PNNL-15955 Rev. 1

Pacific Northwest
National Laboratory
Operated by Battelle for the
U.S. Department of Energy

Geology Data Package for the Single-Shell Tank Waste Management Areas at the Hanford Site

S. P. Reidel
M. A. Chamness

December 2007

Prepared for
CH2M HILL Hanford Group, Inc.,
and the U.S. Department of Energy
under Contract DE-AC05-76RL01830

DISCLAIMER

PACIFIC NORTHWEST NATIONAL LABORATORY
operated by
BATTELLE
for the
UNITED STATES DEPARTMENT OF ENERGY
under Contract DE-AC05-76RL01830

Printed in the United States of America

Available to DOE and DOE contractors from the
Office of Scientific and Technical Information,
P.O. Box 62, Oak Ridge, TN 37831-0062;
ph: (865) 576-8401
fax: (865) 576-5728
email: reports@adonis.osti.gov

Available to the public from the National Technical Information Service,
U.S. Department of Commerce, 5285 Port Royal Rd., Springfield, VA 22161
ph: (800) 553-6847
fax: (703) 605-6900
email: orders@ntis.fedworld.gov
online ordering: http://www.ntis.gov/ordering.htm

This document was printed on recycled paper.
(9/2003)

PNNL-15955 Rev. 1

Geology Data Package for the Single-Shell Tank Waste Management Areas at the Hanford Site

S. P. Reidel
M. A. Chamness

December 2007

Prepared for
CH2M HILL Hanford Group, Inc.,
and the U.S. Department of Energy
under Contract DE-AC05-76RL01830

Pacific Northwest National Laboratory
Richland, Washington 99352

Foreword

This data package discusses the geology of the single-shell tank (SST) farms and the geologic history of the area. The purpose of this report is to provide the most recent geologic information available for the SST farms. This report builds upon previous reports on the tank farm geology and Integrated Disposal Facility geology with information available after those reports were published. Revision 1 presents information on the Post-Ringold basalt-rich gravels in a more clear fashion, provides additional geologic contact data in Table 4.1, replaces a duplicate figure with the correct one, and corrects typographical errors.

Both metric and English units of measurement are used in this document. However, English units are used for descriptions and discussions of drilling activities and samples because that is the system of units used by drillers to measure and report depths and well construction details. To convert feet to meters, multiply by 0.3048; to convert inches to centimeters, multiply by 2.54; to convert meters to feet, multiply by 3.28.

Acknowledgments

The authors acknowledge Frederick M. Mann at CH2M HILL Hanford Group, Inc. (Richland, Washington) for providing project funding and technical guidance. We also greatly appreciate the technical reviews provided by Ann Tallman (independent geologist), Dave Myers and Mike Connelly (both of CH2M HILL, Richland, Washington), Marc Wood (Fluor Hanford, Inc., Richland, Washington), and Bob Bryce (Pacific Northwest National Laboratory). We also are particularly grateful to George Last (PNNL) for his technical peer review of Revision 1, Andrea Currie (PNNL) for copyediting and to Lila Andor, Kathy Neiderhiser, and Mike Parker (PNNL) for final formatting of this report.

Terms

Abbreviations and Acronyms

bgs	below ground surface
BP	before present
CCU	Cold Creek unit
CCU_l	lower Cold Creek unit
CCU_u	upper Cold Creek unit (Cold Creek fine-grained unit)
CD	compact disk
CLEW	Cle Elum-Wallula (deformed zone)
CRBG	Columbia River Basalt Group
DOE	U.S. Department of Energy
DOE-RL	U.S. Department of Energy Richland Operations Office
EC	electrical conductivity
Hf/CCU	Hanford formation/Cold Creek unit
HR-NR	Hog Ranch-Naneum Ridge (anticline)
IDF	Integrated Disposal Facility
OWL	Olympic Wallowa lineament
pH	negative logarithm of the hydrogen ion activity
PNNL	Pacific Northwest National Laboratory
Q_{fg}	Quaternary flood gravels
Q_{fs}	Quaternary flood silt and sand
RCRA	*Resource Conservation and Recovery Act of 1976*
R_{tf}	Ringold Formation, member of Taylor Flat
R_{wi}	Ringold Formation, member of Wooded Island
R_{wia}	Ringold Formation, member of Wooded Island, unit A
R_{wie}	Ringold Formation, member of Wooded Island, unit E
SST	single-shell tank
WMA	waste management area
YFB	Yakima Fold Belt

Units

^{o}	degrees
g	percent acceleration of gravity – a measure of the forces generated during an earthquake
ka	kilo-annum – unit of time equal to one thousand years
lbf/in^2	pound force per square inch
Ma	mega-annum – unit of time equal to one million years
MPa	megapascal
wt%	weight percent

Contents

Figures

Tables

1.0 Introduction

This data package discusses the geology of the single-shell tank (SST) farms, relating the site-specific geology to the region's geologic history. The purpose of this report is to provide the most recent geologic information available for the SST farms and the Integrated Disposal Facility (IDF). This report builds upon previous reports on the tank farm geology (Reidel et al. 2006) and IDF geology (Reidel 2005) with information available after those reports were published. Horton (2007) recently published a companion report to this one that discusses the groundwater flow and contamination beneath the SST farms.

The Hanford Site (Figure 1.1) lies within the Columbia Plateau, a broad plain situated between the Cascade Range to the west and the Rocky Mountains to the east, and is underlain by the Miocene Columbia River Basalt Group (CRBG) (Figure 1.2). The northern Oregon and Washington portion of the Columbia Plateau is often called the Columbia Basin because it forms a broad lowland surrounded on all sides by mountains. In the central and western parts of the Columbia Basin and Pasco Basin where the Hanford Site is located, the basalt is underlain predominantly by Tertiary continental sedimentary rocks and overlain by late Tertiary and Quaternary fluvial and glaciofluvial deposits. All these were folded and faulted during the Cenozoic to form the current landscape of the region.

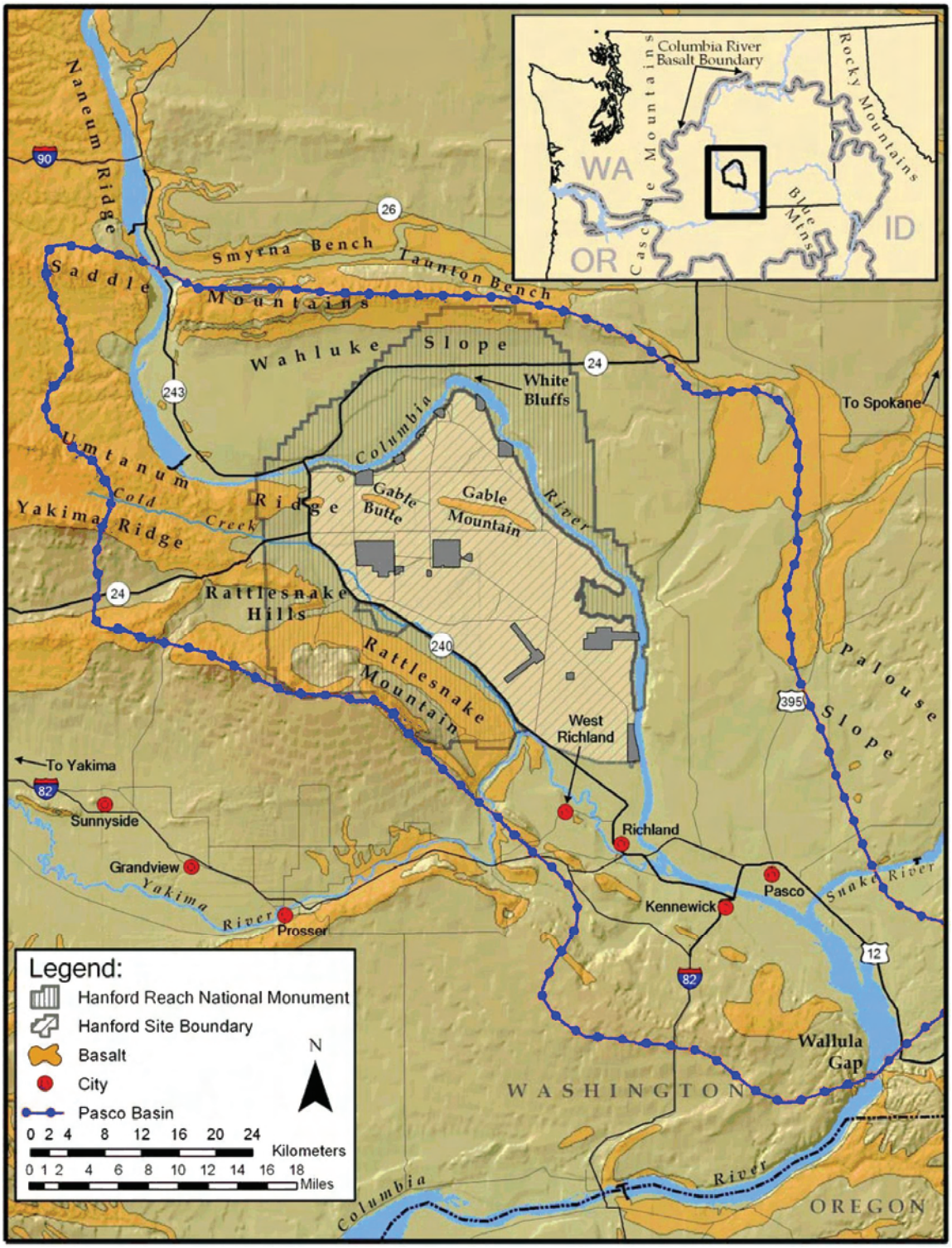

Figure 1.1. Geographic Elements of the Pasco Basin Portion of the Columbia Basin, Washington

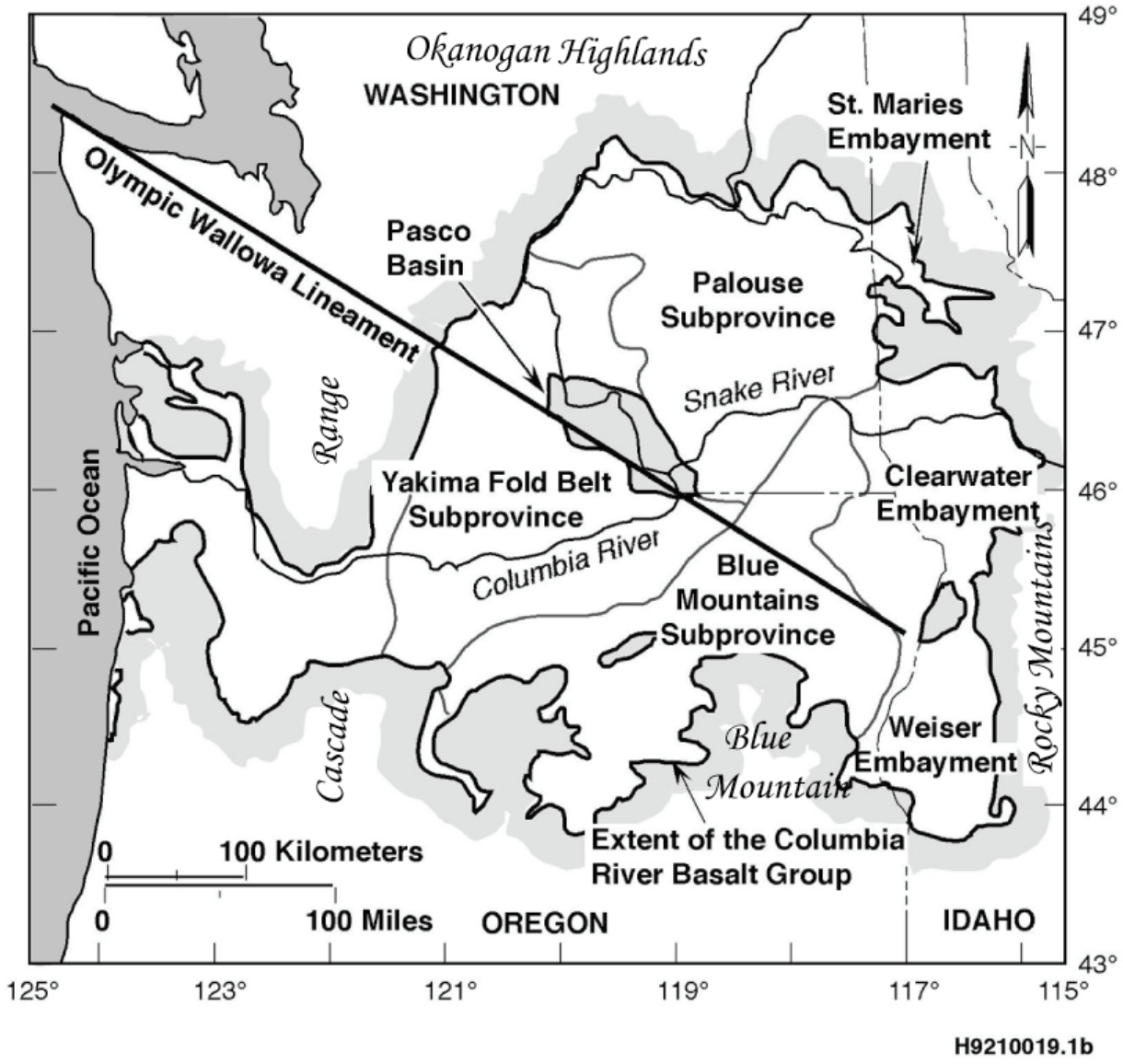

Figure 1.2. Geologic Setting of the Pasco Basin

2.0 Physiographic Setting of the Hanford Site

The physiography of the Hanford Site (Figure 2.1) is dominated by the low-relief plains of the Central Plains physiographic region and anticlinal ridges of the Yakima Folds region (Figure 1.2). The physiography of the Columbia Basin is controlled by the late Cenozoic faulting and folding of the CRBG and overlying sediments of the Ringold Formation. Surface topography in the Columbia Basin has been modified within the past several million years by geomorphic processes related to 1) Pleistocene cataclysmic floods, 2) Holocene eolian activity, and 3) landslides.

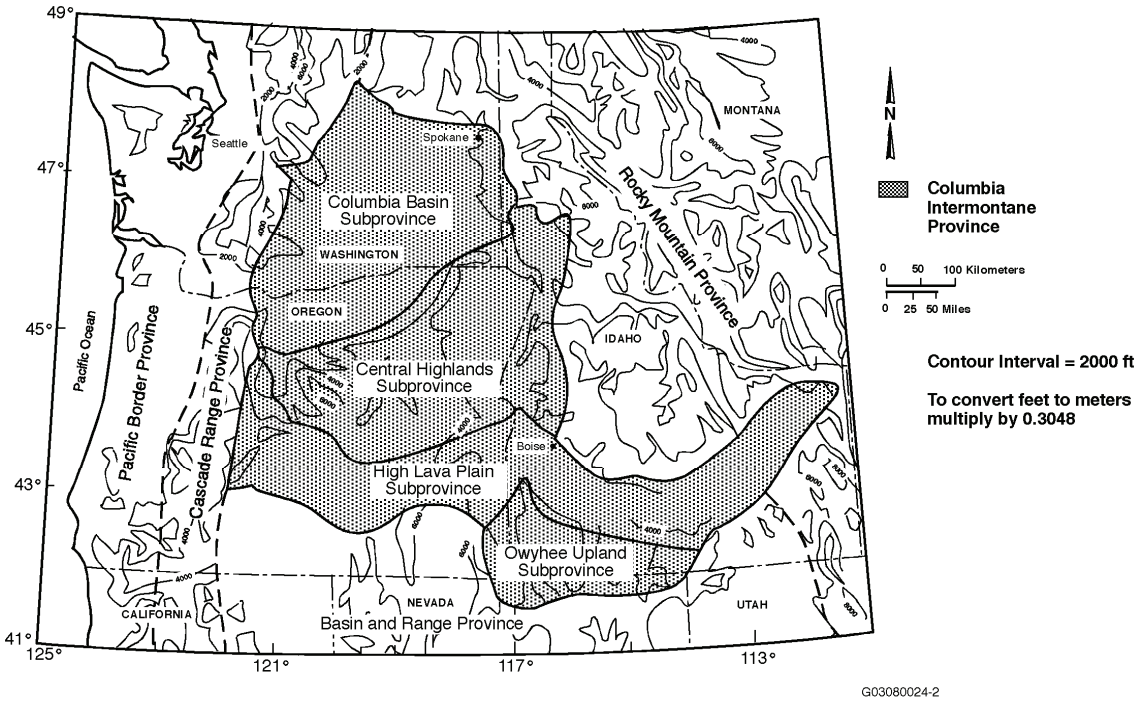

Figure 2.1. Physiographic Map of the Pacific Northwest

Cataclysmic flooding of the Hanford Site occurred when ice dams in western Montana and northern Idaho were breached, allowing large volumes of water to spill across eastern and central Washington (DOE 1989). The last major flood occurred about 13,000 years ago, during the late Pleistocene Epoch. Anastomosing flood channels, giant current ripples, bergmounds, and giant flood bars are among the landforms created by the floods and are readily seen on the Hanford Site. Most of the large landslides in the region occurred when these flood waters eroded steep slopes of the ridges. The single-shell tank (SST) farms are located on a major Pleistocene flood bar, the Cold Creek bar.

Since the end of the Pleistocene, winds have locally reworked the flood sediments, depositing sand dunes in the lower elevations and loess (windblown silt) around the margins of the Pasco Basin. Generally, sand dunes have been stabilized by anchoring vegetation but do become reactivated after vegetation is disturbed, and an active dune field is present in an area on the eastern side of the site. Localized landslides still occur along the Columbia River at the White Bluffs, where irrigation water above the bluffs is reducing friction on some of the bedding planes.

3.0 Geologic History of the Hanford Site

This section describes how the Hanford Site evolved within the context of the Pacific Northwest. It also forms the basis for extrapolating the detailed geology of the tank farms to the surrounding area.

3.1 Structural Setting of the Hanford Site with Respect to the Pacific Northwest

The structure of the Pacific Northwest is controlled by a basement rock assemblage of accreted terranes fused onto the structurally complex North American craton by accretion during the early Mesozoic to early Cenozoic. The accreted terranes form the backbone of the Cascade Range, Okanogan Highlands, and the Blue Mountains. The terranes east of the Cascades now are mostly covered by a thick sequence of Cenozoic rocks that were folded and faulted in a north-south–oriented compressive regime. North-south compression is continuing today east of the Cascades, and this pattern of Cenozoic deformation is expected to continue into the future.

The Columbia Basin is a structurally and topographically low area surrounded by mountains ranging in age from the late Mesozoic to recent (Figure 1.2). The Columbia Basin is composed of two fundamental subprovinces, the Palouse Slope and the Yakima Fold Belt (YFB; Figure 1.2). The Palouse Slope is a stable, undeformed area overlying the old continental craton that dips westward toward the Hanford Site. The YFB is a series of anticlinal ridges and synclinal valleys in the western and central parts of the Columbia Basin. The edge of the old continental craton lies at the junction of these two structural subprovinces east of the Hanford Site.

The Blue Mountains subprovince of the Columbia River flood-basalt province is a northeast trending anticlinorium that extends 250 km from the Oregon Cascades to Idaho and forms the southern border of the Columbia Basin and the southern part of the Columbia Plateau.

3.2 Major Structural Features of the Columbia Basin

Three major structural features are present in the Columbia Basin. One, the YFB, forms the western part of the Columbia Basin. Two features crosscut the Columbia Basin and influence the geology of the Hanford Site. These are the Olympic Wallowa lineament (OWL) (Figures 1.2 and 3.1) and the Hog Ranch-Naneum Ridge (HR-NR) anticline. The OWL passes along the southern boundary of the Hanford Site, and the HR-NR anticline forms the western structural boundary of the Pasco Basin and Hanford Site.

3.2.1 The Olympic-Wallowa Lineament

The OWL (Figure 3.1) is a major topographic feature in Washington and Oregon that crosscuts the Columbia Basin and forms the southern boundary of the Hanford Site (Raisz 1945). This alignment of structural features parallels pre-basalt structural trends along the northwest margin of the Columbia Basin, but it has not been linked to any individual structure (Campbell 1989; Reidel and Campbell 1989).

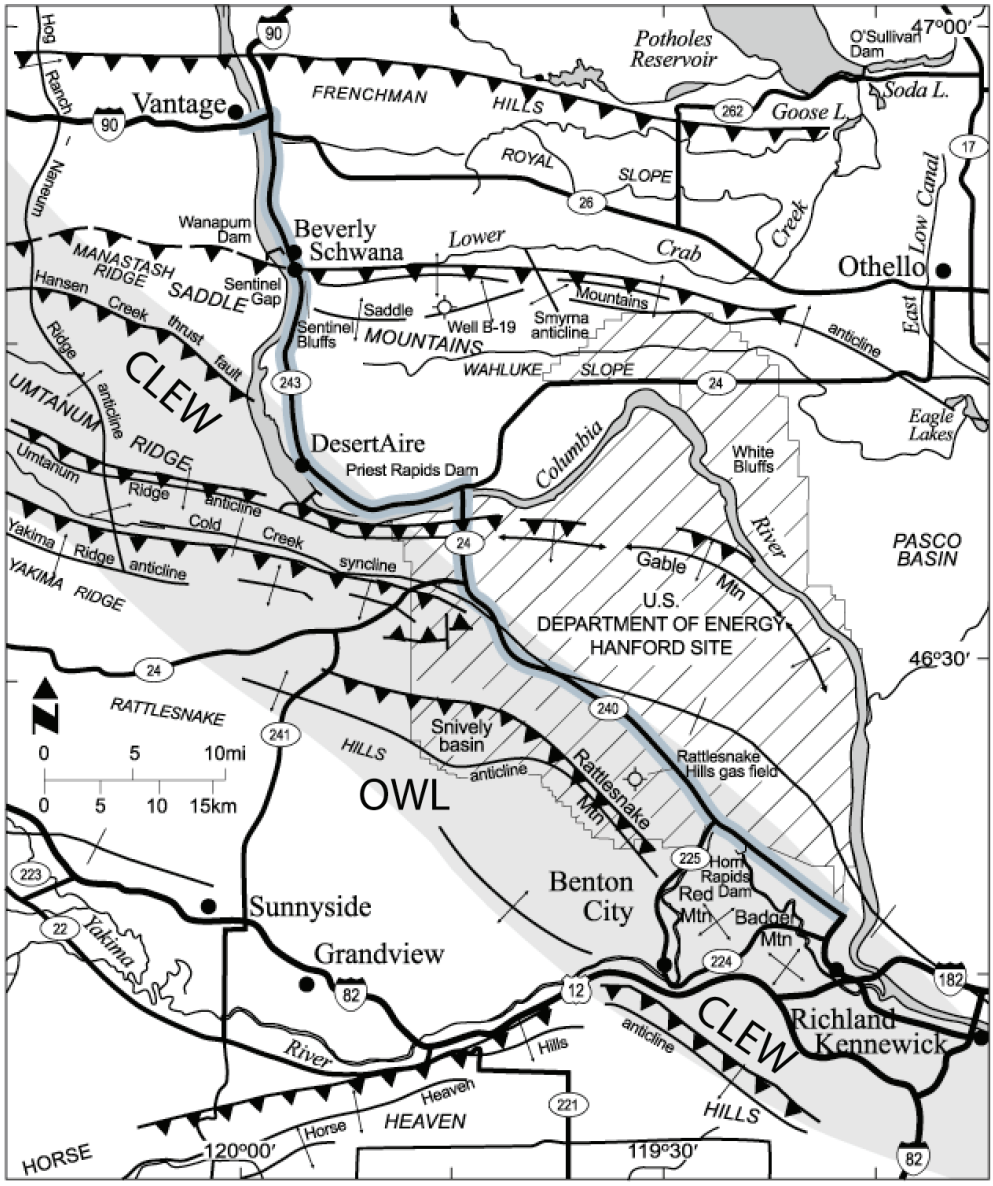

Figure 3.1. Main Structural Features of the Pasco Basin and Surrounding Area

The portion of the OWL that crosses the Columbia Basin is called the Cle Elum-Wallula (CLEW) deformed zone (Figure 3.1) (DOE 1988). It is defined by a 10-km-wide, moderately diffuse zone of anticlines that have an N50ºW orientation. As defined in Davis (1981), the CLEW deformed zone consists of three structural parts: 1) a broad zone of deflected or anomalous fold and fault trends extending south from Cle Elum to Rattlesnake Mountain on the Hanford Site; 2) a narrow belt of topographically aligned domes and doubly plunging anticlines extending from Rattlesnake Mountain to Wallula Gap; and 3) the Wallula fault zone, extending from Wallula Gap to the Blue Mountains.

Northwest of the CRBG margin, numerous northwest- and north-trending faults and shear zones of the Straight Creek fault system lie subparallel to the OWL (Tabor et al. 1984). The Snoqualmie batholith intrudes these faults but is not cut by them, indicating that any possible movement along the OWL at the western margin of the Columbia Basin must be older than the batholith, 17 to 19.7 Ma.

The structural significance of the OWL has been called into question by two recent geophysical studies. Neither a seismic profiling survey (Jarchow 1991) nor a gravity survey (Saltus 1993) could find any obvious geophysical signature for the OWL below the CRBG.

3.2.2 Hog Ranch-Naneum Ridge Anticline

The western structural boundary of the Pasco Basin, the basin containing the Hanford Site, is the Hog Ranch-Naneum Ridge anticline (Figure 3.1). The HR-NR anticline is a broad south-trending anticline in the CRBG that crosses the Yakima Fold Belt in a north-south direction. This south-plunging structure passes through five Yakima Folds and the OWL (Figure 3.1). The HR-NR anticline was active in late to middle Miocene, as demonstrated by thinning of basalt flows across it (Reidel et al. 1989a), but the east-trending Yakima Folds show no apparent offset across this structure (Campbell 1989; Tabor et al. 1984; Reidel et al. 1989a). Growth of the anticline continued from the Miocene to Recent and is evidenced by the highest structural points along the ridges that cross it.

3.2.3 The Yakima Fold Belt

The YFB covers about 14,000 km^2 of the western Columbia Basin (Figure 1.2) and formed as basalt flows and intercalated sediments were folded and faulted under north-south directed compression. The YFB overlies a large pre-basalt basin that has been subsiding since the early Tertiary. The ridges, valleys and basins in the western Columbia Basin are the product of north-south compression that began in the early Tertiary prior to the eruption of the CRBG and continues today. The rates of deformation in the Columbia Basin have declined since the early Tertiary (Reidel et al. 1994). The current rate of ridge growth is estimated at 0.04 mm/yr, and the rate of subsidence in the basin is estimated at 3×10^{-3} mm/yr.

The Hanford Site lies in the Pasco Basin, which is one of the larger structural basins near the eastern limit of the YFB. Deformation in the YFB has controlled the location of the Columbia River system since the late Miocene and the depositional pattern of the post-basalt sediments in the Pasco Basin.

3.2.3.1 Characteristics of the Yakima Folds

The YFB consists of asymmetrical anticlinal ridges and synclinal valleys. The anticlines are typically segmented and usually have a north vergence, although some folds have a south vergence. Synclines are typically asymmetrical with a gently dipping north limb and a steeply dipping south limb. Fold length is variable, ranging from several kilometers to over 100 km; fold wavelengths range from several kilometers to as much as 20 km. Structural relief is typically about 600 m but varies along the length of the fold. The greatest structural relief along the Frenchman Hills, the Saddle Mountains, Umtanum Ridge, and Yakima Ridge occurs where they intersect the north-south trending HR-NR anticline (Reidel et al. 1989a).

Synclines generally form passively, i.e., they are simply lows between two folds. One significant exception to this is the Cold Creek syncline where it crosses the Pasco Basin. Here, the syncline has been actively deforming and subsiding throughout deposition of suprabasalt sediments.

In general, the axial trends produce a “fanning” pattern across the fold belt (Figures 3.1 and 3.2). Anticlines on the western side of the fold belt generally have a N50ºE trend (Swanson et al. 1979a). Anticlines in the central and eastern part of the fold belt have east-west trends except along the CLEW

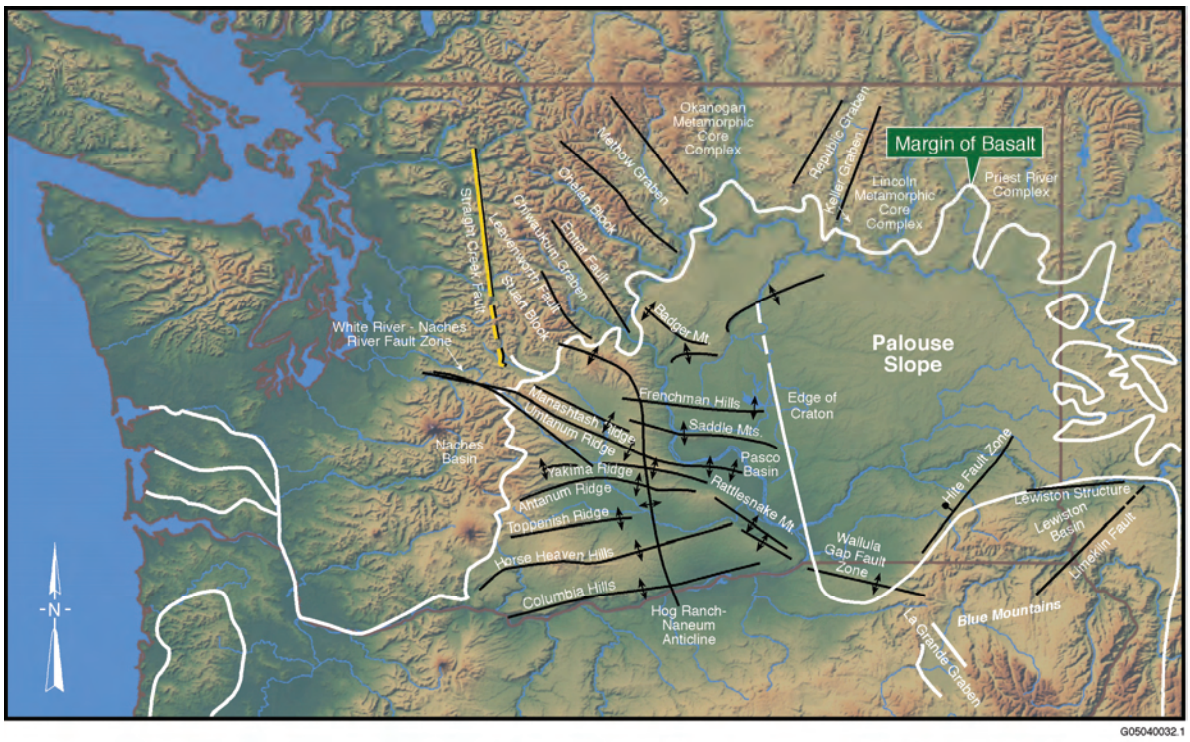

Figure 3.2. General Trend of Yakima Folds Across the Pacific Northwest

deformed zone where a N50ºW trend predominates. The Rattlesnake Hills, Saddle Mountains, and Frenchman Hills have overall east-west trends across the fold belt, but Yakima Ridge and Umtanum Ridge change eastward from east-west to N50ºW in the zone of the CLEW deformed zone. In the central part of the fold belt, the Horse Heaven Hills, the Rattlesnake Hills, and the Columbia Hills have eastward terminations against the CLEW deformed zone.

3.2.3.2 Fold and Fault Geometry

Within the Hanford Site and surrounding area, the geometry of the anticlines typically consists of steeply dipping to overturned north flanks and gently dipping (<5º) south flanks (Figure 3.3). Exceptions, however, include the doubly plunging anticlines within the Rattlesnake-Wallula alignment of the CLEW deformed zone and the conjugate box-fold geometry of parts of the anticlines such as the Smyrna segment of the Saddle Mountains (Reidel 1984). The main variable in fold profiles is the width of the gently dipping limb that varies from as little 5 km to as much as 35 km (Figure 3.3).

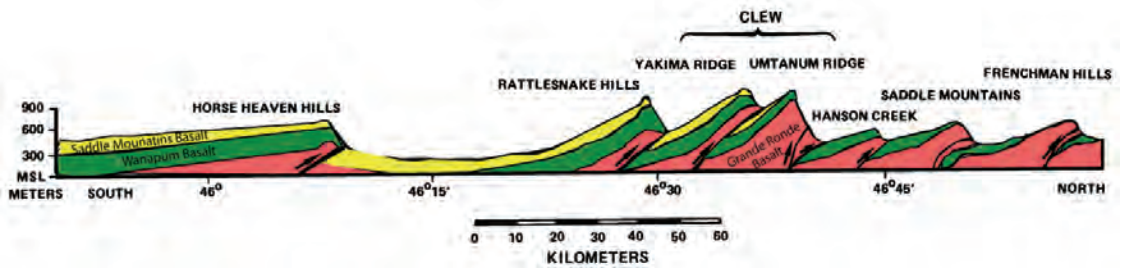

Figure 3.3. Generalized Cross Section Through the Yakima Fold Belt

Segmentation of the anticlines is common throughout the fold belt and is defined by abrupt changes in fold geometry or by places where regional folds die out and become a series of doubly plunging anticlines. Segment lengths are variable but average about 12 km (7 mi) (ranging from 5 to 35 km [3 to 34 mi]) near the Hanford Site; some of the larger segments contain subtler changes in geometry, such as different amplitudes, that could also be considered segment boundaries. Segment boundaries are often marked by cross or tear faults that trend N20ºW to north and display a principal component of strike-slip movement (e.g., Saddle Mountains) (Reidel 1984). Near the Hanford Site, these cross faults are confined to the anticlinal folds and usually occur only on the steeper limb, dying out onto the gentler limb.

Segment boundaries may also be marked by relatively undeformed areas along the fold trend where two fold segments plunge toward each other. For example, the Yakima River follows a segment boundary where it crosses the Rattlesnake-Wallula alignment at the southeast termination of Rattlesnake Mountain (Figure 3.1).

The steep limb of the asymmetrical anticlines is almost always faulted (Figure 3.3). Where exposed, these frontal fault zones have been found to be imbricated thrusts, as, for example, at Rattlesnake Mountain, Umtanum Ridge near Priest Rapids Dam (Bentley 1977; Goff 1981), the Horse Heaven Hills (Hagood 1986), and the Saddle Mountains near Sentinel Gap (Reidel 1984).

Yakima Folds have emergent thrust faults at the ground surface. Faulted material moves along the fault onto the surface in front of the fold, giving the appearance the fault is a low-angle thrust fault with detachment surfaces either within the CRBG, in the sediments below the basalts, or at the basalt-sediment contact. However, where erosion provides deeper exposures into the cores of folds, the frontal faults are observed to be reverse faults (e.g., the Columbia water gap in the Frenchman hills, 45ºS [Grolier and Bingham 1971]; the Columbia Hills at Rock Creek, Washington, 50 to 70ºN). Drilling of the Umtanum fault near Priest Rapids Dam (PSPL 1981) suggests that this fault dips southward under the ridge with a dip of at least 30º to 40º (PSPL 1981) but perhaps as high as 60º (Price and Watkinson 1989).

3.3 Geologic History of the Hanford Site with Respect to the Pacific Northwest

The Hanford Site is a small portion of the Columbia Basin, but the geologic record of the Site is representative of the geologic history of the Pacific Northwest. The following discussion puts the Hanford Site geology into perspective with the regional geologic setting.

3.3.1 Stratigraphy of Rocks Older Than the Columbia River Basalt Group

Rocks older than the CRBG are exposed mainly along the margin of the Columbia Basin. However, they are important to understanding the history of the Hanford Site because many are thought to extend under the basalt and form the foundation of the area. Stratigraphy along the margin of the CRBG is complex and varies widely in both age and lithology. The principal age, lithologies, and importance to the history of Hanford were taken from Reidel et al. (1994) and are summarized below.

- The oldest rocks in the Pacific Northwest are found along the northeast and east margins of the Columbia Basin near the Idaho border. These are late Precambrian and early Paleozoic metavolcanic and metasedimentary rocks (2.3 billion-300 million years before present) interspersed with younger igneous intrusive rocks. These older rocks represent the ancient North American

craton and the remnants of the 1-billion-year-old supercontinent Rodinia that broke apart 750 million years ago to form the Pacific Ocean. The boundary of that rifted margin occurs east of the Hanford Site.

- Late Paleozoic, Mesozoic, and early Cenozoic metavolcanics and metasediments are exposed along the south and western margin of the Columbia Basin. These are the rocks that were added onto the North America Plate remnants of Rodinia between 200 and 50 million years ago. Although many are of similar age to rocks along the north and east margins of the Columbia Basin, they formed as ocean islands and microcontinents far away from the Pacific Northwest. Through the process of plate tectonics, these rocks were carried along on the oceanic plate that collided with the North American Plate beginning 200 million years ago. During the collision process, these ocean islands and microcontinents were accreted onto North America and resulted in the westward growth of North America. Similar accreted terrane rocks are thought to occur deep beneath the Hanford Site.

- Along the west and northwest margin, a series of sedimentary basins formed in early Tertiary time (Campbell 1989). These basins formed in the accreted terranes and are now separated by tectonic "blocks" or uplifts exposing the accreted terranes. The Tertiary rocks extend under the Columbia Basin and Hanford Site and were the targets of oil exploration in the latter half of the 20th century. The rocks include the volcanic and sedimentary rocks that are 50 to 20 million years old and were derived from the erosion of highlands in the Pacific Northwest.

3.3.2 Columbia River Basalt Group and Ellensburg Formation

The CRBG forms the main bedrock of the Columbia Basin and Hanford Site. This consists of over 200,000 km^3 of tholeiitic flood-basalt flows that were erupted between 17 and 6 Ma and now cover approximately 230,000 km^2 of eastern Washington, eastern Oregon, and western Idaho (Camp et al. 2003). Eruptions had volumes as great as 5,000 km^3 (Reidel et al. 1989b), with the greatest amounts being erupted between 16.5 and 14.5 million years before present. The flows were erupted from north-northwest–trending fissures or linear vent systems in north-central and northeastern Oregon, eastern Washington, and western Idaho (Swanson et al. 1979b). These flows are the structural framework of the Columbia Basin, and their distribution pattern reflects the tectonic history of the area over the past 16 million years (Reidel et al. 1989a).

The CRBG has been divided into five formations (Swanson et al. 1979b); only the Grande Ronde Basalt, the Wanapum Basalt, and the Saddle Mountains Basalt are exposed on the Hanford Site (Figure 3.4). The Imnaha Basalt occurs at the base of the Columbia River basalt under the Hanford Site. The Picture Gorge Basalt is not present on the Hanford Site.

The basalt flows of the CRBG are recognized using a combination of lithology, chemistry, and paleomagnetic data (Swanson et al. 1979b). Chemical composition and paleomagnetic data have proven to be the most reliable criteria for flow recognition and correlation. Lithology is reliable for many flows primarily within the Wanapum and Saddle Mountains Basalts, but chemical compositions still are used to confirm identifications.

More than 65% of the CRBG was erupted in a 1-million-year span of the Grande Ronde Basalt. In the field, the Grande Ronde Basalt is divided into four magnetostratigraphic units, which, from oldest to youngest, are Reversed 1, Normal 1, Reversed 2, and Normal 2 (Swanson et al. 1979b). The Grande

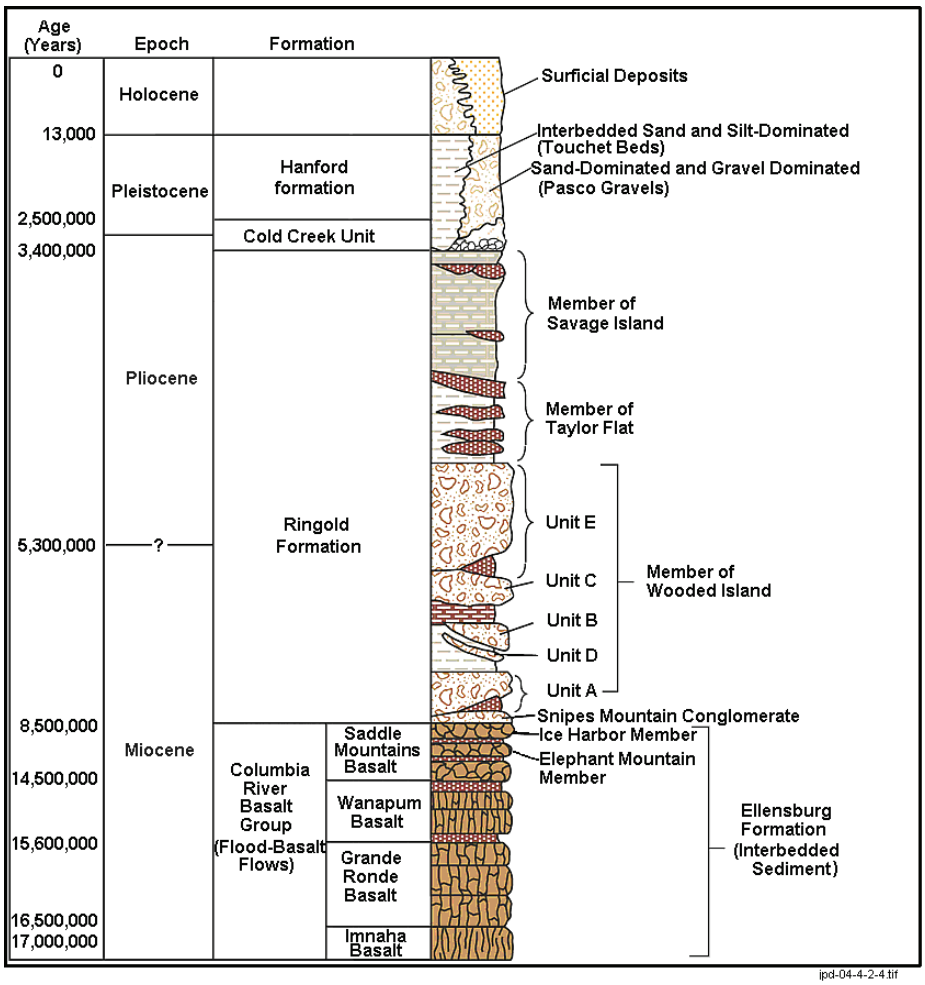

Figure 3.4. Generalized Stratigraphy of the Pasco Basin and Vicinity

Ronde Basalt is further subdivided into 17 groups of flows based on chemical compositions (Reidel et al. 1989b). The Wanapum Basalt has been subdivided into four members, and the Saddle Mountains Basalt has been subdivided into ten members. The Elephant Mountain Member and Ice Harbor Member are the uppermost basalt lava flows at Hanford.

The younger basalt flows of the Wanapum and Saddle Mountains Basalts on the Hanford Site have been locally eroded to various degrees. Some erosion of the basalt occurred between eruptions, as well as before and during deposition of the oldest Ringold sediments. Uplift along anticlinal ridges has resulted in erosion to different depths along the margin of the Pasco Basin and Cold Creek syncline. Within the synclines where the basalt surface is covered by sediment fill, the upper basalt flows have been locally eroded by fluvial activity and proglacial flooding. North of the 200 Areas near Gable Gap, the Saddle Mountains Basalt has been eroded down to the oldest member, the Umatilla Member.

Intercalated with and in some places overlying the CRBG are sedimentary rocks of the Ellensburg Formation (Swanson et al. 1979a). In the western Columbia Basin, the Ellensburg Formation is mostly volcanic-derived sediment; in the central and eastern basin, fluvial sediments of the ancestral Clearwater and Columbia Rivers form the dominant lithologies (Fecht et al. 1987).

3.3.3 Post-Columbia River Basalt Stratigraphy

Most post-CRBG sediments are confined to the synclinal valleys of the YFB. Although the sedimentary record is incomplete, the sedimentation pattern is what is expected in an area with limited rainfall and significant structural development (Fecht et al. 1987). The dominant source of sediment between the upper Miocene to middle Pliocene (10 to 3 million years ago) is the Columbia River system. The upper Ellensburg Formation and the Ringold Formation are the main sediment packages that contain this history and record the migration of rivers and streams into their present channels (Fecht et al. 1987). Capping the sedimentary sequence in the synclines and basins are sediments comprising the Pleistocene Hanford formation deposited during cataclysmic floods and recent eolian deposits.

The upper Ellensburg Formation at the Hanford Site mainly records the path of the ancestral Clearwater-Salmon River system as it flowed from the Rocky Mountains west to its confluence with the Columbia River near the present Priest Rapids Dam. During this time, the Columbia River flowed along the western margin of the Columbia Basin. The Snake River did not enter the Columbia Basin until the end of the Pliocene. The Clearwater-Salmon River geologic record consists of main stream and overbank deposits that occur between lava flows of the Saddle Mountains Basalt. These sediments are important to Hanford because they form part of the confined aquifer system.

Ridges of the YFB were growing during the eruption of the CRBG but usually were buried completely by each new basalt eruption. After the last major basalt eruption, the ridges began to develop significant topography. The highest topography first developed where the ridges intersected the north-south trending HR-NR anticline (Figure 3.1) along the western boundary of the Pasco Basin. Continued uplift of the HR-NR anticline and the ridges of the YFB forced the Columbia River and its confluence with the Salmon-Clearwater River eastward. By 10.5 million years ago, the Columbia River was flowing along the western boundary of the Hanford Site and then turning southwestward through Sunnyside Gap (Figure 3.1) and south past Goldendale, Washington. This is when the Snipes Mountain conglomerate (Figure 3.4), the last Ellensburg Formation unit in the Pasco Basin, was deposited.

Sediment of the Ringold Formation represents evolutionary stages of the ancestral Columbia River as it was forced to change course across the Columbia Basin by the growth of the YFB. Ringold Formation time began approximately 8.5 million years ago when the Columbia River abandoned Sunnyside Gap (Figure 3.1), a water gap through the Rattlesnake Hills, and began to flow across the Hanford Site, leaving the Pasco Basin through the present Yakima River water gap along the southwest end of the Rattlesnake Mountain anticline. The northern margin of the 8.5-million-year-old Ice Harbor basalt controls the Columbia River channel as it exits the Pasco Basin.

The first record of the Columbia River at Hanford is in the extensive gravel and interbedded sand of unit A, Ringold Formation member of Wooded Island (Figure 3.4). The Columbia River was a gravelly braid plain and widespread paleosols.

At about 6.7 million years ago, the Columbia River abandoned the Yakima River water gap along the southeast extension of Rattlesnake Mountain and began to exit the Pasco Basin through Wallula Gap (Figure 3.1). The main channel of the Columbia River in the Pasco Basin was still through Hanford and the 200 Areas. At this time, the Columbia River sediments change to a sandy alluvial system with extensive lacustrine and overbank deposits (Fecht et al. 1987; Reidel et al. 1994; Lindsey 1995). A widespread lacustrine-overbank deposit called the lower mud was deposited over some of the Hanford Site at this time

and is a nearly continuous feature under the 200 West Area and much of the 200 East Area. The lower mud was then covered by another extensive sequence of fluvial gravels and sands. The most extensive of these is called unit E, Ringold Formation member of Wooded Island, but locally other sequences are recognized (e.g., units C and D). Unit E is one of the most extensive Ringold Formation gravels and appears to be continuous under the 200 Areas. To the north near the 100 Areas, Ringold Formation sediments reflect mostly overbank deposition of fine-grained sediments during this time.

The Columbia River sediments became more sand-dominated about 5 million years ago when over 90 m (295 ft) of interbedded fluvial sand and overbank deposits accumulated at Hanford. These deposits are collectively called the Ringold Formation member of Taylor Flat (Lindsey 1995). The fluvial sands of the member of Taylor Flat dominate the lower cliffs of the White Bluffs.

Between 4.8 million years ago to the end of Ringold time at 3.4 million years ago, lacustrine deposits dominated Ringold Formation deposition. A series of three successive lakes is recognized along the White Bluffs and elsewhere along the margin of the Pasco Basin (Lindsey 1995). The lakes probably resulted from damming of the Columbia River farther downstream, possibly near the Columbia Gorge. The lacustrine and related deposits in the Pasco Basin are collectively called the Ringold Formation member of Savage Island.

At the end of Ringold time, the Pacific Northwest underwent regional uplift, resulting in a change in base level for the Columbia River system. Uplift caused a change from sediment deposition to regional incision and sediment removal. Regional incision is especially apparent in the Pasco Basin, where nearly 100 m (328 ft) of Ringold Formation sediment has been removed from the Hanford Area. The regional incision marks the beginning of Cold Creek time and the end of major deposition by the Columbia River.

Regional incision and erosion during Cold Creek time are most apparent in the surface elevation change of the Ringold Formation across the Hanford Site (Figure 3.3). As incision of the Columbia progressed eastward across Hanford, and less erosion occurred on the surface of the Ringold Formation in the 200 West Area, leaving it at a higher elevation than in the 200 East Area (Figure 3.5). The surface of the Ringold Formation in the 200 West Area is consequently also older than that in the 200 East Area and thus was exposed to weathering processes for a much longer time. Less erosion of the 200 West Area surface accounts for the isolated remnants of the fluvial sands of the Ringold Formation member of Taylor Flat. At the north side of 200 East Area, the ancestral Columbia River was able to cut completely through the Ringold Formation to the top of the basalt. The channel can be traced from Gable Gap across the eastern part of the 200 East Area and to the southeast. The greatest amount of incision is near the current river channel.

In the Pasco Basin, the Cold Creek unit records most of the geologic events between the incision by the Columbia River and the next major event, the Missoula floods. The older Ringold Formation surface at the 200 West Area was exposed to weathering, resulting in the formation of a soil horizon on its surface. Because the climate was becoming arid, the resulting soil became a pedogenically altered, carbonate-rich, cemented paleosol. The development of this carbonate-rich paleosol is much greater in the 200 West Area than in the 200 East Area due to longer exposure of the surface. This ancient paleosol is referred to as the lower Cold Creek unit (CCU_l) subunit.

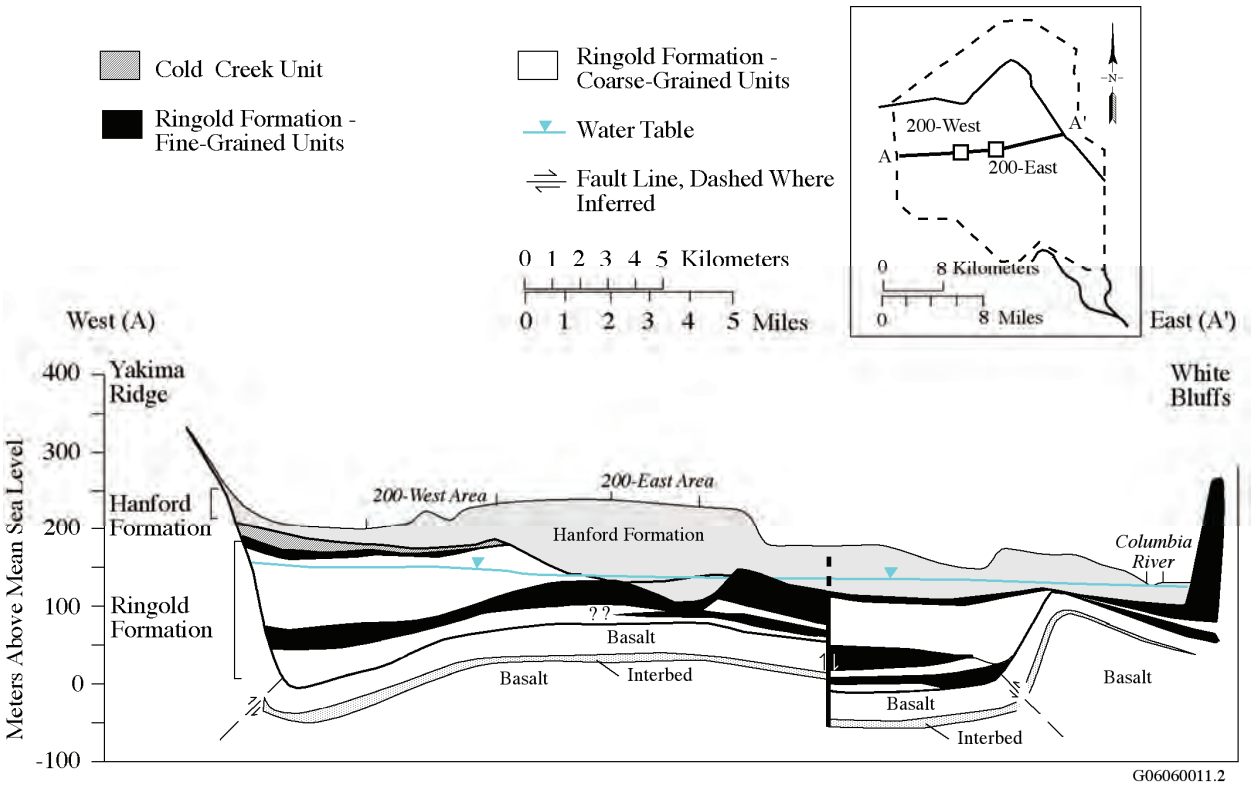

Figure 3.5. Generalized Cross Section Through the Hanford Site

Concurrently, eolian sediments and minor fine-grained flood deposits from streams originating from the nearby ridges were deposited on the paleosol, resulting in a wide variety of sediments that are called the upper subunit of the Cold Creek unit (CCU_u). Because of the long time interval (approximately 3.4 to 2 million years ago), several localized paleosols like the lower Cold Creek unit were able to develop in the upper Cold Creek unit. Throughout Cold Creek time, streams from the Rattlesnake, Yakima, and Umtanum Ridges were carving channels to the Cold Creek drainage, depositing basaltic gravels in their stream beds. These form the side-stream alluvial facies of the Cold Creek unit.

During Cold Creek time in the central Pasco Basin, the Columbia River flowed through Gable Gap, depositing gravels of mixed lithologies in a sand matrix. These gravels, informally called the "Pre-Missoula gravels" (PSPL 1981), overlie the Ringold Formation and are up to 25 m (82 ft) thick. The 200 East Area lies along the boundary between these two geologic environments, undergoing significantly more erosion than beneath the 200 West Area but with some soil development occurring in areas. There may have been other periods of fluvial deposition near the 200 East Area that reworked the existing Ringold Formation gravels. The difficulty and uncertainty in distinguishing between these similar units is reflected in the differences in geologic contacts and their descriptions among authors.

During the Pleistocene, cataclysmic floods inundated the Pasco Basin several times when ice dams failed in northern Washington (Baker et al. 1991). Current interpretations suggest as many as 40 flooding events occurred as ice dams holding back glacial Lake Missoula repeatedly formed and broke. In addition to larger major flood episodes, there were probably numerous smaller individual flood events. Deciphering the history

of cataclysmic flooding in the Pasco Basin is complicated, not only because of floods from multiple sources but also because the paths of Missoula floodwaters migrated and changed course with the advance and retreat of the Cordilleran Ice Sheet.

Along with sedimentological evidence for cataclysmic flooding in the Pasco Basin, high-water marks and faint strandlines occur along the basin margins. Temporary lakes were created when flood waters were hydraulically dammed, resulting in the formation of the short-lived Lake Lewis behind Wallula Gap. High-water mark elevations for Lake Lewis, inferred from ice-rafted erratics on ridges, range from 370 to 385 m (1,214 to 1,261 ft) above sea level.

The sediment deposited by the cataclysmic flood waters has been informally called the Hanford formation because the best exposures and most complete deposits are found there. The coarse-grained flood facies (gravel-dominated facies of DOE-RL 2002) is generally confined to relatively narrow tracts within or near flood channelways. The plane-laminated sand facies (sand-dominated facies of DOE-RL 2002), on the other hand, occurs as a broad sheet over most of the central basin. Paleocurrent indicators within beds of plane-laminated sands are unidirectional, generally toward the south and east within the Pasco Basin.

Rhythmite facies (interbedded silt and sand-dominated facies of DOE-RL 2002) occur in slackwater areas around the margins of the basin and were deposited by multidirectional currents, including upvalley currents. Individual rhythmites become finer and thinner both laterally and vertically upward.

The 200 West and 200 East Areas occur on a major depositional feature called the Cold Creek bar (Figure 3.6). Recent studies using the magnetic polarity of the Hanford formation sediments have shown that the earliest floods may have occurred as long ago as 2 million years. Four magnetic polarity reversals have been found in sediments from core holes in the 200 East Area (Pluhar et al. 2006). These polarity reversals have paleosols at the top of each reversed sequence of sediments. The oldest sediments occur in the ancestral Columbia River channels where the Pre-Missoula sediments occur. The age of the Hanford formation in the 200 West Area is more difficult to determine because only normal-polarity sediments occur here.

Since the end of the Pleistocene, the main geologic process has been wind. After the last Missoula flood drained from the Pasco Basin, winds moved the loose, unconsolidated material until vegetation was able to stabilize it. Stabilized sand dunes cover much of the Pasco Basin, but there are areas, such as along the Hanford Reach National Monument, where sand dunes remain active.

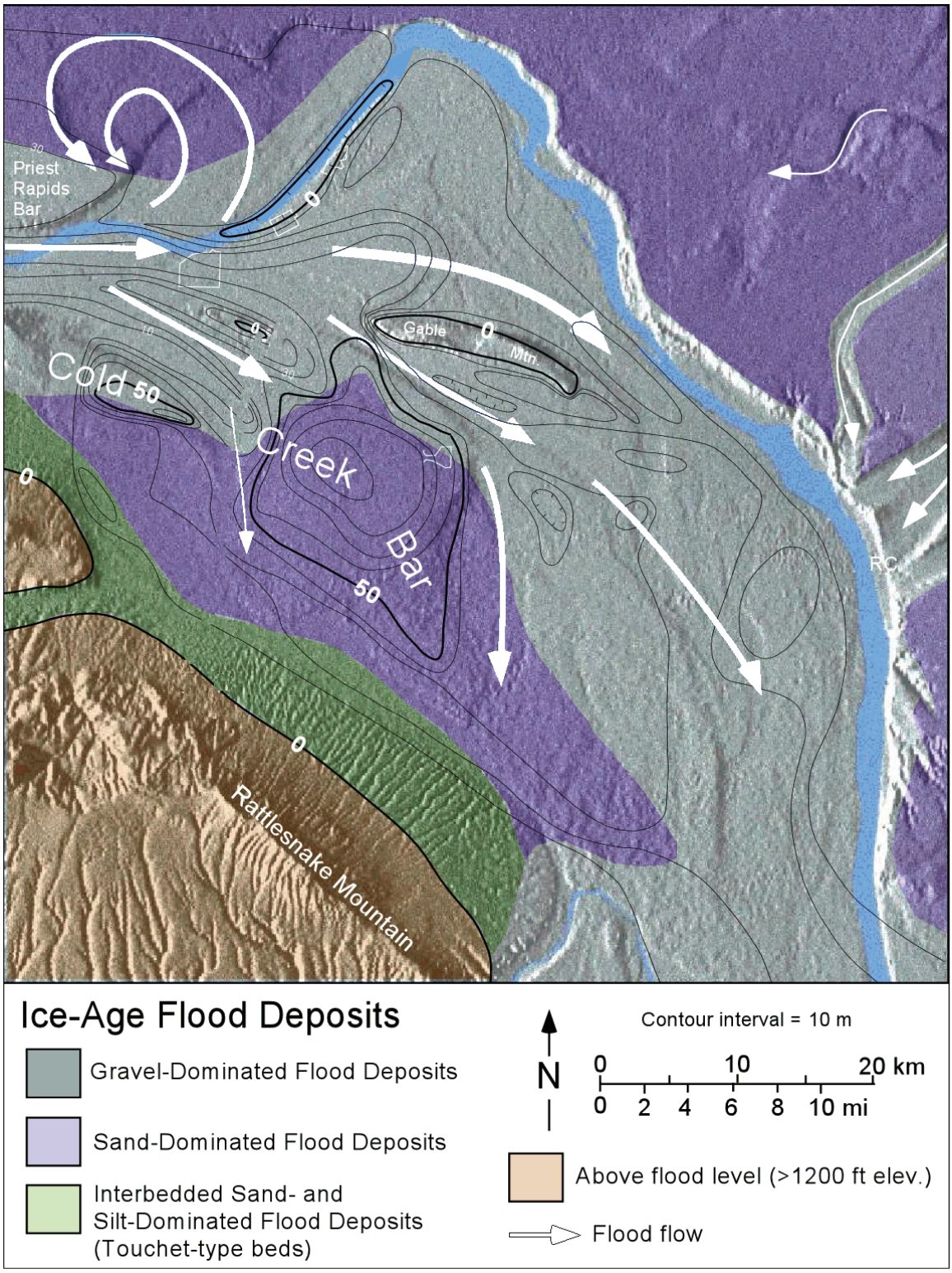

Figure 3.6. Isopach Map of the Ice Age Flood Deposits (Hanford formation)

4.0 Geology of the Pasco Basin and Hanford Site

As discussed in Chapter 3, the events occurring throughout the Pacific Northwest and Columbia Basin are reflected in the sedimentary record in the Pasco Basin and consequently the Hanford Site. This chapter provides a description of the large geologic framework for the Hanford Site.

4.1 Structure of the Hanford Site

The Cold Creek syncline (Figure 4.1) lies between the Umtanum Ridge-Gable Mountain uplift and the Yakima Ridge uplift and is an asymmetric and relatively flat-bottomed structure. The Cold Creek syncline began developing during the eruption of the CRBG and has continued to subside since that time. The 200 Areas lie on the northern flank, and the bedrock dips gently (approximately 5°) to the south. The 300 Area lies at the eastern end of the Cold Creek syncline where it merges with the Pasco syncline. The deepest parts of the Cold Creek syncline, the Wye Barricade depression and the Cold Creek depression, are approximately 7.5 mi southeast of the 200 Areas and southwest of the 200 West Area, respectively (Figure 4.1).

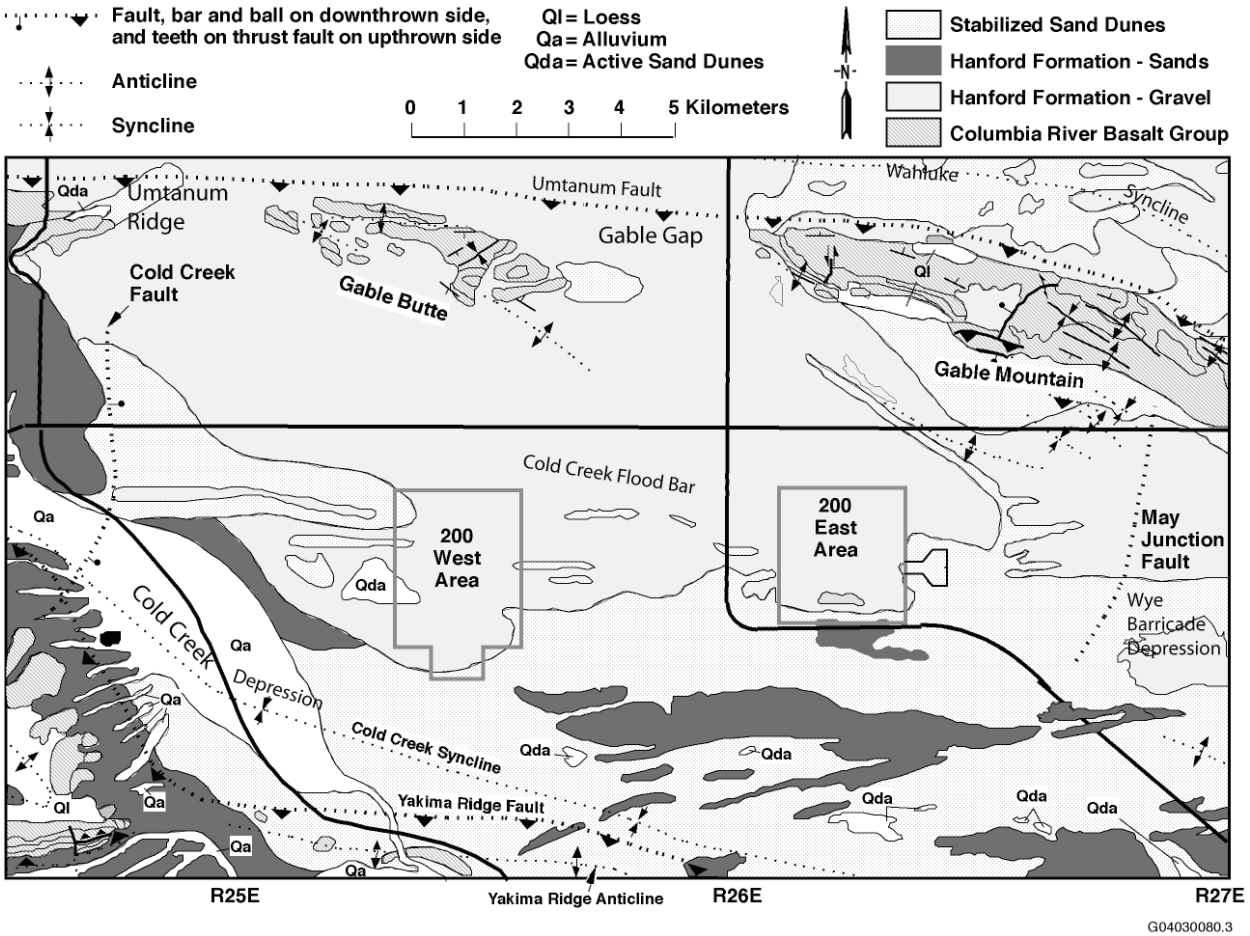

Figure 4.1. Geologic and Geomorphic Map of the 200 Areas and Vicinity

The Wahluke syncline north of Gable Mountain is the principal structural unit that contains the 100 Areas. The Wahluke syncline is an asymmetric and relatively flat-bottomed structure similar to the Cold Creek syncline. The northern limb dips gently (approximately 5°) to the south. The steepest limb is adjacent to the Umtanum-Gable Mountain structure.

The Umtanum Ridge-Gable Butte-Gable Mountain structural trend (Figures 3.1 and 4.1) is a segmented anticlinal ridge extending for a length of 110 km in an east-west direction and passes north of the 200 and 300 Areas and south of the 100 Areas. This structure consists of five segments. From the west, the Umtanum Ridge plunges eastward and joins the Gable Mountain-Gable Butte segment just east of the western boundary of the Hanford Site. The easternmost segment, the Southeast anticline, extends southeast from the eastern boundary of the Gable Mountain-Gable Butte segment.

Umtanum Ridge is an asymmetrical, north-vergent to locally-overturned anticline with a major thrust to high-angle reverse fault on the north side (Figures 3.1 and 4.1) (Goff 1981; Price and Watkinson 1989). Gable Mountain and Gable Butte are two topographically isolated, anticlinal ridges that are composed of a series of northwest trending, doubly plunging, en echelon anticlines, synclines, and associated faults.

The Yakima Ridge uplift extends from west of Yakima, Washington, to the center of the Pasco Basin, where it forms the southern boundary of the Cold Creek syncline south of the 200 West Area (Figures 3.1 and 4.1). The easternmost surface expression of the Yakima Ridge uplift is represented by an anticline that plunges eastward into the Pasco Basin (Myers et al. 1979). The eastern extension of Yakima Ridge is mostly buried beneath late Cenozoic sediments and has much less structural relief than the rest of Yakima Ridge.

4.1.1 Structural Setting of the 200 West Area Tank Farms

The 200 West Area sits on the western part of the Cold Creek bar, which is along the north flank of the Cold Creek syncline (Figure 4.1). The surface of the Columbia River basalt bedrock under the 200 West Area has an overall strike to the northwest and is tilted to the southwest into the Cold Creek depression (Figure 4.1). A deep structural low, the Cold Creek depression, developed along the Cold Creek syncline southwest of the 200 West Area and greatly influences the structural attitudes of the sedimentary layers that overlie the basalt.

4.1.2 Structural Setting of the 200 East Area Tank Farms

The 200 East Area sits on the eastern part of the Cold Creek bar, which is along the northern flank of the Cold Creek syncline (Figure 4.1). Another deep structural low, the Wye Barricade depression, developed along the Cold Creek syncline southeast of the 200 East Area. The May Junction fault is a normal fault that marks the western boundary of the depression.

The 200 East Area sits at the southern end of a series of secondary doubly plunging anticlines and synclines that are associated with the Umtanum-Gable Mountain anticlinal structure (Figure 4.1). WMAs A, AX, B-BX-BY, and C in the 200 East Area lie near the southern flank of the closest secondary anticline. A fault was recently detected during drilling of seismic test boreholes at the Waste Treatment

Plant. The fault caused some displacement in the Pomona Basalt that lies beneath the Elephant Mountain Basalt but is not thought to have caused any displacement in younger basalts or overlying sediments (Barnett et al. 2007).

4.2 Stratigraphy of the Hanford Site

The generalized stratigraphy of the Pasco Basin and Hanford Site is shown in Figure 3.4. The principal rocks exposed at the surface of the surrounding ridges are the CRBG and intercalated sedimentary rocks of the Ellensburg Formation. In the low-lying basins and valleys, these are overlain by younger sedimentary rocks of the Ringold Formation, Cold Creek unit, and the Pleistocene catastrophic flood deposits of the Hanford formation.

4.2.1 Columbia River Basalt Group and Ellensburg Formation

The Elephant Mountain Member is the uppermost basalt flow beneath the 200 Areas and much of the Hanford Site. Where folds and faults have formed basalt ridges, other flows from the Saddle Mountains, Wanapum, and Grande Ronde Formations are exposed.

The Ellensburg Formation is intercalated with and overlies the CRBG in the Pasco Basin and includes epiclastic and volcaniclastic sedimentary rocks (Waters 1961; Swanson et al. 1979b). At the Hanford Site, the Ellensburg Formation consists of sediments deposited by the ancestral Clearwater and Columbia Rivers. Relatively few boreholes in the 200 Areas penetrate the Ellensburg Formation. Those that do generally find tuffaceous siltstones and sandstones, with conglomerates marking ancient main river channels. The Ellensburg stratigraphy of the Hanford Site has been discussed in more detail in Fecht et al. (1987).

4.2.2 Post-Columbia River Basalt Group Sediments

The Hanford Site and tank farms are situated on a sequence of Ringold Formation, Cold Creek unit, and Hanford formation sediments overlying the CRBG (Figure 3.4). The upper Miocene to middle Pliocene record of the Columbia River system in the Columbia Basin is represented by the upper Ellensburg and Ringold Formations. Except for local deposits (e.g., the Cold Creek unit [CCU]), there is a hiatus (erosion or lack of sedimentation) in the stratigraphic record between the end of the Ringold Formation deposition (3.4 Ma) and the beginning of Pleistocene (1.6 Ma) time (DOE 1988; DOE-RL 2002).

Pleistocene to Recent sediments overlying the CRBG at the Hanford Site include cataclysmic flood gravels and slackwater sediments of the Hanford formation; terrace gravels of the Columbia, Snake, and Yakima Rivers; and eolian deposits.

4.3 Geology of the Central Plateau

Because of the need to understand the geologic controls on movement of contaminants in the vadose zone and groundwater, the Central Plateau has become one of the best characterized areas on the Hanford Site. The geology of the Hanford Site has largely been determined using samples from numerous boreholes. Boreholes used in the following discussion are shown in Figure 4.2.

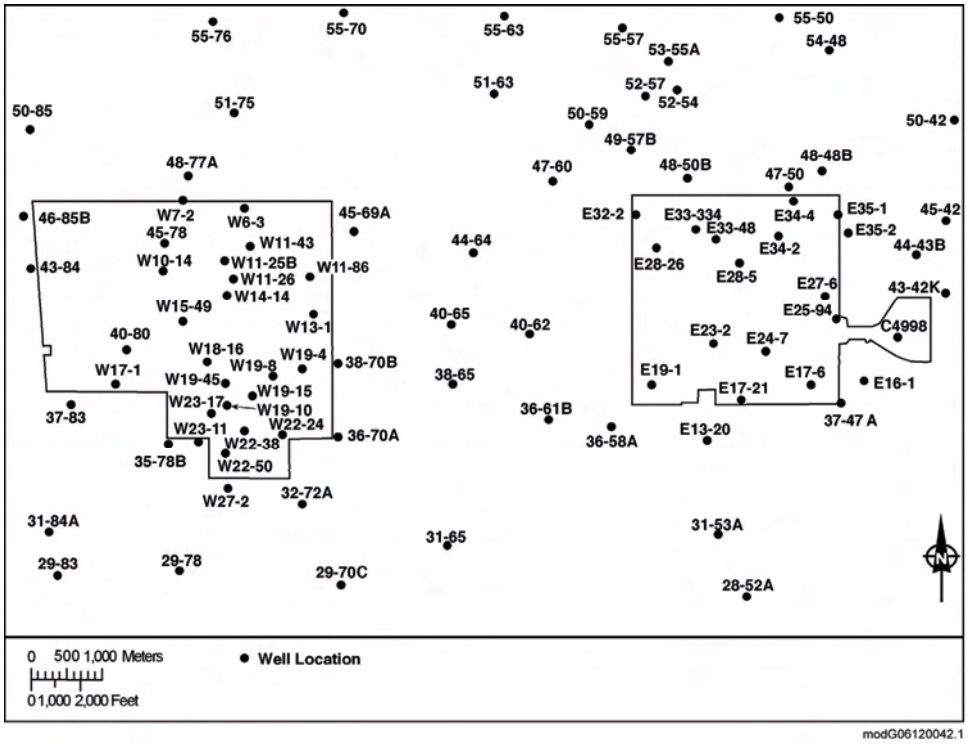

Figure 4.2. Borehole Location Map

Figure 4.3, a fence diagram of the Central Plateau area, depicts the geology above the CRBG. By necessity, Figure 4.3 is highly generalized, depicting the overall consistency of stratigraphy between the 200 East Area and 200 West Area. The major differences are in the thicknesses of the units in response to the geologic history. For example, the Hanford formation thickens to the east as the Ringold Formation thins. This variation is a response to the downcutting by the Columbia River after Ringold Formation time and then further erosion and filling of the erosional channels by Missoula Flood deposits.

4.3.1 Basalt

The uppermost basalt flow beneath the Central Plateau is the Elephant Mountain Member. The top of basalt surface dips to the southwest beneath 200 West Area and to the south-southwest beneath 200 East Area (Figure 4.4). Low-amplitude secondary folds such as the one to the northeast of 200 East Area may occur throughout the area and have probably not been fully identified. Between 200 East Area and Gable Gap to the north, the Elephant Mountain has been eroded to expose underlying basalt flows. There is also a suspected window eroded through the Elephant Mountain near the northeast corner of the 200 East Area.

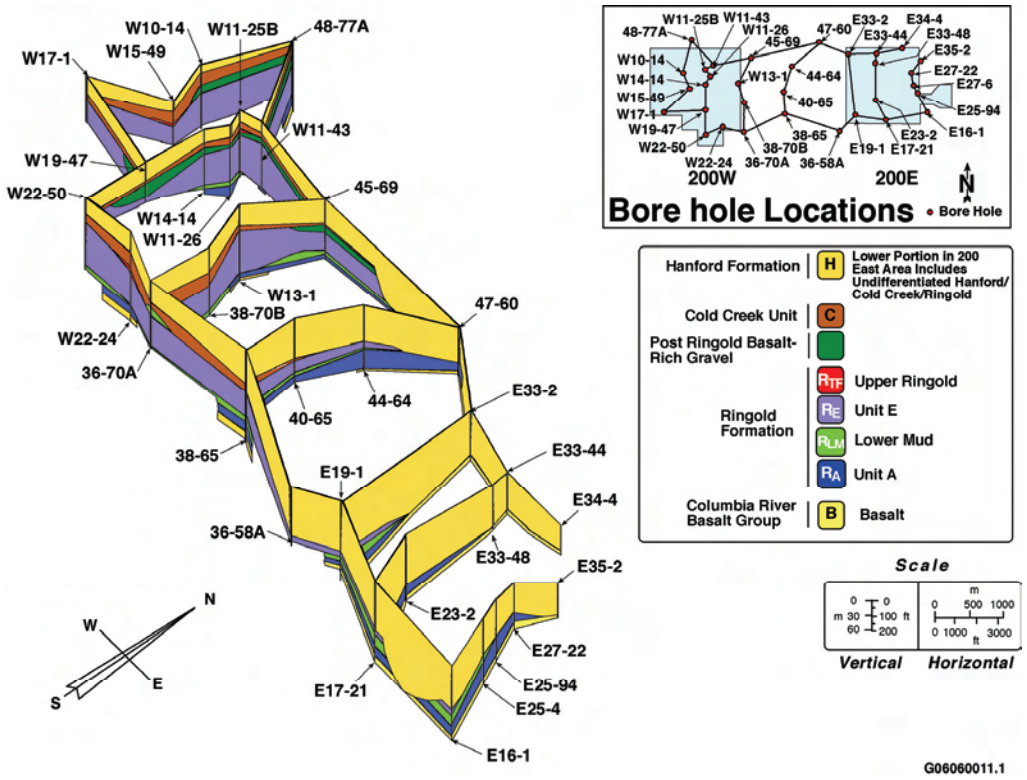

Figure 4.3. Fence Diagram of Sediment Overlying the Columbia River Basalt Group in the Central Plateau, Hanford Site

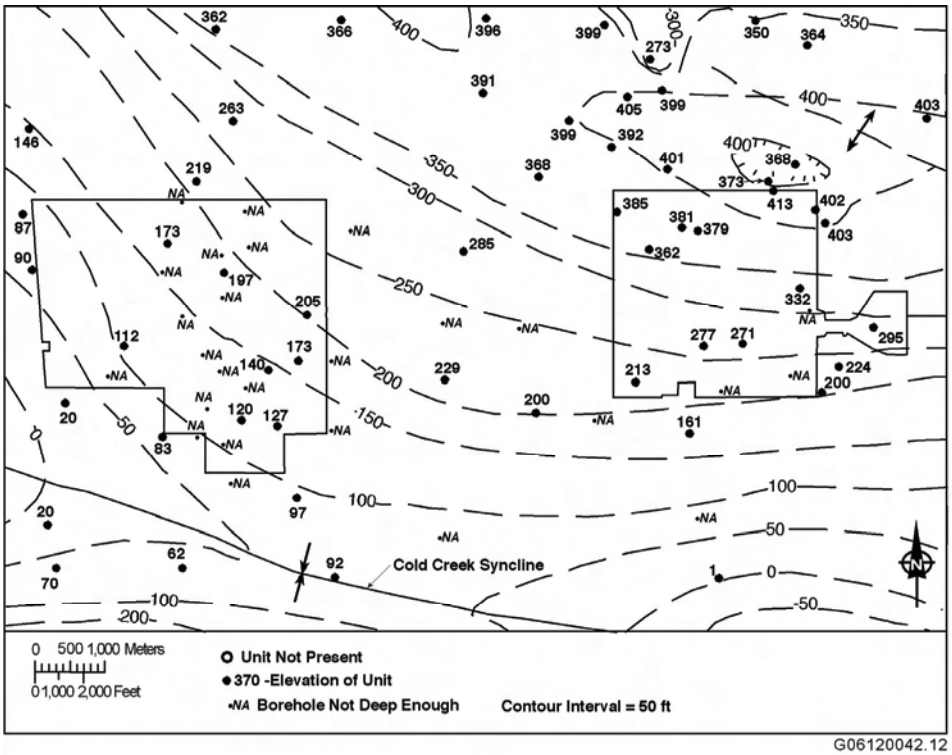

Figure 4.4. Structure Contour Map of the Top of Basalt

4.3.2 Ringold Formation

Although exposures of the Ringold Formation are limited to the White Bluffs on the east side of the Hanford Site and isolated exposures along the Rattlesnake Hills on the west side as well as the Smyrna and Taunton Benches within the Othello Basin, extensive data on the Ringold Formation are available from boreholes at the Hanford Site (e.g., Tallman et al. 1979; DOE 1988). The Ringold Formation at the Hanford Site is up to 185 m thick in the deepest part of the Cold Creek syncline south of the 200 West Area and 170 m thick in the western Wahluke syncline near the 100 B Area. The Ringold Formation pinches out against the Gable Mountain, Yakima Ridge, Saddle Mountains, and Rattlesnake Mountain anticlines. It is largely absent in the northern and northeastern parts of the 200 East Area.

The Ringold Formation consists of semi-indurated clay, silt, pedogenically altered sediment, fine- to coarse-grained sand, and granule to cobble gravel. Ringold Formation strata typically are below the water table on the Hanford Site, and the textural variations influence groundwater flow. The Ringold Formation historically has been divided into a variety of units, facies types, and cycles (Newcomb 1958; Newcomb et al. 1972; Tallman et al. 1979; DOE 1988; Lindsey 1995). However, these terminologies have proven to be of limited use because they are too generalized to account for significant local stratigraphic variation or they were defined in detail for relatively small areas and do not account for basin-wide stratigraphic variation (Lindsey 1991, 1995).

Studies of the Ringold Formation in the Pasco Basin indicate it contains significant stratigraphic variations (Lindsey 1991, 1995) that are best described on the basis of sediment facies. Sediment facies in the Ringold Formation, defined on the basis of lithology, stratification, and pedogenic alteration, include the following:

- The fluvial gravel facies consists of clast-supported granule to cobble gravels with a sandy matrix and intercalated sands and muds. Clast composition is variable but typically includes basalt, quartzite, porphyritic volcanics, and greenstone. Sands generally are quartzo-feldspathic, with less than 25% basalt content. Bedforms have low angle to planar stratification, massive bedding, wide shallow channels, and large-scale cross bedding. The facies was deposited in a gravelly fluvial braidplain characterized by wide, shallow, shifting channels.

- The fluvial sand facies consists of quartzo-feldspathic, cross-bedded and cross-laminated sands that are intercalated with lenticular silty sands, clays, and thin gravels. These sands usually contain <15% basalt lithic fragments, and fining upwards sequences are common. Strata comprising the association were deposited in wide, shallow channels.

- The overbank facies consists of laminated to massive silt, silty fine-grained sand, and paleosols containing variable amounts of pedogenic calcium carbonate. Overbank deposits occur as thin lenticular interbeds in the gravels and sands and as thick laterally continuous sequences. These sediments record deposition in proximal levee to more distal floodplain conditions.

- The lacustrine facies is characterized by plane-laminated to massive clay with thin silt and silty sand interbeds displaying some soft-sediment deformation. Deposits coarsen upwards. Strata were deposited in a lake under standing water to deltaic conditions.

- The alluvial fan facies is characterized by massive to crudely stratified, weathered to unweathered basaltic detritus. These deposits generally are found around the periphery of the basin and record deposition by debris flows in alluvial fan settings and in sidestreams draining into the Pasco Basin.

In the Pasco Basin, the lower half of the Ringold Formation, the member of Wooded Island, is the main unconfined aquifer under the Hanford Site and contains five separate stratigraphic intervals dominated by the fluvial gravels facies. These gravels, designated units A, B, C, D, and E (Figure 3.4, are separated by intervals containing deposits typical of the overbank and lacustrine facies (Lindsey 1991). In the 200 Areas, only fluvial gravel units A and E occur. Between these two gravel units in many places is the lowermost of the fine-grained sequences, designated the lower mud sequence. Fluvial gravel units A and E correspond to the lower basal and middle Ringold Formation units, respectively, as defined by DOE (1988). Gravel units B, C, and D do not correlate to any previously defined units (Lindsey 1991, 1995) and do not occur beneath the tank farms. The lower mud sequence corresponds to the upper basal unit and lower unit as defined by DOE (1988).

The following discussion of the geology of the Central Plateau is based on interpretations of new and old wells for this report (Table 4.1) as well as geologic picks from Williams et al. (2000, 2002) and Thorne et al. (1993). Well locations are shown in Figure 4.2. Specific lithologic descriptions and unit distributions are discussed in more detail in Chapter 5 for each tank farm.

Ringold unit A occurs throughout much of the Central Plateau and ranges from 0 to more than 30 m (0 to 100 ft) thick (Figure 4.5). This unit is thickest to the north and south of the 200 West Area. As can be seen in Figure 4.6, beneath 200 West Area the top of this gravel unit dips to the southwest into the Cold Creek Depression, while beneath the 200 East Area the unit dips to the south into the Cold Creek syncline except in the northern part where it has been eroded. The dip of this unit into the syncline indicates continued structural deformation during and after deposition of the sediments. Generally, unit A is a conglomerate with clasts of basalt and other lithologies in a silty sand matrix intercalated with beds of sand and silt. The sediments may be strongly cemented with silica or calcite in places.

The Ringold Formation lower mud unit has apparently had a more complex history than Unit A in the 200 Areas. As can be seen in Figure 4.7, the lower mud has been eroded from beneath most of the 200 East Area. There is also a poorly defined channel cut through the lower mud unit in the northeastern corner of the 200 West Area. Near 200 East Area, the top of the mud dips to the southeast into the Cold Creek syncline, indicating continuing structural deformation after deposition. In the 200 West Area, the surface of the lower mud unit reflects erosion more than structural deformation, with elevations decreasing in the southern and western parts of 200 West Area and then increasing above the Cold Creek Depression. The lower mud unit ranges in thickness from 0 to 30 m (0 to 103 ft). Thickness of the lower mud increases in the Cold Creek Depression (Figure 4.8), suggesting deformation during deposition of the fine-grained sediments. The lower mud is thickest beneath the 200 East Area and decrease to the south. Figure 4.8 shows a broad zone of decreased thickness bounded by the 50-ft contours that run southeast from the 200 West Area and may trace an old river channel from early in Ringold Formation unit E time. This unit consists primarily of lacustrine silt and clay, with at least one well-developed paleosol noted in the 200 West Area. It is an aquitard, separating the suprabasalt confined aquifer in unit A from the unconfined aquifer in unit E.

Table 4.1. Contact Elevations of Select Boreholes Used in This Report

Well No.	Hanford Well ID	Ground Surface Elevation ft	Contact Picks (Elevation in ft)												
			Top Uppermost Sand	Top Uppermost Gravel	Top Lower Sand	Top Lower Gravel	Top CCU Undiff.	Top CCU_u	Top CCU_l	Post Ringold Basalt-Rich Gravels	Top R_{tf}	Top R_{wie}	Top R_{lm}	Top R_{wia}	Top of Basalt
299-E16-1[a]	A4727	697	674	572	560	482	NP	NP	NP	NP	NP	422	362	298	224
299-E17-21[a]	B8500	735	730	NP	NP	447	NP	NP	NP	NP	NP	400	357	296	197
299-E19-1[a,d]	A5889	734	NP	734	716	479	NP	NP	NP	NP	NP	372	358	304	213
299-E23-2[f]	A4748	720	717	NP	NP	522	NP	NP	NP	NP	NP	NP	NP	352	277
299-E25-94	C4665	693	689	NP	NP	NP	421	421	NP	NP	NP	NP	NP	413	
299-E27-6	A6673	675	NP	674	575	NP	418	420	NP	NP	NP	NP	NP	409	332
299-E32-2	A4830	672	NP	672	592	482	NP	NP	NP	NP	NP	NP	NP	NP	385
299-E34-4	A4879	589	NP	589	NP	NP	NP	NP	NP	NP	NP	NP	NP	NP	413
299-E35-2	A4886	603	NP	603	NP	NP	NP	NP	NP	NP	NP	NP	NP	NP	403
299-W10-14[g]	A4891	701	701	626	NP	NP	586	586	566	564-501	NP	501			
299-W10-24	B8546	686	NP	683	644	627	603	588	558	558-496	NP	496			
299-W11-25B	C4669	688	NP	688	653	NP	597	597	588	564-556	NP	556	282		
299-W11-26	A7287	697	NP	697	632	NP	NP	609	586	549-527	NP	527	289	267	197
299-W11-39	C3117	689	NP	684	655	ND	601	601	589	554-529	NP	529			
299-W11-43	C4694	711	NP	711	684	NP	NP	617	608	591-552	NP	552	NP	299	
299-W11-48	C5243	685	NP	685	658	628	600	600	579	557-501	NP	501	283		
299-W11-86	C5101	731	731	724	666	NP	619	619	609	ND	NP	585	NP	313	240
299-W13-1[b]	C4238	731	NP	731	668	NP	NP	582	566	ND	NP	546	NP	304	205
299-W14-14	B8547	671	NP	671	638	NP	577	577	563	548-506	NP	506	269	233	
299-W15-49[e]	C4301	684	NP	684	655	620	NP	NP	604	NP	523	517	249		
299-W17-1[b]	C4237	651	NP	651	596	NP	NP	551	536	ND	NP	521			
299-W18-16[e]	C4303	682	682	664	632	NP	NP	587	542	532-447	NP	447			
299-W19-45	C3394	675	NP	675	623	NP	NP	542	538	521-450	NP	450			
299-W19-47	C4258	676	NP	668	629	NP	NP	552	538	531-438	NP	438			
299-W22-24[c]	A7845	694	684	654	644	NP	NP	552	509	ND	474	454	229	196	127
299-W22-46	A4977	668	668	607	598	NP	548	548	533	530-483	NP	483			
299-W22-50	B8814	670	656	611	607	NP	541	541	534	NP	NP	528	211	174	
299-W23-17	A7886	666	666	654	NP	NP	541	541	ND	520-484	NP	484			
699-36-58A	A8571	737	737	NP	NP	NP	NP	NP	NP	NP	NP	425			
699-36-70A[c]	A9901	706	706	NP	NP	NP	NP	559	528	486-451	NP	451	274		
699-37-47A[a]	B2822	717	NP	NP	NP	NP	NP	NP	NP	NP	432	407	352	278	200

Table 4.1. (contd)

Well No.	Hanford Well ID	Ground Surface Elevation ft	Contact Picks (Elevation in ft)												
			Top Uppermost Sand	Top Uppermost Gravel	Top Lower Sand	Top Lower Gravel	Top CCU Undiff.	Top CCU_u	Top CCU_l	Basalt-Rich Gravels	Top R_{tf}	Top R_{wie}	Top R_{lm}	Top R_{wia}	Top of Basalt
699-38-65[c]	A5148	755	755	NP	NP	NP	NP	514	NP	NP	NP	473	358	303	229
699-38-70B[b]	C4236	728	NP	721	NP	NP	NP	557	536	ND	NP	449	279	271	
699-40-62[a]	A5158	751	NP	748	711	NP	NP	NP	NP	NP	NP	438	377		
699-40-65[c]	C4235	756	NP	750	724	NP	NP	NP	484	NP	NP	477	391	323	
699-44-64[a]	A5188	727	NP	727	652	NP	NP	NP	NP	NP	NP	467	412	392	285
699-45-69A[c]	A5196	728	NP	726	NP	NP	558	NP	NP	550-503	NP	503	408	368	
699-47-60[a]	A5202	652	NP	652	604	585	NP	NP	NP	NP	NP	NP	NP	426	368
699-48-50B	C5196	609	NP	604	599	ND	ND	ND	ND	ND	ND	ND	ND	NP	400
699-48-77A[c]	A8772	676	NP	676	NP	NP	NP	NP	651	589-541	NP	541	NP	351	219

(a) Numbers below Hanford from Williams et al. 2000 (PNNL-12261).
(b) Numbers below Hanford from Martinez 2004 (WMP-21220).
(c) Numbers below Hanford from Williams et al. 2002 (PNNL-13858).
(d) Numbers from Reidel 2005 (PNNL-14586, Rev. 1).
(e) Numbers below Hanford from Weiss and Walker 2005 (WMP-26333).
(f) Numbers below Hanford from Reidel and Horton 1999 (PNNL-12257).
(g) Numbers below Hanford from Last et al. 1989 (PNL-6820).
NP = Unit not present.
ND = Not determined.

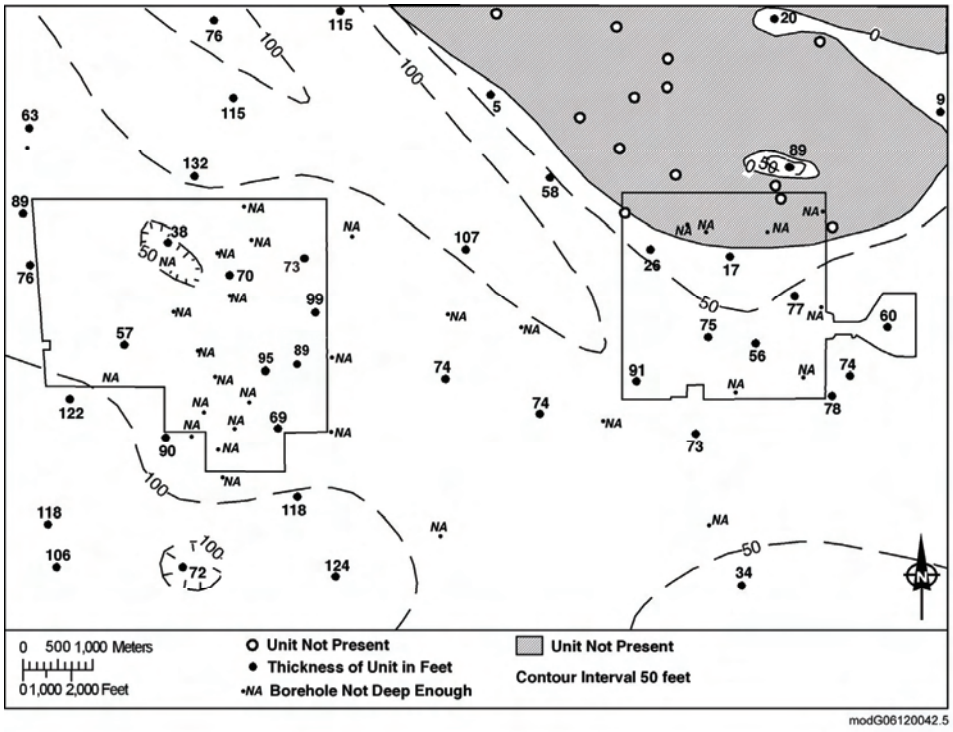

Figure 4.5. Isopach Map of Ringold Unit A

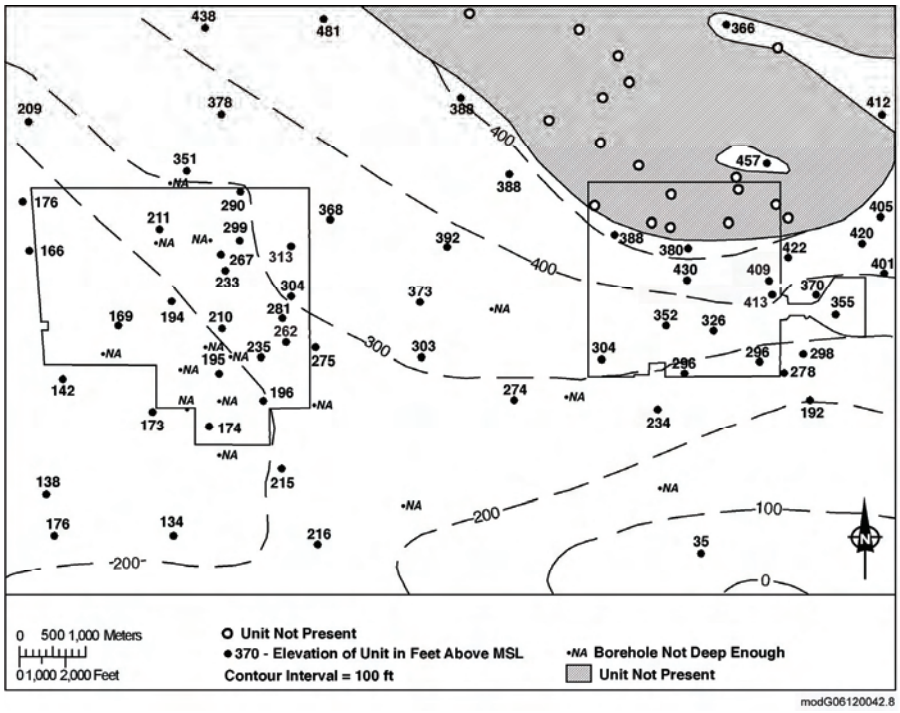

Figure 4.6. Structure Contour Map of Ringold Unit A

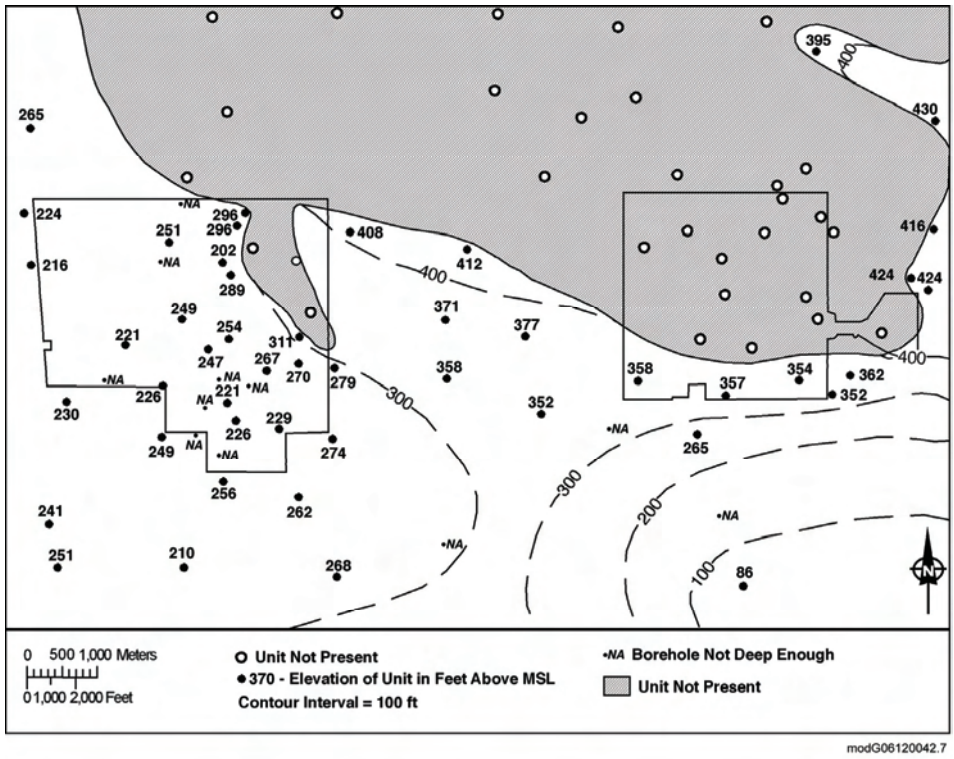

Figure 4.7. Structure Contour Map of Ringold Lower Mud Unit

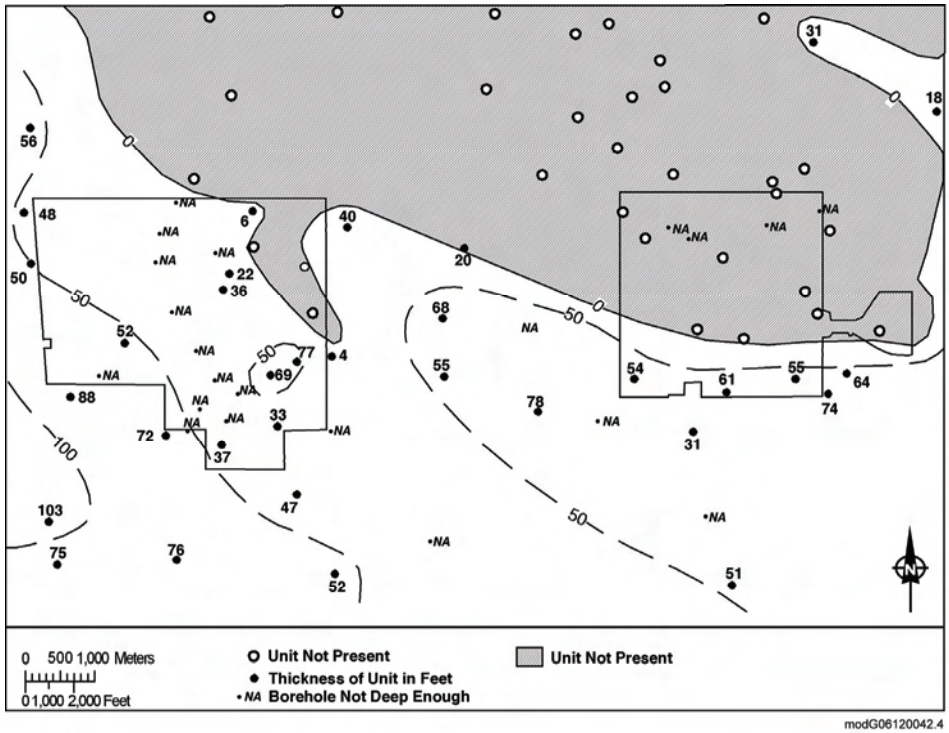

Figure 4.8. Isopach Map of Ringold Lower Mud Unit

Unit E of the member of Wooded Island is by far the thickest of the Ringold Formation units present in the Central Plateau. It consists of well-rounded gravel in a sand and silt matrix deposited by major rivers. Gravel lithologies are varied with sources outside the Columbia Basin. Cementation varies from well- to poorly indurated. Unit E ranges from 0 to more than 90 m (0 to 300 ft) in thickness (Figure 4.9). This variation in thickness is due in part to continued subsidence of the Cold Creek syncline and in part to erosion during the Cold Creek unit and Hanford formation times. Increasing thicknesses to the west of 200 West Area and to the south of 200 East Area are a combination of both processes. Main channels during both Cold Creek and Hanford floods went through Gable Gap and across the northeastern part of 200 East Area, removing unit E from most of that area and leaving a complicated surface in the 200 East Area (Figure 4.10).

In the Pasco Basin, the upper part of the Ringold Formation includes members of Taylor Flat and Savage Island (Lindsey 1995). The member of Taylor Flat consists of a sequence of fluvial sands and overbank deposits while the member of Savage Island consists of lacustrine sediments. The member of Savage Island is found only along the White Bluffs in the eastern Pasco Basin and corresponds to the upper Ringold Formation unit as originally defined by Newcomb (1958). In the 200 West Area, erosional remnants of the member of Taylor Flat consists of fine-grained fluvial sand and overbank facies with localized stringers of calcium carbonate. Member of Taylor Flat sediments are found beneath parts of the T, TX, and TY tank farms and in the vicinity of the U tank farm and are discussed in more detail in Chapter 5.

4.3.3 Pliocene to Pleistocene Transition

Two main alluvial units of the Pliocene to Pleistocene transition are recognized at the Hanford Site—the CCU and the pre-Missoula gravels. Recently, the pre-Missoula gravels were tentatively incorporated into the CCU (DOE-RL 2002); both units are discussed together here.

The laterally discontinuous CCU overlies the tilted and truncated Ringold Formation in an unconformable relationship in the western Cold Creek syncline in the vicinity of 200 West Area (DOE-RL 2002). To the east, the pre-Missoula gravels replace the calcrete and silt-dominated subunits of the CCU. The CCU appears to be correlative to other sidestream alluvial, eolian, and pedogenic deposits found near the base of the ridges bounding the Pasco Basin on the north, west, and south. These sedimentary deposits are inferred to have a late Pliocene to early Pleistocene age on the basis of stratigraphic position and magnetic polarity of interfingering loess units (DOE 1988). Figure 4.11 shows a structure contour map of the Cold Creek unit surface. Because of the difficulty in distinguishing the pre-Missoula gravels from the underlying Ringold and overlying Hanford formation sediments, the structure contour of the CCU does not extend into the 200 East Area. At a coarse scale, the surfaces of the Ringold Formation and the CCU in the 200 West Area (Figures 4.10 and 4.11) dip to the south. This surface also dips to the east between the 200 West and 200 East Areas. Local trends of the CCU are discussed in more detail for each of the tank farms in Section 5.

The CCU is important because its fine-grained sediments and/or its carbonate-rich paleosols can have a significant impact on contaminant movement in the vadose zone. Perched water zones above the CCU have been encountered in several wells in 200 West Area.

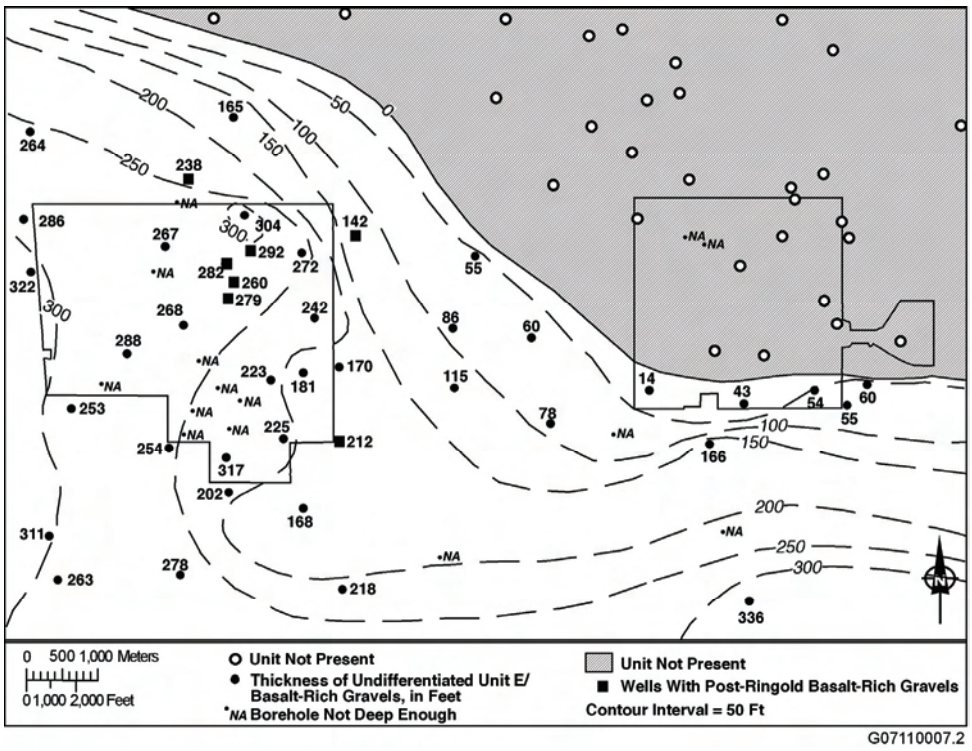

Figure 4.9. Isopach Map of Ringold Unit E

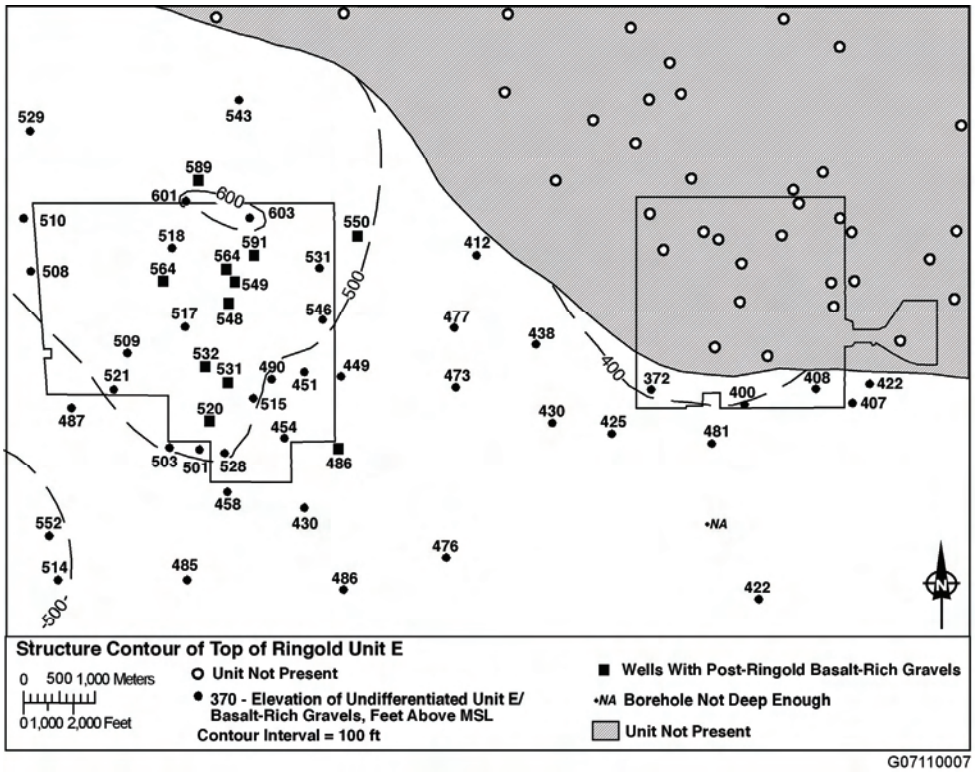

Figure 4.10. Structure Contour Map of Ringold Unit E

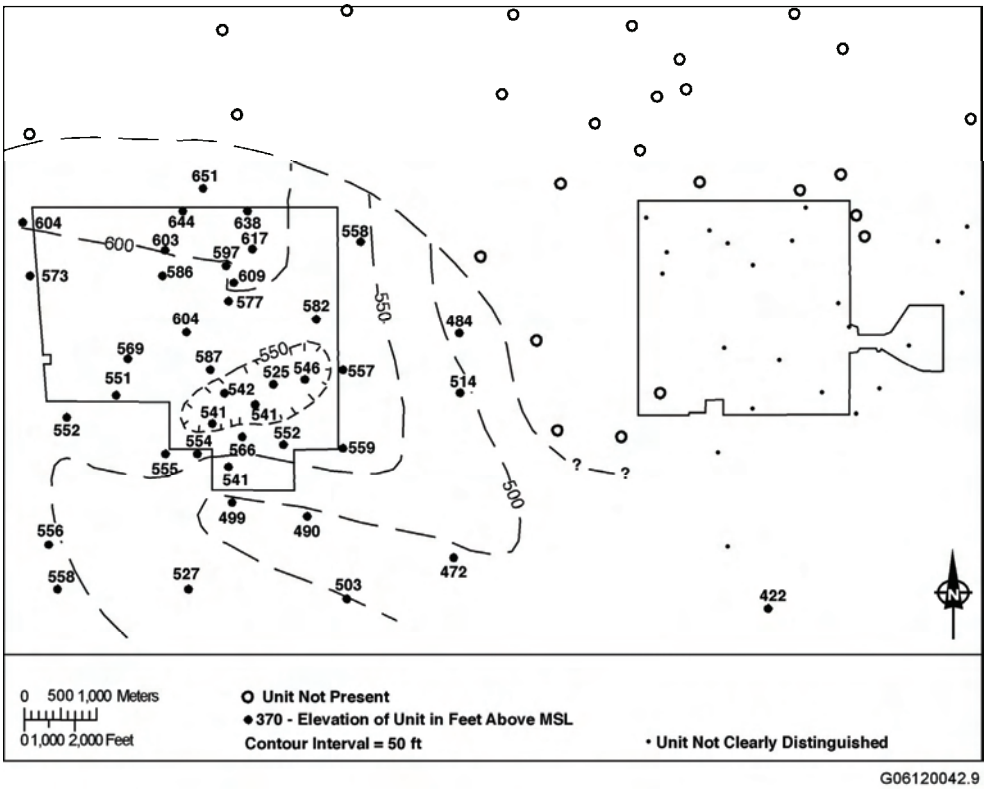

Figure 4.11. Structure Contour Map of Cold Creek Unit

4.3.3.1 Pre-Missoula Gravels – Central Pasco Basin

The Pre-Missoula gravels disconformably overlie the Ringold Formation in much of the central basin and may extend into areas in or near the 200 East Area. The nature of the contact between the pre-Missoula gravels and the overlying Hanford formation is not clear. In addition, it is unclear whether the pre-Missoula gravels overlie or interfinger with the CCU. In this report, we include the Pre-Missoula gravels in the Cold Creek unit because they overlie the Ringold Formation and underlie the Hanford formation, and thus are age-equivalent to the CCU. The gravel lying on basalt beneath much of the northern half of the 200 East Area has been variously interpreted as Ringold Formation unit A, as gravels deposited during Cold Creek time, or as part of the cataclysmic Hanford flood deposits that include some reworked Ringold. The difficulty in distinguishing between these units is reflected in the cross sections for the 200 East SST tank farms presented in Chapter 5.

4.3.3.2 Lower Cold Creek Unit Calcrete and Side-Stream Alluvium – 200 West Area

The lower Cold Creek unit (CCU_l) in the 200 West Area is a highly weathered paleosurface that developed unconformably on top of the Ringold Formation and side-stream alluvium. Other names used to describe this facies have included “caliche” (Brown 1959) and “calcrete” (DOE 1988). The CCU_l consist of basaltic to quartzitic gravels, sands, silt, and clay that are cemented with one or more layers of secondary, pedogenic calcium carbonate. Root traces and animal borrows, as well as other relict soil structures, point to a pedogenic origin for the calcium carbonate, although Slate (1996, 2000) also suggests the calcium carbonate could be associated with paleo groundwater levels. The concentration of calcium carbonate within the CCU_l is generally 20 to 30 wt% but can range from 5 to 70 wt%.

Considerable variability is found within the CCU_l because of natural heterogeneity inherent in soils and soil-forming processes, which vary under different physical, chemical, and biological conditions (e.g., moisture, grain size, aspect, mineralogy, bioturbation, microbial activity). An additional complicating factor is that the land surface during late Pliocene time was locally undergoing changes via fluvial and eolian activity, which resulted in variable rates of aggradation, degradation, and soil development (DOE 1988; Slate 1996, 2000; Wood et al. 2001). The calcium carbonate overprint is superimposed onto a variety of rock types, including silt, quartz-feldpsar-rich sand and gravel, and locally derived basaltic sand and gravel (Slate 1996, 2000; Lindsey et al. 2000).

Fluvial activity included local streams with sources in the nearby basalt ridges which continued to flow through the Cold Creek syncline and 200 West Area. These local side-streams to the Columbia River deposited basaltic gravels across their channels. Most of these side-stream deposits have been found in the ancestral Cold Creek drainage that ran more or less down the Cold Creek syncline (DOE 1988).

Recent review of old and new boreholes through the central portion of 200 West Area have identified gravels up to 26 m (85 ft) thick in a channel cut into Ringold unit E (Table 4.1, Post-Ringold basalt-rich gravels). Basalt content increases abruptly from 20-30% in Ringold Formation gravels to about 50% in the basalt-rich gravels and generally continues to increase toward the top of the unit. In wells 299-W11-25B, 299-W11-39, 299-W14-14, and 699-48-77B, the basalt-rich gravel has been interpreted as lying within or below member of Taylor Flat sediments while in other boreholes it underlies the CCU_l paleosol. The high basalt content is not typical of the Ringold Formation across the Hanford Site. Information is insufficient to determine what this basalt facies represents other than it is probably a sediment of the Cold Creek unit. Because the identification of this unit is based on sparse data, this unit is undifferentiated from Unit E on all maps and figures in this report except Figure 4.3. It is interesting to note that the surface of the undifferentiated sediments forms a fairly smooth consistent contour map, as if both units were later eroded prior to CCU deposition. The contacts for the wells where the Post-Ringold basalt-rich gravels have been identified and shown in Figure 4.3 are given in Table 4.1. More work is needed to determine whether this unit is part of the CCU or Ringold Unit E.

The upper boundary of the CCU_l is usually sharp and distinct in contrast to the lower boundary, which is commonly gradational and overprinted onto the underlying Ringold Formation within the west-central Pasco Basin. The top of the CCU_l is well defined by 1) a contrast in color, 2) an increase in calcium carbonate content and decrease in mud content and sorting, and 3) a sudden drop in total gamma activity (i.e., potassium-40) on borehole geophysical logs (Bjornstad 1990; DOE-GJO 1997). In this data package, the top of the CCU_l is defined as the top of the first pedogenically altered, carbonate-rich, cemented zone accompanied by a sudden drop in natural gamma activity.

The CCU_1 subunit plays a major role in movement of water through the vadose zone in the 200 West Area. The calcrete forms an impermeable barrier in places, causing lateral movement of water from liquid waste disposal sites.

4.3.3.3 Upper Cold Creek Unit Silt-Dominated – 200 West Area

A distinctive silt-rich interval, referred to as the silt-dominated facies of the CCU (DOE-RL 2002) and as Hanford formation/Cold Creek unit (Hf/CCU) deposits, overlies the CCU calcrete facies over most of the 200 West Area (Brown 1960; Tallman et al. 1979; DOE 1988). Recent investigators have included

the “early Palouse soil” (Hanford formation/Plio-Pleistocene deposits) as a subunit of the CCU (Lindsey et al. 1994). Unlike the lower boundary of these strata, which is easily differentiated from the underlying Cold Creek calcrete, the upper contact with the overlying Hanford formation can be difficult to identify in well cuttings. The age of the silt-dominated deposits is bracketed by the Pliocene CCU calcrete (3.4 Ma) and the well-established overlying Missoula flood deposits of the Hanford formation (Pleistocene Epoch). This report will refer to these silt-dominated sediments as the CCU silt-dominated facies (upper Cold Creek unit [Cold Creek fine-grained unit] [$CCU_{u.}$]). Because the upper portion of these deposits may appear similar to or grade upward into the Hanford formation, this interval is referred to in places as undifferentiated Hf/CCU deposits.

Historically, these silt-dominated deposits have been described as a massive, unconsolidated, micaceous, brown to yellow, loess-like silt and minor fine-grained sand (Price and Fecht 1976g; Price and Fecht 1976h; Price and Fecht 1976i; Tallman et al. 1981; DOE 1988; Last et al. 1989; DOE-RL 1993). Brown (1959) originally reported this well-sorted, buff-colored, eolian unit to be up to 21 m (70 ft) thick in the southern portion of the 200 West Area.

More recent investigations have shown that the silt-dominated deposits may contain facies other than eolian silt and fine sand (Lindsey et al. 1994, 2000; Slate 1996). For example, at WMA S-SX, these deposits are composed of mostly intercalated layers of fine sand and silt, more characteristic of alluvial deposits (Lindsey et al. 2000). It appears then that this interval may consist of a mixture of fine-grained deposits under both eolian and alluvial conditions. Regardless of its exact stratigraphic relationship and origin, the silt-dominated sediments are a distinctive lithostratigraphic unit that significantly influences the moisture and contaminant distribution within the vadose zone.

The silt-dominated deposits can be correlated across most of the 200 West Area using fine-grained texture and high natural gamma activity on geophysical logs (DOE 1988; Last et al. 1989). These deposits generally are absent away from the 200 West Area. The top of the silt-dominated interval is identified based on an increase in background gamma activity on geophysical logs (DOE-GJO 1997) and an increase in mud content (up to 75 wt%). Calcium carbonate content often is a few weight percent more than the overlying fine-grained Hanford formation (referred to as the H2 unit by Lindsey [2001a]), and usually is significantly less than that for the underlying pedogenic calcrete facies of the Plio-Pleistocene unit. The basal contact is distinct, indicated by a sharp drop in total gamma activity below and percentage of mud content. Also, compared to the pedogenically altered and cemented Cold Creek unit calcrete, the silt-dominated deposits are relatively loose and friable. Whereas the Hanford formation/ Plio-Pleistocene interval often contains moderate to high concentrations of calcium carbonate, it appears to be evenly disseminated and therefore probably is of detrital origin (Wood et al. 2001).

4.3.3.4 Cold Creek Unit – 200 East Area

The CCU as described above is largely absent from the 200 East Area. The exact origin of the sedimentary deposits overlying the CRBG and underlying the Hanford formation is uncertain and still open to interpretation. These deposits beneath the Hanford formation have been called the Hf/CCU (undifferentiated Hanford/Cold Creek) (Wood et al. 2000) and undifferentiated Hanford formation/Cold Creek unit/Ringold Formation unit (Hf/CCU/RF) (Lindsey et al. 2001b). In this data package, they are placed in the CCU or lower Hanford gravel/CCU undifferentiated because they represent sediments

deposited between the late Pliocene and early Pleistocene. This is the age range of the CCU in the 200 West Area. By assigning these deposits to this unit, only the age is implied, not the origin of the deposits.

Wood et al. (2000) recognized two facies of the Hf/CCU beneath the 200 East Area tank farms: a fine-grained eolian/overbank silt (silt facies Cold Creek unit), up to 10 m thick, and a sandy gravel to gravelly sand facies Cold Creek unit. The thick, silt-rich interval is believed to be a pre-Pleistocene flood fluvial deposit because silty layers associated with Ice Age flood deposits of the Hanford formation in this area are generally much thinner (i.e., a few centimeters or less) (Wood et al. 2000). Where the silt unit is absent, the gravel sequence below the silt unit is indistinguishable from similar-appearing facies of the overlying Hanford formation (Wood et al. 2000). If the thick silt layer predates the Hanford formation, however, then the underlying gravels also must predate the Hanford formation. Thus, the gravel sequence beneath the silt layer must belong to either a mainstream alluvial facies of the ancestral Columbia River (pre-Missoula gravels) or the Ringold Formation.

4.3.4 Quaternary Stratigraphy of the Pasco Basin

Quaternary sediments, as much as 100 m thick within the Pasco Basin, overlie the Ringold Formation and/or CCU at the tank farms. The most extensive of these is the Pleistocene-aged Hanford formation (Figure 3.4), but the sediments also include eolian deposits and recent alluvium.

4.3.4.1 Eolian Deposits

Loess deposits at the Hanford Site contain a detailed Quaternary record; five units are represented within the Pasco Basin (Reidel et al. 1992). These units are informally referred to as L1 through L5 and differentiated on the basis of 1) position relative to other stratigraphic units, 2) color, 3) soil development, and 4) paleomagnetic polarity. They are discussed in more detail in Section 6.

4.3.4.2 Hanford Formation

The Hanford formation is the main stratigraphic unit at the surface of the tank farms. The Hanford formation consists of pebble to boulder gravel, fine- to coarse-grained sand, and silt. These deposits are divided into three facies: 1) gravel-dominated, 2) sand-dominated, and 3) sand- and silt-dominated. These facies are referred to as coarse-grained deposits, plane-laminated sand facies, and rhythmite facies, respectively, in DOE (1988). The rhythmites also are referred to as the Touchet Beds. The Hanford formation is thickest beneath the Cold Creek bar, particularly in the vicinity of the 200 East Area, where it is over 100 m thick (Figure 4.12).

The gravel-dominated facies association generally consists of coarse-grained basaltic sand and granule to boulder gravel. These deposits display massive bedding, plane to low-angle bedding, and large-scale planar cross-bedding in outcrop. The gravel facies dominates the Hanford formation in the 100 Areas north of Gable Mountain, the northern part of the 200 East and West Areas, and the eastern part of the Hanford Site including the 300 Area. The gravel-dominated facies was deposited by high-energy flood waters in or immediately adjacent to the main cataclysmic flood channelways.

The sand-dominated facies association consists of fine- to coarse-grained sand and granule gravel displaying plane lamination and bedding and, less commonly, plane bedding and channel-fill sequences in

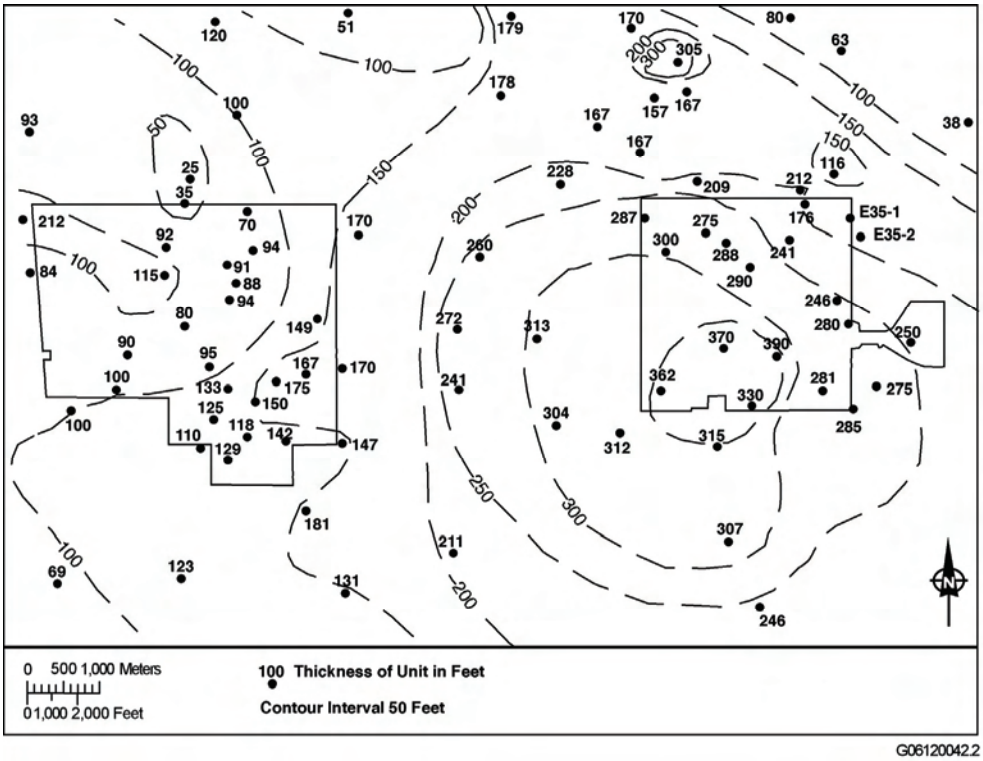

Figure 4.12. Isopach Map of Hanford Formation

outcrop. These sands may contain small pebbles and rip up clasts in addition to pebble-gravel interbeds and silty interbeds less than 1 m thick. The silt content of these sands is variable. These sands typically are basaltic, commonly being referred to as black, gray, or salt-and-pepper sands. This facies is most common in the central Cold Creek Syncline, in the central to southern parts of the 200 East and 200 West Areas. The laminated sand facies was deposited adjacent to main flood channelways during the waning stages of flooding. The facies is transitional between the gravel-dominated facies and the rhythmite facies.

The interbedded sand- and silt-dominated facies association consists of thinly bedded, plane-laminated and ripple cross-laminated silt and fine- to coarse-grained sand that commonly display normally graded rhythmites a few centimeters to several tens of centimeters thick (Myers et al. 1979; DOE 1988; DOE-RL 2002). This facies is found throughout the central, southern, and western Cold Creek syncline within and south of the 200 East and 200 West Areas. These sediments were deposited under slackwater conditions and in back-flooded areas (DOE 1988).

Cataclysmic floods inundated the Pasco Basin several times during the Pleistocene when ice dams failed in northern Washington and Idaho. Net erosion by these floods was minimal and probably associated with only the earliest floods; later floods only partially incised into older flood deposits before backfilling. The Hanford formation usually is divided into units based on facies association (e.g., H1, H2, and H3 of Lindsey [1995]). However, it is difficult to correlate between these units for any distance because no characteristics have been identified that can be used to distinguish layers if the facies are the same. Because of the difficulty in correlating a specific layer in the Hanford formation across a larger area, the discussion in this section does not distinguish units within the Hanford formation.

Recent work on subdividing the Missoula flood deposits at the Hanford Site has shown that paleomagnetic polarity is a useful technique (Pluhar 2003; Pluhar et al. 2006). In a detailed study at the 200 East Area, four magnetic polarity reversals were recognized (Figure 4.13). These reversals were equated to the Brunhes normal subchron (present to 780,000 years BP) and the Matuyama reversal subchron (780,000 to 1.76 Ma). The Matuyama reversal has a normal excursion at 1 Ma, which Pluhar attributed to the normally magnetized sediments between the upper and lower reversal. The age of the lowest reversal is constrained by the lower limit of 1.76 Ma of the Matuyama subchron.

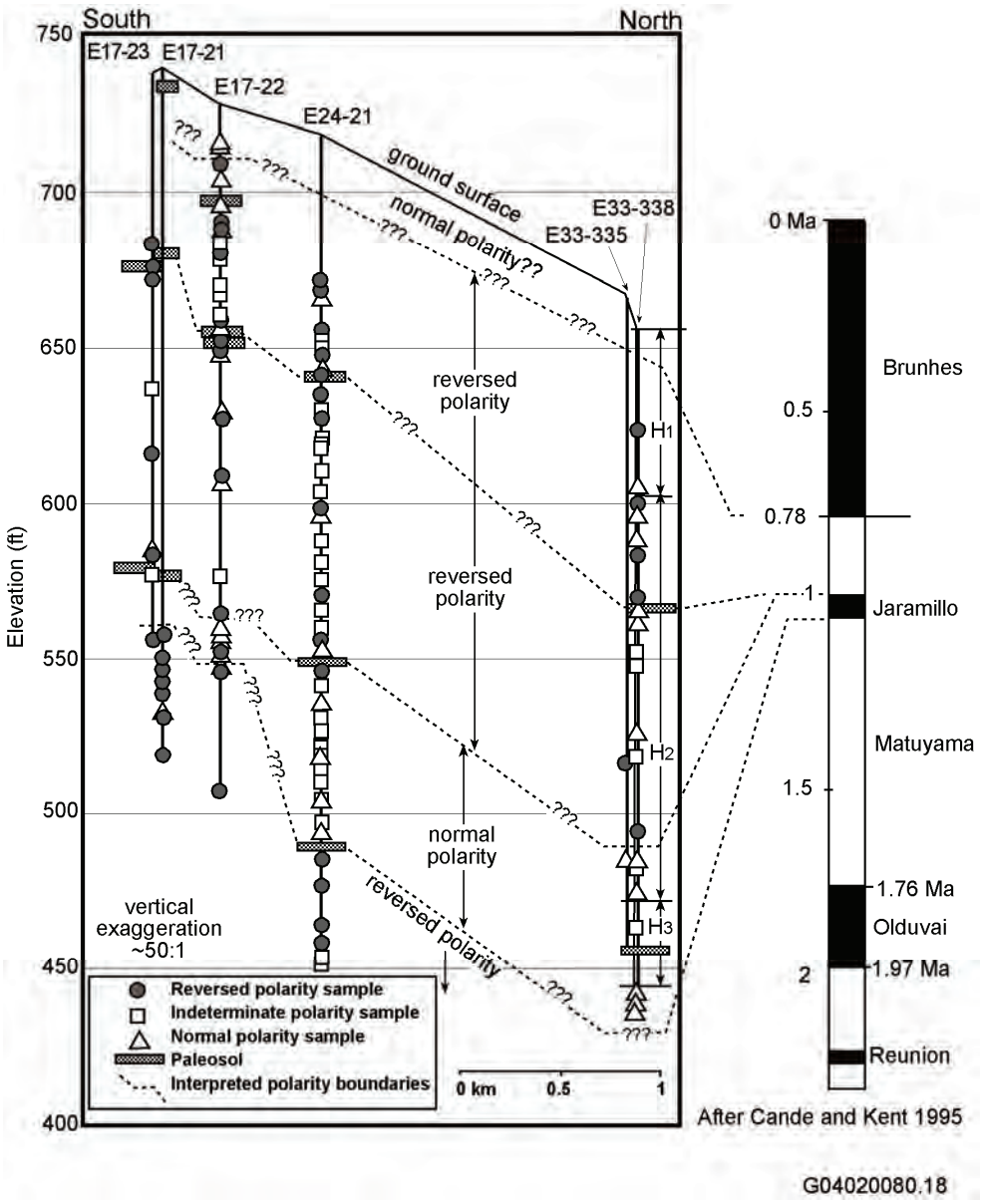

Figure 4.13. Stratigraphic Correlations in the 200 East Area Based on Stratigraphy and Magnetic Polarity (Pluhar et al. 2006)

In the 200 West Area, mainly normally polarized sediments were found with two possible reversed horizons. Pluhar et al. (2006) interpreted the Hanford formation at the 200 West Area as being deposited during the Brunhes normal subchron (present to 780,000 years BP) and the two possible reversals as short magnetic excursions during the Brunhes subchron.

The results of the Pluhar et al. (2006) study suggest that the Hanford formation sediments at the 200 East Area are older than those in the 200 West Area. This further implies that the Hanford subdivisions—upper coarse-dominated (H1), sand-dominated (H2), and lower coarse-dominated (H3) (Lindsey 1995)—are not the same flooding event in both areas and, thus, cannot be correlated across the Cold Creek bar.

4.3.5 Clastic Dikes

Clastic dikes are vertical to subvertical sedimentary structures that crosscut normal sedimentary layering and could locally affect the vertical and horizontal movement of water and contaminants. Clastic dikes are a common geologic feature of Pleistocene flood deposits of the Hanford formation, although they also have been found in the underlying Ringold Formation and in CRBG and intercalated sedimentary interbeds. Clastic dikes on the Hanford Site have been described in detail in Fecht et al. (1999).

Clastic dikes typically occur in swarms and occur as regularly shaped polygonal patterns, irregularly shaped polygonal patterns, pre-existing fissure fillings, and random occurrences. Regular polygonal networks resemble four- to eight-sided polygons. Dikes in irregularly shaped polygon networks generally are crosscutting in both plane and cross section, resulting in extensive segmentation of the dikes. Clastic dikes often occur in zones of pre-existing weakness.

Clastic dikes typically show a wide range in width, depth, and length. They are especially notable within the sand- and silt-dominated facies of the Hanford formation. The vertical extent of clastic dikes has been observed to range from 30 cm to greater than 55 m (~1 to 180 ft), while width ranges from about 1 mm to greater than 2 m (0.04 in. to more than 6.6 ft).

In general, a clastic dike is composed of an outer skin of clay with coarser infilling material. Clay linings are commonly 0.03 mm to 1.0 mm (0.012 in. to 0.039 in.) thick, but linings up to about 10 mm are known. The clay skins may have a great influence on transport both within and adjacent to the clastic dikes. The width of individual infilling layers ranges from as little as 0.01 mm (0.0039 in.) to more than 30 cm (11.8 in.), and their length can vary from about 0.2 m (0.66 ft) to more than 20 m (65.6 ft). Infilling sediments are typically poorly to well-sorted sand but may contain clay, silt, and gravel.

Clastic dikes have been reported at several of the SST waste management areas (WMAs). Price and Fecht (1976g, 1976h) stated that clastic dikes were detected in the S and SX tank farms but could not be mapped. Clastic dikes (and/or polygonally patterned ground often associated with clastic dikes) have also been observed at a number of locations surrounding the 200 West Area SST farms, including the SY tank farm to the north, the Environmental Restoration and Disposal Facility to the east, and throughout Cold Creek Valley to the south and west (including the former 216-S-16 pond). Tallman et al. (1979) indicated that identification of clastic dikes in the 200 West Area also was based on examination of cable-tool drilling samples. Horton and Johnson (2000) reported that possible clastic dikes had been encountered by at least two *Resource Conservation and Recovery Act of 1976* (RCRA) groundwater monitoring wells south of the SX tank farm (i.e., 299-W22-48 and 299-W22-50). Lindsey et al. (2000) also noted a few

structures suggestive of clay skins on clastic dikes in splitspoon samples from well 299-W22-50. Clastic dikes have been found also in the 200 East Area at the Integrated Disposal Facility and the Waste Treatment and Immobilization Plant.

Some clastic dikes were noted during excavation of the T, TX, and TY tank farms (Price and Fecht 1976i, 1976j, 1976k), and clastic dikes were previously reported for two boreholes (299-W15-134 and 299-W15-180) within the TX tank farm (Wood et al. 2001). Borehole C3381 intersected a dike in the Hanford formation H2 unit; borehole 299-W10-27 appears to have intersected two dikes, one in the Hanford formation H2 unit and another in the R_{tf}.

Clastic dikes are present in all SST WMAs but actual locations were not mapped when the tank farms were constructed. To estimate the potential intersections, Johnson et al. (1999) created a plausible hypothetical network of clastic dikes for the S and SX tank farms (Figure 4.14) based on polygonally patterned ground mapped between Army Loop Road and State Highway 240 and scaled based on the best cell size estimate from Fecht et al. (1999).

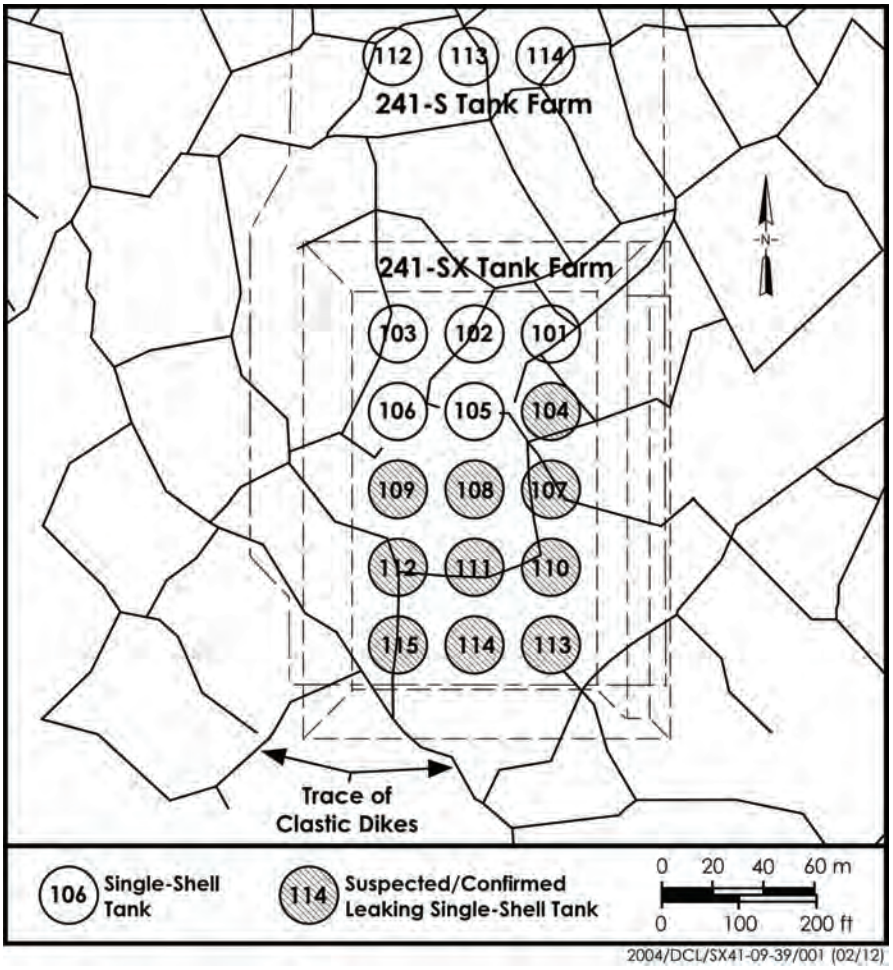

Figure 4.14. Hypothetical Projection of Clastic Dikes into the S and SX Tank Farms. These are not actual dikes but an example of how they might occur.

4.3.6 Volcanic Ash Deposits

Volcanism in the Cascade Range has been active throughout the Pleistocene Epoch (approximately 2 million years before present [BP] to 10,000 years BP), and throughout the Holocene Epoch (10,000 years BP to present). The eruption history of the Holocene best characterizes the most likely types of activity in the next 100 years. Many volcanoes have been active in the last 10,000 years, including Mount Mazama (Crater Lake) and Mount Hood in Oregon, and Mount St. Helens, Mount Adams, Mount Baker, and Mount Rainier in Washington. The Quaternary sediments recorded these eruptions in the form of ash deposits that are interlayered with the sediments.

4.3.7 Surface Soil

Hajek (1966) lists and describes 15 different soil types on the Hanford Site, varying from sand to silty and sandy loam. The 200 East Area consists of the Burbank Loamy Sand, the Ephrata Sandy Loam, and the Rupert Sand. The Rupert Sand has now been reclassified as the Quincy Sand (Neitzel et al. 1996). The 200 West Area consists of the Quincy Sand and the Burbank Loamy Sand. The SST WMAs in the 200 East Area are developed in the Burbank Loamy Sand and the Ephrata Sandy Loam. The SST WMAs in the 200 West Area are developed mainly in the Quincy Sand.

The Burbank Loamy Sand is dark-colored, coarse-textured soil underlain by gravel. The surface soil is usually about 40 cm (16 in.) thick but can be 76 cm (30 in.) thick. The gravel content of the subsoil ranges from 20 to 80%. The surface of the Ephrata Sandy Loam is dark–colored, and the subsoil is dark grayish-brown, medium-textured soil underlain by gravelly material, which may continue for many feet. The Quincy Sand (formerly Rupert Sand) is brown to grayish-brown coarse sand grading to dark grayish-brown at about 90 cm (35 in.). Quincy Sand developed under grass, sagebrush, and hopsage in coarse sandy alluvial deposits that were mantled by windblown sand.

Soil horizons have been disturbed or removed over much of the surface within the 200 East and West Area boundaries. It can still be found in undisturbed areas within and between these areas.

5.0 Geology of the Single-Shell Tank Farms

SST farms S, SX, T, TX, TY, and U are located in the 200 West Area; SST farms A, AX, B, BX, BY, and C are located in the 200 East Area (Figure 5.1). This chapter describes the geology of those tank farms.

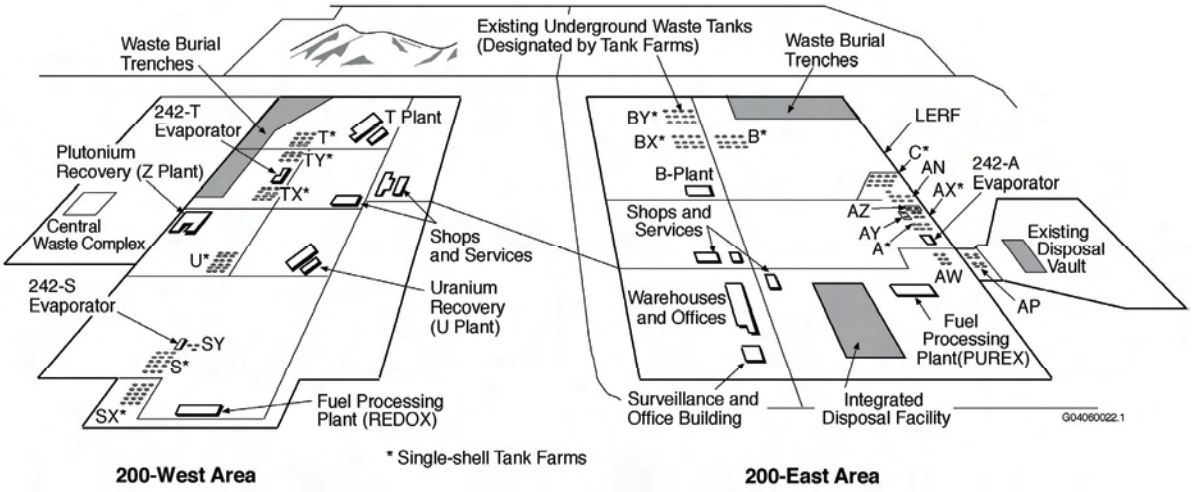

Figure 5.1. Activities in the 200 Areas

5.1 Source of Data

Data used in this compilation were obtained from published reports, unpublished data on surface geologic studies, and from borehole data. Some figures are directly from various published reports, leading to a mixture of English and metric units. Where possible, both units are shown, but this was not possible in all cases.

The surface geology and geomorphology of the Hanford Site has been mapped and published in (Reidel and Fecht 1994a, 1994b). The principal geologic units exposed at the surface are fluvial and eolian sands and backfill (Reidel and Fecht 1994a, 1994b).

Subsurface information comes from borehole data consisting of drilling logs, archived samples, and geophysical logs. These are the principal data sets used to interpret the subsurface at the SST farms. In addition, numerous reports describing the geology of the area and vicinity are available and are a valuable source of information (e.g., Tallman et al. 1979; DOE 1988; Connelly et al. 1992a; Williams et al. 2000, 2002). Older geophysical logs include some logs from surrounding waste disposal sites obtained prior to discharge of effluent and provide an additional source of information for stratigraphic correlations.

Particle size distribution and calcium carbonate content information are available for some boreholes from the ROCSAN database and studies on the Integrated Disposal Facility well samples. The ROCSAN database, created by Rockwell Hanford Operations, contains particle size distribution data. New data are no longer added but the database is available through the Virtual Library maintained by Fluor Hanford. ROCSAN data were considered only for those samples collected by drive barrel because hard-tool drilling pulverizes the sediments so that results are not representative of actual particle size distribution. Other methods of drilling were rarely used during the period ROCSAN was being updated.

Calcium carbonate and moisture contents are available for some boreholes. Available data are in the borehole packages on file at PNNL and in various reports. The data were obtained from discrete samples collected by the borehole geologist during drilling. The moisture data were used to supplement the geologist's log and the gross gamma-ray log in determining lithologic variations. For obvious reasons, moisture data are valuable for only those samples collected above the water table.

Gross gamma-ray logs and neutron moisture logs exist for many of the boreholes used for Chapter 3 of the SST performance assessment (DOE-ORP 2006). These logs were used in the interpretation of the geology at the SST farms.

Finally, drill cuttings are available from most of the boreholes used for the ROCSAN database and the information in Chapter 3 of the SST performance assessment (DOE-ORP 2006). The same precautions pertaining to the ROCSAN data pertain to the physical samples. That is, drill cuttings obtained from hard tool drilling methods will yield an unrepresentative particle size distribution; lithologies, however, remain unchanged. All available physical samples are on file in the Hanford Geotechnical Sample Library currently under custody of Fluor Hanford.

5.2 Uncertainty in Stratigraphic Interpretations

The principal source of uncertainty for the lateral continuity of the layers and thickness of the beds is borehole data. Surface mapping is well controlled at the Hanford Site and has been done by geologists with extensive mapping experience at the Hanford Site and in the Columbia Basin. The quality of subsurface data is related to the drilling technique, the logging of the borehole, and the sample collection. Subtle differences between some stratigraphic units such as silty sandy layers of the Hanford formation and units of the underlying Ringold Formation (e.g., upper Ringold and intercalated silty units) make identification of the contact difficult. The quality of the drillers' and geologists' logs, archived samples, and use of geophysical logs becomes crucial to reducing this type of uncertainty.

In addition to the uncertainty in borehole data, there is uncertainty in the geometric shape of the sediment body. Because of the nature of the cataclysmic flooding that produced the Hanford formation, very few analogs are available for comparison to the Hanford Site. Borrow pits in the Pasco Basin and excavations at the Hanford Site provide a glimpse into the geometric shape of a sediment body, but often the nature of the sediment body must be interpreted from boreholes.

5.2.1 Uncertainty Due to Drilling Techniques and Logging

Most boreholes at the Hanford Site have been drilled using cable-tool techniques and, less often, air rotary techniques. Newer boreholes now are drilled using the Becker-Hammer technique that allows high-quality core samples to be recovered. The principal source of uncertainty here is in the depth and thickness of the sedimentary beds due to straightness of the boreholes, which have not been surveyed for straightness. However, this is deemed to be minor because most boreholes have been shown to have only minor deviations when the groundwater pumps and risers were installed.

Cable-tool drilling has been the standard technique from earliest drilling at the Hanford Site because drive-barrel drilling can be done without adding water and cuttings are easy to contain. The borehole advances by use of drive barrel or hard tool and driven temporary casing. Hard-tool drilling routinely requires added water in the vadose zone. The technique generally provides acceptable sample control and has proven successful. More recently, in uncontaminated areas, air rotary has been the preferred technique.

There are several disadvantages to cable-tool drilling:

- Samples can be difficult to retain in the drive barrel, especially samples from very dry zones.
- Gravels are not easily retrieved because they are not easily retained in the drive barrel.
- Cemented units or large gravels must be drilled with a "hard tool," which breaks up the sample and alters the grain-size distribution of samples.
- Water added during hard-tool use in a cable tool invalidates moisture logs.

The disadvantages to air rotary drilling are as follows:

- Samples can be difficult to retrieve. The quantity of sample is often related to the air pressure used.
- Low pressures in the air line can result in excessive grinding of particles by bits; thus, the sample may not be representative of the sediment body.

Most boreholes prior to the 1980s were drilled without a well-site geologist present to log the samples. Thus, the only records of early drilling are drillers' logs that vary in the quality of the sample description. Drillers' logs are extremely inconsistent because a driller's attention is focused on operating the rig and not on describing the samples. The quality of the geologists' logs also varies from borehole to borehole. For example, a geologist new to the site will recognize the major sediment changes in drill cuttings but may not recognize the subtler changes that also represent changes in stratigraphy.

Many boreholes at the Hanford Site were completed without the benefit of being geophysically logged. Geophysical logging can be an important tool for determining the depth of lithologic changes. Geophysical logs show subtle lithology differences stemming from differing amounts of natural gamma-ray emitters (most commonly potassium-40). Gamma-ray response typically is proportional to clay and silt abundance and can provide information on changes in grain size. When geophysical logs are used along with the well-site geologists' logs and archived samples, the uncertainty in the depth of lithologic changes is reduced.

5.2.2 Uncertainty Due to Borehole Coverage

Borehole coverage is usually dictated by factors other than addressing a geologic problem. Therefore, the coverage of boreholes is generally inadequate to address many geologic problems. For the Hanford Site 200 Areas, borehole coverage is good because characterization studies for various projects were conducted and because of the installation of groundwater wells.

5.2.3 Uncertainty Due to Sampling

Sample retrieval is often difficult, and sample quantities are limited. Vadose zone drilling is difficult for sample recovery because the samples are typically dry and not easily retained in the drive barrel. As indicated above, the grain size of the sample can also be affected by the drilling technique, such as in hard tool drilling that generates an increase in the fine-grained portion of the sediment samples.

To perform certain tests, samples from several depths often must be composited. Also, certain tests performed on samples in the past may have destroyed the integrity of the sample. In the past, particle size testing resulted in loss of fines when the samples were returned to the Hanford Geotechnical Sample Library.

5.3 Geology of the 200 West Area Single-Shell Tank Farms

Information presented below is primarily from a series of reports by Hanford contractors in the late 1990s and early 21st century on the subsurface conditions of each of the single-shell tank farms.

5.3.1 Geology of Waste Management Area S-SX

Geologic characteristics of WMA S-SX (Figure 5.2) have been extensively studied. Price and Fecht (1976g, 1976h) presented an initial detailed interpretation of the geology. DOE-GJO (1996) presented an interpretation of the geology that was based primarily on geophysically logged groundwater monitoring wells constructed around the perimeter of the tank farm in the early 1990s. In Johnson and Chou (1998), the geologic interpretation was refined and updated. Johnson et al. (1999) further described the geology and other subsurface contaminants. Lindsey et al. (2000) provided additional interpretations on the geology. Most recently, Sobczyk (2000) presented a reinterpretation of the geology based on gross gamma-ray logs of 98 boreholes within the SX tank farm and the most recently published geology reports of the area by Johnson et al. (1999) and Lindsey et al. (2000). Detailed geologic and geochemical characterization of two boreholes is given in Serne et al. (2002a, 2002b). As noted in Section 4, the natural vertical and horizontal variations in fluvial sediments limit the distinctive characteristics that can be used to identify different geologic layers. Consequently, authors may interpret the geology and select contacts at differing depths for the same geologic layer. The main source of geologic information for the S and SX tank farms is borehole information. The key boreholes used for the compilation of geologic data on the S and SX tank farms are given in Table 5.1.

The S and SX tank farms were constructed in the upper Hanford formation sediments underlying the 200 West Area, along the north limb of the Cold Creek syncline (Figure 4.4). Stratigraphic units in the vadose zone underlying or adjacent to these tank farms include CRBG, the Miocene- to Pliocene-age Ringold Formation, the CCU, the Hanford formation, and backfill materials (Figure 5.3 and Table 5.2). More detailed cross sections of the geology of WMA S-SX are shown in Figures 5.4 through 5.9.

All but the surface of the Hanford formation have a general tendency to dip west to southwest toward the axis of the Cold Creek syncline (Figure 5.10). The water table lies in the Ringold Formation, and the unconfined aquifer is located entirely in the Ringold Formation.

5.3.1.1 Columbia River Basalt Group

The Elephant Mountain Member of the CRBG lies at an elevation of approximately 26 m (85 ft) above mean sea level beneath the S and SX tank farms (a depth of approximately 175 m [575 ft]) and dips gently to the southwest toward the axis of the Cold Creek syncline (Figure 4.4) (Price and Fecht 1976g, 1976h; DOE-RL 1993; Johnson et al. 1999). It forms the base of the suprabasalt confined aquifer contained in Ringold formation unit A.

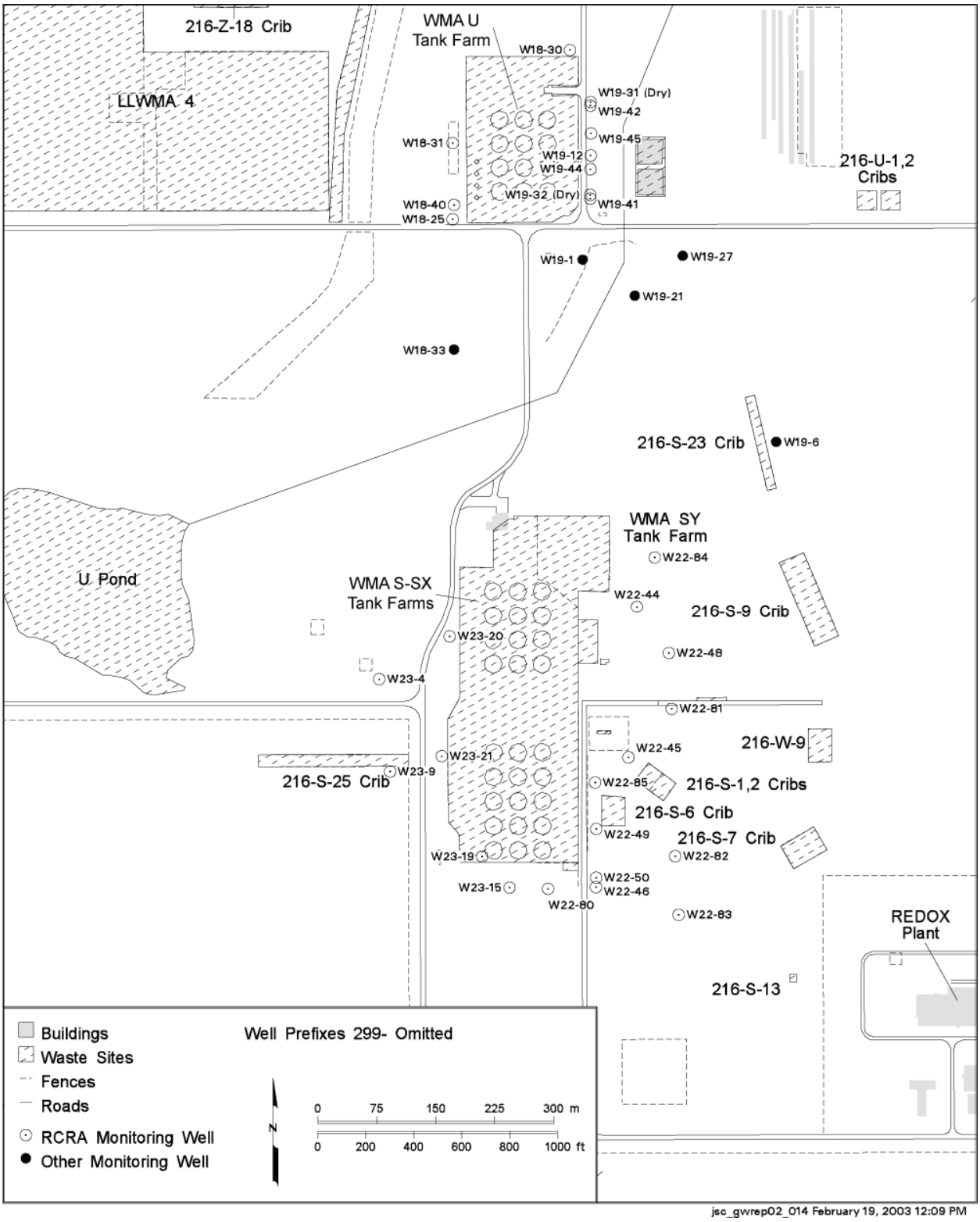

Figure 5.2. Well Location Map for Waste Management Areas S-SX and U

Table 5.1. Stratigraphic Contact Elevations for Boreholes in Waste Management Area S-SX[a]

Well No.	Ground Surface Elevation ft[b]	Contact Picks (Elevation in ft)[b]											
		Top H1a	Base of H1a gravel	Top of H1 gravel	Top H2 sand	Top H3 gravel	Top CCU_u	Top CCU_l	Top R_{tf}	Top R_{wie}	Top R_{lm}	Top R_{wia}	Top of Basalt
W22-15	672	672	652	625	615	NP	557	534	NP	525			
W22-17	671	671	649	632	614	NP	554	NP	NP	524			
W22-27	681	NP	665	640	605	NP	554	544	NP	495	236	180	124
W22-38	684	NP	NP	667	634	NP	566	539	NP	497			
W22-39	665	NP	659	615	608	NP	544	NP	NP	518			
W22-44	675	NP	662	639	615	NP	541	NP	NP	523			
W22-45	663	NP	659	630	625	NP	544.6	517	NP	490			
W22-46	668	NP	659	607	598	NP	548	533	NP	530			
W22-50	670	NP	656	611	607	NP	541	534	NP	528	211	174	
W23-1	662	NP	NP	620[c]	595	NP	545	505	NP	500			
W23-2	661	NP	NP	614[c]	607	NP	533	506	NP	504			
W23-3	661	NP	NP	604	584	NP	536	516	NP	497			
W23-4	663	663	624	554	NP	NP	544	514	NP	497			
W23-5	664	NP	655	609	594	NP	541	523	NP	494			
W23-7	664	NP	NP	623	614	NP	543	504	NP	488			
W23-9	664.5	NP	624	568	NP	NP	554	509	NP	494			
W23-10	664.8	NP	609	569	559	NP	544	515	NP	493			
W23-11	664	NP	616	575	NP	NP	554	514	NP	501			
W23-13	663	NP	623	590	568	NP	538	510	NP	508			
W23-14	661	NP	626	586	561	NP	538	509	NP	508			
W23-15	652	NP	640	595	577	NP	526	505	NP	500			
W23-16	670	670	623	588	583	NP	545	517	NP	515			
W23-17	666	666	641	551	NP	NP	541		NP	520			
W23-57	664	NP	NP	620[c]	586	NP	542						
W23-62	665	NP	NP	613[c]	596								
W23-64	663	NP	NP	595	568								
W23-68	664	NP	NP	590	575								
W23-73	661	NP	NP	611[c]	597								
W23-74	661	NP	NP	611[c]	600								

Table 5.1. (contd)

Well No.	Ground Surface Elevation ft[(b)]	Contact Picks (Elevation in ft)[(b)]											
		Top H1a	Base of H1a gravel	Top of H1 gravel	Top H2 sand	Top H3 gravel	Top CCU_u	Top CCU_l	Top R_{tf}	Top R_{wie}	Top R_{lm}	Top R_{wia}	Top of Basalt
W23-94	662	NP	NP	590	573	NP	534						
W23-100	661	NP	NP	596									
W23-105	661	NP	NP	594									
W23-108	661	NP	NP	592	567								
W23-109	661	NP	NP	597									
W23-113	661	NP	NP	589									
W23-117	661	NP	NP	588									
W23-121	661	NP	NP	582	570	NP	538						
W23-125	660	NP	NP	611[(c)]	592	NP	531						
W23-143	661	NP	NP	600	580	NP	532						
W23-163	661	620[(c)]	NP	NP	592								
W23-171	661	620[(c)]	NP	NP	595		538						
W26-12		676	649	604	595	NP	554						

(a) Johnson et al. (1999). This list includes all relevant boreholes drilled since that report was published.

(b) Multiply by 0.3048 to convert feet to meters.

(c) Elevation of unit at bottom of tank farm excavation.

CCU_1 = Lower Cold Creek fine-grained unit).

CCU_u = Upper Cold Creek unit (Cold Creek fine-grained unit).

GA = Gravel unit A, Hanford formation (lower gravel-dominated).

GB = Gravel unit B, Hanford formation (upper gravel-dominated).

H1 = Hanford formation, unit H1; equivalent to upper gravel-dominated.

H2 = Hanford formation, unit H2; equivalent to sand-dominated.

H3 = Hanford formation, unit H3; equivalent to lower gravel-dominated.

NP = Not present.

R_{lm} = Ringold Formation, lower mud unit.

R_{tf} = Ringold Formation, member of Taylor Flat.

R_{wia} = Ringold Formation, member of Wooded Island, unit A.

R_{wie} = Ringold Formation; member of Wooded Island, unit E. See Table 4.1 for differentiated Ringold Unit E and post-Ringold basalt-rich gravels.

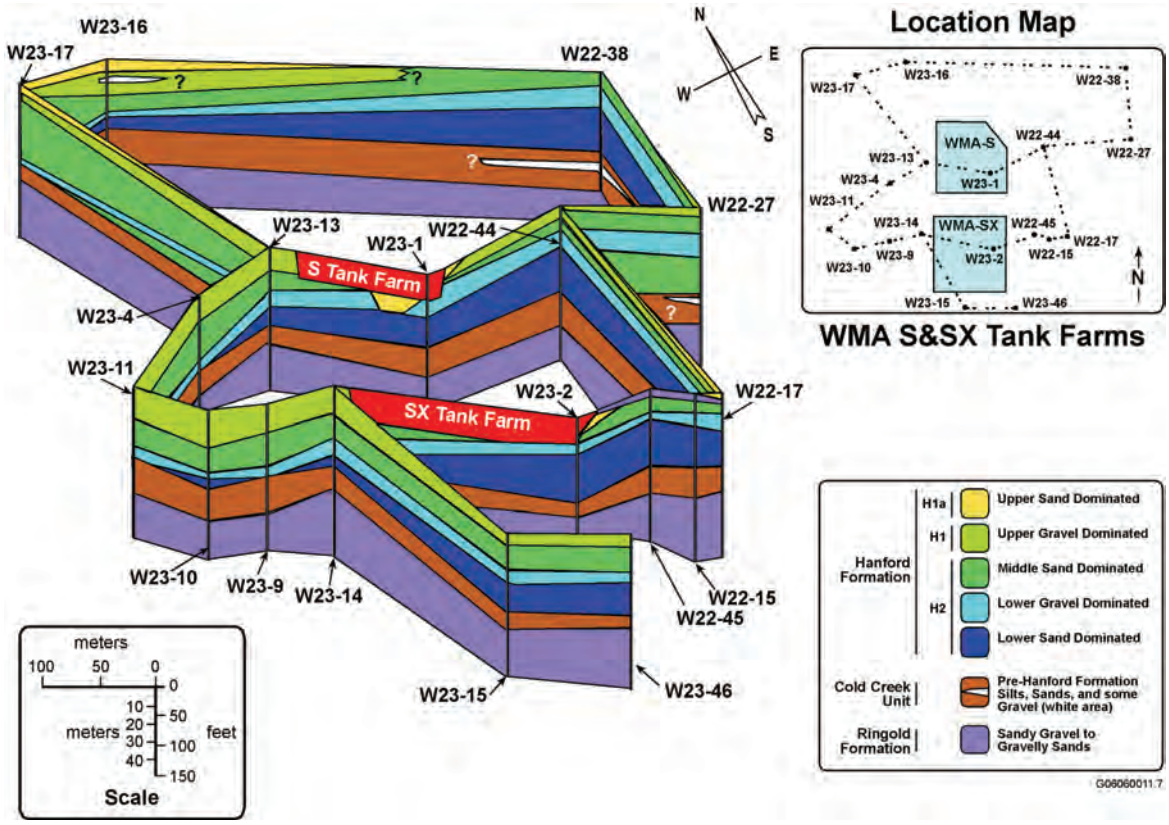

The top sand layer corresponds to subunit H1a. Gravel Unit B is subunit H1, and the next three lower units (sand, Gravel Unit A, and sand) compose the subunit H2.

Figure 5.3. Fence Diagram of Stratigraphy Underlying Waste Management Area S-SX (Johnson et al. 1999)

5.3.1.2 Ringold Formation

The Ringold Formation lies directly on top of the CRBG and is approximately 125 m (410 ft) thick beneath the S and SX tank farms (Figure 5.3 and Table 5.2). The group locally consists of the units of Ringold Formation Member of Wooded Island. At WMA S-SX, there are three principal stratigraphic facies in the R_{wi} unit: 1) the fluvial gravels of unit A, 2) a fine-grained, paleosol-lacustrine sequence referred to as the lower mud unit, and 3) fluvial gravels of unit E (Table 5.2). Ringold Formation unit E forms the main unconfined aquifer beneath the 200 West Area. Member of Taylor Flat sediments are not present beneath WMA S-SX.

The thickness of Ringold Formation unit A is approximately 30 m (100 ft) (DOE-RL 1993). Tallman et al. (1979) describe this unit as silty-sandy gravel that is composed predominantly of gravel supported by a coarse-to-fine sand matrix with intercalated, lenticular beds of sand and silt.

The thickness of the overlying lower mud unit is approximately 12 to 30 m (40 to 100 ft) (Tallman et al. 1979; DOE-RL 1993). This unit consists predominantly of mud (i.e., silt and clay); the lower portion contains well-developed argillic to calcic paleosol sequence (DOE 1988). The lower mud is an aquitard separating the confined and unconfined suprabasalt aquifers.

Table 5.2. Stratigraphic Terminology and Unit Thickness for the S and SX Tank Farms

Stratigraphic Symbol	Formation	Facies/Subunit	Description	Thickness
Holocene/Fill	NA	Backfill	Poorly-sorted gravel to medium sands and silt derived from the Hanford formation (Price and Fecht 1976g, 1976h).	18.6 m
H1a	Hanford formation	Sand	Sand to silty sand sequence occurs sporadically on either side of both tank farms and in a channel beneath SX farm	0–8 m
		Unit H1b – gravelly sand, upper gravel-dominated unit	Top coarse sand and gravel sequence equivalent to the Johnson et al. (1999) "Gravel Unit B." This is not shown on Figure 5.2 due to the scale of the drawing.	12 m
		Unit H1a – slightly silty sand; upper sand-dominated unit	Fine sand and silt sequence	9–12 m
H1		Unit H1 – lower gravel-dominated unit	Middle coarse sand and gravel sequence equivalent to "Gravel Unit A" described by Johnson et al. (1999) and "Hanford Unit A" described by Sobczyk (2000).	1–10 m
H2		Unit H2 – slightly silty sand; lower sand-dominated unit	Lower fine sand and silt sequence	24.3 m
CCU_u and/or Hf/CCU	Cold Creek unit	Upper	Very fine sand to clayey silt sequence is interstratified silt to silty very fine sand and clay deposits at least partially correlative with the "early Palouse soils" described by Tallman et al. (1979) and DOE (1988) and the "unnamed Hanford formation [?] or Plio-Pleistocene Deposits [?]" described by Lindsey et al. (2000), and the Hf/PP deposits in Wood et al. (2001).	10.7 m
CCU_l		Lower	Carbonate-rich sequence. Weathered and naturally altered sandy silt to sandy gravel, moderately to strongly cemented with secondary pedogenic calcium carbonate.	1–4 m
R_{wie}		Member of Wooded Island	Moderate to strongly cemented, well-rounded gravel and sand deposits, and interstratified finer-grained deposits.	Unit E: 75–85 m; Lower Mud: 12–30 m; Unit A: 30 m

CCU_l = Lower Cold Creek unit.
CCU_u = Upper Cold Creek unit (Cold Creek fine-grained unit).
Hf/CCU = Hanford formation/Cold Creek unit.
NA = Not applicable.
R_{wie} = Ringold Formation, member of Wooded Island, unit E.

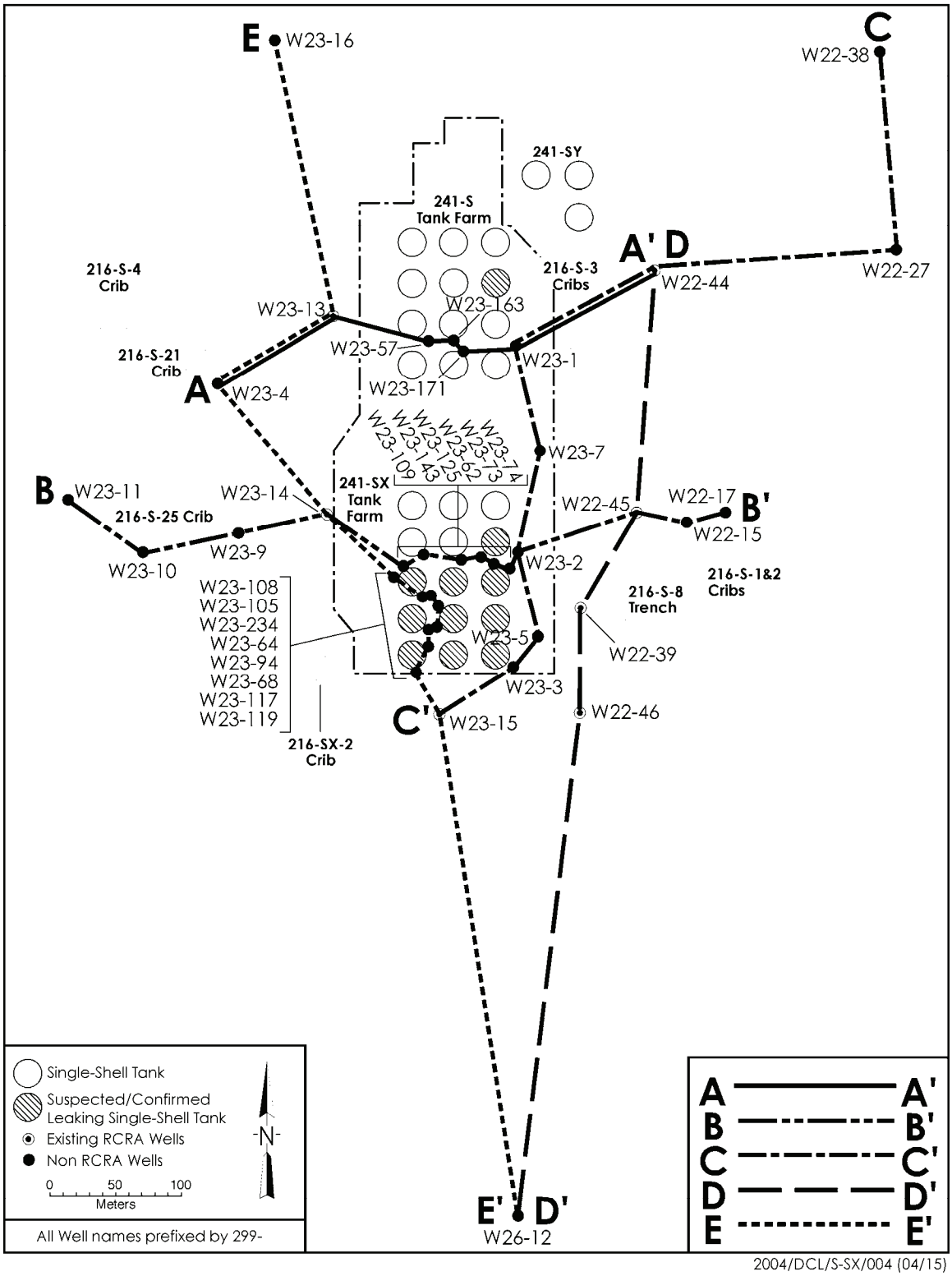

Figure 5.4. Location Map for Cross Sections (modified from Johnson et al. 1999)

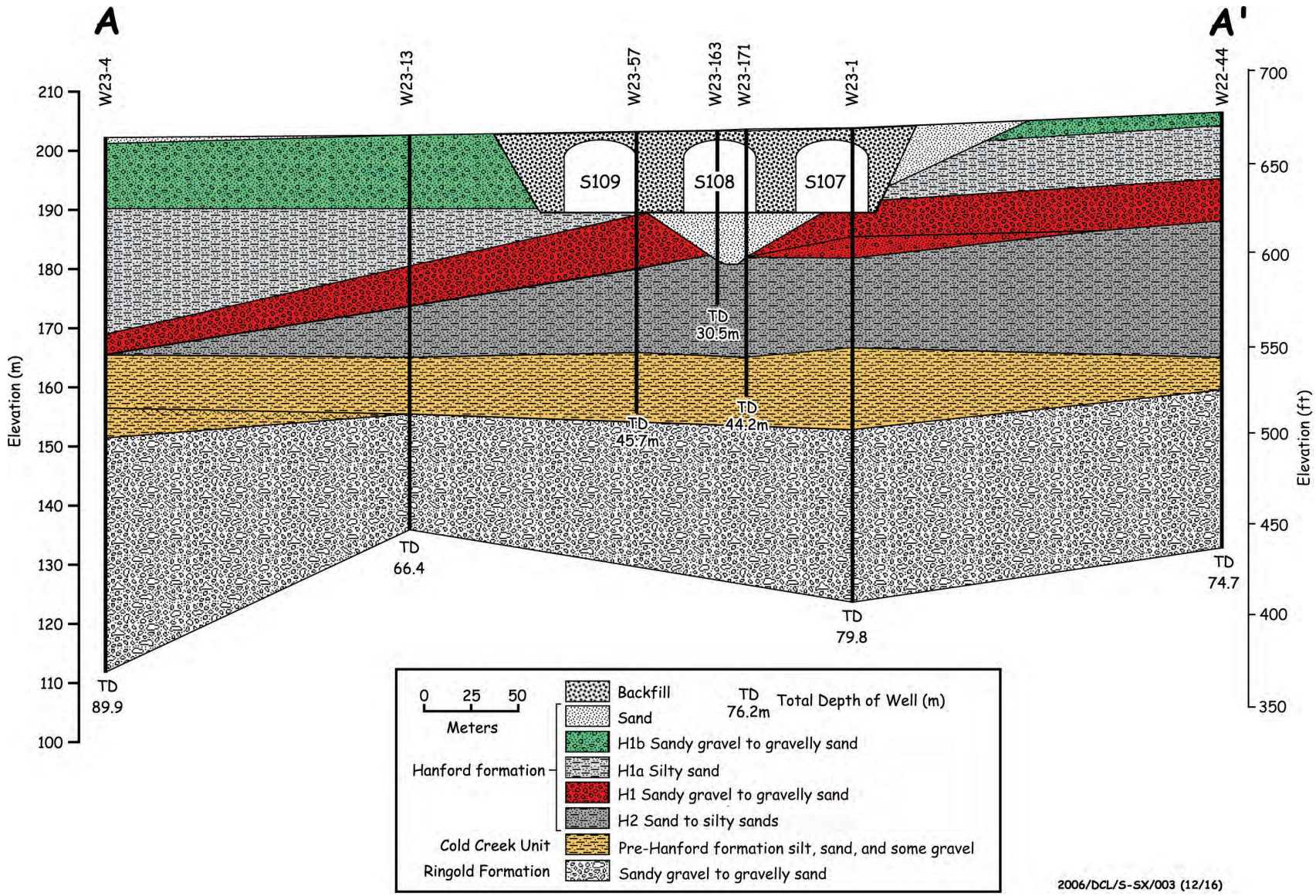

Figure 5.5. Geologic Cross-Section A-A' from the S and SX Tank Farms (modified from Johnson et al. 1999)

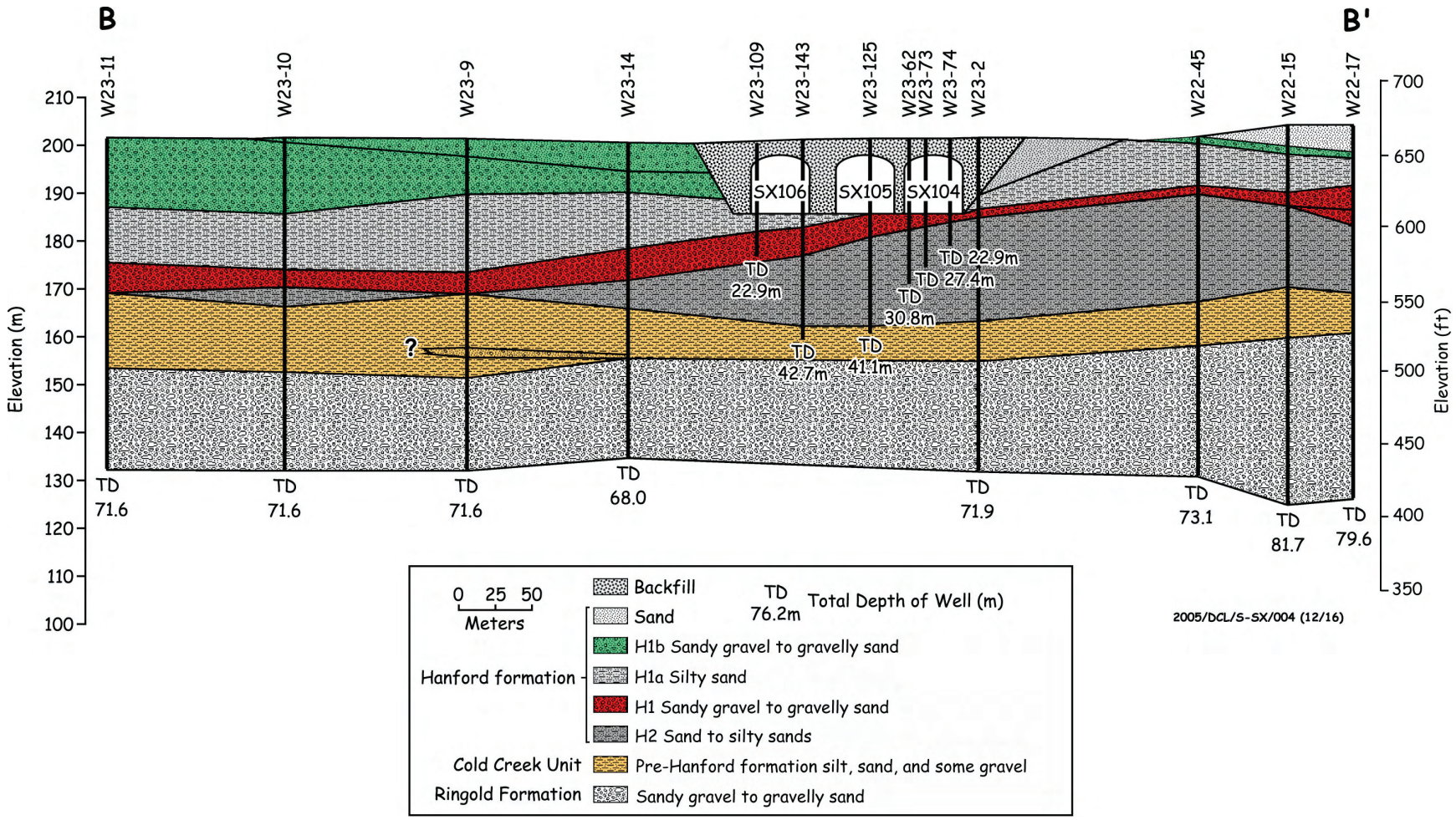

Figure 5.6. Geologic Cross-Section B-B' from the S and SX Tank Farms (modified from Johnson et al. 1999)

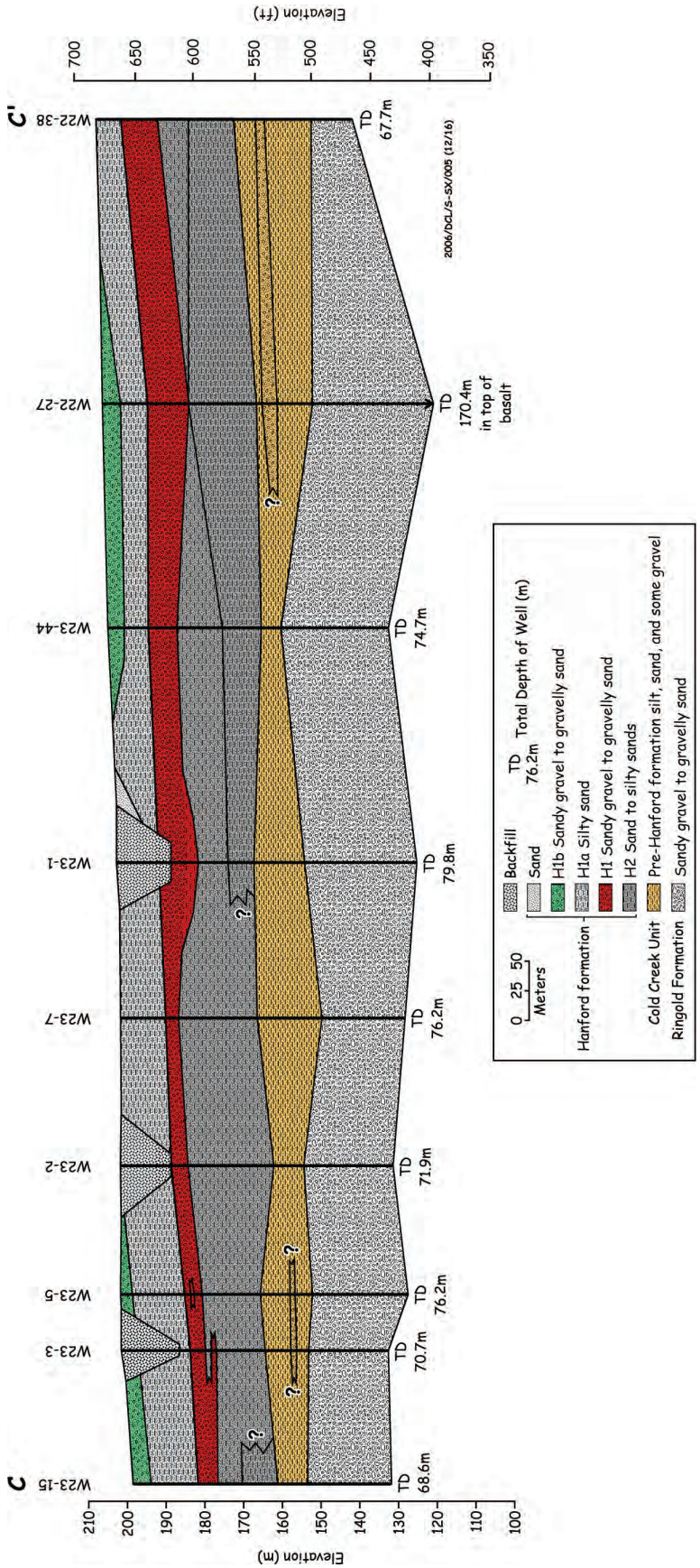

Figure 5.7. Geologic Cross-Section C-C' from the S and SX Tank Farms (modified from Johnson et al. 1999)

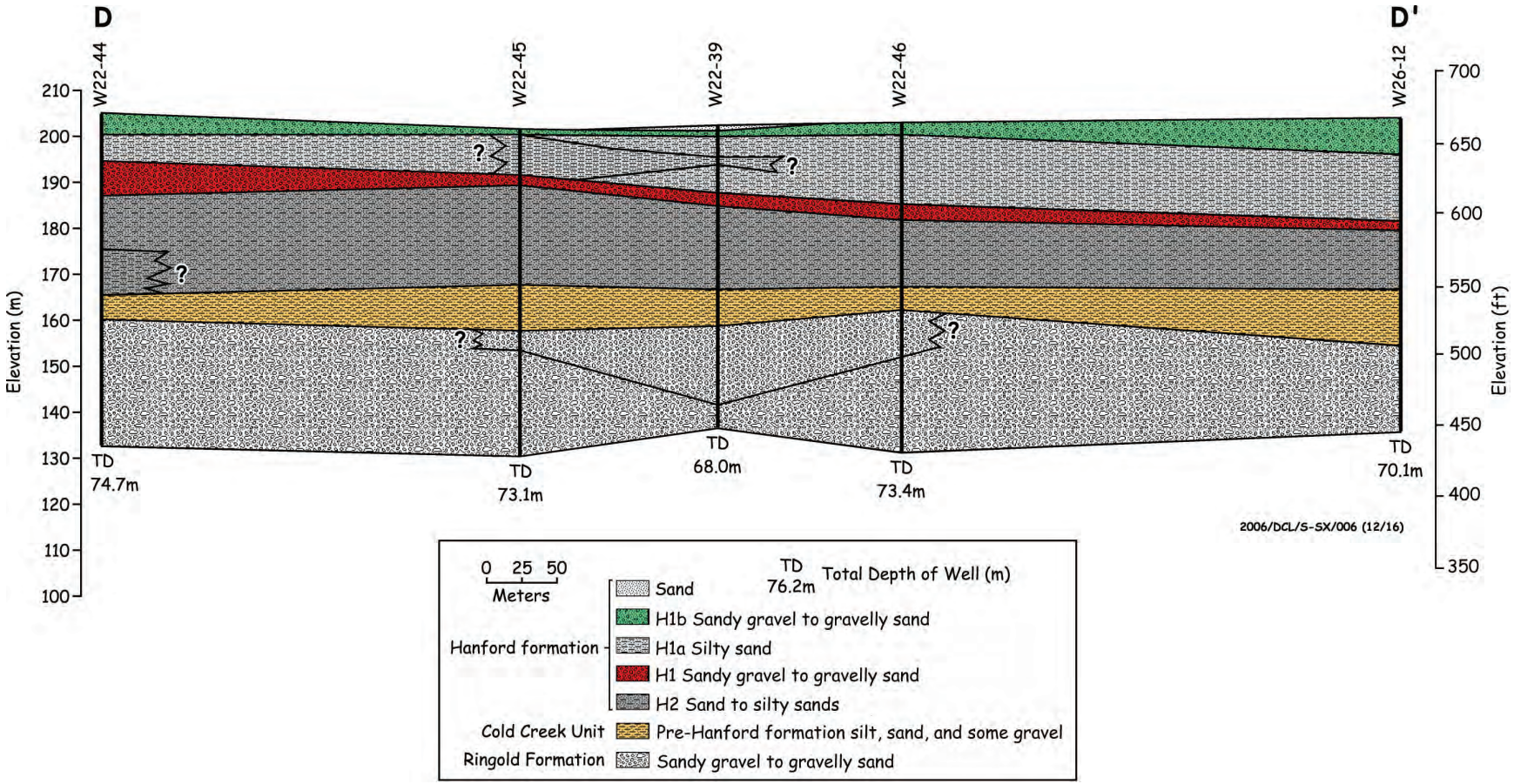

Figure 5.8. Geologic Cross-Section D-D' from the S and SX Tank Farms (modified from Johnson et al. 1999)

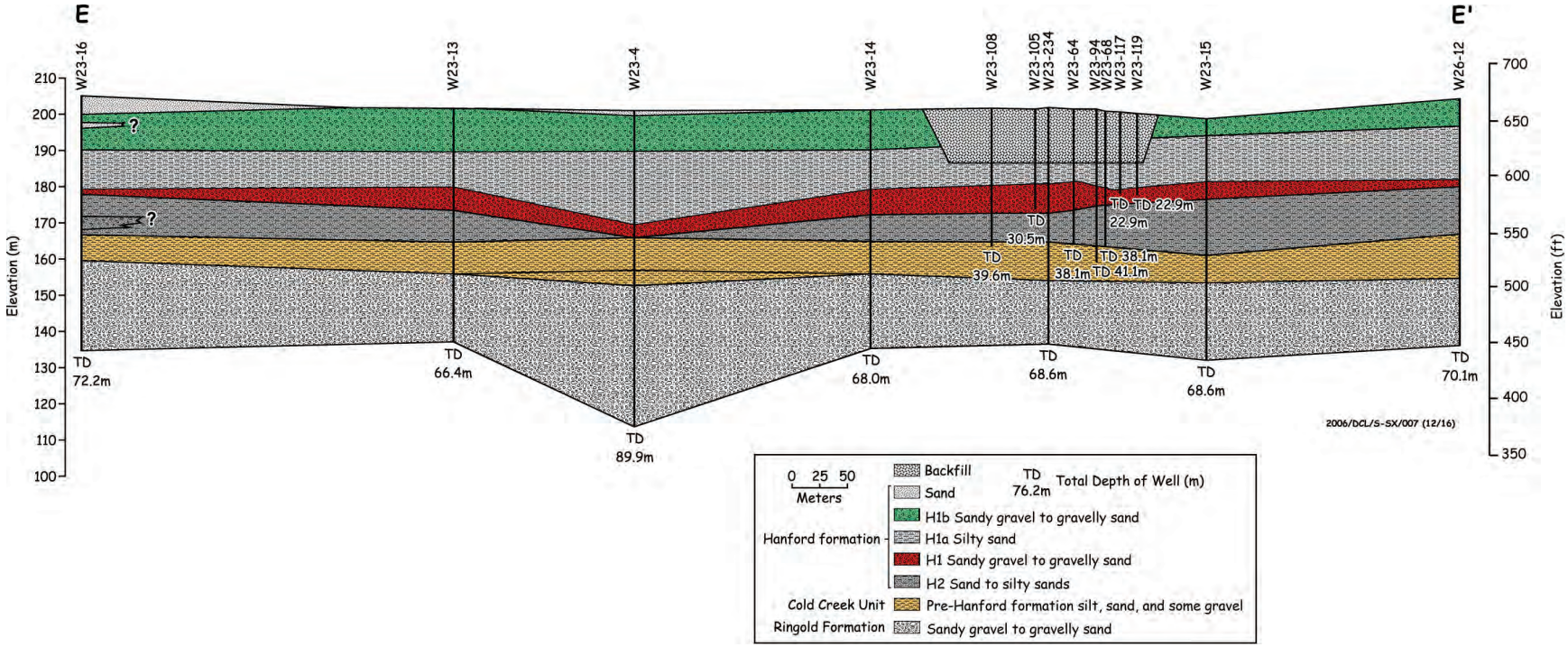

Figure 5.9. Geologic Cross-Section E-E' from the S and SX Tank Farms (modified from Johnson et al. 1999)

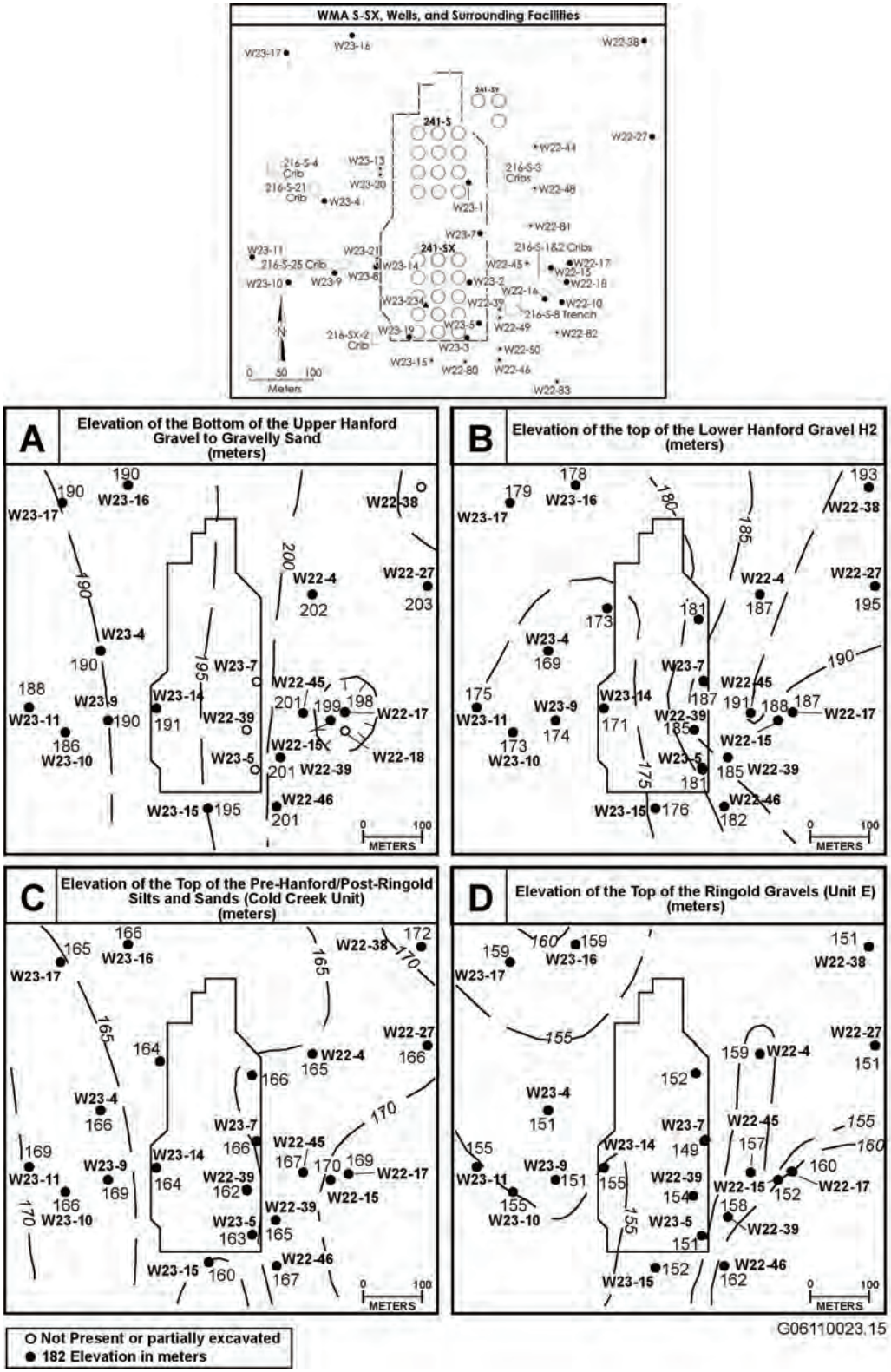

Elevation contours in subgraphs A and C mark the bottom of subunits H1 and H2, respectively.

Figure 5.10. Elevation Contour Maps on Top of Stratigraphic Unit Underlying Waste Management Area S-SX (modified from Johnson et al. 1999)

The thickness of unit E is estimated to be approximately 75 to 85 m (250 to 280 ft) (Tallman et al. 1979; DOE-RL 1993). This unit consists of well-rounded, clast-supported pebbles and small cobbles in a matrix of sand and mud. The amount of cementation is variable, with the lower portion of this unit described as moderately- to well-indurated conglomerate (Tallman et al. 1979). However, zones of poorly indurated gravel and sand also occur within this zone. The upper part of the unit is generally poorly indurated. Borehole data in the immediate vicinity of the S and SX tank farms indicate that this upper portion is dominated by sandy gravel and muddy sandy gravel, with sand to muddy sand beds becoming more prevalent toward the top of the unit.

5.3.1.3 Cold Creek Unit

The CCU includes the "early Palouse soils," "unnamed Hanford formation [?] or Plio Pleistocene Deposits [?] and Plio Pleistocene unit," and Hanford formation/Plio-Pleistocene deposits described in Wood et al. (2001). Two distinct facies of the CCU are recognized beneath the SX tank farm; these consist of an upper (CCU_u) and lower (CCU_l) subunit (Table 5.2). The coarse-grained, side-stream alluvial facies (DOE 1988; Slate 1996, 2000) of subunit CCU_l is not present beneath the S and SX tank farms. The eastern edge of this gravel facies occurs along the southwest boundary of the 200 West Area. The combined total thickness of the CCU is up to 13.1 m (43 ft) in the vicinity of the S and SX tank farms (Figure 5.3 and Table 5.2). Subunit CCU_u is relatively thick (up to 10.7 m [35 ft]), compared to the subunit CCU_l, which measures only 1 to 4 m (4 to 13 ft) in thickness.

The lower subunit CCU_l is characterized by pedogenic calcium carbonate cement occurring as either one discrete layer or as a diffuse zone. This suggests slow or negligible aggradation and/or subsequent erosion during paleosol development. In contrast, other areas to the west and south show up to five separate calcic horizons separated by relatively noncalcareous, uncemented sand, silt, and even indigenous basaltic sand and/or gravel of the side-stream facies (Slate 1996, 2000).

Calcium carbonate content generally does not exceed 25 wt% in the vicinity of the S and SX tank farms.

Unconformably overlying subunit CCU_l is the upper subunit CCU_u which consists of interstratified, uncemented fine sand, silt, and/or clay that displays only rare very weak soil development in the vicinity of the S and SX tank farms. Subunit CCU_u sediments appear to be predominantly fluvial overbank types of deposits intercalated with some eolian deposits (Johnson et al. 1999; Lindsey et al. 2000; Slate 2000). This subunit can be difficult to distinguish from fine-grained Hanford sediments in borehole samples, but a slight increase in calcium carbonate content and gamma log response are used to differentiate CCU_u sediments from those of the Hanford formation.

Plot C in Figure 5.10 shows a low amplitude north-south trending trough in the CCU surface that runs beneath the S and SX tank farms and may be related to an ancestral Cold Creek era drainage system or to erosion during Hanford formation floods.

5.3.1.4 Hanford Formation

Pleistocene-age deposits of the Hanford formation overlie the CCU and represent the dominant vadose zone materials directly beneath the S and SX tank farms. Paleomagnetic polarity data collected from the Hanford formation at the S and SX tank farms have all been normal polarity and, thus, do not

provide a means to further subdivide the sediments based on age as has been done at the 200 East Area (Pluhar 2003). Three subunits are identified in the S-SX area; the H2, H1, and H1a subunits in ascending order.

Subunit H2, the lower fine sand and silt sequence of the Hanford formation (Table 5.2), consists primarily of interstratified silty sands. This sequence generally thins from about 24.3 m (80 ft) east of the S and SX tank farms to approximately 10.7 m (35 ft) west of these tank farms. Johnson and Chou (1998) suggest that this thinning may signify some scouring on top of the subunit, perhaps associated with a secondary flood channel similar to the north-south trending flood channel that bisects Cold Creek bar. The grain-size within the Hanford H2 subunit appears to coarsen upward slightly. Johnson et al. (1999) and Sobczyk (2000) report that the top of this unit generally dips about 6° to the southwest with some local relative highs and lows present throughout (Figure 5.10). Below subunit H2 are slightly finer-grained deposits of interstratified very fine sand, silt, and clay associated with the upper subunit CCU_u, as defined by a diagnostic increase in total gamma activity on borehole geophysical logs (Johnson et al. 1999; Sobczyk 2000; Wood et al. 2001).

Subunit H2 is bounded above by subunit H1 (Table 5.2), which is a coarse unit dominated by gravel to gravelly sand and intercalated coarse sand that can be correlated beneath the S and SX tank farms. This middle sequence is referred to as “Gravel Unit A” in Johnson et al. (1999) and as “Hanford Unit A” in Sobczyk (2000) and is equivalent to the H1 unit described in DOE-GJO (1996) and Lindsey et al. (2000). Subunit H1 ranges in thickness from 1 m (3 ft) to nearly 10 m (30 ft) beneath the S and SX tank farms. Sobczyk (2000) reports subunit H1 to be thickest beneath tank SX-102, where coarse-grained flood deposits backfilled an apparent channel eroded into the top of the underlying subunit H2.

Particle size results using dry sieving for 100 selected samples from seven wells drilled in and around the tank farm show that this unit averages approximately 30% gravel, 66% sand, and only 4% mud. This is compared to the materials directly above and below it, that both average <1% gravel, nearly 90% sand, and 9% mud. Based on the modified Folk/Wentworth classification scheme, the classification of the average particle size for subunit H1 falls near the boundary between the sandy gravel and gravelly sand classes.

Above the coarse facies of subunit H1 lies an upper fine sand to silty-sand sequence (Johnson et al. 1999) equivalent to subunit H1a (Table 5.2) described in Lindsey et al. (1994, 2000), and the “silty sand” described in Sobczyk (2000). This sequence consists predominantly of interstratified slightly silty medium to very fine sands and ranges in thickness from 0 m, where it was removed during excavation of the tank farm, to about 9 to 12 m (30 to 40 ft) to the southwest. Johnson et al. (1999) and Sobczyk (2000) reported that the top of this unit dips slightly (approximately 2°) to the southwest. Sobczyk (2000) also suggested that this unit may become coarser-textured to the west.

A coarse-grained sand to gravelly sand unit overlies the fine-sand sequence of subunit H1a (Table 5.2) and appears to be intercalated with sandy gravel to the west. This unit is equivalent to Gravel Unit B (Johnson et al. 1999) and Hanford Unit B (Sobczyk 2000). It is the uppermost stratigraphic unit in the tank farm area, but is completely missing beneath the tank farm, where it was removed during construction. In surrounding boreholes, however, this unit ranges from a few meters in thickness to the east up to 12 m (40 ft) to the west.

5.3.1.5 Backfill

Price and Fecht (1976g, 1976h) describe the backfill surrounding the SSTs as consisting predominantly of poorly-sorted cobbles, pebbles, and coarse to medium sands to silt derived from the Hanford formation. Lindsey et al. (2000) describe the backfill as relatively non-cohesive, friable, massive sand with variable amounts of silt and pebbles. A hardened zone at the base of the backfill was also observed, extending to a depth of approximately 19 m (61 ft) that was significantly harder and drier than the overlying materials.

5.3.2 Geology of Waste Management Areas T and TX-TY

The geology of the T, TX, and TY tank farms and vicinity is well understood as a result of several decades of site characterization activities. It has been described in numerous reports (Price and Fecht 1976i, 1976j, 1976k; Tallman et al. 1979; Last et al. 1989; Connelly et al. 1992b; DOE-GJO 1997; Wood et al. 2001).

The T, TX, and TY tank farms (Figure 5.11) were constructed into the upper Hanford formation sediments underlying the 200 West Area, along the north limb of the Cold Creek syncline (Figure 4.4). The main source of geologic information for the tank farms is borehole information (Table 5.3). Detailed geologic and geochemical characterization of a number of boreholes is given in Serne et al. (2004a, 2004b). Stratigraphic units underlying or adjacent to these tank farms (in ascending order) include the CRBG, the Miocene- to Pliocene-age Ringold Formation, the CCU, the Hanford formation, and backfill materials (Figure 5.12 and Table 5.4). Detailed cross sections through the tank farms are shown in Figures 5.13 through 5.15. All but the surface of the Hanford formation have a general tendency to dip west to southwest toward the axis of the Cold Creek syncline (Figures 5.16 and 5.17).

5.3.2.1 Columbia River Basalt Group

The bedrock underlying the T, TX, and TY tank farms is Elephant Mountain Member; the bedrock strikes northwest-southeast with a southwest dip into the Cold Creek syncline. The Elephant Mountain Member is encountered only in 299-W11-26 in the area of WMAs T and TX-TY. That well hit basalt at an elevation of 60 m (197 ft) above sea level (Figure 4.4, Table 5.3).

5.3.2.2 Ringold Formation

The Ringold Formation was deposited on the CRBG and is up to 185 m (600 ft) thick in the Cold Creek syncline. Under the T, TX, and TY tank farms, the Ringold Formation consists mainly of fluvial gravels and sands; these belong to the R_{wi} unit and the R_{tf} (Lindsey et al. 2001b).

The Ringold Formation, member of Wooded Island, unit A overlies the Elephant Mountain Member beneath WMAs T and TX-TY (Table 6.4). Unit A is a pebble to cobble gravel with up to 15% sand and very little silt. Some interstratified sand horizons occur within the gravel, and there are some highly cemented zones. Unit A is 21 m (70 ft) thick in well 299-W11-26, the well closest to the T, TX, and TY tank farms penetrating the entire Ringold Formation.

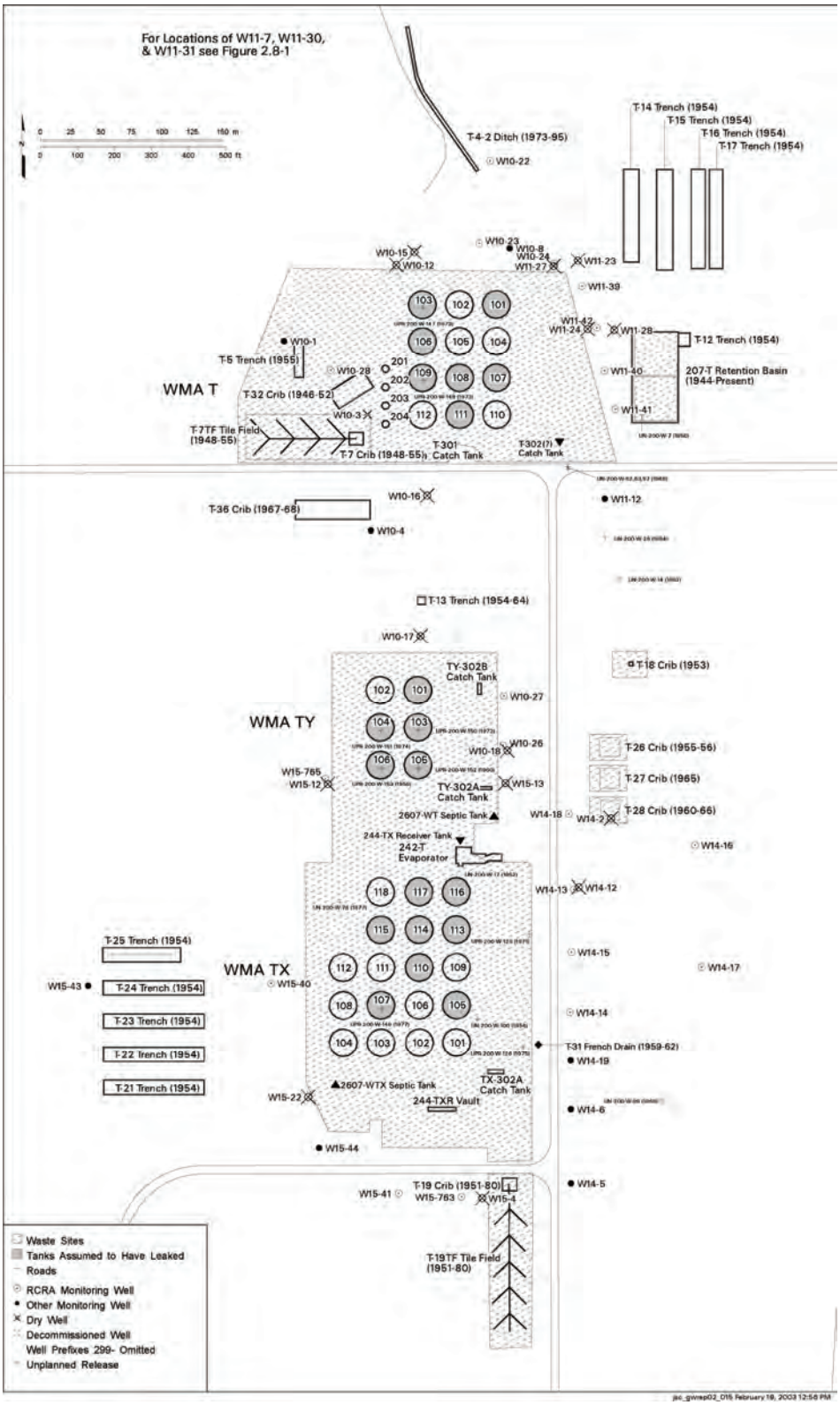

Figure 5.11. Well Location Map for Waste Management Areas T and TX-TY

Table 5.3. Stratigraphic Contact Elevations for Boreholes in Waste Management Areas T and TX-TY[a]

Well No.	Ground Surface Elevation ft[b]	Contact Picks (elevation in ft)[b]									
		Top H1 gravel	Top H2 sand	Top H3 gravel	Top CCU_u	Top CCU_l	Top R_{tf}	Top R_{wie}	Top R_{lm}	Top R_{wia}	Top of Basalt
W10-1	672	672	610	NP	596	578	562	531			
W10-3	671	648	ND	ND	586	578	561	544			
W10-8	677	677	633	ND	592	583	561	552			
W10-12	672	673	612	NP	590	582	559	537			
W10-15	672	662	612	NP	599	579	557	537			
W10-16	670	664	615	NP	587	575	565	541			
W10-17	671	671	629	NP	581	571	559	543			
W10-18	671	665	627	NP	584	574	556	541			
W10-23	678	670	635	ND	598	590	568	547			
W10-24	686	683	644	627	603	588	578	558			
W10-26	672	669	630	ND	584	575	562	545			
W10-27	672	668	628	ND	583	574	559	547			
W10-196	671	663	663	ND	589	579	566	550			
W11-12	679	679	651	NP	588	576	NP	552			
W11-27	681	671	646	NP	596	586	561	554			
W11-28	689	689	649	NP	592	584	565	546			
W11-39	689	684	655	ND	601	589	570	554			
W11-40	688	685	656	ND	600	585	570	554			
W11-41	688	685	651	ND	597	588	568	557			
W11-42	690	687	651	NP	597	590	574	564			
W14-5	665	663	636	NP	577	564	NP	541			
W14-6	665	665	623	ND	577	562	NP	549			
W14-12	667	662	633	NP	573	565	NP	541			
W14-13	670	665	637	ND	581	572	558	545			
W14-14	671	671	638	NP	577	563	561	548	269	233	
W14-15	671	669	633	ND	584	568	555	548			
W14-18	667	665	637	NP	581	574	558	545			
W15-22	667	667	620	NP	565	557	547	541			

Table 5.3. (contd)

Well No.	Ground Surface Elevation ft[(b)]	Contact Picks (elevation in ft)[(b)]									
		Top H1 gravel	Top H2 sand	Top H3 gravel	Top CCU_u	Top CCU_l	Top R_{tf}	Top R_{wie}	Top R_{lm}	Top R_{wia}	Top of Basalt
W15-41	666	666	614	ND	573	562	554	545			
W15-71	671	622	622	ND	568	559	NP	539			
W15-75	670	640	621	ND	570	562	NP	539			
W15-126	671	626	616								
W15-128	670	621	617								
W15-134	671	622	622								
W15-166	671	622	618	ND	571	561					
W15-765	670	668	630	ND	581	575	561	544.6			

Wood et al. (2001). This list includes all relevant boreholes drilled since that report was published.
Multiply by 0.3048 to convert feet to meters.
CCU_l = Lower Cold Creek unit.
CCU_u = Upper Cold Creek unit (Cold Creek fine-grained unit).
H1 = Hanford formation, unit H1; equivalent to gravel-dominated.
H2 = Hanford formation, unit H2; equivalent to sand-dominated.
R_{lm} = Ringold Formation, lower mud unit.
R_{tf} = Ringold Formation, member of Taylor Flat.
R_{wia} = Ringold Formation, member of Wooded Island, unit A.
R_{wie} = Ringold Formation, member of Wooded Island, unit E. See Table 4.1 for differentiated Ringold Unit E and post-Ringold basalt-rich gravels.
ND = Not determined.
NP = Not present.

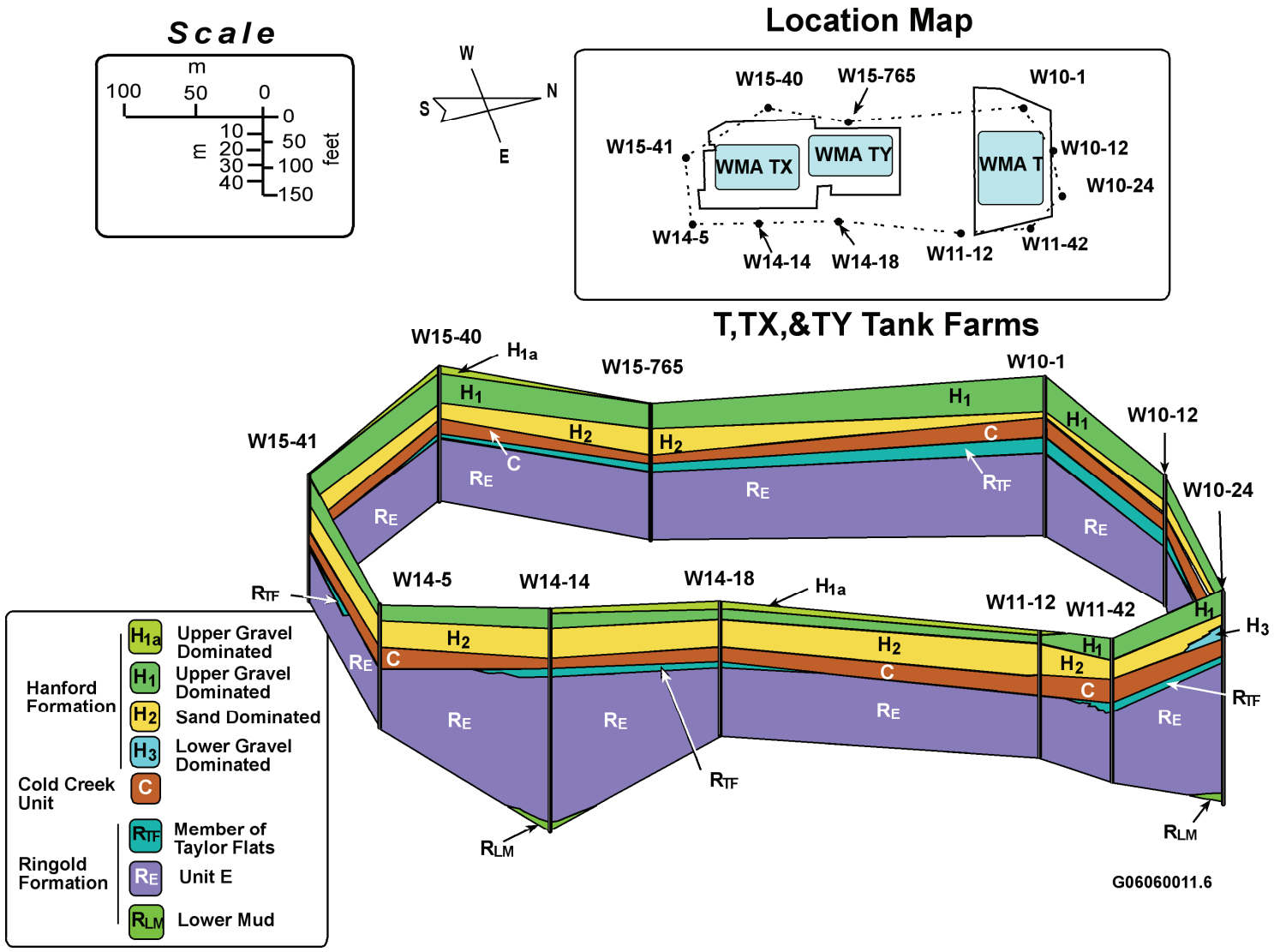

Figure 5.12. Fence Diagram Showing the Relationship Between Stratigraphic Units at the T, TX, and TY Tank Farms

Table 5.4. Stratigraphic Terminology and Unit Thickness for the T, TX, and TY Tank Farms

Stratigraphic Symbol	Formation	Facies/Subunit	Description	Thickness
Backfill	NA	Backfill – Anthropogenic	Gravel-dominated consisting of poorly to moderately sorted cobbles, pebbles, and coarse to medium sand with some silt derived from coarse-grained Hanford formation (H1 unit) excavated around tanks (Price and Fecht 1976i, 1976j, 1976k; Wood et al. 2001); occasional layers of sand to silty sand occur near the base of the backfill sequence.	18 m
H1	Hanford formation	Unit H1 (Gravel-dominated facies association). Cataclysmic flood deposits (high-energy)	Gravel-dominated flood sequence; composed of mostly poorly-sorted, basaltic, sandy gravel to silty sandy gravel. Equivalent to the upper gravel sequence discussed by Last et al. (1989), the Q_{fg} documented by Reidel and Fecht (1994b), Hanford Gravel Unit A of Johnson et al. (1999), coarse-grained sequence (H1 unit) of Wood et al. (2001) and gravel facies of unit H1 of Lindsey et al. (2001b), and gravel-dominated facies association of DOE-RL (2002).	10–12 m
H2		Unit H2 (Sand-dominated facies association). Cataclysmic flood deposits (moderate energy)	Sand-dominated flood sequence; composed of mostly horizontal to tabular cross-bedded sand to gravelly sand. Some sand beds capped with thin layers of silty sand to sandy silt. Equivalent to Hanford Sands of Johnson et al. (1999), Fine-Grained Sequence (H2 unit) of Wood et al. (2001) and unit H2 of Lindsey et al. (2001b), the sandy sequence of Last et al. (1989) and Lindsey et al. (1992), and to Q_{fs} documented by Reidel and Fecht (1994b), and sand-dominated facies association of DOE-RL (2002).	9–18 m
H3		Unit H3 (Gravel-dominated facies association). Cataclysmic flood deposits (high-energy)	Gravel-dominated flood sequence; composed of poorly sorted, basaltic, sandy gravel. Distinguished from the H2 sands by a sharp decrease in gamma response in the gravels.	0–10 m
Hf/CCU	Undifferentiated Hanford formation and Cold Creek unit	NA	Silty sequence. Similar to Cold Creek unit but distinguished by having a lower natural gamma response.	2–5 m
CCU_u	Cold Creek unit	Upper subunit Post-Ringold Formation eolian and/or overbank alluvial deposits	Silty sequence; consisting of interstratified well-sorted silt and fine sand. Uncemented but may be moderately to strongly calcareous from detrital $CaCO_3$. Equivalent to the "early Palouse soil" (Tallman et al. 1979; DOE 1988; DOE-GJO 1997) and the Hf/PP deposits of Wood et al. (2001). Also equivalent to the upper Plio-Pleistocene unit in Lindsey et al. (2001b) and the fine-grained, laminated to massive lithofacies of the Cold Creek unit DOE-RL (2002).	2–7 m

Table 5.4. (contd)

Stratigraphic Symbol	Formation	Facies/Subunit	Description	Thickness
CCU_l		Lower subunit Calcic paleosols developed on eroded Ringold or post-Ringold Formation eolian and/or fluvial deposits	Calcic paleosol sequence; consisting of interbedded layers of pedogenically altered to unaltered gravel, sand, silt, and/or clay, cemented together with one or more layers of secondary $CaCO_3$, originally referred to as "caliche" (Brown 1959). Since then the name has evolved from the Plio-Pleistocene unit (DOE 1988; DOE-GJO 1997; Slate 2000), the Plio-Pleistocene calcrete facies (DOE 1988; Wood et al. 2001), the lower Plio-Pleistocene unit (Lindsey et al. (2001b), and the coarse- to fine-grained, $CaCO_3$-cemented lithofacies of the Cold Creek unit (DOE-RL 2002).	0–8 m
R_{tf}	Ringold Formation	Member of Taylor Flat Ancestral Columbia River System fluvial channel, crevasse splay, and overbank deposits	Fine-grained Ringold Formation sequence consisting of interstratified, well-bedded fine to coarse sand to silt. Equivalent to the upper Ringold Formation unit (DOE 1988).	10 m
R_{wi} unit		Member of Wooded Island Ancestral Columbia River System braided-stream deposits	Coarse-grained Ringold Formation sequence, consisting of mostly moderately sorted, quartzitic sandy gravel to silty sandy gravel. Equivalent to middle Ringold unit (DOE 1988) and the Ringold Formation unit E and unit A gravels (Wood et al. 2001; Lindsey et al. 2001b). Contains mud (LM).	Unit E: 85 m; LM: 6–11 m; Unit A: 20 m

$CaCO_3$ = Calcium carbonate.
CCU_l = Lower Cold Creek unit.
CCU_u = Upper Cold Creek unit (Cold Creek fine-grained unit).
Hf/CCU = Hanford formation/Cold Creek unit.
LM = Lower mud unit.
NA = Not applicable.

The lower mud unit overlies Ringold Formation unit A and is a fine-grained lacustrine deposit. The lower mud is 7 m (22 ft) thick in well 299-W11-26 (Table 5.3) and appears to be continuous under the WMAs, although it pinches out a few thousand feet to the east. The top of the lower mud unit generally conforms to the top of basalt, dipping gently (~6º) to the southwest.

The lower mud unit is equivalent to hydrogeologic unit 8 of Williams et al. (2002). They describe hydrogeologic unit 8 as separating the suprabasalt aquifer into an upper unconfined aquifer in the sediments above the lower mud unit and a lower, confined aquifer in the Ringold Formation unit A. Groundwater in the unconfined aquifer and the confined Ringold Formation unit A aquifer does not flow vertically through hydrogeologic unit 8 (Williams et al. 2002). Where the lower mud unit is not present such as the paleochannel in the northeast corner of 200 West Area (Figure 4.7), the suprabasalt aquifer is a single system.

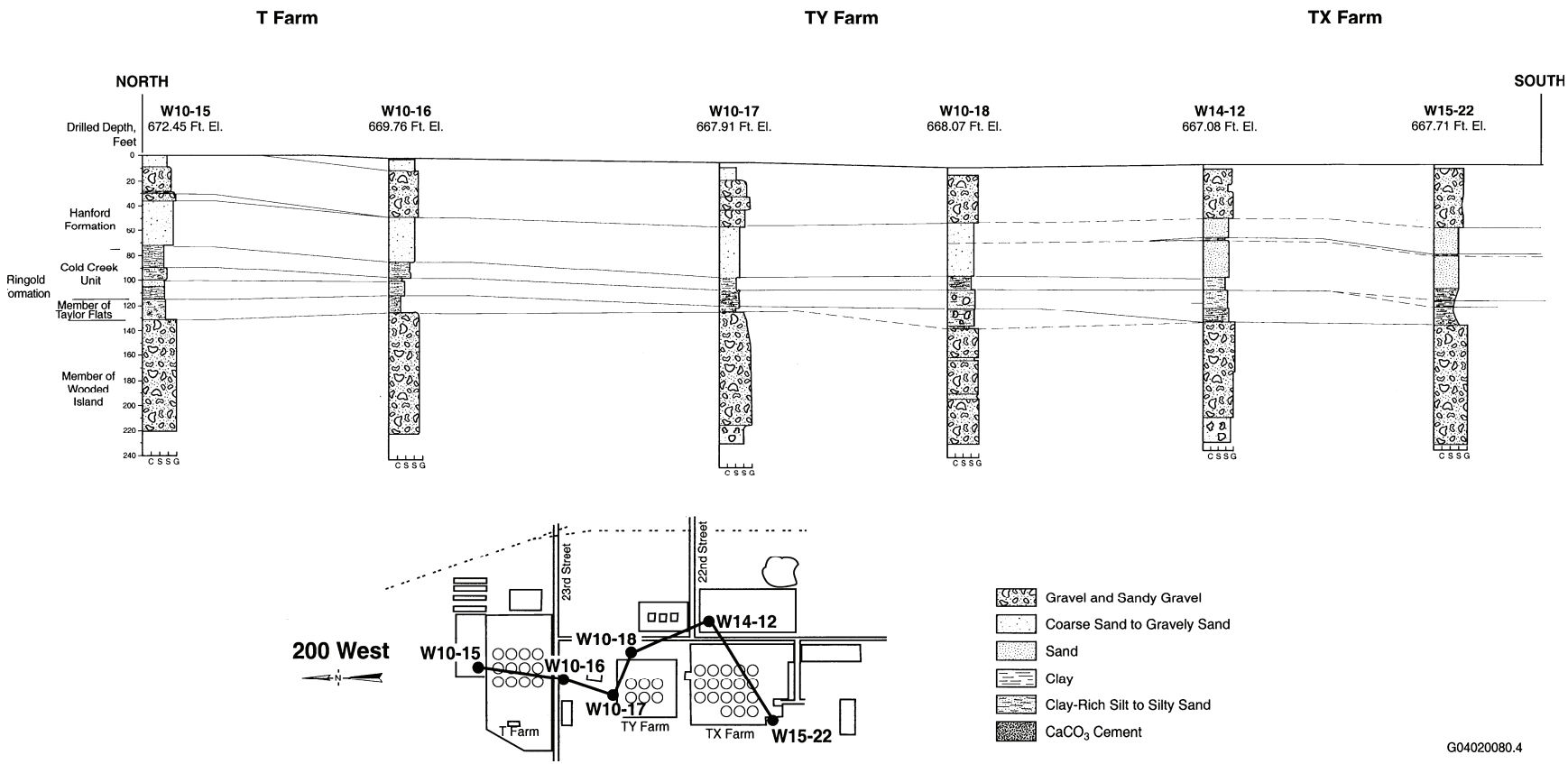

Figure 5.13. Cross Section Through the T, TX, and TY Tank Farms (based on Hodges and Chou 2001)

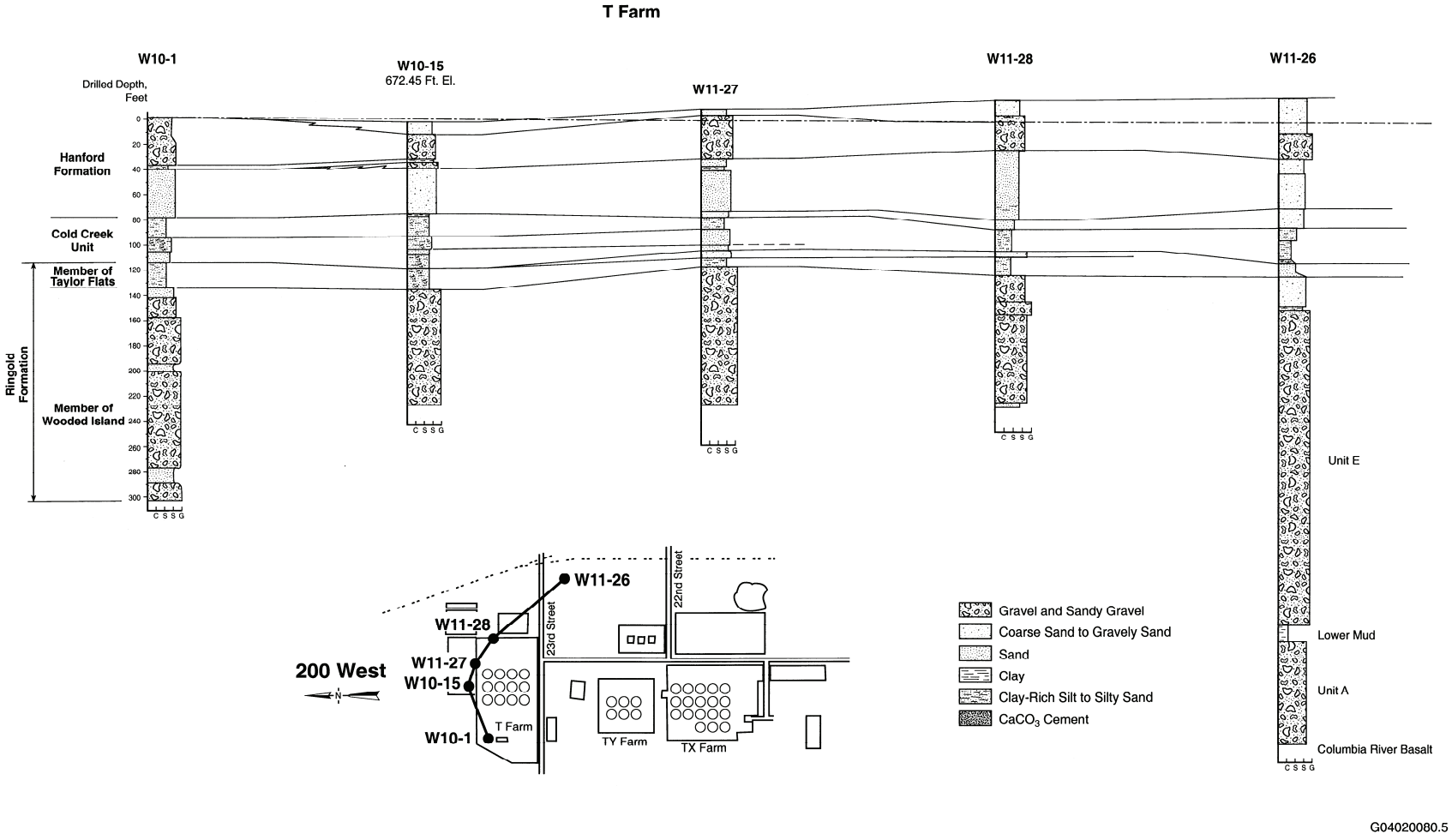

Figure 5.14. Cross Section Through the T Tank Farm (based on Hodges and Chou 2001)

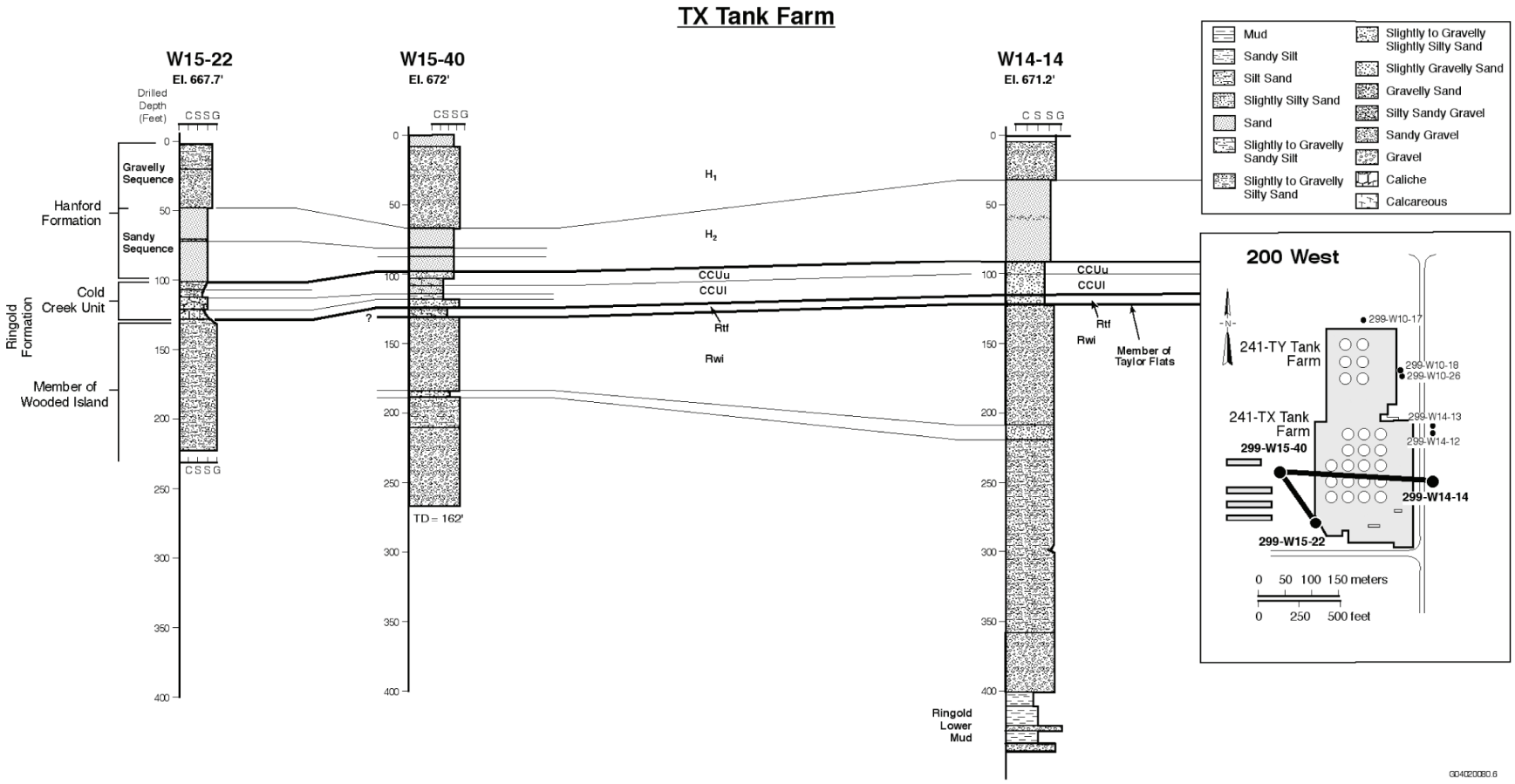

Figure 5.15. Cross Section Through the TX Tank Farm (based on Hodges and Chou 2001)

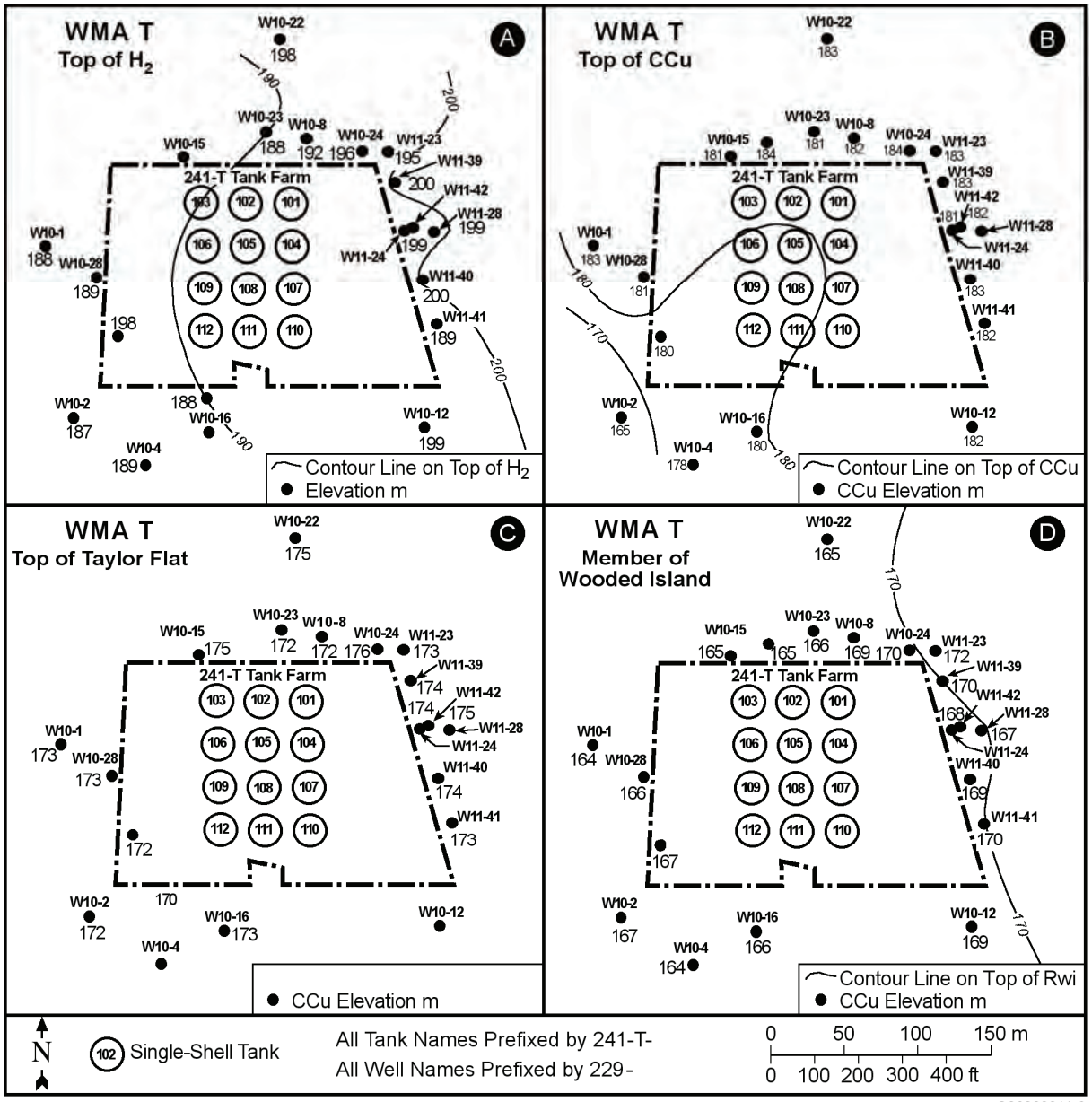

Figure 5.16. Structure Contour Maps on Selected Units Beneath the T Tank Farm

Overlying the lower mud unit is the Ringold unit E. The contact between the two is easily distinguished on natural gamma logs by unit E's considerably lower gamma activity. Unit E is described as a pebble to cobble gravel with a fine- to coarse-grained sand matrix. Gravel content is usually >60 to 70%. Occasionally, features interpreted as large boulders were encountered during drilling. The sediments are variably consolidated, usually poorly sorted, and show variable amounts of calcium carbonate. Iron oxide staining is common. "Slow drilling," "hard drilling," "switched to hard tool" are common comments on the geologists' logs when drilling in unit E sediments. Unit E is between 39 m and 85 m thick; the upper boundary of unit E dips slightly toward the west or southwest beneath WMA T (Figures 5.16 and 5.17). The unconfined aquifer lies in unit E.

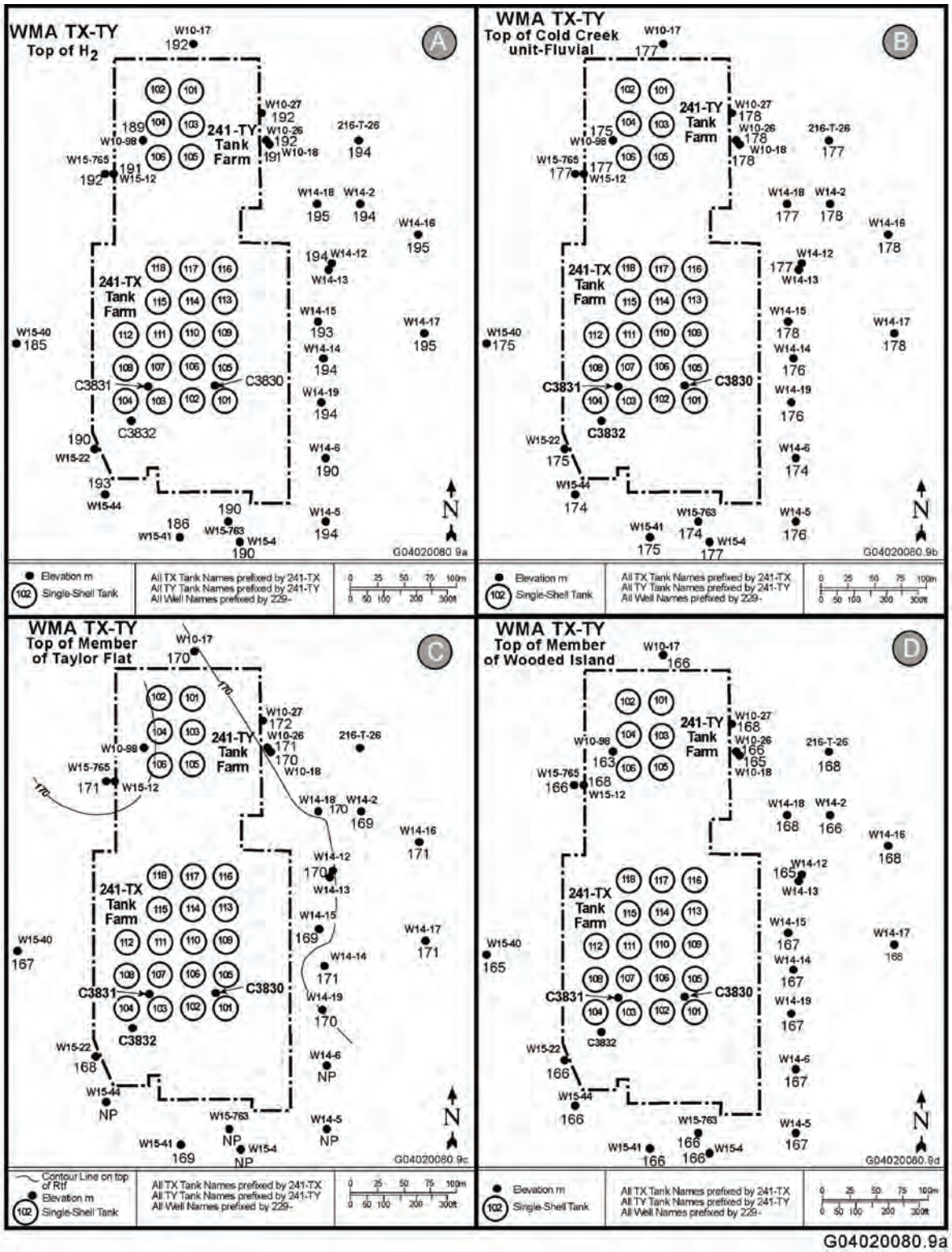

Figure 5.17. Structure Contour Maps of Selected Units Beneath Waste Management Area TX-TY

During construction of the Central Plateau fence diagram for this report, a basalt-rich gravel was identified below what has been interpreted previously as member of Taylor Flat sediments. As discussed in Section 4, up to 80% of these gravels are basalt clasts, which is unusual for Ringold unit E gravels. This gravel has been identified in wells 299-W11-26, 299-W11-25B, and 299-W14-14, as well as in other wells in the northern 200 West Area (Table 4.1) and seems to run roughly north-south. The basalt-rich gravel lies above the water table and does not affect groundwater flow but could affect flow through the vadose zone. It is not shown on Figures 5.13, 5.14, or 5.15.

Overlying these sediments is the Ringold member of Taylor Flat. These sediments range in thickness from 10 m (30 ft) thick in the north to none near the southern boundary of the TX tank farm (Figures 5.18 and 5.19). The R_{tf} is a mixture of fluvial-sand and overbank facies associations consisting of bedded, unconsolidated to consolidated and poorly to well-sorted sandy silt, sand, and silty sand. Local pebbly areas occur. In places, calcium carbonate occurs as stingers and nodules of calcite, whereas in other places no calcium carbonate exists. The lower boundary of this unit is easily recognized by the difference in texture. The upper surface dips gently toward the west-southwest (Figures 5.16 and 5.17).

5.3.2.3 Cold Creek Unit

The CCU lies unconformably on the tilted and truncated Ringold Formation surface. Weathering and soil development associated with the overlying CCU is often overprinted the R_{tf} and/or the R_{wie}. Because the degree of post-Ringold Formation pedogenesis decreases with depth, the contact with the overlying CCU is gradational and generally defined by an upward increase in gamma activity from naturally occurring radionuclides, increase in calcium carbonate content, and/or decrease in mud content (indicative of more cementation).

The CCU_u and the CCU_l are present beneath the T, TX, and TY tank farms. The CCU_l subunit consists of calcium carbonate-cemented silt, silty sand, and sandy silt with some gravel in places (Table 5.4). In most wells, the calcium carbonate is fairly continuous with depth throughout the unit, but in others there are caliche-rich and caliche-poor zones. In well 299-W11-38 (adjacent to and replaced by well W11-42), three distinct caliche zones were recognized. The CCU_l subunit ranges in thickness from 2 to 10 m (8 to 32 ft) with an average thickness of 5 m (17 ft) under the WMAs (Figures 5.18 and 5.19).

The CCU_u consists of unconsolidated, fine-grained, fluvial-overbank and/or eolian facies sediments generally thought to be derived from the eolian reworking of the underlying R_{tf} and/or the underlying CCU_l (Brown 1960; DOE 1988). These sediments are slightly- to well-consolidated, moderately- to well-sorted silt and sandy silt. They may contain calcium carbonate but lack the cementation found in the underlying calcic paleosols. The CCU_u is between 2 and 7 m (6 and 22 ft) in thickness (Figures 5.18 and 5.19). The surface of the unit dips gently to the southwest.

The driller's log for well 299-W10-2, drilled in 1951 about 35 m (115 ft) southwest of T tank farm, noted perched water from 26 to 31 m (85 to 102 ft) depth. This closely corresponds to the top and bottom of the CCU_u in the well. Perched water also was found in 1994 just above the contact of the CCU_u and the overlying Hanford formation in well 299-W10-22, north of WMA T. Although perched water has not been found beneath WMA T, the CCU_u sediments extend throughout the area so that perched water may occur locally in areas that have not been drilled.

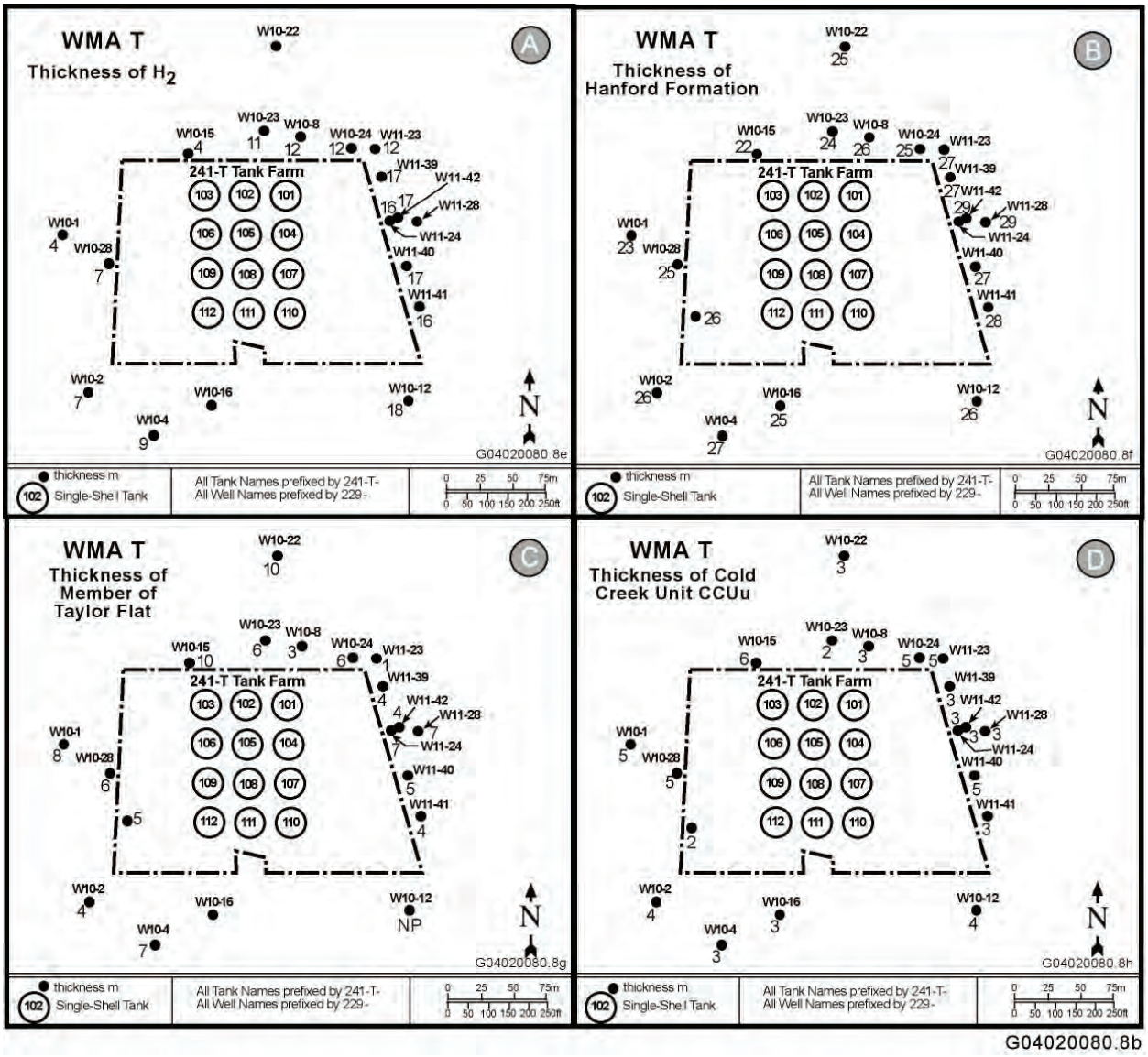

Figure 5.18. Thickness of Selected Stratigraphic Units in Waste Management Area T

The CCU_u has been called the Hanford/CCU by some workers because of its indeterminate age; that is, it appears to have some characteristics similar to the CCU and some characteristics of the silt-rich part of the Hanford formation. Regardless of its exact age and origin, the CCU silt-rich facies is a distinctive lithostratigraphic unit that can be correlated across most of the 200 West Area based on its fine-grained texture and high natural gamma activity on geophysical logs (DOE 1988; Last et al. 1989). Although the exact age of the CCU_u is in question, the upper and lower contacts of this subunit can be readily established. Thus for this report, the CCU_u will be retained for all deposits defined by the criteria above. The age, however, is not necessary to map the unit.

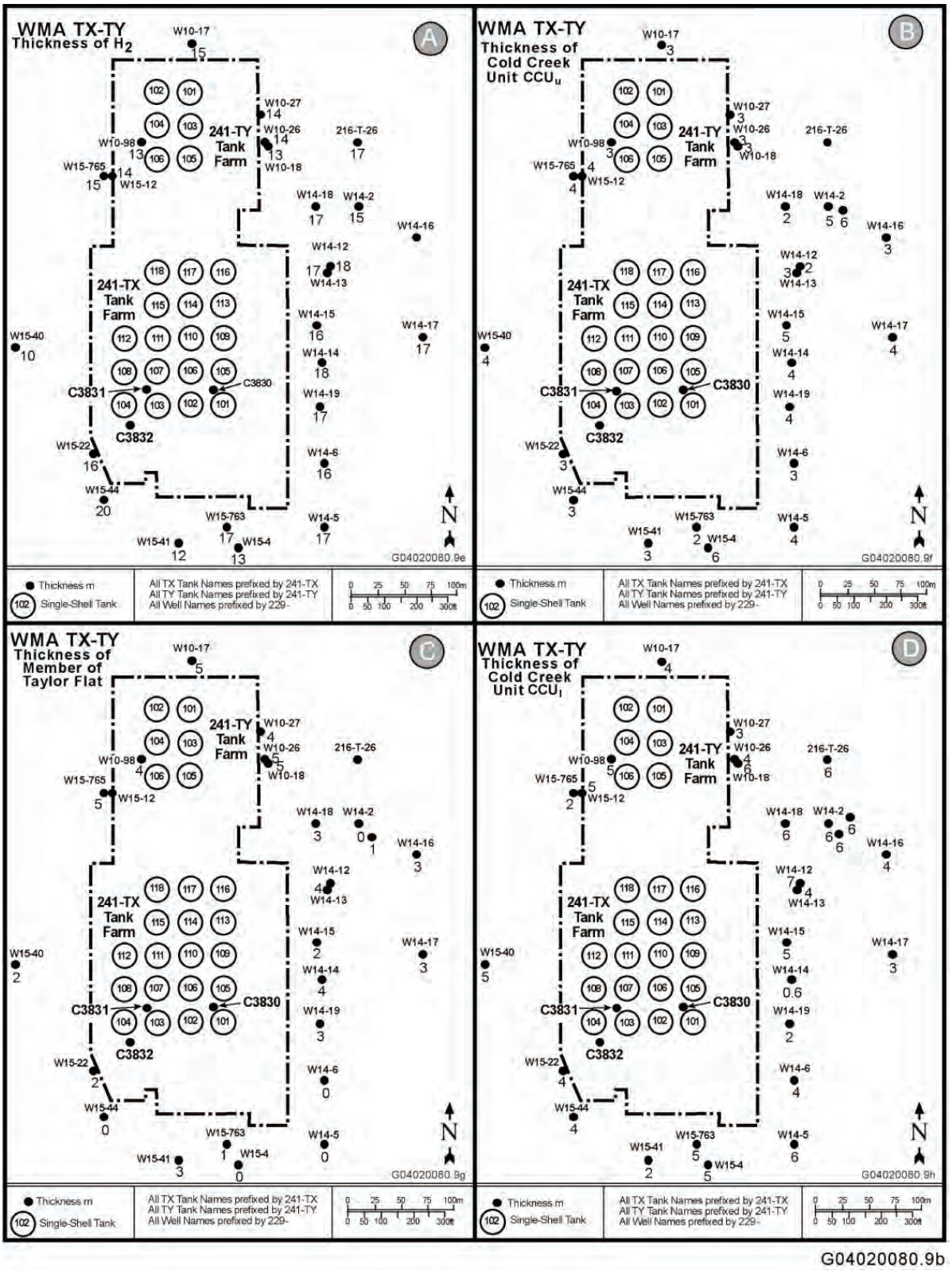

G04020080.9b

Figure 5.19. Thickness of Selected Stratigraphic Units in Waste Management Area TX-TY

5.3.2.4 Hanford Formation

The Hanford formation at the T, TX, and TY tank farms is about 27.4 m (90 ft) thick (Figure 5.12 and Table 5.4) subdivided into a lower sand-dominated and an upper gravelly subunit. These are the H1 and H2 units of Lindsey (1991). A third subunit, the H3 lower gravel subunit, has been identified in a well just north of the T tank farm but does not extend beneath the tank farms. The contact between the two is marked by a sharp increase in total natural gamma from the upper gravelly unit to the lower sandy unit.

The sand-dominated sequence H2 subunit is described on borehole logs as variably bedded silty sand, sand, and slightly gravelly to gravelly sand. The sediments are poorly- to well-sorted and unconsolidated. Fine-grained, silt-rich lenses are common and range from about 5 to 10 cm up to about 30 cm in thickness. Based on observations of outcrop and intact core, the sand-dominated sequence is interpreted to have been deposited during the waning stages of glacial flooding.

The H2 subunit ranges from about 4 to 20 m (13 to 66 ft) in thickness beneath WMAs T and TX-TY (Figures 5.18 and 5.19). The sandy beds are salt-and-pepper sands ranging from about 30% basaltic and 70% felsic sand to 70% basaltic and 30% felsic sand. The sequence is not cemented but does contain zones with calcium carbonate as small concretions and as coatings on grains. Thin silt lenses cap some individual beds within the Hanford formation sand-dominated sequence. These lenses are generally 0.15 m or less in thickness but range up to about 0.3 m (0.9 ft) thick. The silt lenses cannot be correlated among boreholes.

The base of the H2 subunit is recognized by a change from the finer-grained silty sand to coarser-grained deposits that is also reflected by a decrease in natural gamma activity from CCU to H2 sediments. The top of the sand-dominated sequence is more difficult to distinguish and is usually picked at the top of the shallowest sand bed that is >3 m (10 ft) thick beneath gravel-dominated deposits. In some wells, this corresponds to an increase in natural gamma activity within the sand-dominated sequence. The Hanford formation sand-dominated sequence tends to be thicker beneath the eastern part of WMAs T and TX-TY and has a slight dip toward the west or southwest (Figures 5.16 and 5.17).

The H1 subunit overlies the H2 subunit everywhere beneath the T, TX, and TY tank farms, except where the H1 unit has been removed by excavation. The H1 subunit generally is thicker in the western portion of WMAs T and TX-TY, perhaps because of higher energy deposition associated with the north-south trending paleochannel. The gravel-dominated sequence is described as consisting of silty sandy gravel and sandy gravel with some interbedded sand and silty sand. The Hanford formation gravel-dominated sequence varies from 6 to 17 m (20 to 55 ft) thick in the area. At some wells, the sequence lies at the surface, whereas in other wells, the sequence is covered by a thin layer of Holocene sediment. Much of the entire unit was removed from most, if not all, of the tank farms during construction and replaced as backfill after construction was complete. The base of the gravel-dominated sequence was picked at the top of the first sand or silty sand sequence that is at least 3 m (10 ft) thick. This contact may be somewhat arbitrary, particularly in boreholes with only a driller's log and no natural gamma log available.

5.3.2.5 Holocene Deposits and Backfill

Holocene deposits overlie the Hanford formation near WMAs T and TX-TY but have been removed from within the tank farms. These deposits are limited to windblown silt and sand. Eolian sheet sands occur sporadically at the surface and generally are less than 1 to 2 m thick. Backfill material occurs to about the 15-m (50-ft) depth in the tank farm. The backfill is poorly sorted, gravelly sand to sandy gravel (Price and Fecht 1976i, 1976j, 1976k) from the gravel-dominated sequence of the Hanford formation.

5.3.3 Geology of Waste Management Area U

WMA U is located on the Hanford Site in the south central portion of the 200 West Area between WMA S-SX to the south and WMAs T and TX-TY to the north (Figures 5.1 and 5.2). The geology of WMA U is well understood and has been described in several reports. These reports include Price and Fecht (1976l), Hodges and Chou (2000), Smith et al. (2001), and Lindsey (1991, 1995).

Geologic characterization of WMA U is based principally on borehole logs (i.e., geologic and drillers' logs) from 25 boreholes near the tank farm (Table 5.5). The logs describe the physical and chemical characteristics of the subsurface system and include data such as grain size distribution, calcium carbonate content, and moisture content. Interpretation is based also on existing reports that describe the regional, Hanford Site, 200 Areas, and local geology.

WMA U lies within a shallow, north-south–oriented topographic low. This low formed within the southwestern extent of a flood bar deposit known as the Cold Creek bar and likely represents a braided stream channel that cuts across the bar (Figure 4.1). Within the U tank farm, isolated anthropogenic topographic depressions occur just southwest of tank U-110 and northwest of tank U-109. Until run-on and run-off controls were recently constructed around the site, these depressions were conducive to the collection and subsequent infiltration of surface run-off.

Stratigraphic units beneath WMA U (from oldest to youngest) include Miocene age CRBG; late Miocene- to Pliocene-age fluvial gravel; sand and silt of the Ringold Formation; Pliocene- to Pleistocene-age gravel, sand, and silt, including calcic paleosol of the CCU; Pleistocene-age flood gravels and sand of the Hanford formation; and recent Holocene sediments (Table 5.6 and Figure 5.20). Boreholes used in the analysis are shown in Figure 5.21. Figures 5.22 through 5.25 show more detailed geology of WMA U. The sequence of suprabasalt sediment is about 170 m (560 ft) thick at WMA U (Wood and Jones 2003; Smith et al. 2001).

Except for the surface of the sediments, most sedimentary layers tilt gently to the southwest (<1º). This is consistent with other 200 West Area WMAs where the layers tilt southwest into the Cold Creek syncline.

5.3.3.1 Columbia River Basalt Group

The CRBG forms the bedrock beneath WMA U. The Elephant Mountain Member of the Saddle Mountain Basalt Formation is the uppermost and youngest basalt beneath WMA U. Depth to basalt is about 170 m (560 ft) beneath WMA U. The Elephant Mountain Member is about 25 m (80 ft) thick in the 200 West Area (Myers et al. 1979).

Table 5.5. Stratigraphic Contact Elevations for Boreholes in Waste Management Area U[a,c]

Well Number	Ground Surface Elevation ft[b]	Contact Picks (Elevation in ft)[b]									
		Top H1 gravel	Top H2 sand	Top CCU	Top CCU_u	Top CCU_l	Top R_{tf}	Top R_{wie}	Top R_{lm}	Top R_{wia}	Top of Basalt
W15-5	675	675	615	560	560	548	NP	542	247	196	148
W18-19	670	670	624	545	NP	NP	NP	531			
W18-30	669	669	623	554	554	545	NP	538			
W18-31	661	661	640	548	548	535	NP	531			
W19-1	672	672	630	548	548	531	NP	525			
W19-3	693	693	591	515	NP	NP	NP	500			
W19-4	713	708	NP	546	NP	NP	470	451	270	193	173
W19-8	700	700	NP	525	NP	NP	NP	490	267	198	140
W19-10	680	680	617	545	545	528	NP	521	230	203	118
W19-13	693	693	583	523	NP	NP	NP	513			
W19-14	691	691	579	529	NP	NP	NP	519			
W19-15	691	691	586	544	544	528	525	515			
W19-16	693	693	602	553	NP	NP	NP	526			
W19-17	695	695	590	535	NP	NP	NP	510			
W19-18	699	699	591	539	NP	NP	NP	516			
W19-22	686	686	608	546							
W19-27	690	80	611	536	536	519	516	506			
W19-31	661	661	616	541	NP	NP	NP	521			
W19-32	674	674	629	549	NP	NP	NP	524			
W19-41	675	675	631	548	548	535	NP	529			
W19-42	674	674	630	558	558	538	NP	532			
W19-45	675	675	623	542	542	538	NP	450			
W19-47	676	668	629	552	552	538	NP	438			
W21-1	699	699	NP	528	528	502					
W22-27	679	679	610	854	554	541	524	495	236	180	125

(a) Bjornstad (2004). This list includes all relevant boreholes drilled since that report was issued.
(b) Rounded to nearest foot, multiply by 0.3048 to convert feet to meters.
(c) Weiss and Walker (2005).
CCU = Cold Creek unit.
CCU_l = Lower Cold Creek unit.
CCU_u = Upper Cold Creek unit (Cold Creek fine-grained unit).
H1 = Hanford formation, unit H1; equivalent to gravel-dominated.
H2 = Hanford formation, unit H2; equivalent to sand-dominated.
R_{lm} = Ringold Formation, lower mud unit.
R_{tf} = Ringold Formation, member of Taylor Flat.
R_{wia} = Ringold Formation, member of Wooded Island, unit A.
R_{wie} = Ringold Formation, member of Wooded Island, unit E. See Table 4.1 for differentiated Ringold Unit E and Post-Ringold basalt-rich gravels.
NP = Not present.

Table 5.6. Stratigraphic Terminology and Unit Thickness for the U Tank Farm

Stratigraphic Symbol	Formation	Facies/Subunit	Description	Thickness[(a)]
Backfill	NA	Backfill – Anthropogenic	Gravel-dominated consisting of poorly to moderately sorted cobbles, pebbles, and coarse to medium sand with some silt derived from coarse-grained Hanford formation (H1 unit) excavated around tanks (Price and Fecht 1976l; Wood et al. 2001); occasional layers of sand to silty sand occur near the base of the backfill sequence.	12 m
H1	Hanford formation	Unit H1 – (Gravel-dominated facies association). Cataclysmic flood deposits (high-energy)	Gravel-dominated flood sequence; composed of mostly poorly-sorted, basaltic, sandy gravel to silty sandy gravel. Equivalent to the upper gravel sequence discussed by Last et al. (1989), the Q_{fg} documented by Reidel and Fecht (1994b), Hanford Gravel Unit A of Johnson et al. (1999), coarse-grained sequence (H1 unit) of Wood et al. (2001) and gravel facies of unit H1 of Lindsey et al. (2001b), and gravel-dominated facies association of DOE-RL (2002).	2–7 m
H2		Unit H2 – (Sand-dominated facies association). Cataclysmic flood deposits (moderate energy)	Sand-dominated flood sequence; composed of mostly horizontal to tabular cross-bedded sand to gravelly sand. Some sand beds capped with thin layers of silty sand to sandy silt. Equivalent to Hanford Sands of Johnson et al. (1999), Fine-Grained Sequence (H2 unit) of Wood et al. (2001) and unit H2 of Lindsey et al. (2001a), the sandy sequence of Last et al. (1989), and to Q_{fs} documented by Reidel and Fecht (1994b) and sand-dominated facies association of DOE-RL (2002).	24 m
Hf/CCU	Undifferentiated Hanford formation and Cold Creek unit	NA	Silty sequence. Similar to Cold Creek unit but distinguished by having a lower natural gamma response.	4–8 m
CCU_u	Cold Creek unit	Upper subunit post-Ringold Formation eolian and/or overbank alluvial deposits	Silty sequence; consisting of interstratified well-sorted silt and fine sand. Uncemented but may be moderately to strongly calcareous from detrital $CaCO_3$. Equivalent to the "early Palouse soil" (Tallman et al. 1979; DOE 1988; DOE-GJO 1997) and the Hf/PP deposits of Wood et al. (2001). Also equivalent to the upper Plio-Pleistocene unit in Lindsey et al. (2001b) and the fine-grained, laminated to massive lithofacies of the Cold Creek unit DOE-RL (2002).	3–6 m

Table 5.6. (contd)

Stratigraphic Symbol	Formation	Facies/Subunit	Description	Thickness[(a)]
CCU_l		Lower subunit calcic paleosols developed on eroded Ringold Formation or post-Ringold Formation eolian and/or fluvial deposits	Calcic paleosol sequence; consisting of inter-bedded layers of pedogenically altered to unaltered gravel, sand, silt, and/or clay, cemented together with one or more layers of secondary $CaCO_3$, originally referred to as "caliche" (Brown 1959). Since then the name has evolved from the Plio-Pleistocene unit (DOE 1988; DOE-GJO 1997; Slate 2000), the Plio-Pleistocene calcrete facies (DOE 1988, Wood et al. 2001), the lower Plio-Pleistocene unit (Lindsey et al. 2001b), and the coarse- to fine-grained, $CaCO_3$-cemented lithofacies of the Cold Creek unit (DOE-RL 2002).	1–2 m
R_{tf}	Ringold Formation	Member of Taylor Flat Ancestral Columbia River System fluvial channel, crevasse splay, and overbank deposits	Fine-grained Ringold Formation sequence consisting of interstratified, well-bedded fine to coarse sand to silt. Equivalent to the upper Ringold Formation unit (DOE 1988).	Absent
R_{wi}		Member of Wooded Island Ancestral Columbia River System braided-stream deposits	Coarse-grained Ringold Formation sequence, consisting of mostly moderately sorted, quartzitic sandy gravel to silty sandy gravel. Equivalent to middle Ringold Formation unit (DOE 1988) and the Ringold Formation unit E gravels (Wood et al. 2001; Lindsey et al. 2001b). Well-stratified clay and interbedded silt and silty sand is equivalent to the lower mud Ringold Formation unit (DOE 1988). Fluvial gravels with intercalated sands are equivalent to the basal Ringold Formation unit (DOE 1988) and the Ringold Formation unit A gravels (Wood et al. 2001; Lindsey et al. 2001b).	Unit E: 90 m; LM: 15 m; Unit A: 30 m

(a) Multiply by 3.281 to convert meters to feet.
$CaCO_3$ = Calcium carbonate.
CCU = Cold Creek unit.
CCU_l = Lower Cold Creek unit.
CCU_u = Upper Cold Creek unit (Cold Creek fine-grained unit).
Hf/CCU = Hanford formation/Cold Creek unit.
LM = Lower mud unit.
NA = Not applicable.
Q_{fg} = Quaternary flood gravels.
Q_{fs} = Quaternary flood silt and sand.
R_{tf} = Ringold Formation, member of Taylor Flat.
R_{wi} = Ringold Formation, member of Wooded Island.

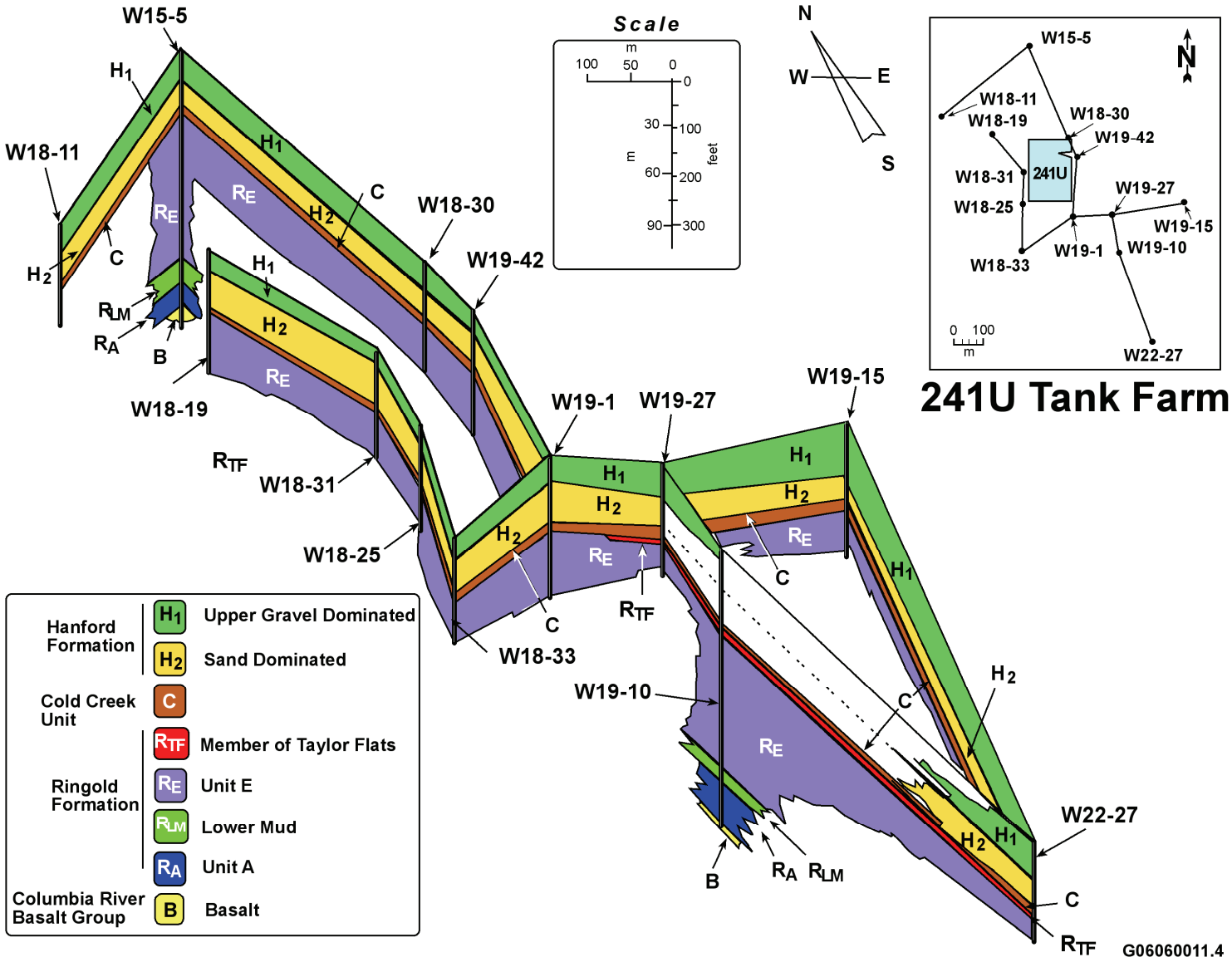

Figure 5.20. Fence Diagram Showing the Relationship Between Stratigraphic Units at Waste Management Area U

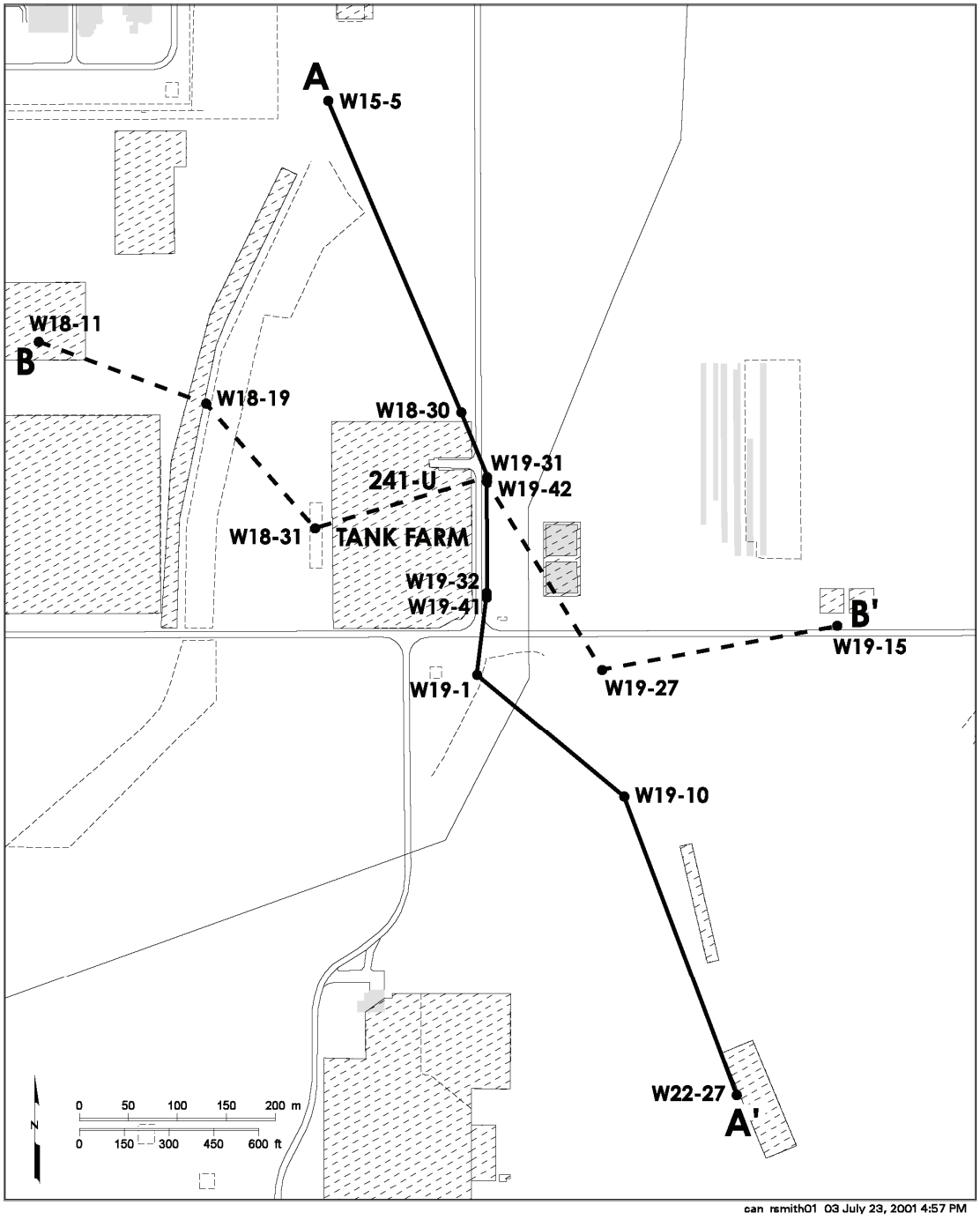

Figure 5.21. Location of Boreholes Used in This Report and Cross-Section Lines of Waste Management Area U for Figures 5.22 and 5.23

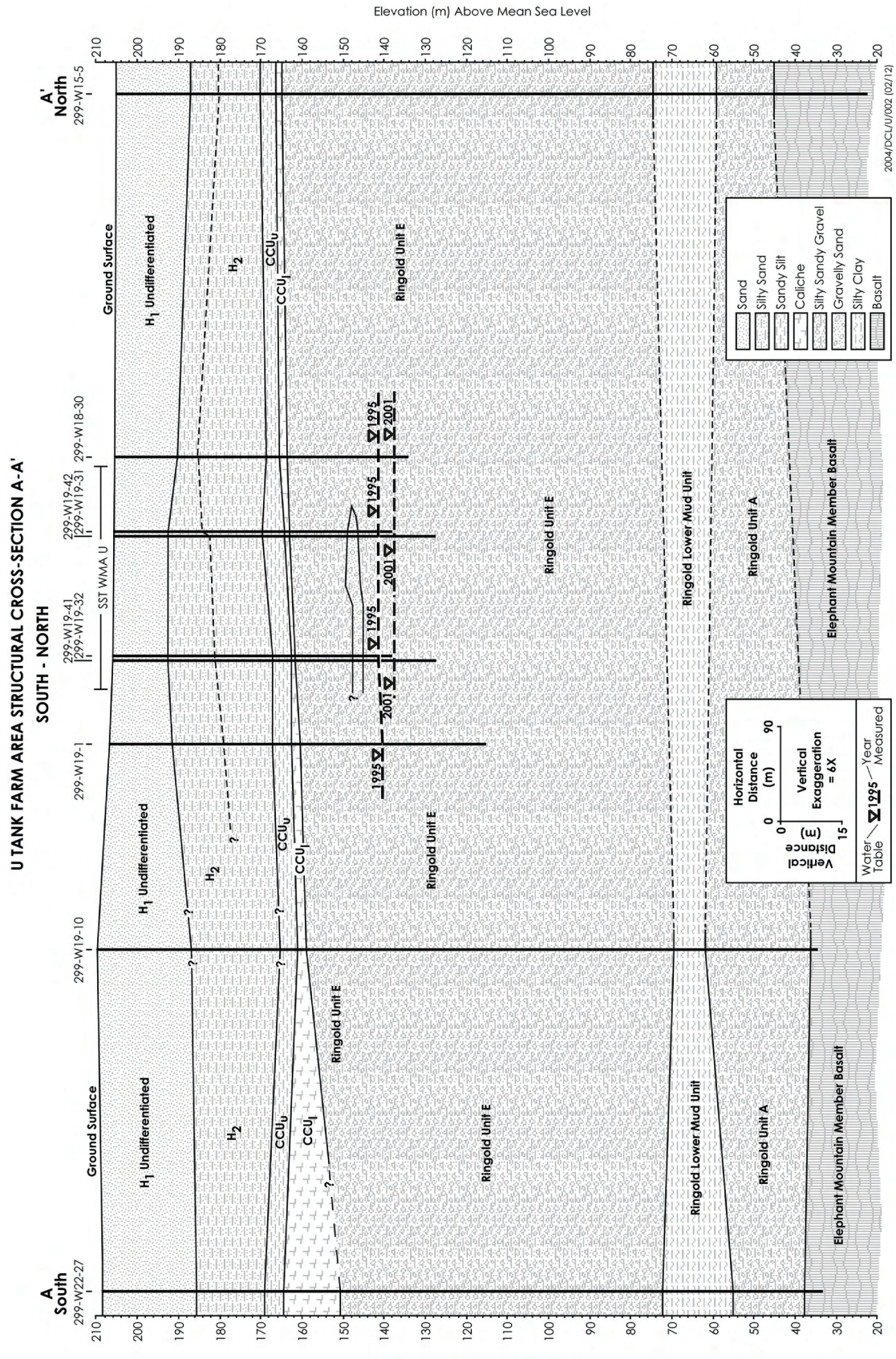

Figure 5.22. North–South Geologic Cross Section of Waste Management Area U (modified from Smith et al. 2001)

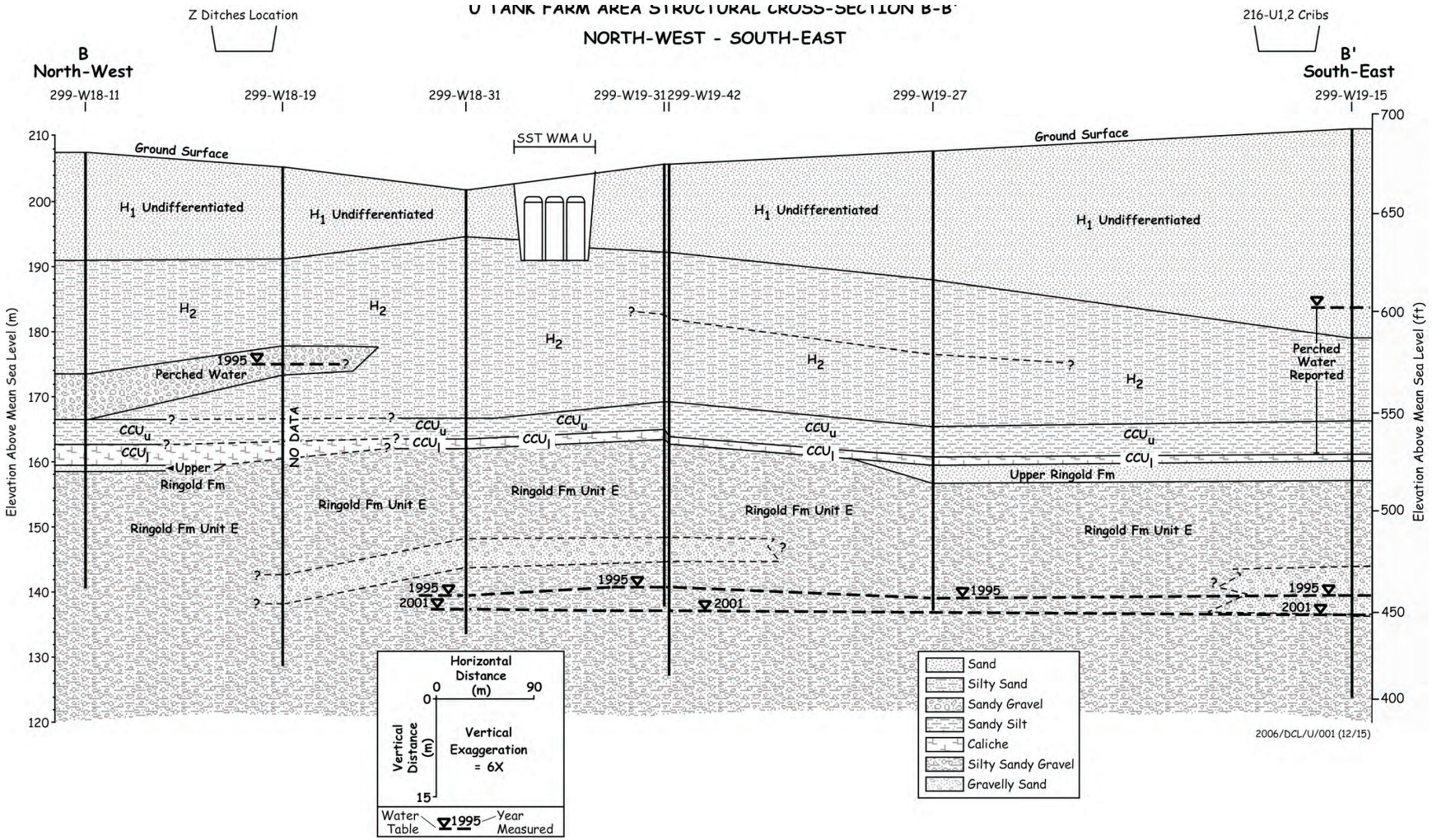

Figure 5.23. Northwest–Southeast Geologic Cross Section of Waste Management Area U (modified from Smith et al. 2001)

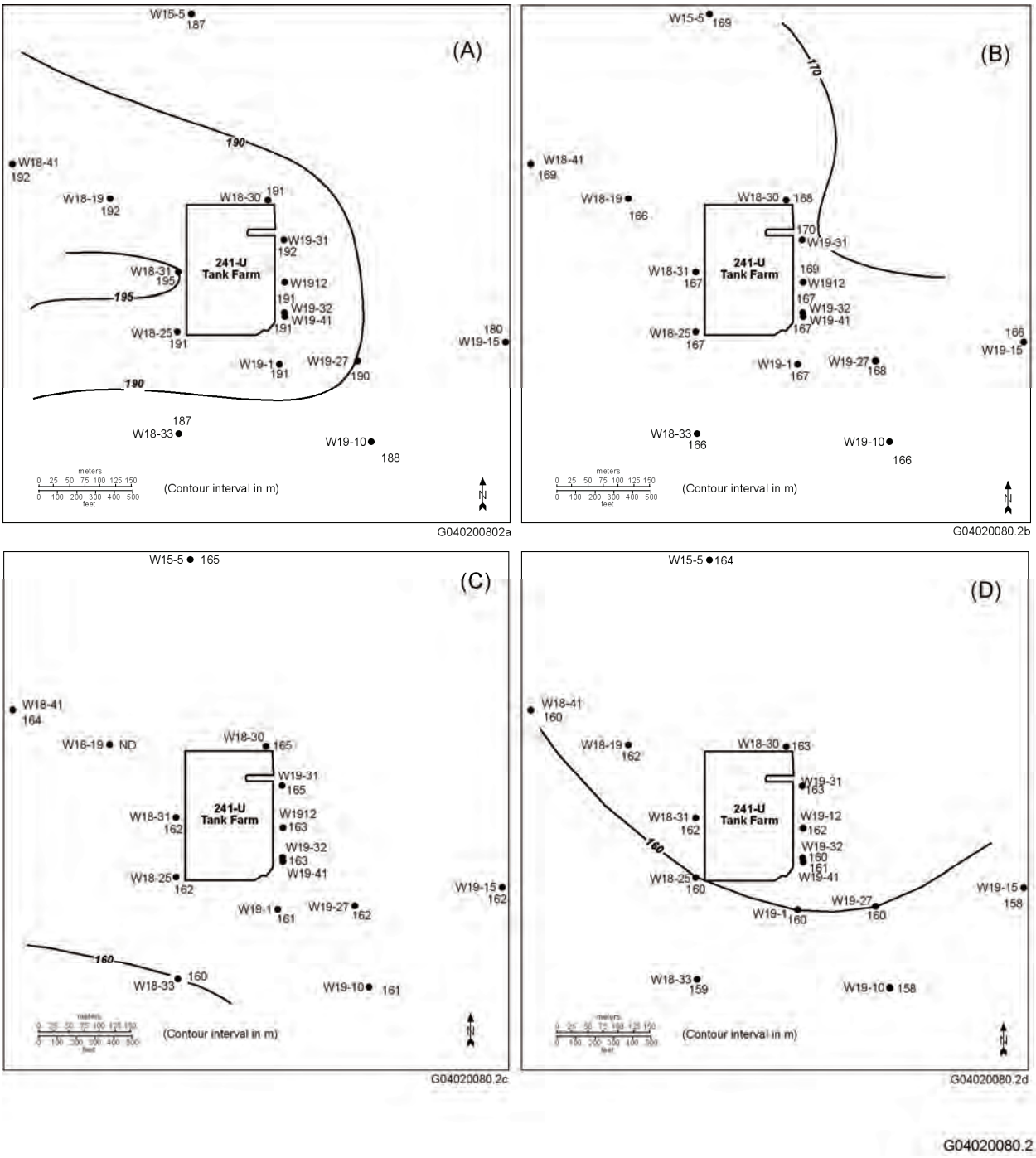

(A) Structure contour map on surface of Hanford formation, unit H2; equivalent to middle sand-dominated.

(B) Structure contour map on surface of upper Cold Creek unit.

(C) Structure contour map on surface of lower Cold Creek unit.

(D) Structure contour map on surface of Ringold Formation, member of Wooded Island, unit E.

Figure 5.24. Structure Contour Maps of Waste Management Area U (modified from Smith et al. 2001)

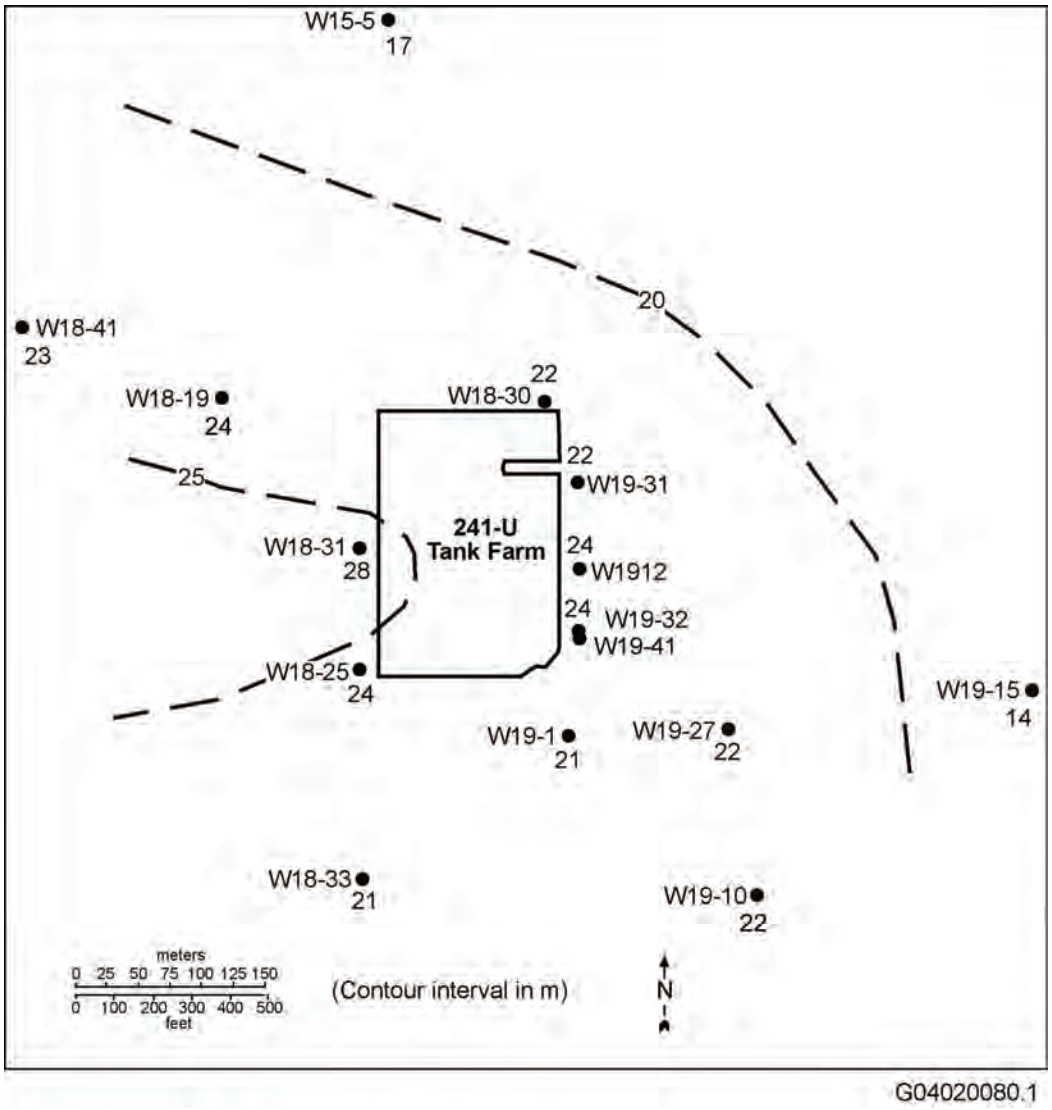

Figure 5.25. Isopach Map of the Hanford H2 Unit at Waste Management Area U (modified from Smith et al. 2001)

5.3.3.2 Ringold Formation

The Ringold Formation overlies the Elephant Mountain Member and consists of fluvial lacustrine sediments that were deposited by the ancestral Columbia River drainage system. Near the WMA, three units of the member of Wooded Island (Lindsey 1995) are present—in ascending order, these are unit A, the lower mud unit, and unit E. The member of Taylor Flat is absent beneath WMA U, although it is found to the southeast and northwest (Figures 5.20, 5.22, and 5.23).

Unit A, the lowest subunit, consists of fluvial gravels with intercalated sands. Unit A is up to 30 m (98 ft) thick and dips to the south-southwest (WHC 1991; Smith et al. 2001) (Table 5.6 and Figure 5.20). The lower mud unit, a lacustrine mud deposit, overlies unit A and is approximately 15 m (50 ft) thick. The lower mud unit is an aquitard and forms the bottom of the unconfined aquifer beneath WMA U. It is characterized by well-stratified clay and interbedded silt and silty sand (Singleton and Lindsey 1994).

Unit E is the uppermost sequence of the Ringold Formation beneath WMA U. Like unit A, unit E consists of fluvial gravels with intercalated sands. Where the lower mud unit is not present outside the WMA, it is commonly undistinguishable from unit A. Unit E is about 90 m (295 ft) thick, is the host stratum for the unconfined aquifer, and dips gently to the southwest (Figure 5.24) (Smith et al. 2001).

During preparation of this report, a basalt-rich gravel was identified below what has been interpreted as member of Taylor Flat sediments in the T-TX tank farm area. In wells 299-W19-45 and 299-W19-47, up to 80% of the gravels are basaltic, which is more like the CCU side-stream facies than Ringold Formation unit E gravels. This gravel has been identified in the northern 200 West Area (Table 4.1), and seems to run roughly north-south. The basalt-rich gravel lies above the water table and does not affect groundwater flow but could affect flow through the vadose zone. It is not shown in Figures 5.22 or 5.23.

5.3.3.3 Cold Creek Unit

The CCU unconformably overlies the Ringold Formation (Wood and Jones 2003) and basalt-rich gravel and is divided into two subunits, the CCU_l and the CCU_u. The CCU_l is a caliche-rich zone about 1 to 2 m (3 to 6 ft) thick that developed on the paleo-surface of the Ringold Formation. It is a calcium carbonate-rich layer with locally derived basalt detritus, silt-rich deposits, and reworked Ringold Formation material. The calcium carbonate zones are probably discontinuous and occur as layers, nodules, and clast coatings. The upper subunit (CCU_u) is a silt-rich, sandy soil about 3 to 6 m (9 to 15 ft) thick that is relatively uniform and shows little depositional structure. Both subunits dip slightly to the southwest (Figure 5.24). The fine-grained nature of this unit has significant influence on the vertical movement of moisture in the vadose zone. Perched water above the CCU has been found to the east beneath the 216-U-14 ditch and 216-U-1 and U-2 cribs in the past.

5.3.3.4 Hanford Formation

The Hanford formation consists of sediments deposited during several episodes of cataclysmic flooding and consists of pebble-to-boulder gravel, fine- to coarse-grained sand, and silt. The Hanford formation is divided into two major sequences based on lithology beneath WMA U—lower sand-dominated (H2) and upper gravel-dominated sequences (H1).

The lower sand-dominated sequence (H2) consists primarily of a sand layer that averages about 24 m (79 ft) thick across WMA U (Figure 5.25) (Wood and Jones 2003). It thins to the east and northeast and dips to the east as well (Figure 5.24, plot A). Repetitive sequences of very thin, flat-lying lamina of silt and sand have been observed in intact core samples and may provide a sedimentary structure that influences moisture movement in the vadose zone.

The upper gravel-dominated sequence (H1) is distinguished from the sand-dominated sequence by a marked difference in grain-size distribution. A significant fraction of the upper unit is gravels with less sand, indicating deposition in a higher-energy environment. In the vicinity of WMA U, the contact between the two units is irregular. The unit varies between 2 and 7 m (8 and 22 ft). Beneath WMA U, the contact between the two sequences is near the base of the original excavation along the eastern edge of the tank farm. The contact is closer to the surface toward the west and northwest and therefore has had little influence on tank waste migration.

5.3.3.5 Holocene Deposits and Backfill

Holocene-aged deposits in the 200 West Area are dominated by eolian sand. These sands tend to consist of very fine- to medium-grained, occasionally silty sands. Eolian deposits were removed from WMA U during construction of the tank farm. The tank farms were excavated to a depth of about 12 m (40 ft) during construction and backfilled with silt, sand, and gravel of the Hanford formation and eolian sand.

5.4 Geology of the 200 East Area Single-Shell Tank Farms

SST farms A, AX, C, B, BX, and BY are located in the 200 East Area (Figure 5.1). Because of their proximity, WMAs A-AX and C are discussed together.

5.4.1 Geology of Waste Management Areas A-AX and C

This section provides a detailed description of geologic and stratigraphic relationships beneath tank farms A, AX, and C and adjoining areas of the 200 East Area (Figure 5.26). The discussion of these parameters is based on a compilation of historical information (Brown 1959; Price and Fecht (1976a, 1976b, and 1976f; Tallman et al. 1979; Lindsey et al. 1992; Jones et al. 1998; and Williams et al. 2000) and some new interpretations allowed by new borehole emplacement and research conducted in calendar year 2003 (Williams and Narbutovskih 2003, 2004). Detailed geologic and geochemical characterization of recent boreholes is given in Brown et al. (2006). The most recent detailed description of the A, AX, and C tank farms is that in Wood et al. (2003), and most of the discussion presented below is built on that report.

Numerous wells have been drilled over the years in the vicinity of the SSTs. Table 5.7 provides geologic contacts for those wells used in the following geologic discussion and cross sections. Figure 5.27 shows well locations. For some wells, several interpretations of stratigraphic contacts or "picks" have been rendered by various authors over the years. Most of the illustrations presented here reflect picks represented by Wood et al. (2003) with some modification arising from new well logs.

The A, AX, and C tank farms were built in Hanford formation sediments. Based on Wood et al. (2003), seven stratigraphic units lie beneath WMAs A-AX and C. From oldest to youngest, the primary geologic units are

- CRBG
- undifferentiated CCU fine unit and/or Ringold Formation (CCU/R)
- undifferentiated Hanford formation gravel and/or CCU gravel and/or Ringold Formation, unit A (H3/CCU/R)
- Hanford formation – lower gravel-dominated sequence (H3 unit)
- Hanford formation – sand-dominated sequence (H2 unit)
- Hanford formation – upper gravel-dominated sequence (H1 unit)
- recent deposits.

The CCU is equivalent to the "Plio-Pleistocene Unit" in Wood et al. (2003). Cross sections (Figures 5.28 through 5.37) illustrate the distribution and thicknesses of these units.

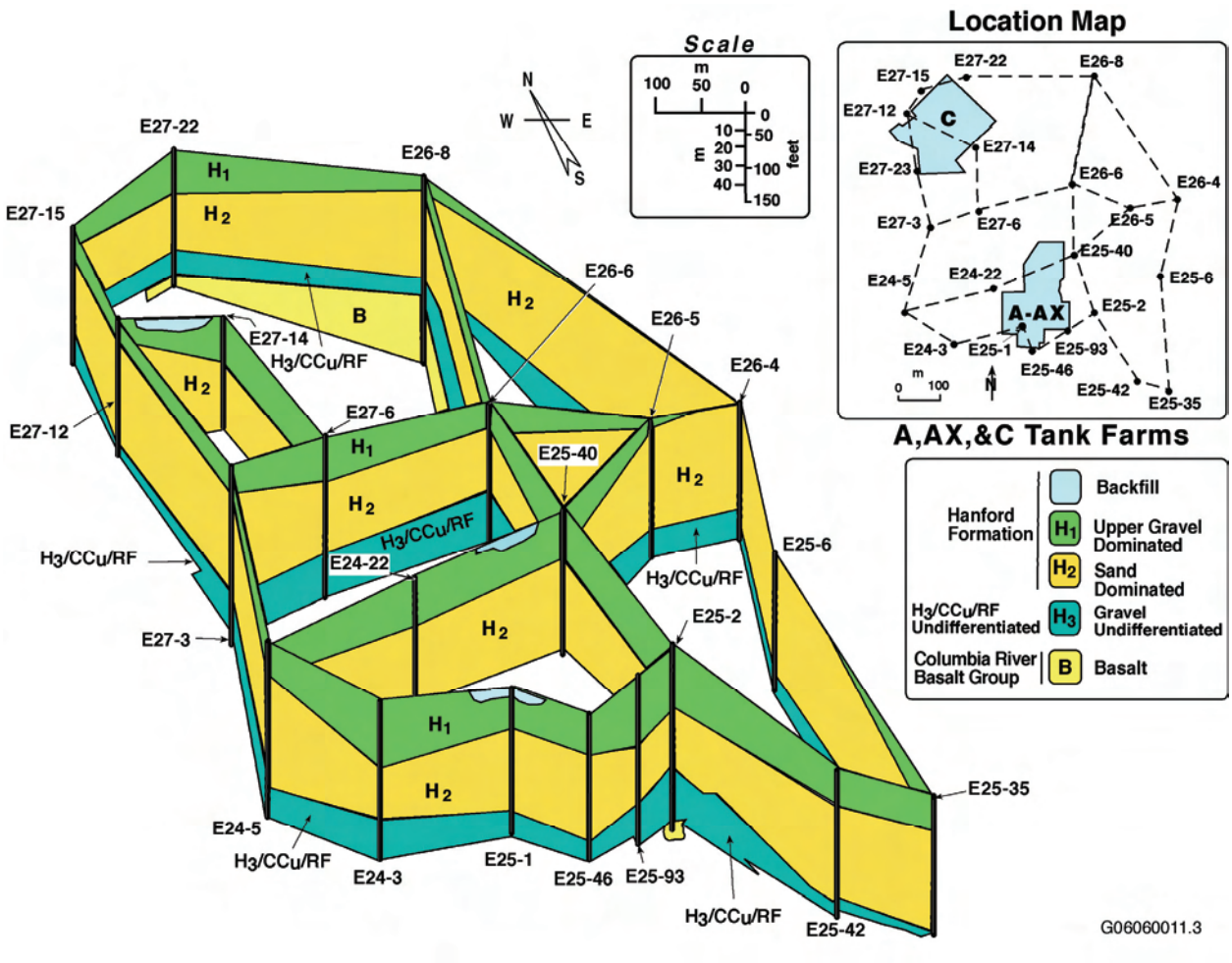

Figure 5.26. Fence Diagram of the A, AX, and C Tank Farms

5.4.1.1 Columbia River Basalt Group

The Elephant Mountain Member is the uppermost basalt flow beneath the A, AX, and C tank farms and lies at an elevation of approximately 100 m (328 ft) above mean sea level and dips gently to the southwest toward the axis of the Cold Creek syncline (Figure 5.36) (Price and Fecht 1976a, 1976b, 1976f; DOE 1988). Up to 15 m (50 ft) of topographic relief exists on the basalt surface as a result of tectonic deformation and/or erosion.

Four boreholes (299-E25-2, 299-E26-8, 299-E27-3, and 299-E27-6) in WMAs A-AX and C extend to the top of basalt. One borehole (299-E26-8) fully penetrated the Elephant Mountain Member and advanced through the first sedimentary interbed (Rattlesnake Ridge) into the underlying Pomona Member of the CRBG (Figure 5.33). In this borehole, the Elephant Mountain Member and the Rattlesnake Ridge Interbed were 27 m (90 ft) and 15 m (50 ft) thick, respectively.

Table 5.7. Stratigraphic Contact Elevations for Boreholes in Waste Management Areas A-AX and C[(a)]

Well Number	Ground Surface Elevation ft[(b)]	Contact Picks (Elevation in ft)[(b)]					
		Top H1 gravel	Top H2 sand	Top H3 gravel	Top CCU_u/R	Top CCU_l/R	Top of Basalt
E24-4	700	670	615	NP	NP	440	
E24-5	699	699	644	NP	NP	439	
E24-13	691	691	571	NP	421	401	
E24-20	689	689	589	NP	414	409	
E25-1	694	663	609	NP	434	414	
E25-2	677	663	557	472	422	412	322
E25-6	662	NP	662	472	397	392	
E25-7	660	NP	660	340	NP	395	
E25-35	675	675	605	465	415	405	
E25-41	672	672	572	472	417	402	
E25-42	686	686	600	460	NP	415	
E25-46	698	698	605	NP	425	415	
E25-48	683	683	593	463	423	403	
E25-93	680	669	560	435	NP	375	
E26-4	649	649	635	515	425	415	
E26-5	652	652	632	507	NP	422	
E26-6	655	655	595	485	410	406	
E26-8	620	620	585	NP	NP	NP	370
E27-3	685	685	650	NP	408	NP	333
E27-4	672	646	562	NP	NP	432	
E27-6	675	674	575	NP	420	409	332
E27-12	661	661	591	NP	NP	436	
E27-13	670	670	550				
E27-14	659	689	650	NP	NP	434	
E27-15	654	654	593	NP	NP	429	
E27-21	673	673	608	NP	NP	433	
E27-22	632	632	552	NP	NP	417	364
E27-23	675	664	575	NP	NP	450	

(a) Bjornstad (2004) and Wood et al. (2003).

(b) Multiply by 0.3048 to convert feet to meters.

NP = Unit not present.

CCU_u/R = Undifferentiated Cold Creek unit/Ringold Formation fine-grained sediments.

CCU_l/R = Undifferentiated Cold Creek unit/Ringold Formation coarse-grained sediments.

H1 = Hanford formation, unit H1; equivalent to upper gravel-dominated.

H2 = Hanford formation, unit H2; equivalent to sand-dominated.

H3 = Hanford formation, unit H3; equivalent to lower gravel-dominated.

R_{wia} = Ringold Formation, Member of Wooded Island, unit A.

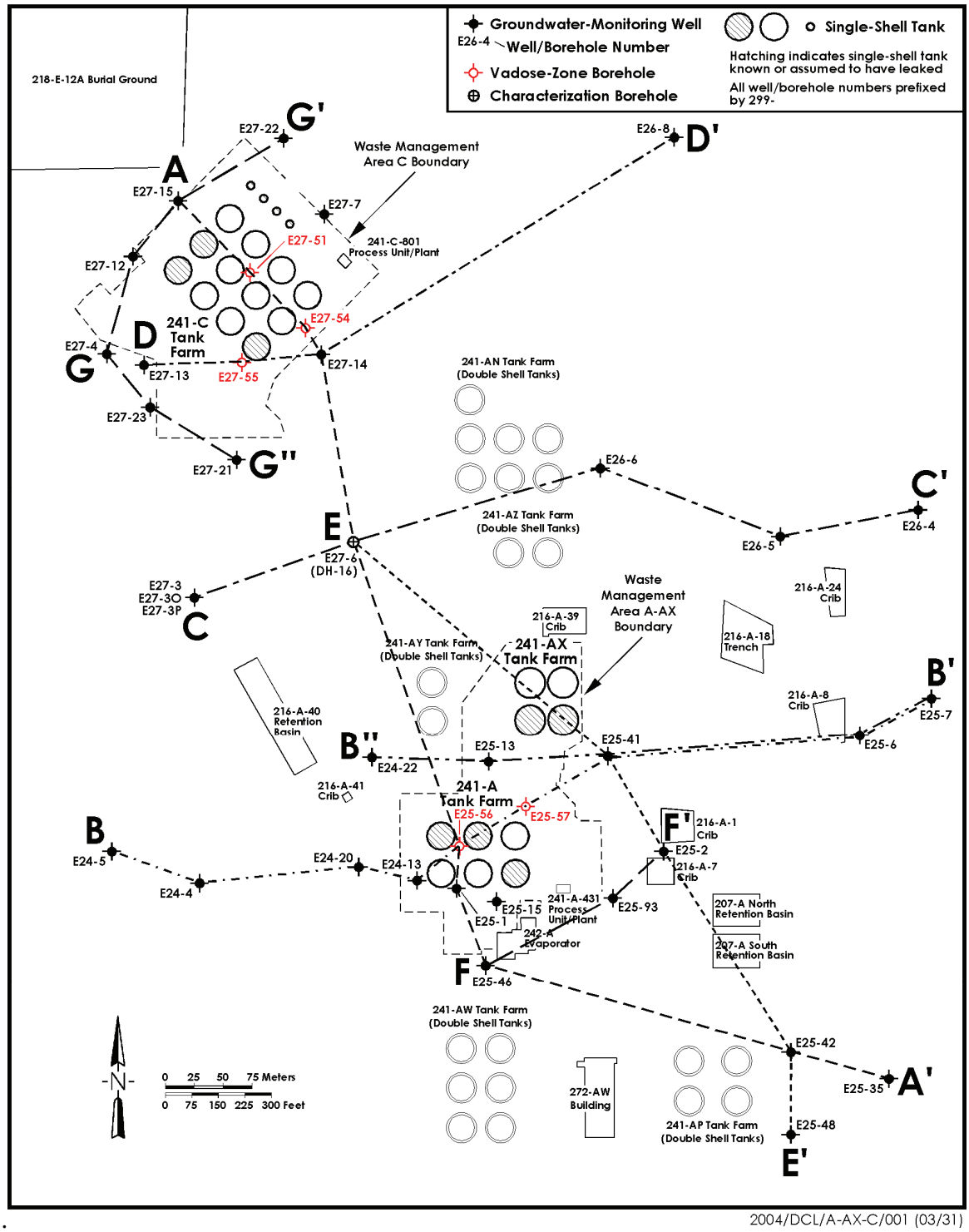

Figure 5.27. Well and Cross-Section Locations for the A, AX, and C Tank Farms and Adjoining Areas of the 200 East Area

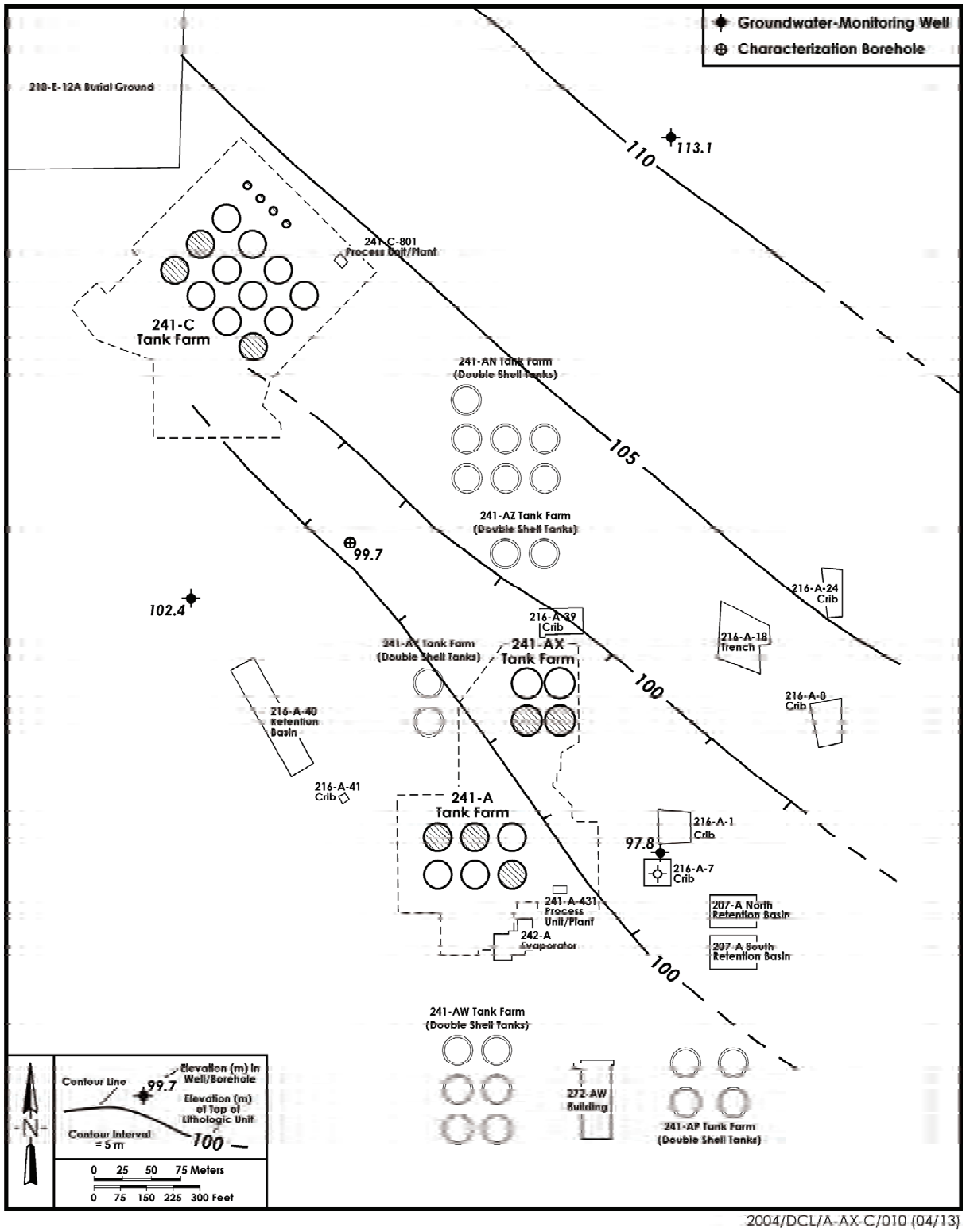

Figure 5.28. Structure Contour Map of the Top of Basalt at the A, AX, and C Tank Farms

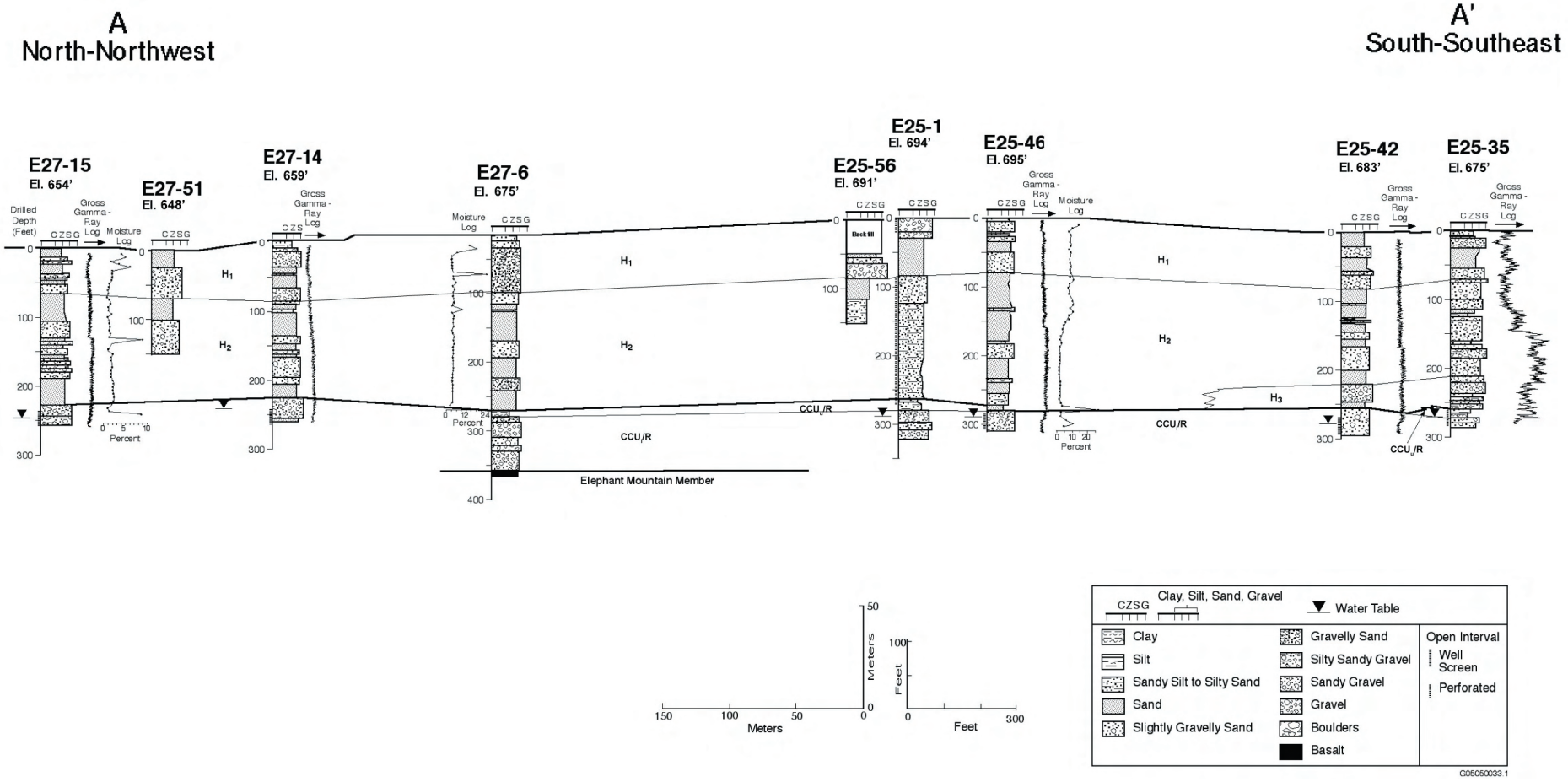

Figure 5.29. **C**ross-Section A-A' at the A, AX, and C Tank Farms (modified from Wood et al. 2003)

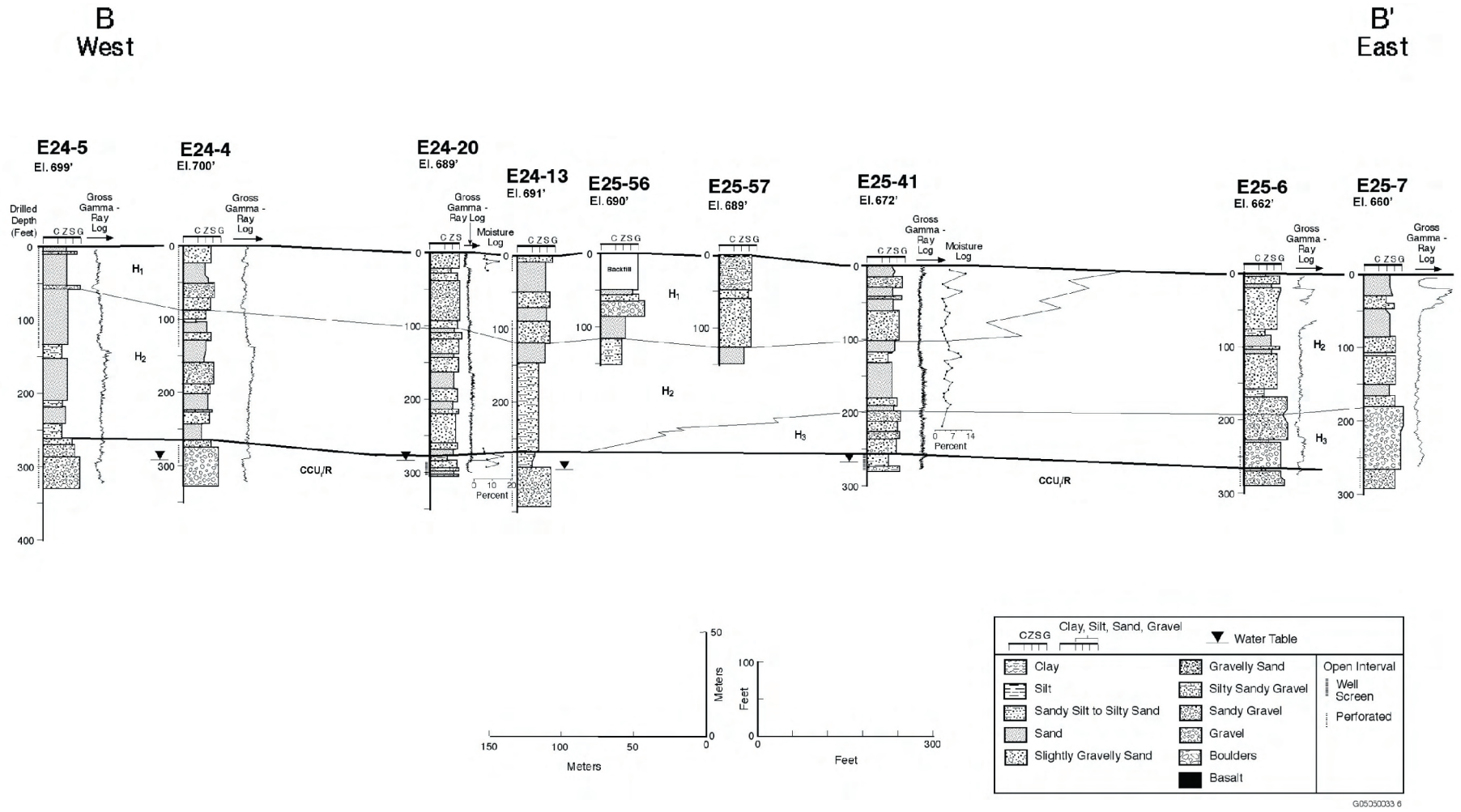

Figure 5.30. Cross-Section B-B' at the A, AX, and C Tank Farms (modified from Wood et al. 2003)

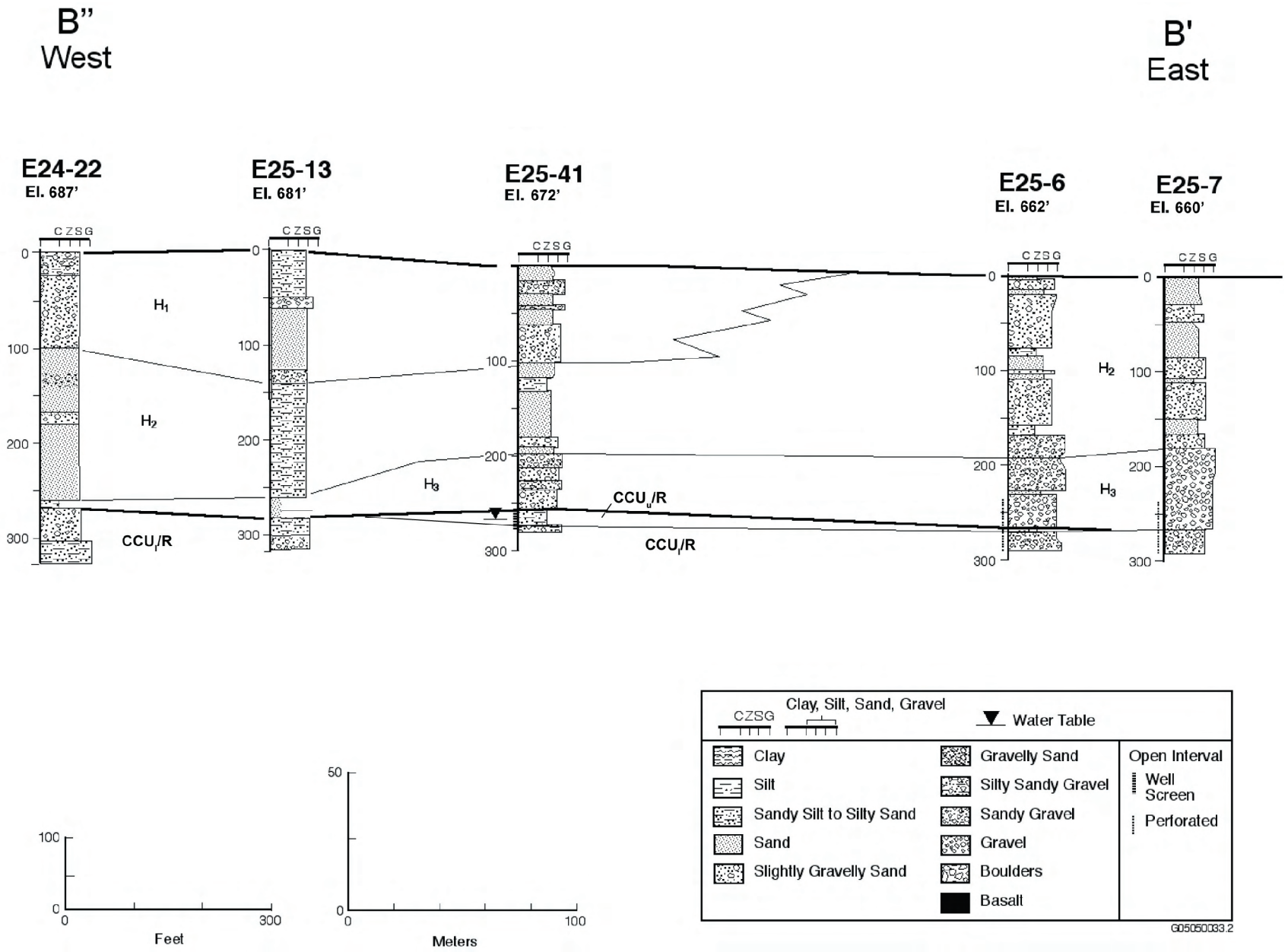

Figure 5.31. Cross-Section B"-B' at the A, AX, and C Tank Farms (modified from Wood et al. 2003)

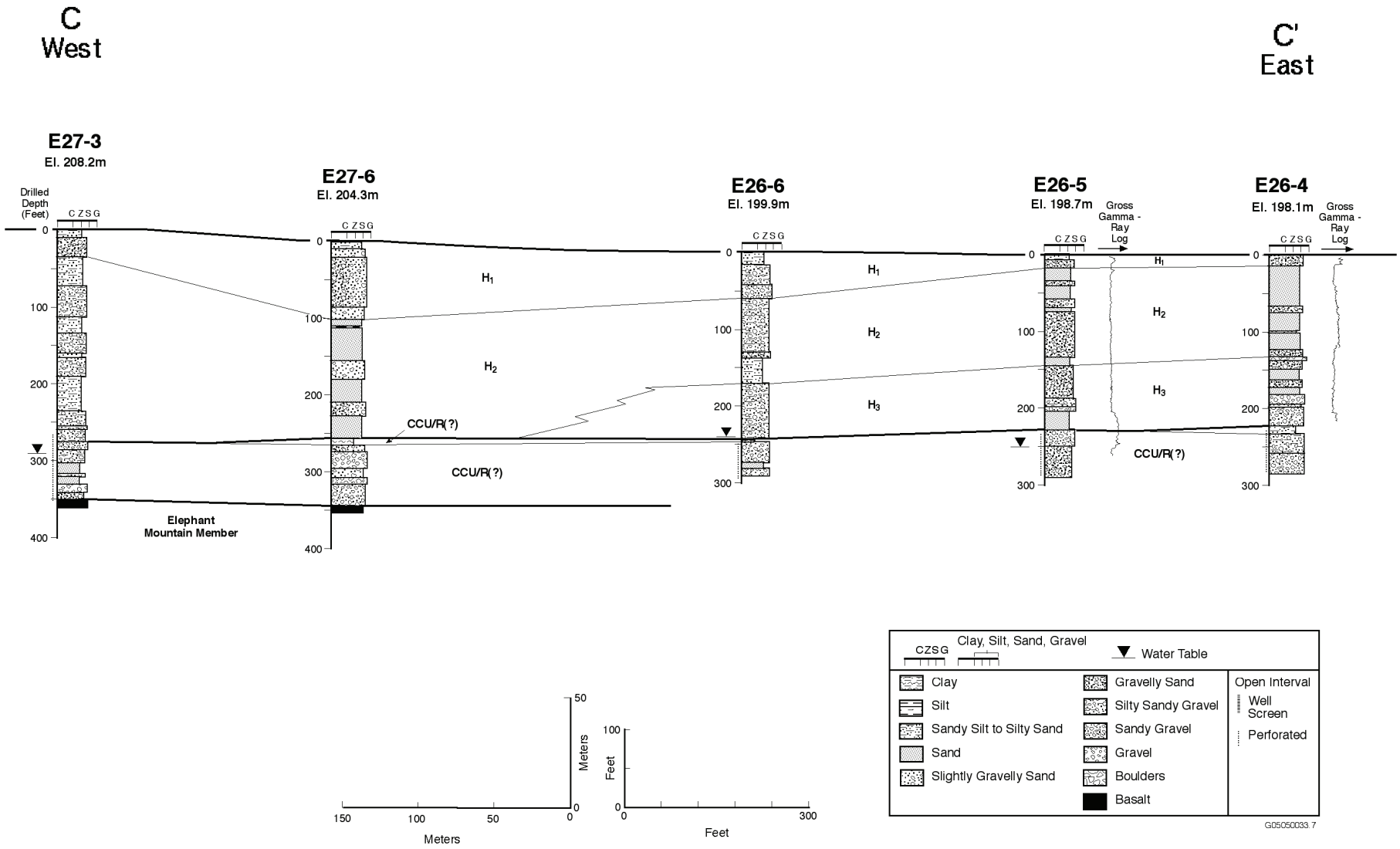

Figure 5.32. Cross-Section C-C' at the A, AX, and C Tank Farms (modified from Wood et al. 2003)

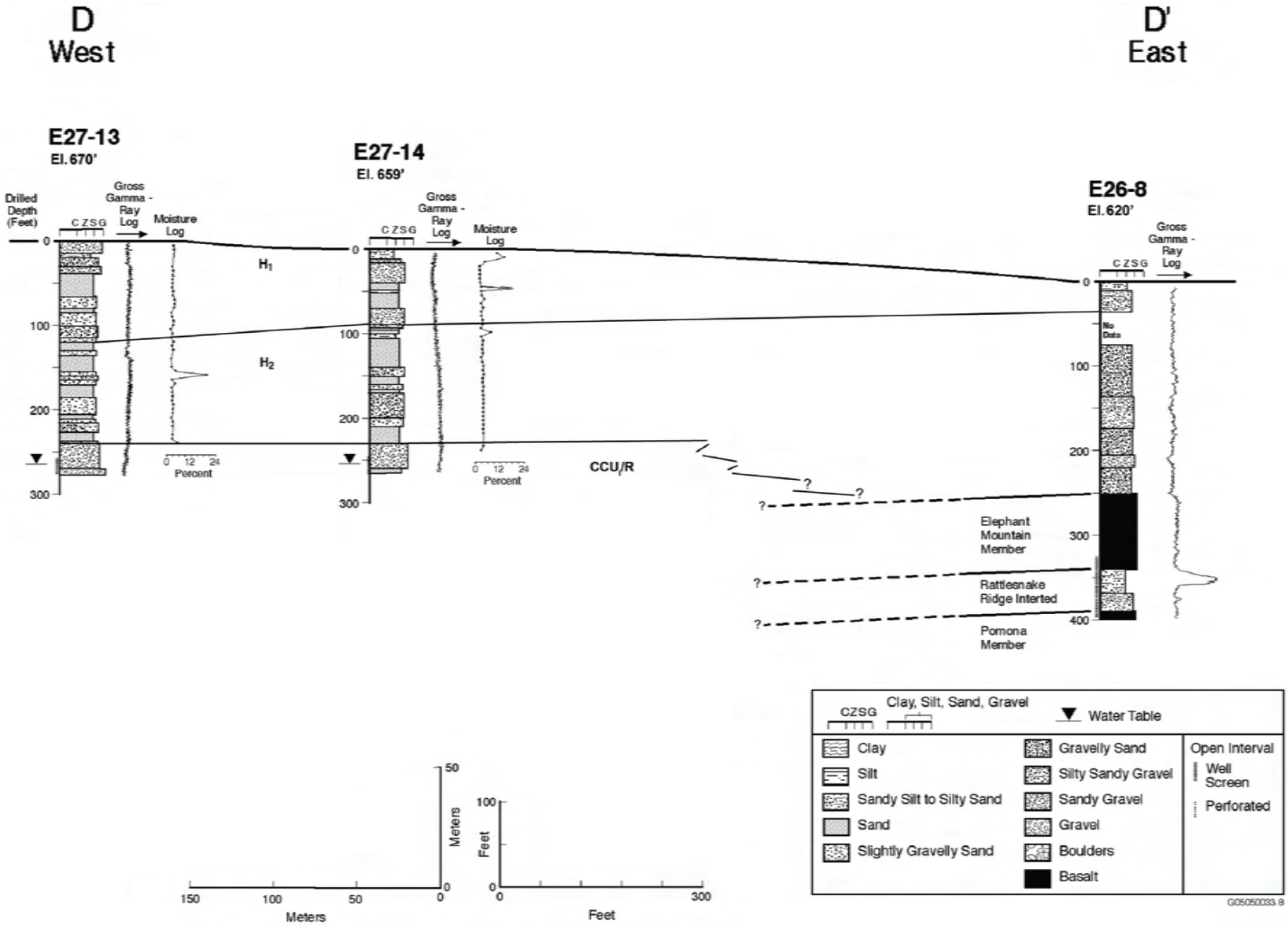

Figure 5.33. Cross-Section D-D' at the A, AX, and C Tank Farms (modified from Wood et al. 2003)

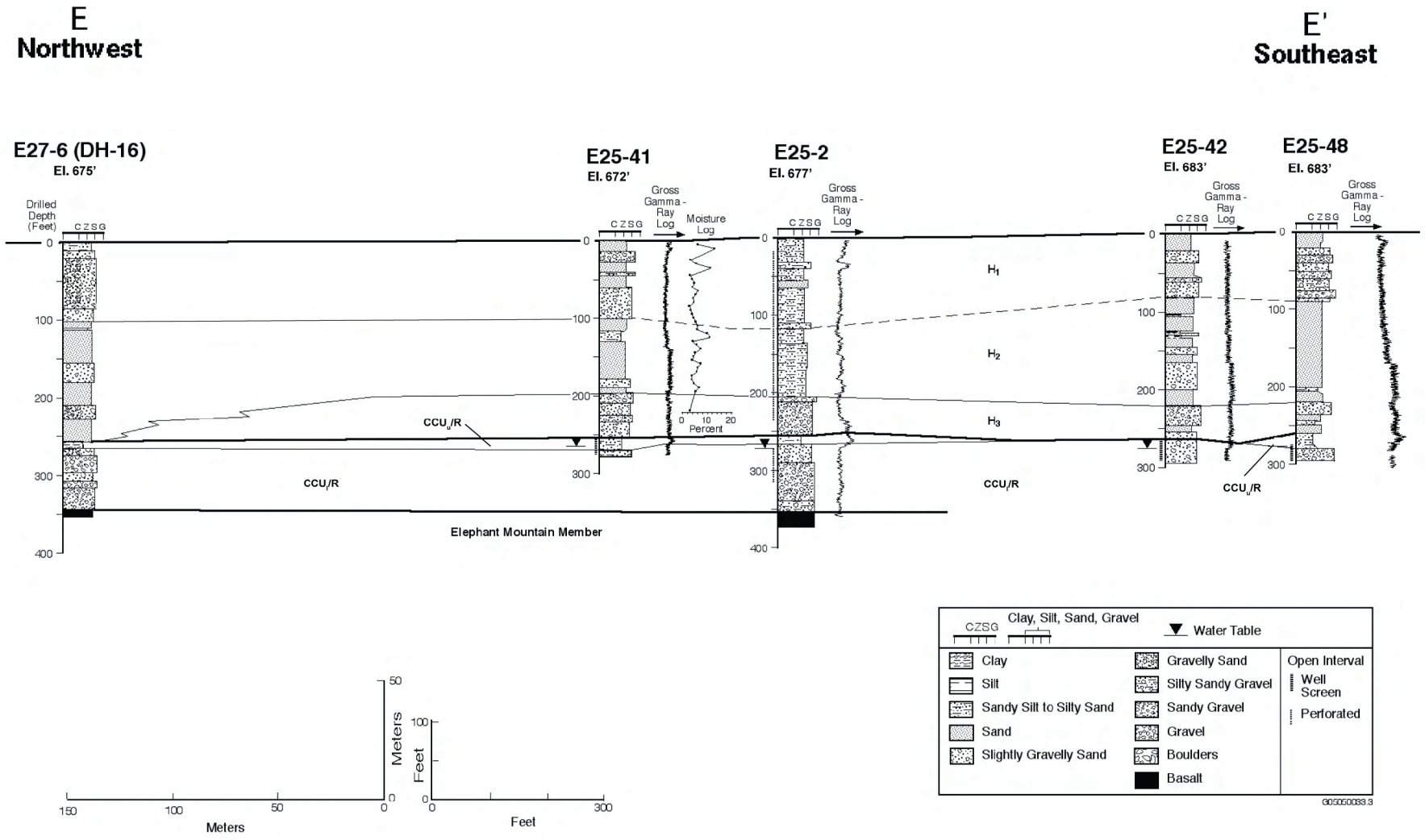

Figure 5.34. Cross-Section E-E' at the A, AX, and C Tank Farms (modified from Wood et al. 2003)

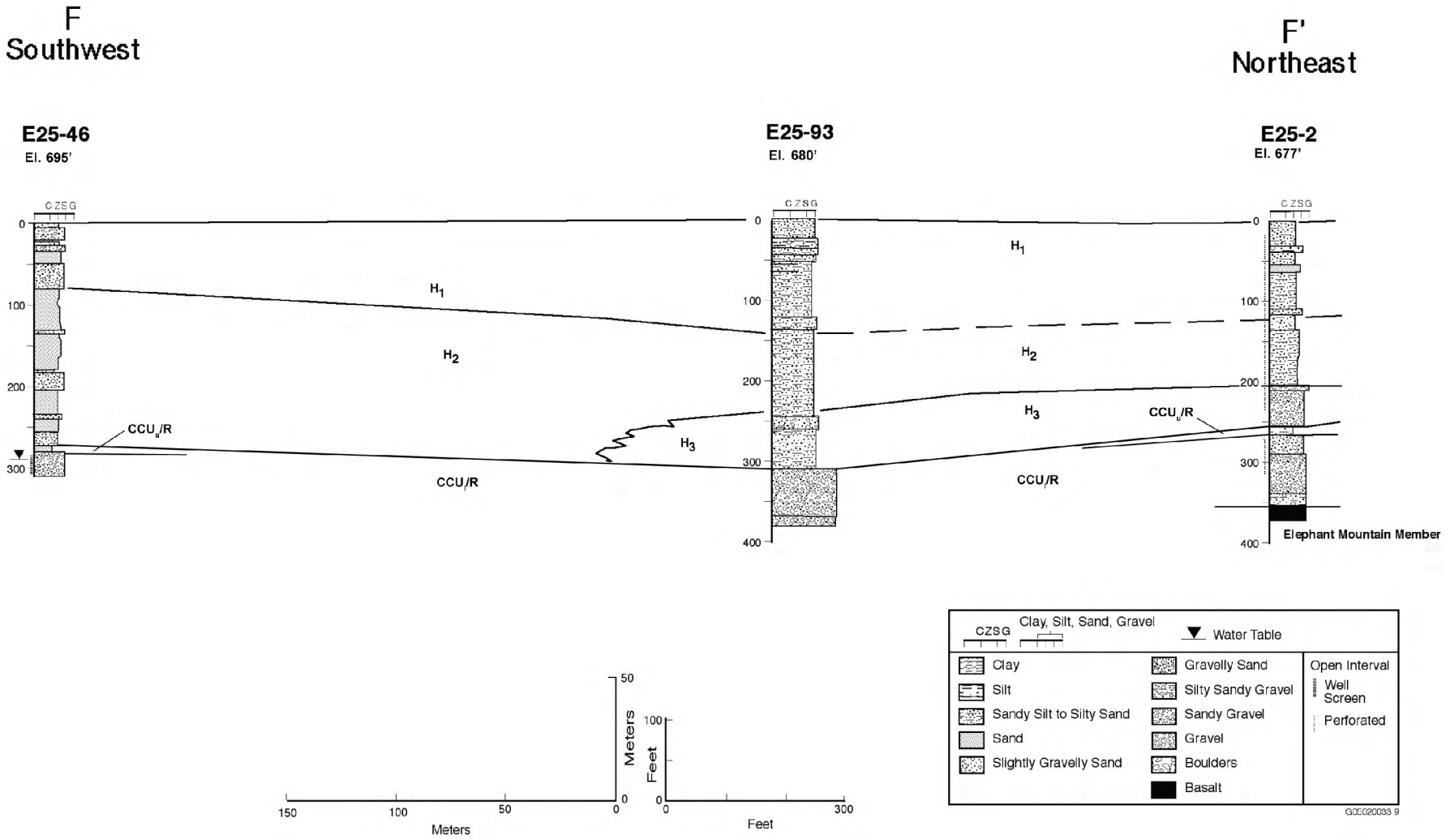

Figure 5.35. Cross-Section F-F' at the A, AX, and C Tank Farms (modified from Wood et al. 2003)

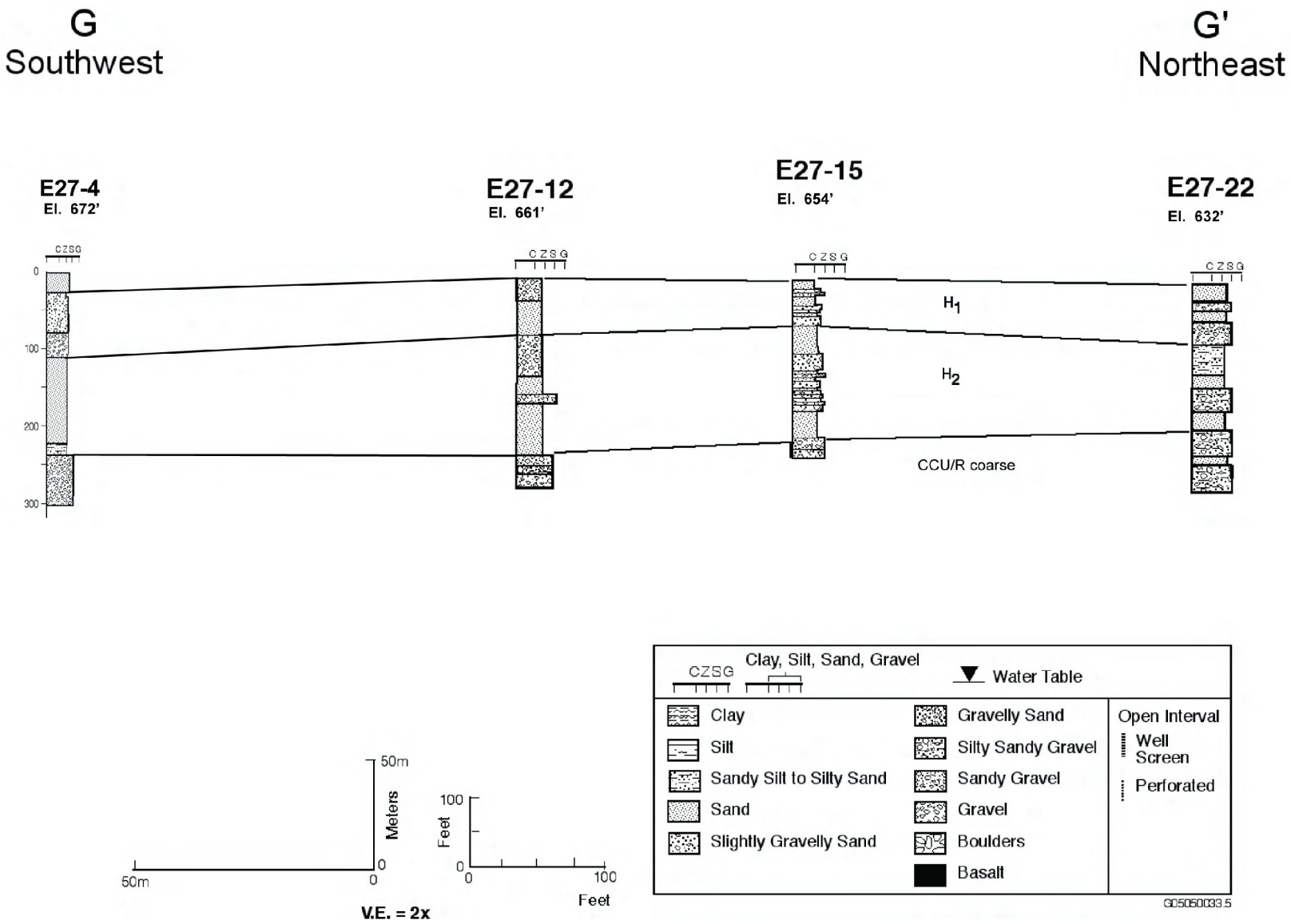

Figure 5.36. Cross-Section G-G' at the A, AX, and C Tank Farms (modified from Wood et al. 2003)

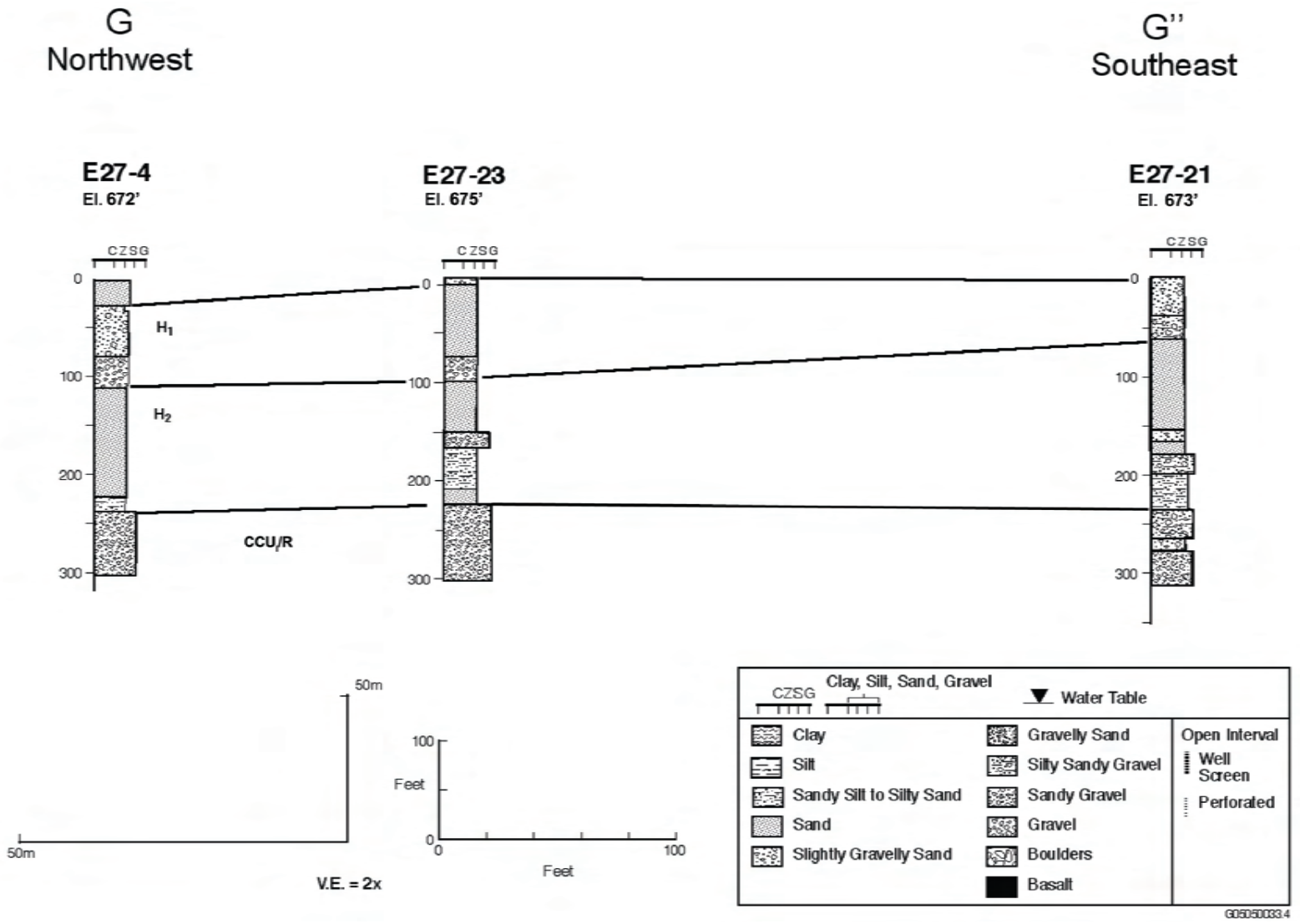

Figure 5.37. Cross-Section G-G″ at the A, AX, and C Tank Farms (modified from Wood et al. 2003)

5.4.1.2 Undifferentiated Hanford and/or Cold Creek Unit and/or Ringold Formation

WMAs A-AX and C lie along the edge of a paleochannel that eroded much or all of the Ringold Formation during CCU and/or Hanford time. Because of the difficulty in distinguishing reworked Ringold Formation gravels and Pre-Missoula mainstream Columbia River gravels from original Ringold Formation gravels, these units are undifferentiated here and shown on the cross sections as CCU-Ringold (CCU/R) or as Hanford-CCU-Ringold gravels (H3/CCU/R). A similar problem arises with fine-grained sediments overlying the basal gravels. In places, these fine-grained layers appear to correlate to Ringold Formation sediments, based in part on color, but in other areas appear to be more closely related to CCU or even Hanford formation sediments. Therefore, the lower fine-grained sediments are also undifferentiated here.

Gravelly facies immediately overlying basalt within most of the study area belong to the H3/CCU/R. An exception is in the northeast of WMA C near borehole 299-E26-8, where the top of basalt rises above the CCU_l/R, leaving Hanford formation sediments lying directly on top of basalt (Figure 5.33). The CCU_l/R consists of predominantly sandy pebble- to cobble-sized gravel with occasional boulders. Mineralogically, the sand fraction consists of 15 to 60% basalt grains with generally less than 1 wt% calcium carbonate. The total thickness of this unit is less than 27 m (90 ft), based on a limited number of boreholes where the upper and lower boundaries are represented. The top of undifferentiated Hanford-CCU-Ringold gravels ranges from about 120 to 130 m (390 to 425 ft) elevation above mean sea level.

A coarse-grained unit, undifferentiated Hanford-CCU-Ringold gravels, is found in most boreholes beneath WMA A-AX but not beneath WMA C. It occurs at a depth of about 79 m (260 ft) (Figures 5.28 through 5.37) and ranges in thickness from 0-7 m (0-21 ft). Descriptions of this unit vary significantly, which may be due to 1) subjective descriptions and/or interpretations by different drillers and geologists; 2) heterogeneities within the unit, which may include multiple lithologic units (i.e., CCU silts overlying Ringold Formation mud); or 3) a combination of the above. Where present, this fine-grained unit is described in about half of the boreholes as a blue-, gray-, or olive-colored clay or mud; remaining borehole logs describe the unit as a tan to brown sandy silt to “heavy” silt, which may display a laminated to mottled structure. The former description fits that of Ringold Formation paleosol facies (DOE 1988), whereas the latter fits descriptions for the Cold Creek silt facies (Wood et al. 2000), interpreted as eolian-overbank in origin. Unlike most other fine-grained units in the 200 Areas, the undifferentiated Cold Creek silt and/or Ringold Formation mud unit is generally noncalcareous, containing only a few weight percent or less calcium carbonate.

Some gross gamma-ray logs show a moderate increase in activity occasionally accompanied by an increase in moisture. No perched water was noted on top of the sequence (Caggiano and Goodwin 1995), but the water table was higher in the past. Thus, the increased moisture content may be a remnant of a higher water table.

5.4.1.3 Hanford Formation

The Hanford formation makes up the majority of the suprabasalt sedimentary sequence beneath WMAs A-AX and C, ranging in thickness from 61 to 83 m (200 to 275 ft). The Hanford formation has been divided into three informal units (H1, H2, and H3 from top to bottom) in the 200 East Area. These units do not correspond to similarly named units in the 200 West Area.

The H3 unit is the Hanford formation's lower gravel-dominated sequence in the area and overlies undifferentiated Cold Creek/Ringold Formation deposits. This sequence is equivalent to the lower coarse-grained unit of the Hanford formation of Last et al. (1989), to the lower gravel–dominated sequence of Lindsey et al. (1992), and to the Hanford formation H3 sequence of Lindsey et al. (1994).

The H3 unit consists of clast-supported, sandy, pebble to boulder gravel to matrix-supported pebbly sand. This unit appears in the east and southeast parts of the study area, but appears to be missing from beneath most of WMA A-AX and all of WMA C. The unit is probably absent from these areas because of lateral facies changes that take place between gravel-dominated facies to the north and sand-dominated facies to the south away from the axis of primary flood channel that exists north and east of the study area. The surface of the H3 unit slopes to the south and west, with the highest elevations occurring in the northeast and east portions of the study area.

The H2 unit is continuous beneath WMAs A-AX and C. It overlies the undifferentiated CCU/R units or the H3 unit where present. The H2 unit is equivalent to the middle sand unit (Last et al. 1989), the fine sequence of Lindsey et al. (1992), and the Hanford formation H2 sequence of Lindsey et al. (1994).

Dominantly a fine- to coarse-grained sand, the H2 unit also contains lenses of silty sand to slightly gravelly sand. Minor sandy gravel to gravelly sand beds occur sporadically. Consolidation ranges from loose to compact. Cementation is very minor or absent. Silt lenses and thinly interbedded zones of silt and sand are common but are not abundant in the H2 unit. These thin (<0.3 m [1 ft]) fine-grained zones generally cannot be correlated between boreholes and are not reflected in the gross gamma-ray logs or moisture data. Sampling intervals are probably too large to detect such thin zones. The fine structure observed in some older gross gamma-ray logs may reflect changes in the silt content that were not detected during drilling.

The upper portion of H2 may have been scoured by a southeast trending Ice Age flood channel, associated in part with deposition of the overlying gravelly H1 unit. This is indicated by a south to southeast-trending trough present at the top of the H2 unit (Figures 5.29, 5.30, 5.31, 5.34, and 5.35). Furthermore, over 40 m (130 ft) of relief exists on top of the H2 unit at right angles to the axis of this trough (Figures 5.29 and 5.30). These same figures show that H2 is interpreted to occur at the surface in the easternmost part of the study area where the overlying H1 unit is missing.

The H1 upper gravel sequence is equivalent to the upper coarse-grained unit of Last et al. (1989), the upper gravel sequence of Lindsey et al. (1992), and the Hanford formation H1 sequence of Lindsey et al. (1994). This unit consists of predominantly loose, sandy gravel to gravelly sand, with minor beds of sand to silty sand. Coarser beds may contain boulder-sized materials. Occasional thin, discontinuous lenses of fine sand and silt may also be present.

Figures 5.29 through 5.32 show the H1 unit thickens near the center of the study area and beneath WMA A-AX where it reaches approximately 30 m (100 ft) thick.

5.4.1.4 Recent Deposits

Two types of recent deposits are present in WMAs A-AX and C—1) eolian sand and silt and 2) backfill material. Backfill is found within the tank farms and other disturbed areas. Fine to medium sand to silty sand caps the sedimentary sequence outside the tank farms. These fine-grained eolian deposits are up to 6 m (20 ft) thick and contain up to 10 wt% calcium carbonate associated with recent soil development.

5.4.2 Geology of Waste Management Area B-BX-BY

The geology of the B, BX, and BY tank farms and vicinity is well understood as a result of several decades of site characterization activities. It has been described in numerous reports, including Price and Fecht 1976c, 1976d, 1976e; Tallman et al. 1979; Last et al. 1989; Connelly et al. 1992a; DOE-GJO 1997; Wood et al. 2000; and Lindsey et al. 2001a.

The B, BX, and BY tank farms were constructed into the upper Hanford formation sediments underlying the 200 East Area, along the north limb of the Cold Creek syncline (Figure 4.1). The upper surface of Cold Creek bar in the 200 East Area forms a broad plain at about 210 m (700 ft) elevation. The WMA is located on the grade that slopes gently to the northeast from the Cold Creek bar.

The main source of geologic information for the WMA is borehole information (Figure 5.38 and Table 5.8). Stratigraphic units underlying or adjacent to these tank farms (in ascending order) include CRBG, the Miocene- to Pliocene-age Ringold Formation, the CCU, the Hanford formation, and backfill materials (Figure 5.39 and Table 5.9). More detailed geologic cross sections through the WMA are shown in Figures 5.41 through 5.43. Detailed physical and geochemical characterizations of recently drilled vadose zone boreholes have been described in Lindenmeier et al. (2002, 2003) and Serne et al. (2002a).

5.4.2.1 Columbia River Basalt Group

The bedrock underlying the B, BX, and BY tank farms is the CRBG; the bedrock strikes northwest-southeast with a southwest dip into the Cold Creek syncline (Figure 4.4). The uppermost basalt unit is the Elephant Mountain Member of the Saddle Mountain Basalt. It is also the base of the unconfined aquifer in the WMA B-BX-BY area. The Elephant Mountain Member is at depths of 70 to 100 m (230 to 320 ft). There is about 8 m (26 ft) of relief on the surface of the basalt, which is mainly the result of post-basalt erosion. However, the orientation of the relief on the top of basalt also corresponds in orientation with the secondary anticlines of the Yakima Folds just north of 200 East Area (Reidel and Fecht 1994b).

5.4.2.2 Ringold Formation

The Ringold Formation is largely absent under the B, BX, and BY tank farms. The Ringold Formation has been removed by fluvial downcutting of the ancestral Columbia River and cataclysmic Pleistocene flooding (Lindsey et al. 2001a). The R_{wi} unit is present south of the WMA in the central part of 200 East Area (Figures 4.3 and 4.5).

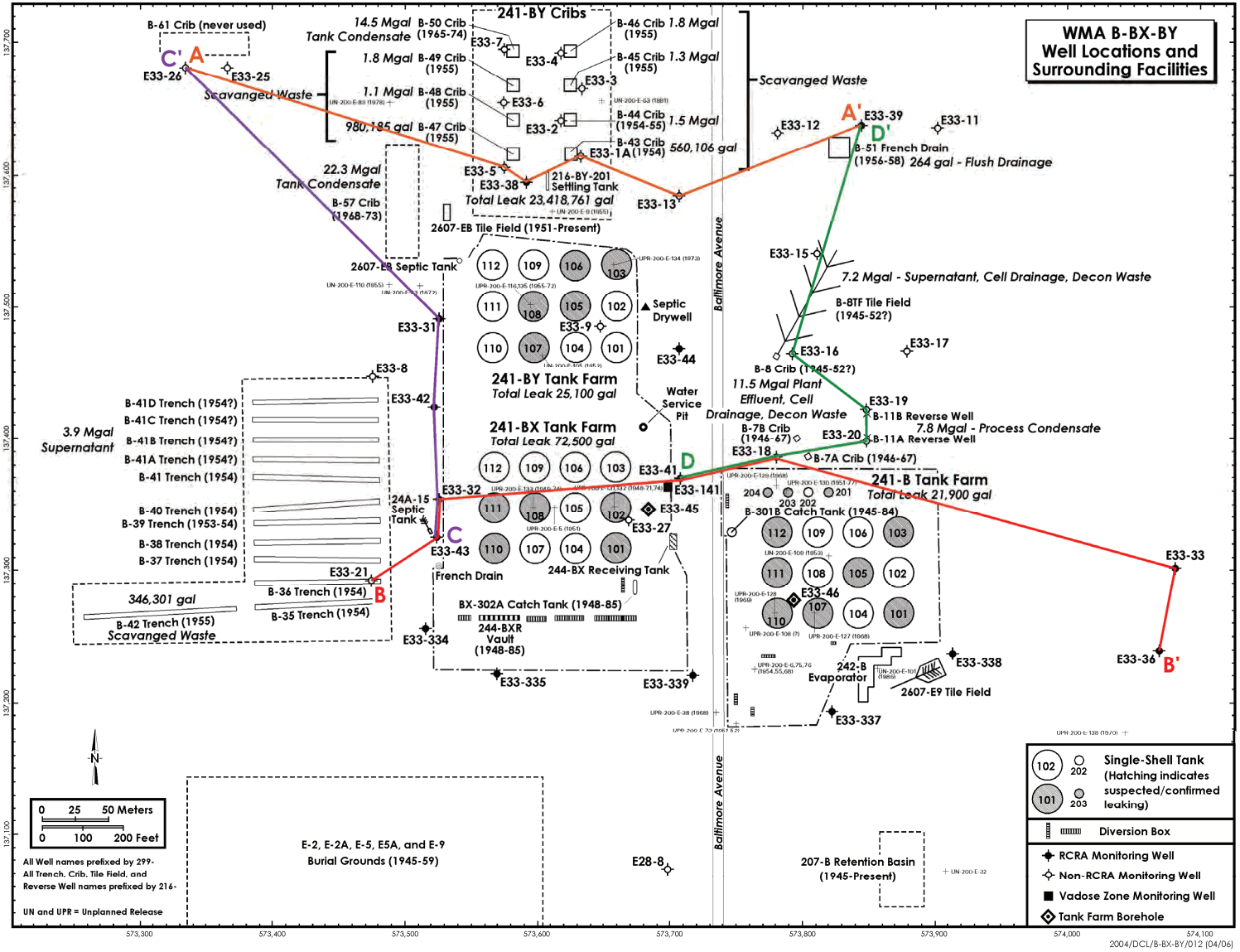

Figure 5.38. Location of Cross Sections Through Waste Management Area B-BX-BY (modified from Wood et al. 2000)

Table 5.8. Stratigraphic Contact Elevations for Boreholes in Waste Management Area B-BX-BY[a]

Well No.	Ground Surface Elevation ft[b]	Contact Picks (Elevation in ft)[b]								
		Top H1 gravel	Top H2 sand	Top H3 gravel	Top Hf/CCU_u	Top Hf/CCU_l	Top R_{wie}	Top R_{lm}	Top R_{wia}	Top of Basalt
E33-1	630	NP	605	NP	NP	459	NP	NP	NP	389
E33-5	632	NP	582	NP	NP	452	NP	NP	NP	397
E33-13	626	NP	606	NP	NP	436	NP	NP	NP	391
E33-16	642	NP	618	NP	439	422	NP	NP	NP	402
E33-18	653	NP	607	NP	443	NP	NP	NP	NP	383
E33-19	649	NP	614	NP	444	429	NP	NP	NP	404
E33-20	652	NP	616	NP	443	432	NP	NP	NP	402
E33-21	664	NP	620	NP	NP	424	NP	NP	NP	384
E33-26	630	NP	600	NP	NP	480	NP	NP	NP	390
E33-31	648	NP	583	NP	453	450	NP	NP	NP	398
E33-32	657	NP	617	NP	437	427	NP	NP	NP	387
E33-33	641	NP	604	NP	441	431	NP	NP	NP	391
E33-36	644	NP	604	NP	NP	NP	NP	NP	NP	384
E33-39	624	NP	594	NP	NP	444	NP	NP	NP	394
E33-41	651	NP	616	NP	436	411	NP	NP	NP	391
E33-42	650	NP	595	NP	NP	415	NP	NP	NP	390
E33-43	662	NP	617	NP	452	432	NP	NP	NP	387

(a) Bjornstad (2004) and Wood et al. (2000).
(b) Multiply by 0.3048 to convert feet to meters.
CCU = Cold Creek unit.
Hf/CCU = Hanford formation/Cold Creek unit undifferentiated.
H1 = Hanford formation, unit H1; equivalent to upper gravel-dominated.
H2 = Hanford formation, unit H2; equivalent to sand-dominated.
H3 = Hanford formation, unit H3; equivalent to lower gravel-dominated.
R_{wia} = Ringold Formation, Member of Wooded Island, unit A.
NP = Not present.

5.4.2.3 Undifferentiated Hanford Formation/Cold Creek Unit

The exact origin of the sedimentary deposits overlying the CRBG and underlying the H2 unit is uncertain and still open to interpretation, as is the case at the A-AX and C WMAs. Recent reports have designated deposits beneath the H2 unit as the undifferentiated Hanford formation/Cold Creek unit (Wood et al. 2000) and Hanford formation/Cold Creek unit/Ringold Formation unit (Lindsey et al. 2001a). Others call these deposits the H3 unit (Serne et al. 2002c). The Hf/CCU designation is used in Table 5.8 and in the following cross sections. Wood et al. (2000) recognized two facies of the Hf/CCU beneath the B, BX, and BY tank farms—a fine-grained eolian/overbank silt (silt facies) and a sandy gravel to gravelly sand facies.

The thick silt-rich interval is believed to be primarily a pre-Pleistocene flood deposit because silty layers associated with coarse-grained Pleistocene flood deposits in this area are generally only a few centimeters thick (Wood et al. 2000). The texture, structure, and color of the thick silt layer are all identical to that of the early Palouse soil (Tallman et al. 1979; DOE 1988), more recently referred to as the CCU_u, which is widely distributed beneath the 200 West Area (Johnson et al. 1999; Wood et al. 2000; DOE-RL 2002). Here, the fine-grained facies is referred to as the undifferentiated Hanford formation/ CCU fine subunit (Hf/CCU fine).

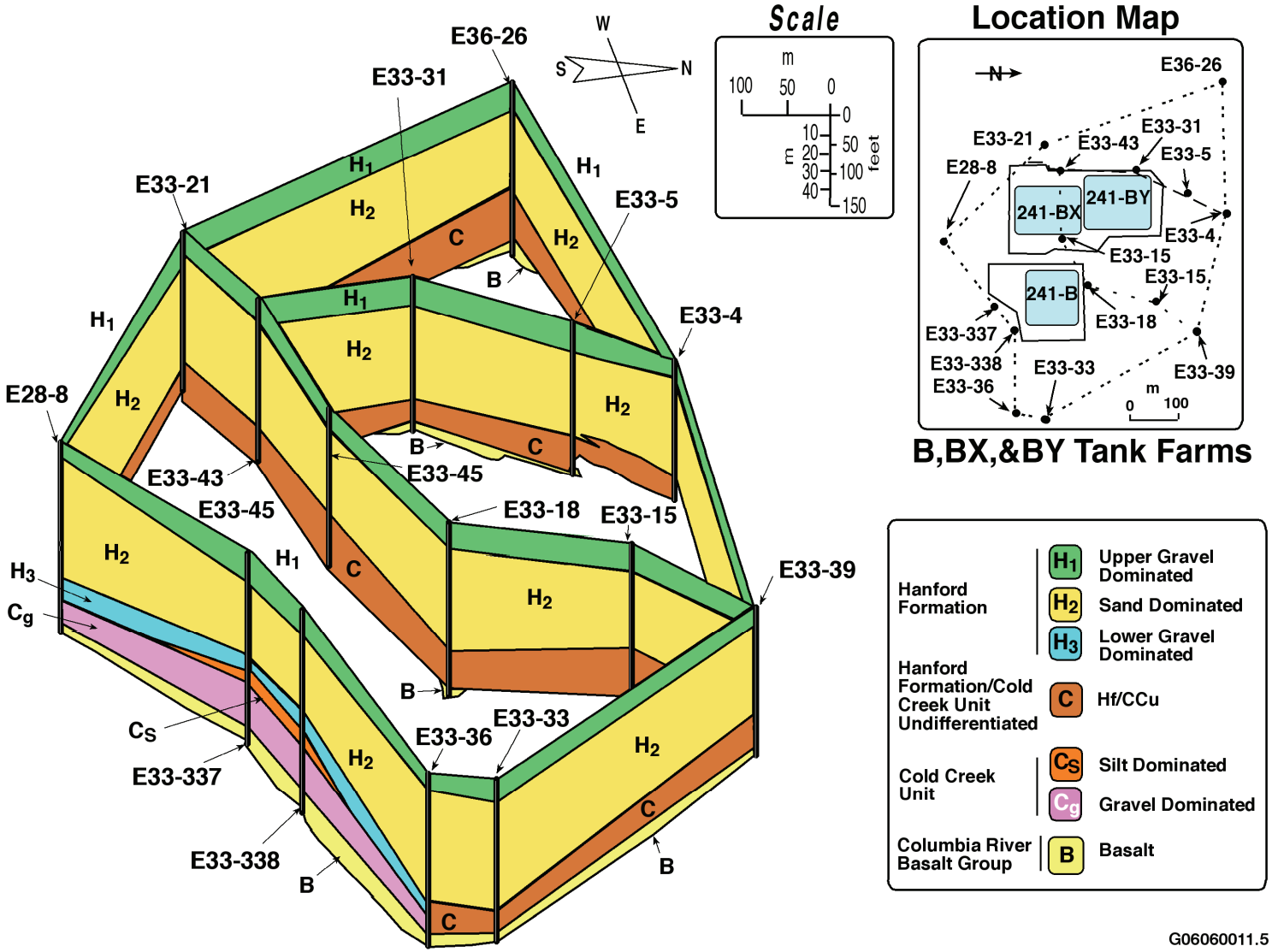

Figure 5.39. Fence Diagram Showing the Relationship Between Stratigraphic Units at the B, BX, and BY Tank Farms

Table 5.9. Stratigraphic Terminology and Unit Thickness for the A-AX and C Tank Farms

Stratigraphic Symbol	Formation	Facies/ Subunit	Description	A-AX Thickness	C Thickness
Backfill	NA	Backfill – Anthropogenic	Gravel-dominated consisting of poorly to moderately sorted cobbles, pebbles, and coarse to medium sand with some silt derived from coarse-grained Hanford formation (H1 unit) excavated around tanks (Price and Fecht 1976a, 1976b, 1976f; Wood et al. 2003); occasional layers of sand to silty sand occur near the base of the backfill sequence.	10 m	10 m
H1	Hanford formation	Unit H1 – (Gravel-dominated facies association). Cataclysmic flood deposits (high-energy)	Gravel-dominated flood sequence; composed of mostly poorly sorted, basaltic, sandy gravel to silty sandy gravel. Equivalent to the upper gravel sequence discussed by Last et al. (1989), the Q_{fg} documented by Reidel and Fecht (1994b), coarse-grained sequence (H1 unit) of Wood et al. (2003) and gravel facies of unit H1 of Lindsey et al. (2001a), and gravel-dominated facies association of DOE-RL (2002).	20–30 m	10–30 m
H2		Unit H2 – (Sand-dominated facies association). Cataclysmic flood deposits (moderate energy)	Sand-dominated flood sequence; composed of mostly horizontal to tabular cross-bedded sand to gravelly sand. Some sand beds capped with thin layers of silty sand to sandy silt. Equivalent to Fine-Grained Sequence (H2 unit) of Wood et al. (2003) and unit H2 of Lindsey et al. (2001b), the sandy sequence of Last et al. (1989) and Lindsey et al. (1992), to Q_{fs} documented by Reidel and Fecht (1994b), and sand-dominated facies association of DOE-RL (2002).	30–65 m	45–>70 m
H3		Unit H3 – (Gravel-dominated facies association). Cataclysmic flood deposits (high-energy)	Gravel-dominated flood sequence; composed of open framework gravel and poorly sorted, basaltic, sandy gravel to silty sandy gravel. Equivalent to the lower coarse-grained unit of the Hanford formation of Last et al. (1989), to the lower gravel sequence of Lindsey et al. (1992) and to the Hanford formation, H3 sequence of Lindsey et al. (1994).	0–20 m	0
CCU_u/R	Undifferentiated Cold Creek unit and Ringold Formation and /or lower Hanford gravel	Upper subunit	Silty sequence; locally thick layer of silt overlying the gravelly sediments of the lower subunit. Silt facies is light olive-brown to tan colored, massive, well-sorted, fine, calcareous silt to sand with pedogenetic traces (i.e., root casts).	0–6 m	0
CCU_l/R		Lower subunit	Lower gravel sequence equivalent to pre-Missoula gravels; sandy gravel to gravelly sand beneath the silt-dominated facies and above the top of basalt. Occurs as muddy, sandy gravel to sandy gravel. Moderate to uncemented with some caliche fragments. In the absence of CCU_u, this cannot be distinguished from H3.	0–>15 m	0–25 m

Table 5.9. (contd)

Stratigraphic Symbol	Formation	Facies/ Subunit	Description	A-AX Thickness	C Thickness
R_{wi}	Ringold	R_{wi} unit – Ancestral Columbia River System braided-stream deposits	Coarse-grained Ringold Formation sequence, consisting of mostly moderately sorted, quartzitic sandy gravel to silty sandy gravel. Equivalent to middle Ringold Formation unit (DOE 1988) and the Ringold Formation unit E gravels (Wood et al. 2003; Lindsey et al. 2001a).	Probably not present	Probably not present

CCUu/R = Upper Cold Creek unit/Ringold Formation.
CCU_l/R = Lower Cold Creek unit/Ringold Formation.
H1 = Hanford formation, unit H1; equivalent to upper sand-dominated.
H2 = Hanford formation, unit H2; equivalent to middle sand-dominated.
H3 = Hanford formation, unit H3; equivalent to lower sand-dominated.
NA = Not applicable.
Q_{fg} = Quaternary flood gravels.
Q_{fs} = Quaternary flood silt and sand.
R_{wi} = Ringold Formation, member of Wooded Island.

The silt layer has an irregular surface (Figure 5.39) and may not extend much beyond WMA B-BX-BY. The silt facies of the Hf/CCU is divided into two distinctive beds. The upper bed consists of a light olive-brown- to tan-colored, massive, well-sorted fine calcareous silt to sand. Pedogenetic traces (i.e., root casts) occur locally. The silt bed is present locally mainly in the B tank farm area where the silt layer is up to 10 m (30 ft) thick. In well 299-E33-338, it is 3 m (9.9 ft) thick (Figure 5.37). Elsewhere, it either was not deposited or more likely was eroded.

A sequence of sandy gravel to gravelly sand occurs at the B, BX, and BY tank farms beneath the silt facies and above the top of basalt that represents either cataclysmic flood deposits or ancestral Columbia River deposits. Where the fine-grained facies is absent, the gravel sequence below the silt unit is indistinguishable from similar-appearing facies of the H3 unit that is found in other areas such as WMA A-AX (Wood et al. 2000). However, geophysical logs have been able to detect a calcium carbonate layer in several wells, suggesting that, locally, it can be distinguished from the Hanford formation in the absence of the silt-dominated sediment. Prior to the discovery of the thick silt layer, reported in Wood et al. (2000), gravels overlying basalt bedrock were always included in the Hanford formation (Tallman et al. 1979; Last et al. 1989; Connelly et al. 1992a; Lindsey et al. 1992). If the thick silt layer predates the Hanford formation, however, then the underlying gravels must also predate the Hanford formation. Thus, the gravel sequence beneath the silt layer must belong to either a mainstream alluvial facies of the ancestral Columbia River (CCU time) or possibly the Ringold Formation, which was deposited by the ancestral Columbia River. This unit is referred to as the Hf/CCU coarse subunit in this report.

In core, this sediment occurs as muddy sandy gravel to sandy gravel, consisting of approximately 30 to 80% gravel, 15 to 65% sand, and up to 15% mud (Lindenmeier et al. 2003). The gravel clasts consist of a mixture of mostly quartzite, basalt, and some highly weathered friable granite. Where unbroken, the gravel clasts are subrounded to rounded and range up to at least 60 mm in diameter (intermediate axis). The matrix ranges from mostly very fine sand to poorly-sorted coarse to medium sand, with variable mud content. These materials are moderate to uncemented with some caliche fragments.

The thickness of the gravel-dominated sediments ranges from 10 to 30 m (30 to 100 ft) (Figures 5.38 through 5.41). The upper surface of the sandy gravel to gravelly sand has approximately 10 m of relief

Table 5.10. Stratigraphic Terminology and Unit Thickness for the B, BX, and BY Tank Farms

Stratigraphic Symbol	Formation	Facies/Subunit	Description	Thickness[(a)]
Backfill	NA	Backfill – Anthropogenic	Gravel-dominated consisting of poorly to moderately sorted cobbles, pebbles, and coarse to medium sand with some silt derived from coarse-grained Hanford formation (H1 unit) excavated around tanks (Price and Fecht 1976c, 1976d, 1976e; Wood et al. 2000); occasional layers of sand to silty sand occur near the base of the backfill sequence.	12 m
H1	Hanford formation	Unit H1 – (Gravel-dominated facies association). Cataclysmic flood deposits (high-energy)	Gravel-dominated flood sequence; composed of mostly poorly-sorted, basaltic, sandy gravel to silty sandy gravel. Equivalent to the upper gravel sequence discussed by Last et al. (1989), the Q_{fg} documented by Reidel and Fecht (1994b), Hanford Gravel Unit A of Johnson et al. (1999), coarse-grained sequence (H1 unit) of Wood et al. (2000) and gravel facies of unit H1 of Lindsey et al. (2001a), and gravel-dominated facies association of DOE-RL (2002).	Up to 20 m
H2		Unit H2 – (Sand-dominated facies association). Cataclysmic flood deposits (moderate energy)	Sand-dominated flood sequence; composed of mostly horizontal to tabular cross-bedded sand to gravelly sand. Some sand beds capped with thin layers of silty sand to sandy silt. Equivalent to Hanford Sands of Johnson et al. (1999), Fine-Grained Sequence (H2 unit) of Wood et al. (2000) and unit H2 of Lindsey et al. (2001a), the sandy sequence of Last et al. (1989) and Lindsey et al. (1992), and to Q_{fs} documented by Reidel and Fecht (1994b), and sand-dominated facies association of DOE-RL (2002).	30–60 m
Hf/CCU_u	Undiffentiated Hanford formation/Cold Creek unit	Upper Post-Ringold Formation eolian and/or overbank alluvial deposits	Silty sequence; consisting of interstratified well-sorted silt. Uncemented but may be moderately to strongly calcareous from detrital $CaCO_3$. Equivalent to the "early Palouse soil" (Tallman et al. 1979; DOE 1988; DOE-GJO 1997) and the Hf/PP deposits of Wood et al. (2000). Also equivalent to the upper Plio-Pleistocene unit in Lindsey et al. (2001a) and the fine-grained, laminated to massive lithofacies of the Cold Creek unit DOE-RL (2002).	0–10 m
Hf/CCU_l		Lower gravel resulting from eroded Ringold or post-Ringold Formation fluvial deposits	Gravelly sequence; consisting of open framework gravel and sandy gravel to gravelly sand; may be equivalent to pre-Missoula gravels in part and/or to H3 gravel facies of the Hanford formation where the fine facies is not present. It is possible some of these gravels are remnants of Ringold Formation unit A gravels.	10–30 m

(a) Multiply by 3.281 to convert meters to feet.

$CaCO_3$ = Calcium carbonate.

CCU_l = Lower Cold Creek unit.

CCU_u = Upper Cold Creek unit.

Hf/CCU = Hanford formation/Cold Creek unit.

NA = Not applicable.

Q_{fg} = Quaternary flood gravels.

Q_{fs} = Quaternary flood silt and sand.

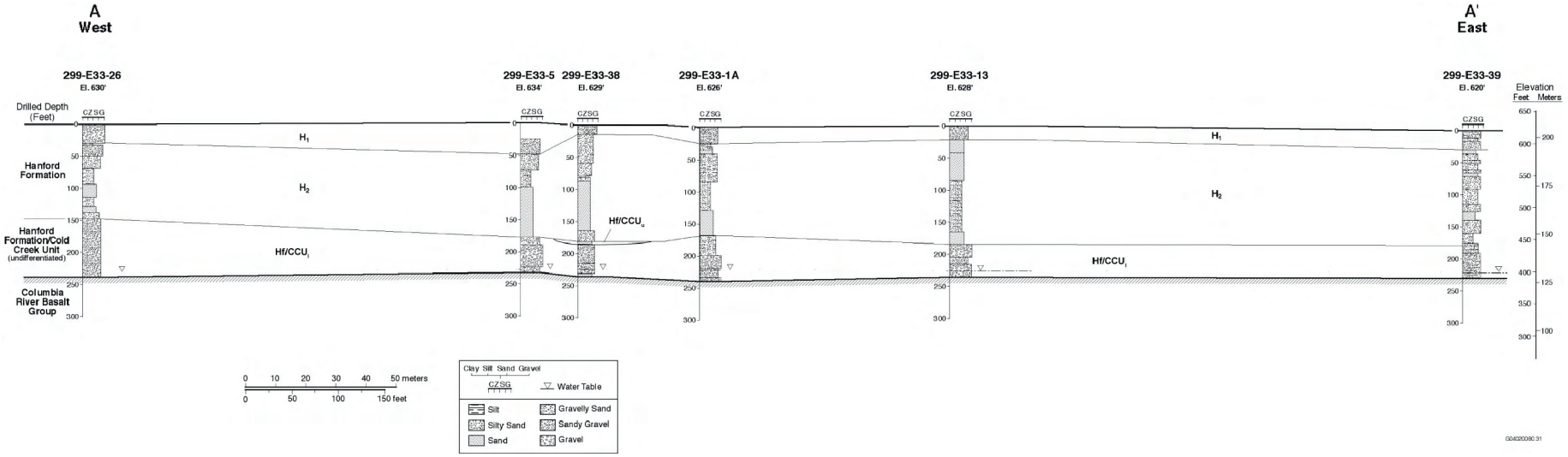

Figure 5.40. Cross-Section A-A' at Waste Management Area B-BX-BY (modified from Wood et al. 2000)

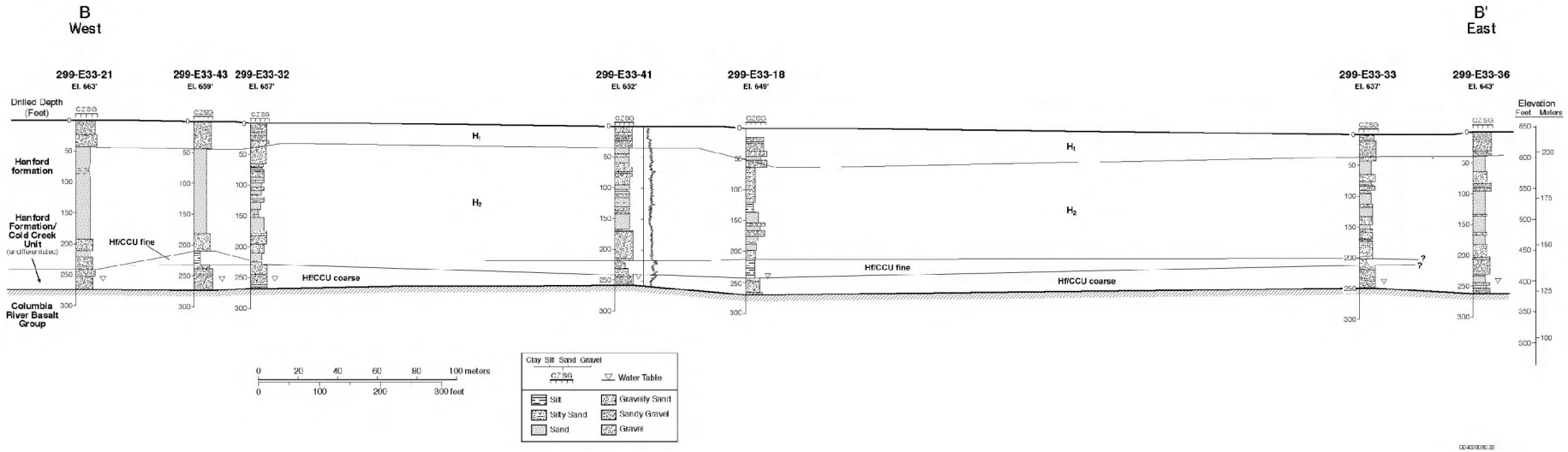

Figure 5.41. Cross-Section B-B' at Waste Management Area B-BX-BY (modified from Wood et al. 2000)

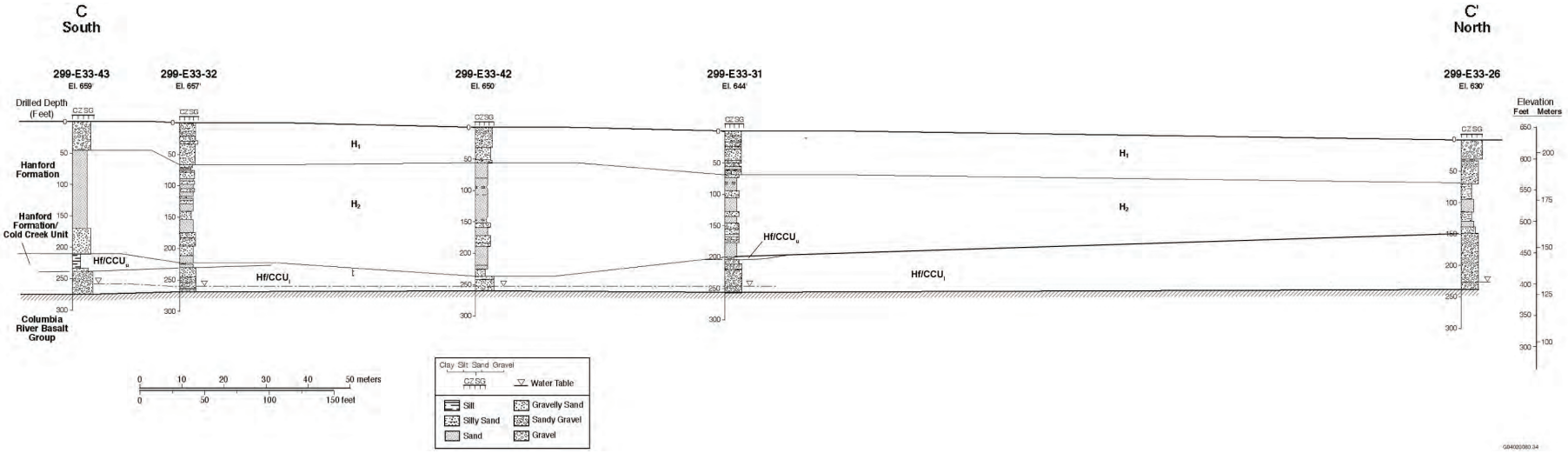

Figure 5.42. Cross-Section C-C' at Waste Management Area B-BX-BY (modified from Wood et al. 2000)

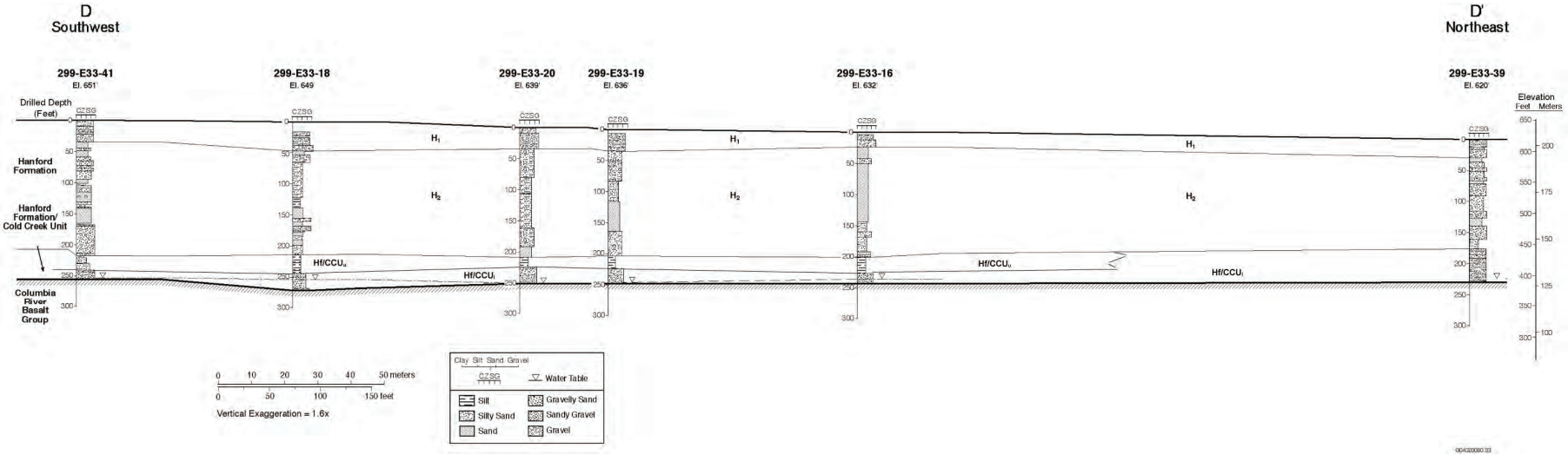

Figure 5.43. Cross-Section D-D' at Waste Management Area B-BX-BY (modified from Wood et al. 2003)

(Wood et al. 2000). There is a depression in this unit over the northwest corner of the B tank farm. The depression appears to be filled with the overlying silt-dominated sediments. The gravel facies is thinnest and structurally low while the silt facies is thickest here, suggesting that it was eroded before the depression was backfilled with silt (Wood et al. 2000).

5.4.2.4 Hanford Formation

The Hanford formation at the B, BX, and BY tank farm ranges from about 46 to 70 m (150 to 225 ft) thick (Figures 5.38 through 5.41) and consists of a series of massive sands intercalated with beds of sand and gravelly sands, and thinner lens of silts and clayey silts. It can be subdivided into a lower undifferentiated Hanford formation/CCU gravel-dominated unit, a lower sand-dominated unit (H2), and an upper gravel-dominated unit (H1). The contacts between the three are marked by a sharp increase in total natural gamma from the gravelly units to the sandy unit.

The lower undifferentiated Hanford/CCU sediments are discussed above. Overlying them is the H2 unit, consisting of a sand-dominated sequence. The H2 unit is predominantly a poorly- to well-sorted, medium- to coarse-grained sand with some silt layers (Wood et al. 2000). The upper part of the H2 unit is slightly coarser than the lower part, with occasional pebbles floating in a coarse sand matrix. With depth, the medium to coarse sand becomes more frequently interstratified with layers of fine- to medium-grained sand. The salt-and-pepper appearance of the sand is distinctive and caused by the approximately equal concentrations of basalt and quartz and feldspar. The H2 unit ranges from 30 m (110 ft) in the north to 60 m (200 ft) in the central and southern parts of the WMA (Wood et al. 2000). Two thin (<0.5 ft), fine-grained silty layers were observed within the Hanford formation, H2 unit in borehole 299-E33-338 (Lindenmeier et al. 2003).

H1, the upper gravel-dominated unit, consists of mostly sandy gravel to silty sandy gravel, with lesser amounts of gravelly sand. Thin (0.5-ft) silt layers are locally present within this sequence. The gravels are multi-lithologic but generally contain a high percentage of basalt. The gravel clasts are generally subrounded to well–rounded, and the finer fraction is described as mostly very coarse to coarse sand with perhaps as much as 5 to 7% mud. The samples generally display no cementation or obvious sedimentary structure.

Paleomagnetic data have been used to subdivide the Hanford formation based on magnetic polarity reversals. Three polarity reversals have been identified in samples from boreholes 299-E33-335 and 299-33-338 in the WMA B-BX-BY area, while four reversals have been identified at the Integrated Disposal Facility site to the south (Figure 4.13).

The lowermost Hanford/CCU gravels have normal polarity. The H2 sediment has three polarities. The lower and middle parts have normal polarity, and the upper part of the H2 unit has reversed polarity. The H1 unit has primarily reversed polarity; the upper part of H1 unit was not sampled but it probably has the normal polarity of the current Earth magnetic field. The polarity sequences correlate well with the Integrated Disposal Facility site (discussed in Chapter 6). The oldest reversed polarity found at the Integrated Disposal Facility site appears not to be present at WMA B-BX-BY.

5.4.2.5 Holocene Deposits and Backfill

Locally up to 13 m (45 ft) of backfill are present at WMA B-BX-BY. The backfill is poorly sorted, gravelly sand to sandy gravel (Price and Fecht 1976c, 1976d, 1976e) from the gravel-dominated sequence of the Hanford formation.

6.0 Geology of the Integrated Disposal Facility

The Integrated Disposal Facility (IDF) is located south of the 200 East Area tank farms. The geology of the IDF trench, which was constructed in 2004–2005, is summarized in Reidel and Fecht (2005). The location is important in understanding the geology of the 200 East Area tank farms because of the detailed characterization work in the trench exposure. The geology presented in this chapter is from Reidel (2005).

6.1 Site Stratigraphy

The stratigraphy at the new IDF site consists of the Hanford formation and Ringold Formation overlying the CRBG. Surficial sediments are mainly eolian deposits consisting of reworked Hanford sands and silts.

The stratigraphy and the stratigraphic model developed for this study are summarized in Figure 6.1 and Table 6.1. The stratigraphy has been determined using data from numerous boreholes in the vicinity (Figure 6.2) and detailed cross sections (Figures 6.3, 6.4, 6.5, and 6.6).

The stratigraphy of the new IDF site is divided from youngest to oldest into the following units:

- eolian deposits
- Hanford formation, upper gravel-dominated facies
- Hanford formation, sand-dominated facies
- Hanford formation, lower gravel-dominated facies
- Ringold Formation
  - unit E
  - lower mud
  - unit A
- Columbia River Basalt Group.

A series of gravel and sand/silt units can be recognized in the Hanford formation layers (Table 6.1). These units are not formally defined but are tentatively correlated across the IDF site. Additional work will be necessary to verify these correlations. They are shown on the cross sections and in Table 6.1.

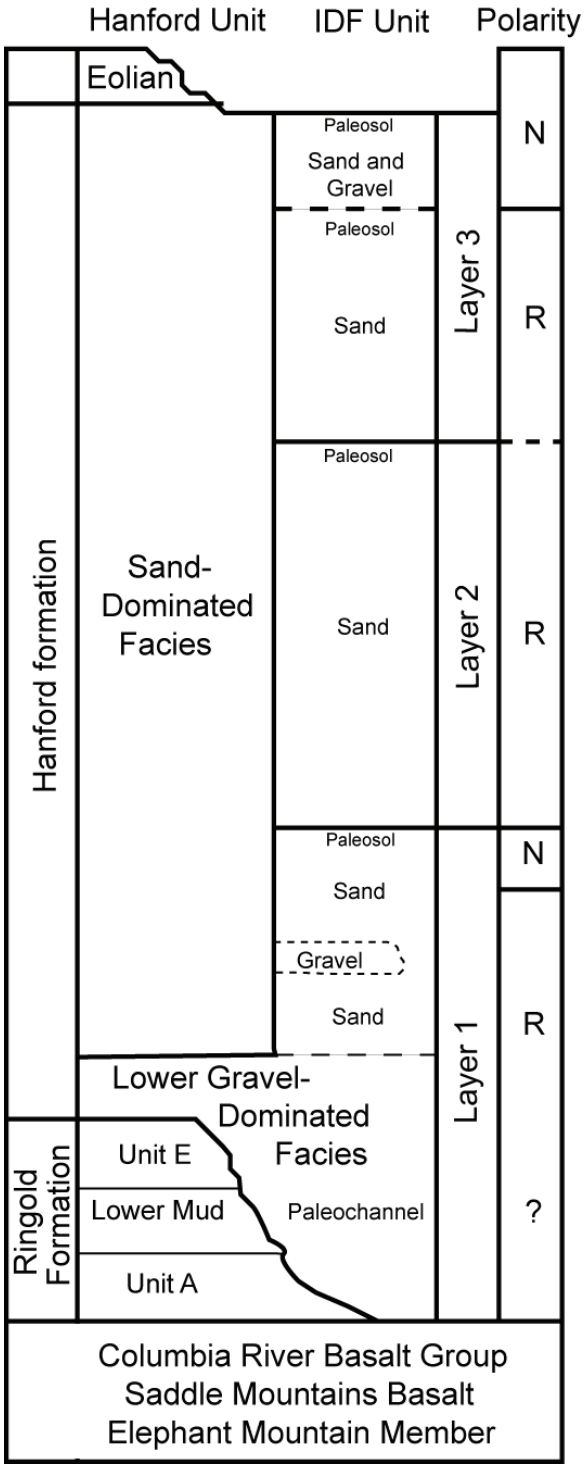

Figure 6.1. Integrated Disposal Site Stratigraphy

Table 6.1. Stratigraphic Contact Elevations for Boreholes in the Integrated Disposal Site (ft[a])

Borehole	Surface Elevation [brass cap or casing (C)]	Back-fill	Surface Sand (S)	Top of Layer 3 (L3)	Top of Layer 2 (L2)	Top of Layer 1 (L1)	Top of Sandy Gravel 1 (G1)	Top of Sand 1 (S1)	Top of Sandy Gravel 2 (G2)	Top of Sand to Silty Gravelly Sand 2 (S2)	Top of Gravel 3 (G3)	Top of Sand to Silty Sand 3 (S3)	Top of Gravel 4 (G4)	Thickness of Hanford Forma-tion	Top of Ringold	Top R_{wie}	Top R_{lm}	Top R_{wia}	Thickness of Ringold	Basalt
E13-10	733(C)	N	733	ND	ND	ND	NP	733	713	705	537	514	494	239	449	449	ND	ND	ND	ND
E17-12	719 (C)	N	719	669	647	564	704	694	NP	694	497	479	429	ND	ND	ND	ND	ND	ND	ND
E17-13	719 (C)	31	NP	ND	647	ND	ND	689	NP	689	494	469	424	ND	ND	ND	ND	ND	ND	ND
E17-17	717	N	716	ND	651	ND	716	702	NP	702	492	442	417	ND	ND	ND	ND	ND	ND	ND
E17-18	718	N	717	ND	648	ND	713	693	626	616	483	458	426	ND	ND	ND	ND	ND	ND	ND
E17-20	717	N	716	ND	646	ND	706	696	676	671	497	436	416	ND	ND	ND	ND	ND	ND	ND
E17-21[b]	735	N	735	730	677	572	730	720	715	705	523	505	447	238	400	400	357	296	173	197
E17-22	723.7	N	723.7	722	650	ND	NP	722	NP	717.7	507	485.7	449	ND	ND	ND	ND	ND	ND	ND
E17-23	734.4	N	734.4	733	672	576	NP	733	711	705.4	501	498.4	453	ND	ND	ND	ND	ND	ND	ND
E17-25	738.3	N	738.3	NP	NP	NP	NP	737	729	727.3	504	479	445	ND	ND	ND	ND	ND	ND	ND
E17-26	735.17	N	735.17	ND	ND	ND	NP	NP	NP	NP	505	485	455	ND	ND	ND	ND	ND	ND	ND
E18-1	716	N	ND	ND	ND	ND	720	700	675	660	545	535	NP	215	505	505	ND	ND	ND	ND
E18-3	718	N	718	ND	656	ND	715	703	ND	656	546	542	NP	235	483	483	ND	ND	ND	ND
E18-4	718	N	718	ND	ND	ND	715	699	668	658	ND	568	NP	232	486	486	ND	ND	ND	ND
E19-1	736 (C)	N	736	ND	ND	ND	735	716	686	672	520	506	NP	250	486	486	346	306	285	201
E23-1	710 (C)	N	0 to 5	ND	665	ND	704	NP	689	665	489	477	454	ND	417	409	ND	ND	ND	ND
E23-2	721 (C)	0	720	ND	ND	ND	NP	720	NP	605	520	500	484	290	430	430	ND	ND	166	264
E24-4	697 (C)	20	696	ND	646	ND	NP	696	611	ND	ND	ND	472	270	ND	ND	ND	ND	ND	ND
E24-7	716 (C)	N	716	ND	652	ND	716	708	NP	708	500	486	448	380	336	336	ND	ND	70	266
E24-16	715	N	715	ND	656	ND	714	706	626	616	460	425	410	ND	ND	ND	ND	ND	ND	ND
E24-17	716	N	716	ND	659	ND	711	706	NP	706	464	524	421	ND	ND	ND	ND	ND	ND	ND
E24-18	716	N	716	ND	664	ND	715	699	NP	699	506	481	456	325	391	391	ND	ND	ND	ND
E24-21	714	N	714.40	714	636	544	706	702	NP	702	479	473	444	ND	ND	ND	ND	ND	ND	ND
E24-24	721.46	N	721.46	NA	NA	NA	NP	NP	NP	NP	502	492	437	ND	ND	ND	ND	ND	ND	ND
37-47A	716	N	716	ND	ND	ND	NP	716	NP	716	526	NP	474	284	432	432	350	304	231	201
C3828	737.5	N	737.53	ND	575	ND	NP	737.5	NP	728.5	503	475	460	ND	ND	ND	ND	ND	ND	ND

(a) Multiply by 0.3048 to convert feet to meters.

(b) Top of basalt from C4562, approximately 20 ft away.

N = No backfill.

NA = Not available.

ND = Not determined; unit could be present but cannot be recognized in logs.

NP = Not present.

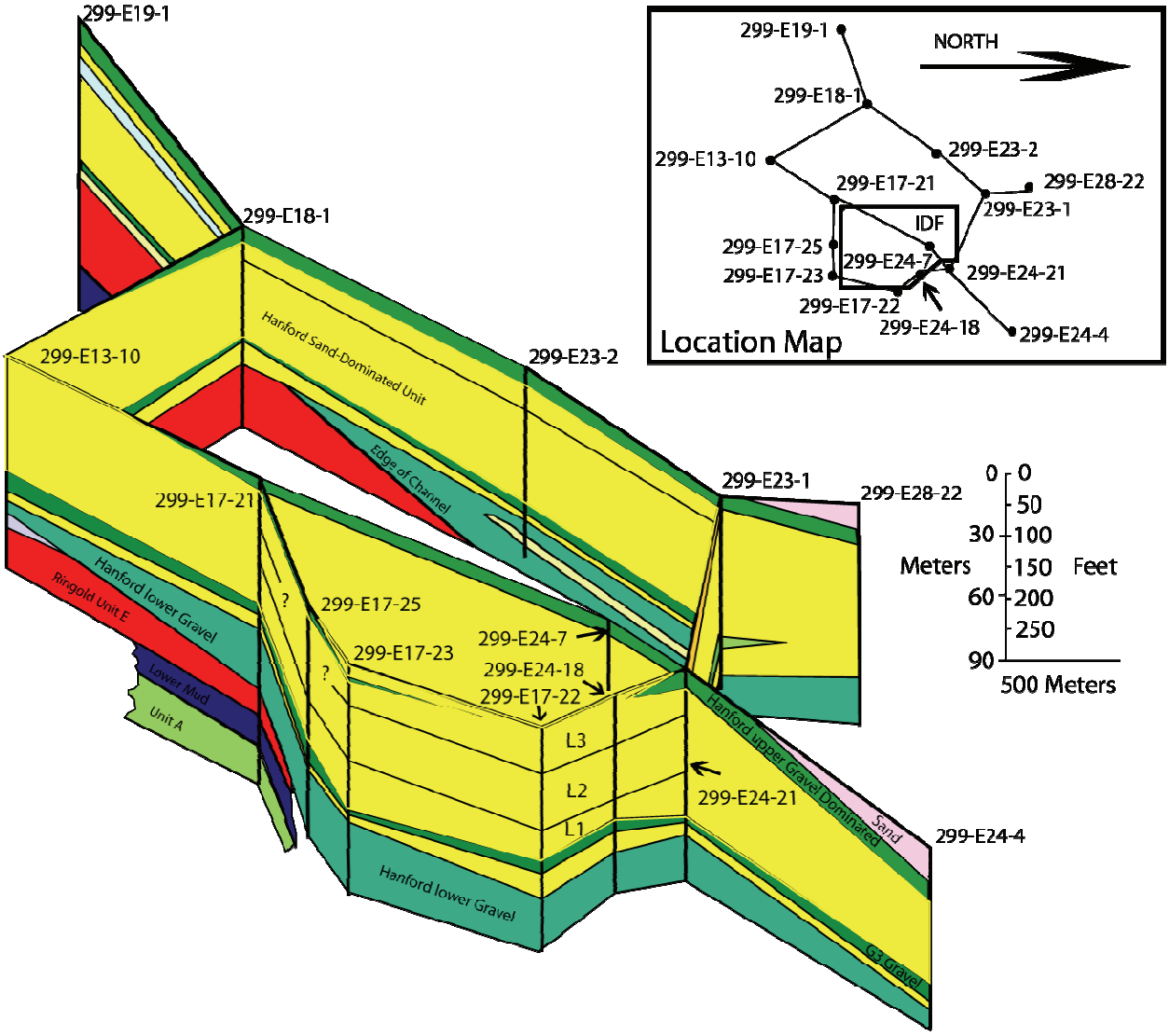

Figure 6.2. Fence Diagram of the IDF Site and Vicinity (modified from Reidel 2005)

6.1.1 Columbia River Basalt Group

Previous studies (Reidel and Fecht 1994a) have shown that the Elephant Mountain Member of the CRBG underlies the IDF site, forming the base of the suprabasalt aquifers. No erosional windows are known or suspected to occur in the IDF site area. Figures 4.4 and 6.3 show the elevation of the top of the CRBG under the 200 East Area and vicinity. Borehole C4562 adjacent to 299-E17-21 encountered the Elephant Mountain Member vesicular flow top at 165 m (540 ft) below ground surface (59.4 m [195 ft] above mean sea level).

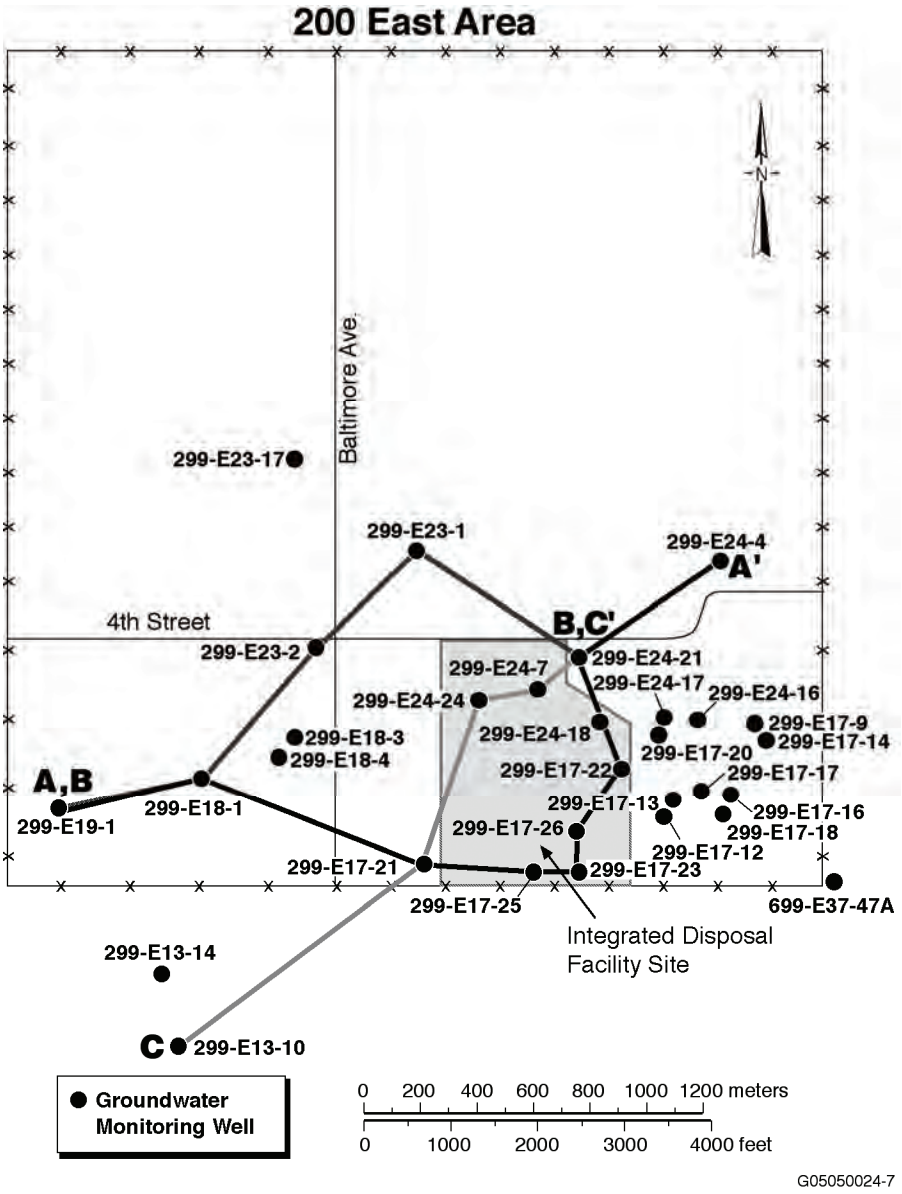

Figure 6.3. Locations of Cross Sections A-A', B-B', and C-C' (modified from Reidel 2005)

6.1.2 Ringold Formation

Because few boreholes penetrate the entire Ringold Formation at the IDF site, data at depth are limited. The Ringold Formation reaches a maximum thickness of 87 m (285 ft) on the west side of the IDF site and thins eastward. It consists of three units of Ringold Formation member of Wooded Island; unit A, lower mud, and unit E. The Ringold Formation member of Taylor Flat is not present at the IDF site but has been identified in the southeast corner of the 200 East Area in borehole 299-E37-47A. These sediments pinch out or were eroded beneath the IDF site.

The surface of the Ringold Formation is irregular beneath the IDF site area (Figures 6.4, 6.5, and 6.6). A northwest-southeast–trending erosional channel is centered along the northeast portion of the site. The deepest portion near boreholes 299-E24-7 and 299-E24-21 (Figure 6.6) is in the northern portion of the

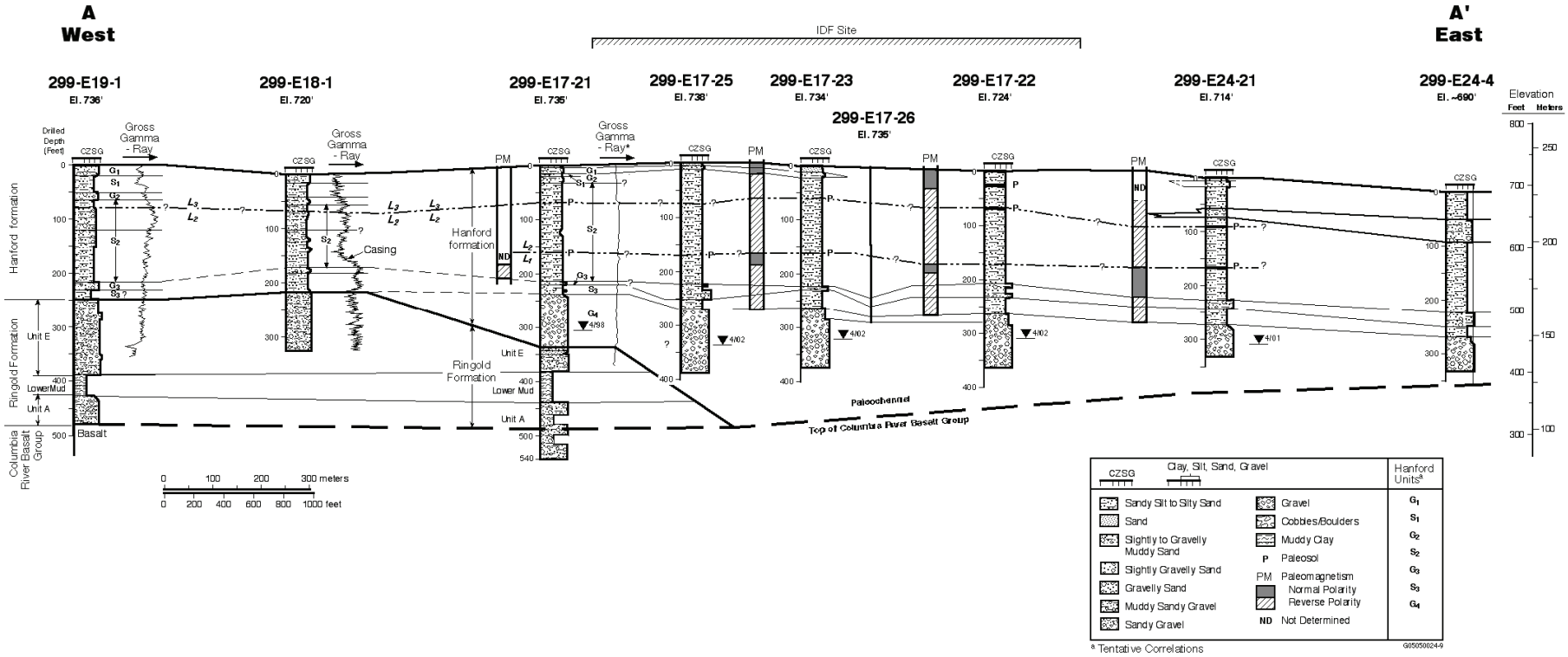

Figure 6.4. Cross-Section A–A' Across the IDF Site (modified from Reidel 2005)

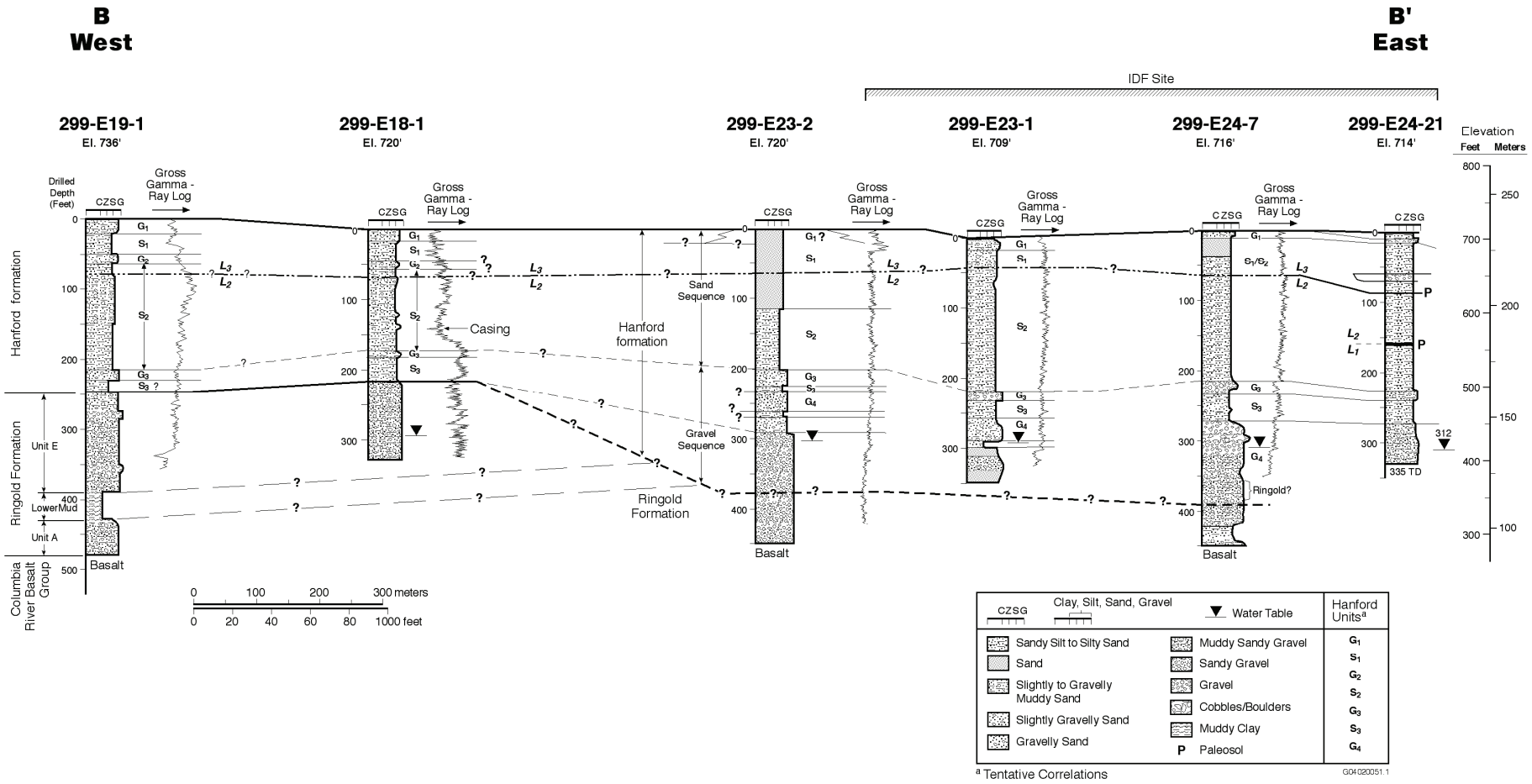

Figure 6.5. Cross-Section B–B' Across the IDF Site (modified from Reidel 2005)

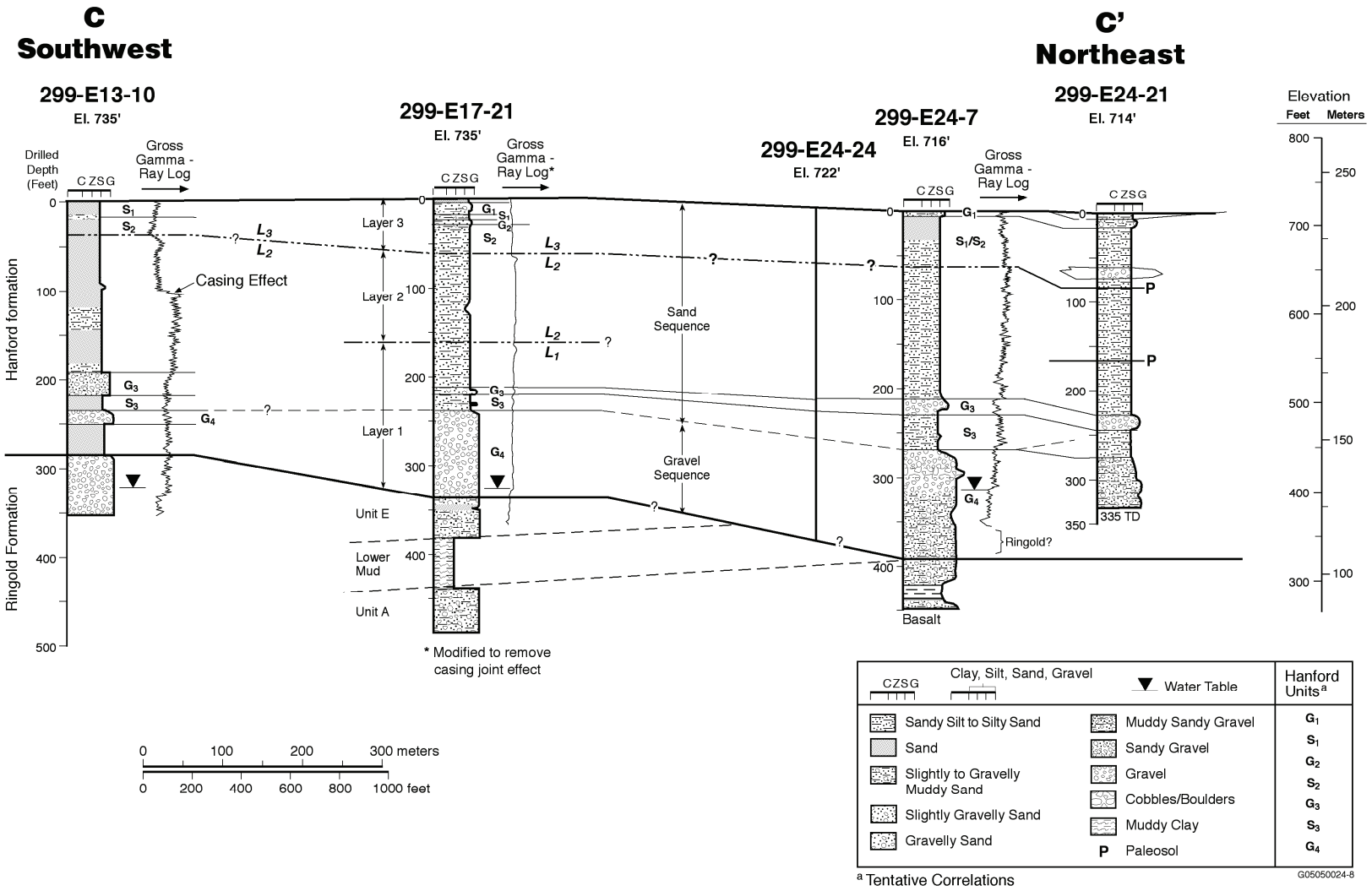

Figure 6.6. Cross-Section C–C' Across the IDF Site (modified from Reidel 2005)

IDF site. Near wells 299-E17-23 and 299-E17-22, the channel may have cut all the way down to basalt. This trough is interpreted to be a smaller part of a much larger trough under the 200 East Area resulting from scouring by the Missoula floods or post-Ringold Formation fluvial incision prior to the Missoula floods.

Based on only three, possibly four, boreholes penetrating Ringold Formation unit A in the study area (Table 6.1), this unit is interpreted to overlie the CBRG across much of the IDF site. New groundwater well 299-E17-26 may have penetrated this unit near the base of the well, according to the well-site geologist's log. If it did, then this would represent an isolated outcrop in the paleochannel that underlies the IDF site.

Unit A is 30 m (100 ft) thick on the west side of the IDF site but pinches out to the northeast (Figures 6.3, 6.4, 6.5, and 6.6). Unit A is sandy gravel consisting of both felsic and basaltic rocks. There are occasional yellow to white interbedded sand and silt with silt and clay lenses. One silt layer occurs at 142 to 145 m (465 to 475 ft), and a second was encountered in a borehole drilled next to 299-E17-21 for shear wave velocity measurements (borehole C4562) from 151 to 157 m (495 to 515 ft). Green-colored, reduced-iron staining is present on some grains and pebbles. Although the entire unit appears to be partially cemented, the zone produced abundant water in well 299-E17-21.

A maximum of 19 m (61 ft) of the Ringold Formation lower mud was encountered on the east and south sides of the IDF site. The uppermost part (about 1.2 m [4 ft]) consists of a yellow sandy to silty mud. The silty mud grades downward into about 10 m (34 ft) of blue mud with zones of silt to slightly silty mud. The blue mud, in turn, grades down into 7 m (23 ft) of brown silty mud with organic-rich zones and occasional wood fragments. The lower mud, like unit A, is absent in the center of the IDF site (Figures 6.3 and 6.4).

Ringold Formation unit E overlies the lower mud and underlies the Hanford formation. Unit E is as much as 15 m (50 ft) of sandy gravel to gravelly sand with scattered large pebbles and cobbles up to 10 inches in size. The gravel consists of both felsic and basaltic clasts, which are well-rounded with a sand matrix supporting the cobbles and pebbles. Cementation of this unit ranges between slight and moderate. The upper contact of unit E is not easily identified at the IDF site. In the western part of the study area, unconsolidated gravels of the Hanford formation lie directly over the Ringold Formation unit E gravels, making exact placement of the contact difficult. The dominance of basalt in the Hanford formation and the general absence of any cementation are the key criteria used for distinguishing them here (Reidel et al. 1998). In the central and northeast part of the area, unit E is interpreted to have been eroded (Figures 6.3, 6.4, 6.5, and 6.6). Unconsolidated gravels and sands typical of the Hanford formation replace them.

6.1.3 Hanford Formation

The Hanford formation is as much as 116 m (380 ft) thick in and around the IDF site (Figure 6.5A). The Hanford formation reaches its greatest thickness along a northwest-southeast–trending trough under the eastern part of the IDF site and thins to the southwest along the margin of the trough (Figures 6.3, 6.4, 6.5, 6.6, and 6.7).

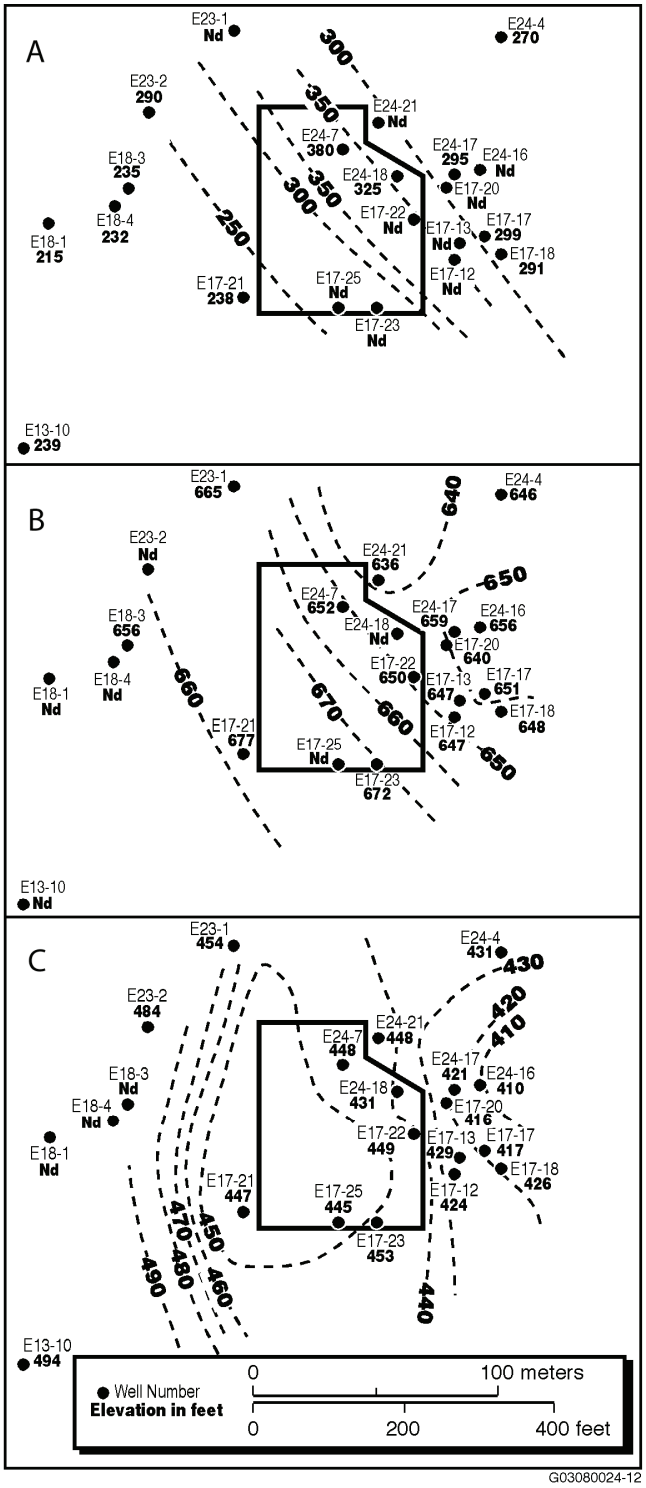

Figure 6.7. Isopach and Structure Contour Maps for the Hanford Formation at the IDF Site A. Thickness of the Hanford Formation. B. Elevation of the Top of Layer 2. C. Elevation of the Top of the Lower Gravel-Dominated Layer. Dashed lines show approximate contour or isopleth (modified from Reidel 2005)

The Hanford formation consists of poorly sorted pebble to cobble gravel and fine- to coarse-grained sand, with lesser amounts of interstitial and interbedded silt and clay. In previous studies of the IDF site, the Hanford formation was described as consisting of three units: an upper and lower gravelly facies and a sandy facies between the two gravelly units. The upper gravelly facies appears to be thin or absent in parts of the IDF area. In Table 6.1, the elevations of the tops of several of the more distinct and tentatively correlated units of the Hanford formation are given.

6.1.3.1 Lower Gravel-Dominated Facies

The lowermost part of the Hanford formation encountered beneath the IDF site consists of the lower gravel-dominated facies, which is equivalent to the gravel-dominated facies of DOE (2002). Drill core and cuttings from these boreholes indicate that the unit is clast-supported pebble- to cobble-gravel with minor amounts of sand in the matrix. The cobbles and pebbles are almost exclusively basalt with no cementation. In outcroppings, these deposits display massive bedding, plane to low-angle bedding and large-scale planar forset cross-bedding, but such features typically cannot be observed in borehole core. At the northeast end of the IDF site, the Hanford formation is over 33 m (109 ft) thick in borehole 299-E24-21 and thins to the southwest (27 m [88 ft] thick in 299-E17-21). The lower gravel decreases in elevation across the IDF site (Figure 6.5C).

6.1.3.2 Sand-Dominated Facies

The upper portion of the Hanford formation ranges from 82 m (270 ft) to 186 m (283 ft) of fine to coarse-grained sand with minor amounts of silt and clay and some gravelly sands. This sequence is equivalent to the sand-dominated facies of DOE-RL (2002).

The texture of the sand-dominated facies changes across the IDF site, reflecting a higher-energy environment for the floodwater to the northeast and east part of the site.

6.1.3.3 Upper Gravel-Dominated Facies

The upper gravel-dominated facies is present as a relatively thin layer across much of the IDF site (Figure 6.3). Texturally it is very similar to the lower gravel-dominated facies.

6.1.3.4 Paleosols

Three main paleosols (soils) were identified in the sand-dominated facies core and one gravel unit that allow the Hanford formation to be subdivided into at least three layers. The paleosol horizons represent intervals when no sediments were deposited and soil development took place between periods of Pleistocene cataclysmic flooding. The paleosols have abrupt upper contacts and less well defined lower contacts. The paleosols are typically 4–6 in. thick, bioturbated, a lighter color than the surrounding sediments, and characterized by a slightly higher moisture content (e.g., borehole C3177-170 depth below ground surface, 5.26%). Calcium carbonate development is also present, suggesting that these paleosols represent the Stage I carbonate morphology.

Layer 1. A poorly developed paleosol of sand and silt slightly cemented by calcium carbonate (Stage I or II carbonate development) defines the top of this layer. Only the upper several inches show any cementation, but elevated concentrations of calcium carbonate extend to a depth of about 3 m (10 ft) below the top. Calcium carbonate fragments and grain coatings were found at greater depths.

Layer 1 may be as much as 1 to 1.7 million years old, based on interpretation of the paleomagnetism (Figure 4.13) (Pluhar et al. 2003).

Layer 2. Layer 2 is capped by a paleosol that occurs at approximately 198 m (650 ft) elevation under the IDF site, although disseminated flakes of calcium carbonate and calcium carbonate-cemented sand grains suggesting Stage II carbonate development are disseminated throughout. Layer 2 is older than 13 ka and younger than 720 ka and has a normal magnetic polarity (Figure 4.13). This layer is probably part of the Matuyama reversed polarity that began about 0.78 Ma. The surface of Layer 2 decreases in elevation eastward under the site (Figure 6.7B).

Layer 3. Layer 3 has two paleosols, although one is not present everywhere in the IDF site. It also has two polarity reversals—a reverse polarity at the base of the sequence and a normal polarity between the surface and the top of the reverse polarity (Figure 4.13) (Pluhar et al. 2006).

The uppermost paleosol is a 3-m (1.1-ft) thick, oxidized and leached zone of fine-grained sand and silt with some pebbles with a 10-cm (4-in.) caliche zone (sand and silt cemented by calcium carbonate). This forms the surface of much of the IDF site north of the eolian deposits. The lower paleosol caps the lower 8 to 10 m (25 to 30 ft) of Layer 3 and is the top of the reversed polarity zone. Several minor silt lenses are locally present but are discontinuous.

6.1.4 Clastic Dikes

Although there is no evidence for clastic dikes on the surface of the IDF site, a clastic dike was encountered during the drilling of well 299-17-24 between 155.5 ft and 157.5 ft, and clastic dikes were mapped in the trench. Clastic dikes may occur in both Hanford and Ringold sediments.

6.1.5 Eolian Unit

Eolian deposits cover the southern part of the IDF disposal site. Borehole 299-E17-21 was sited on a stabilized sand dune. The eolian unit is composed of fine- to coarse-grained sands with abundant silt, as layers and as material mixed with the sand. Calcium-carbonate coating found on the bottom of pebbles and cobbles in drill core through this unit is typical of Holocene caliche development in the Columbia Basin. This unit is equivalent to mapping unit Qd, Holocene Dune Sand, of Reidel and Fecht (1994a, 1994b).

7.0 Tectonic Development of the Hanford Site

The geologic history of the Pacific Northwest from the Precambrian to the present and the resulting geologic structures that have developed at the Hanford Site significantly affect the seismic hazards of the Site (Geomatrix 1996). This section summarizes the principal tectonic events in the development of the Hanford Site and their hazards.

7.1 Summary

Microseismicity, high in situ stress conditions, and the geometry of Quaternary-Holocene faulting indicate that the basin is still experiencing north-south compression. Although known late-Cenozoic faults are found exclusively on the anticlinal ridges, earthquake focal mechanisms and strain measurements suggest that most stress release is occurring in the synclinal areas. No earthquake events have been shown to be related to known faults.

7.2 Contemporary Stress and Strain

7.2.1 Seismicity

Seismic monitoring at the Hanford Site began when the U.S. Geological Survey installed a small array of seismograph stations around the Site in summer 1969. In 1982, a closely spaced seismic network was installed at the Hanford Site to characterize the microseismicity on the Site for a possible subsurface geologic repository for high-level waste. This network operated until 1988 when the number of stations was reduced. Earthquakes of magnitudes 1.0 (Coda Amplitude Magnitude) and larger are currently being located at the Hanford Site, and earthquakes of magnitude 2.5 and larger are located throughout most of eastern Washington. Figures 7.1 through 7.3 summarize the location of historical and more recent seismic activity in the Columbia Basin.

7.2.2 Earthquake Environments

Past seismic hazard studies at the Hanford Site have shown that earthquakes can be related to three crustal layers (Table 7.1) and five general sources (Table 7.2). All layers and sources are monitored at the Hanford Site except the Cascadia Subduction Zone, which is monitored by the University of Washington.

7.2.3 Vertical Patterns

Three horizontal layers of seismicity (seismic stratigraphy) are related to the stratigraphy of the Hanford Site and vicinity—the CRBG, the pre-basalt sediments, and the crystalline basement (Table 7.1). About 75% of the earthquakes originated in the CRBG layer. The pre-basalt sedimentary layer has had 8% of the events and the crystalline basement has had 17%.

7.2.3.1 Shallow Earthquakes in the Basalts

The majority of the seismicity at the Hanford Site and the surrounding area comes from the basalt layer, which extends from the surface to approximately 4 km under the Site.

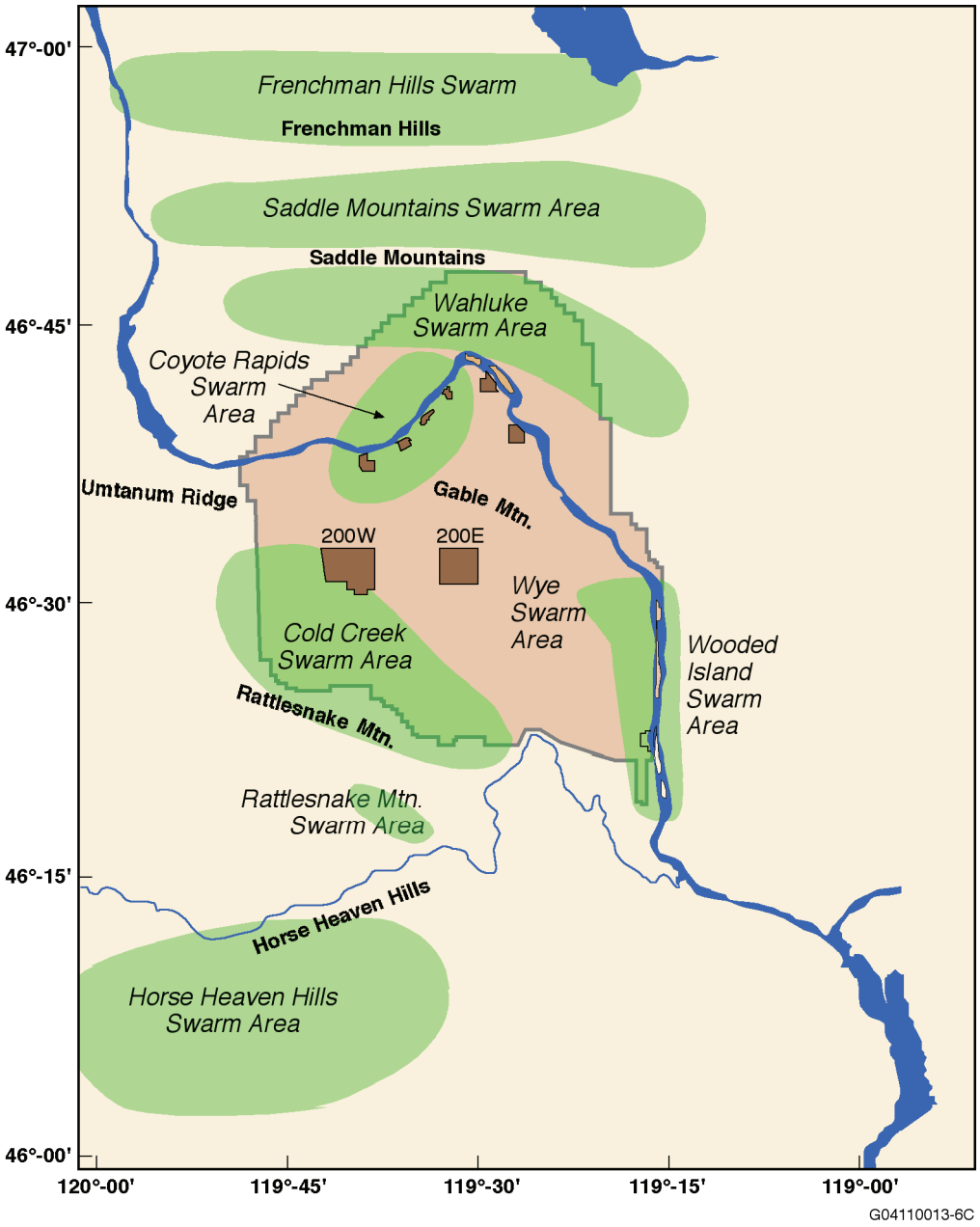

Figure 7.1. Earthquake Swarm Areas in the Pasco Basin

7.2.3.2 Earthquakes in Sedimentary Rock Below the Basalt

The seismicity in the pre-basalt sedimentary rock appears to be confined to the top 3 km. The seismicity of this sedimentary layer at the Hanford Site is relatively low when compared to the basalt layer but may be related to localized detachment zones related to the growth of the anticlinal structures.

7.2.3.3 Earthquakes in the Crystalline Basement

Deep earthquakes below 10 km appear to be concentrated in the west and southwest portion of the Hanford Site. The deepest earthquakes located below the Hanford Site are shallower than 30.0 km.

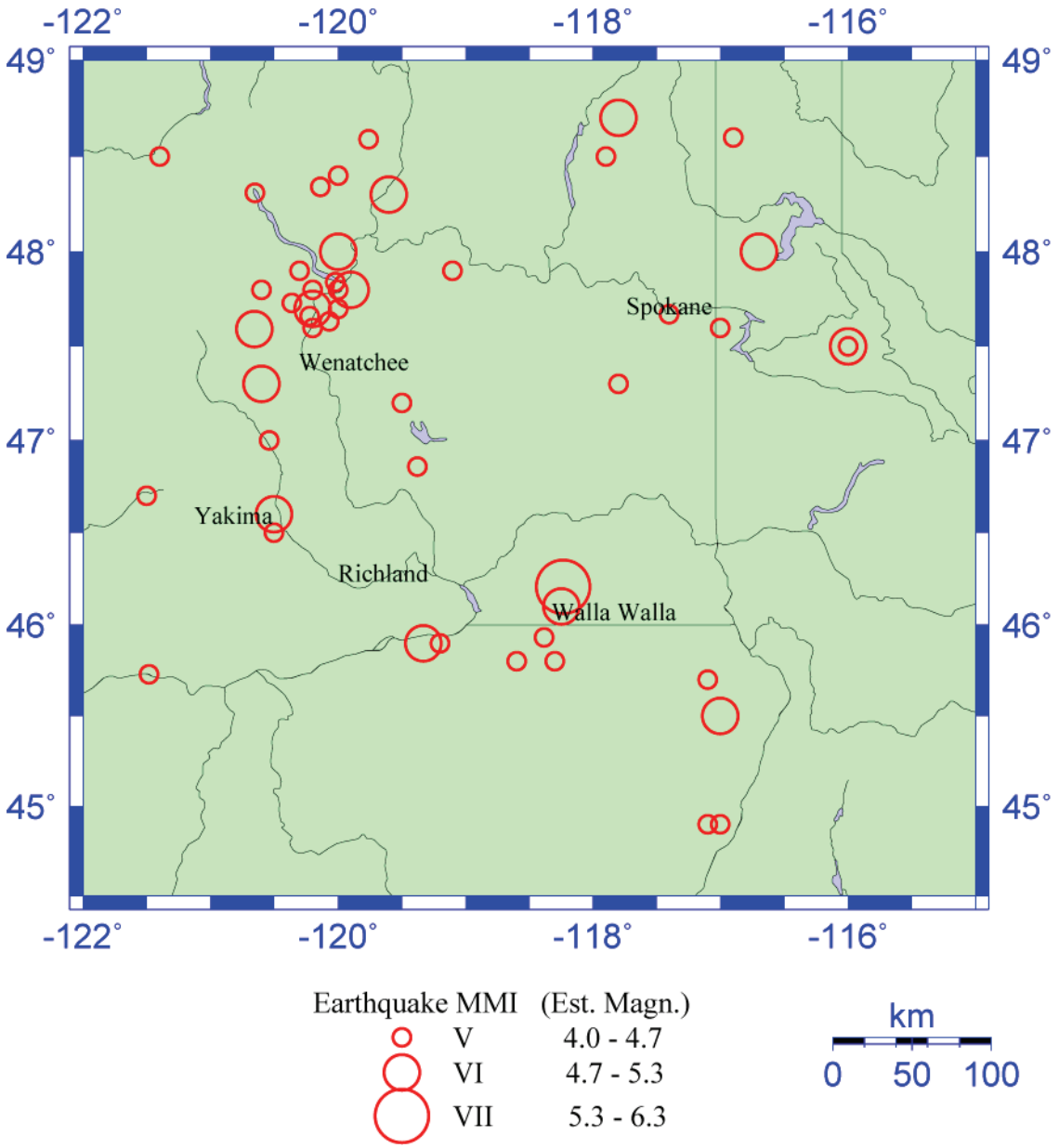

Includes all earthquakes between 1850 and 1969 with a Modified Mercalli Intensity of V or larger or a Richter magnitude of 4 or larger.

Figure 7.2. Historical Seismicity of the Columbia Basin and Surrounding Area

Using first-motion data from the Eastern Washington Regional Network and from the Basalt Waste Isolation Project, focal mechanisms show faulting that strikes between N30ºW and N80ºW. While the west-northwest strike is consistent, the throw on the assumed faults is not. These data indicate reverse faults or strike-slip faults.

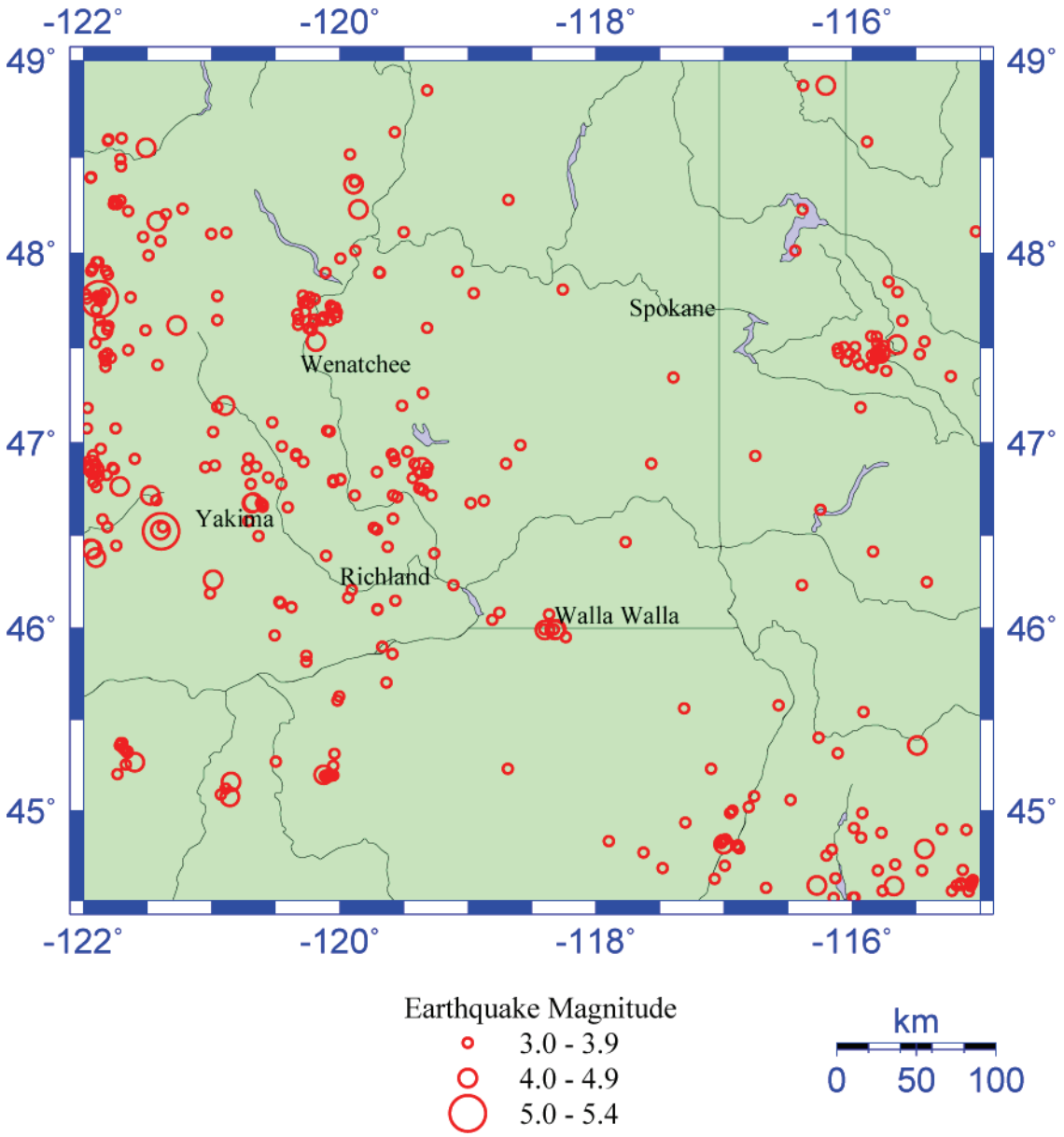

All earthquakes from 1969 to 2001 with a Richter magnitude of 3 or larger are shown.

Figure 7.3. Seismicity of the Columbia Basin and Surrounding Areas as Measured by Seismographs

Table 7.1. Depths of Earthquakes

Layer	Depth
Columbia River Basalt Group	0–5 km
Pre-basalt sediments	5–10 km
Crystalline basement	>10 km

Table 7.2. Principal Locations of Earthquakes

Area	Layer
Major reverse faults on ridges	Mainly basalt, also pre-basalt sediments
Secondary faults on ridges	Basalt
Swarm area	Basalt
Basement	Crystalline basement
Cascadia subduction zone	Lithosphere - plate tectonic boundary

7.3 Spatial Patterns

Past studies (Geomatrix 1996) have concluded that there are five different tectonic environments (earthquake sources) where earthquakes can occur near the Hanford Site and in the Columbia Basin of eastern Washington (Table 7.2):

- reverse/thrust faults in the CRBG associated with major anticlinal ridges such as Rattlesnake Mountain, Yakima Ridge, and Umtanum Ridge (Figure 3.1)
- secondary faults occurring on the major anticlinal ridges
- small geographic areas of unknown geologic structure that produce clusters of events (swarms), usually in the CRBG in synclinal valleys
- basement source structures – Because very little is known about geologic structures in the crystalline basement beneath the Hanford Site, earthquakes cannot be directly tied to a mapped fault.
- the Cascadia Subduction Zone – This source recently has been postulated to be capable of producing a magnitude 9 earthquake.

7.3.1 Floating Earthquakes

A special tectonic environment covering the entire Columbia Basin, including the Hanford Site, is considered to be a “floating” earthquake. A floating earthquake is one that, for seismic design purposes, can happen anywhere in a tectonic province and is not associated with any known geologic structure. It can be floated anywhere in the province.

7.3.2 Earthquake Swarm Areas

The major source of earthquakes at the Hanford Site is swarm activity. There are three areas of significant swarm activity: the Wooded Island Swarm Area, Coyote Rapids Swarm Area, and the Saddle Mountains Swarm Area. Several less active areas are shown in Figure 7.1. These swarm areas are located in synclinal areas in the YFB, and the majority of earthquakes at the Hanford Site occur in these swarms.

Although the swarm earthquakes (magnitude 0 to 4) are geographically correlated with the YFB, they do not tend to align along the projections of the fault traces (Figure 7.4). The Wooded Island Swarm Area, near the 300 Area, occurs at the eastern edge of the YFB where it abuts against the Palouse Slope. This boundary marks the suture zone between the old accreted terranes to the west and the stable Precambrian-Paleozoic craton to the east (Reidel et al. 1994). This zone also is marked by an abrupt increase in thickness of basalt and sub-basalt sediment over the accreted terranes and abrupt thinning of basalt and sediment over the craton.

The Coyote Rapids Swarm Area is at the horn of the Columbia River between the 100 K and 100 N areas; it occurs over no known geologic structure. The swarm lies at the intersection of two paleoslopes that make a northeast-southwest trough extending from Spokane, Washington, to the Columbia Gorge. This zone may be an old basement weakness zone, but there is no known reason for the swarm to occur in its present position.

The Saddle Mountains Swarm Area is along the north side of the Saddle Mountains. The swarm area is north of the Saddle Mountains fault zone in an area that has no mapped geologic structures. There is evidence for recent (post 13,000 years) faulting, but this faulting is part of the Saddle Mountains fault zone. The cause of the earthquake swarm is not known at this time.

7.3.3 Magnitude of Earthquakes

Earthquake activity at the Hanford Site and in the Columbia Basin is summarized in Tables 7.3 and 7.4 and in Figures 7.2 and 7.3. There is no direct comparison between Richter magnitude (not calculated as Coda Amplitude Magnitude), Modified Mercalli Intensity, and ground accelerations.

The largest magnitude earthquake on the Hanford Site was a 3.8 magnitude earthquake on October 25, 1971, in the Coyote Rapids Swarm Area (Figures 7.1 and 7.3). The largest recent, felt earthquake was a 3.3 magnitude earthquake on June 12, 1995, in the Wooded Island Swarm Area (Figure 7.1). The largest regional earthquake was the 5.7 Milton-Freewater earthquake on July 16, 1936 (Figure 7.2); this earthquake occurred 100 km southeast of the Hanford Site. The 1936 Milton-Freewater earthquake was estimated to have a peak acceleration of 0.03 *g*.

Although the swarm earthquakes (magnitude 0 to 4) are geographically correlated with the YFB, they do not tend to align along the projections of the fault traces (Figure 7.4).

7.3.4 Contemporary Stress in the Cold Creek Syncline

Geodetic surveys (DOE 1988) were performed across the Pasco Basin to determine rates of shortening. The data suggest north-south shortening but the rate of shortening is not statistically significant at the 95% confidence level and the measurements are within the error limits of the recording instruments.

Contemporary stress measurements were performed at the Hanford Site in the 1980s as part of the U.S. Department of Energy Basalt Waste Isolation Project. Core disking and spalling in boreholes drilled in the Cold Creek syncline indicate relatively high in situ stress (DOE 1988). Hydraulic fracturing tests were conducted in boreholes in the Cold Creek syncline at about 1 km depth (DOE 1988). The results also indicated high in situ stress. The maximum horizontal stress ranges from 52.6 to 67.4 MPa (7,630 to

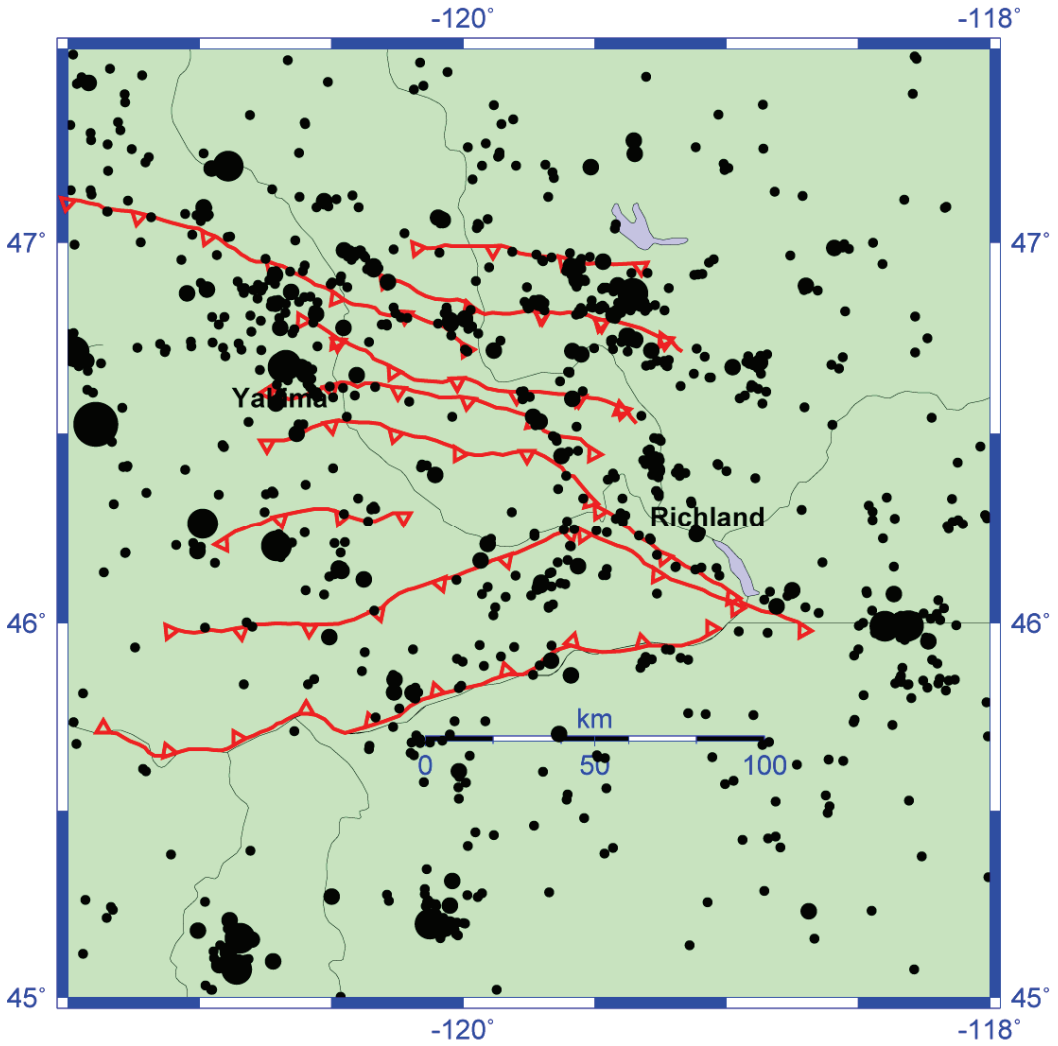

The Yakima Folds and Thrust Faults are shown in red; triangle marks are on the upthrown side of the faults.

Figure 7.4. Relationship of Small Earthquakes to Geologic Structures

9,780 lbf/in^2); the minimum horizontal stress ranges from 30.3 to 35.7 MPa (4,400 to 5,180 lbf/in^2) with a mean horizontal to vertical ratio of 1.77 + 0.20. The mean orientation of induced fractures, and the direction of the maximum horizontal stress, is consistent with north-south compression (Reidel et al. 1994).

7.4 Geologic Hazards

7.4.1 Volcanic Hazard Assessment

Two types of volcanic hazards have affected the Hanford Site in the past 20 million years:

- continental flood basalt volcanism that produced the CRBG, which underlies the Hanford Site, outcropping in the surrounding ridges, which is no longer a hazard
- volcanism associated with the Cascade Range, which still remains a hazard due to ash fall.

Table 7.3. Earthquakes Equal to or Greater Than Modified Mercalli Intensity V in Columbia Plateau and Surrounding Area from 1870 through 1980[a,b,c]

Date	Universal Time	Epicentral Intensity[d] Magnitude	Coordinates	Location/Remarks
March 5, 1892	LT	VI	46.6°N 120.5°W	North Yakima, Washington
March 5, 1893	LT	VI	45.9°N 119.3°W	Umatilla, Oregon
July 5, 1911	08:00	V	47.0°N 120.5°W	Ellensburg, Washington
February 28, 1918	23:15	V	46.5°N 120.5°W	Yakima, Washington
November 1, 1918	17:20	VI	46.7°N 119.5°W	Corfu, Washington
September 14, 1921	11:00	VI	46.1°N 118.25°W	Dixie-Walla Walla, Washington
September 18, 1934	24:00 LT	V	47.0°N 120.5°W	Ellensburg, Washington
September 26, 1934	16:15 LT	V	47.0°N 120.5°W	Ellensburg, Washington
September 26, 1934	16:45	V	47.0°N 120.5°W	Ellensburg, Washington
September 26, 1934	21:15	V	47.0°N 120.5°W	Ellensburg, Washington
October 19, 1934	23:31 LT	V	47.0°N 120.5°W	Ellensburg, Washington
November 1, 1934	07:28	V	47.0°N 120.5°W	Ellensburg, Washington
November 2, 1934	15:17 LT	V	47.0°N 120.5°W	Ellensburg, Washington
July 16, 1936	07:07:49.0	VII, 6.1 MS 5.75 ML	46.2°N 118.20°W	Milton-Freewater, Oregon (WCC Relocated)
July 18, 1936	16:30	V	46.9°N 118.4°W	Milton-Freewater, Oregon
August 4, 1936	09:19	V	45.8°N 118.6°W	Helix, Oregon
August 28, 1936	04:39	V	45.9°N 118.4°W	Milton-Freewater, Oregon
February 23, 1942	14:03	V	47.6°N 120.2°W	Wenatchee-Chelan Falls, Washington
October 31, 1944	11:34:28.7	V	47.8°N 120.6°W	Fish Lake, Washington
January 13, 1948	06:55:00	V	47.9°N 120.3°W	Lucerne-Waterville, Washington
January 7, 1951	22:45:00	V	45.9°N 119.2°W	McNary, Oregon
January 20, 1959	About 23:15	V	46.2°N 118.2°W	Milton-Freewater, Oregon
July 23, 1966	01:57:08.8	4.3 MB	47.2°N 119.5°W	Ephrata, Washington
December 20, 1973	01:08:28.2	V,4.4 MC	46.9°N 119.35°W	2.4-km depth Corfu, Washington
April 8, 1979	07:29:37.8	4.2 MC	46.0°N 118.4°W	Walla Walla, Washington (UW)

(a) Davis (1981).

(b) DOE (1988).

(c) Latitude and longitude are used to define the location of historical earthquakes. Some times and coordinates have been modified from the original source times and coordinates to better reflect the possible error of these early earthquakes.

(d) Modified Mercalli Intensity.

LT = Local time.

MB = Body-wave magnitude.

MC = Coda-length magnitude.

ML = Local magnitude.

MS = Surface-wave magnitude.

UW = University of Washington.

WCC = Woodward-Clyde Consultants.

Table 7.4. Earthquake Listing for the Columbia Plateau and Surrounding Area from 1866 to 1966[a, b, c]

Date	Universal Time	Intensity[d]/ Magnitude	Coordinates	Remarks
Earthquakes with Magnitude ≥3 or Intensity ≥IV, 1866 to 1966				
November 24, 1866	18:10	IV	45.6°N 121.2°W	The Dalles, Oregon
December 15, 1872	05:40	VIII	49.0°N 121.0°W	Lake Chelan, Washington
September 2, 1891	10:30 LT	IV	47.1°N 118.4°W	Ritzville, Washington
September 17, 1891	04:30	IV	44.9°N 121.0°W	Salem, Oregon
February 29, 1892	10:45	IV	45.6°N 121.2°W	The Dalles, Oregon
March 5, 1892	LT	VI	46.6°N 120.5°W	North Yakima, Washington
March 5, 1893	LT	VI	45.9°N 119.3°W	Umatilla, Oregon
December 15, 1897	LT	V	47.8°N 120.0°W	Lakeside, Washington
October 18, 1905	23 LT	V	47.8°N 120.0°W	Chelan, Washington
January 2, 1906	LT	VI	48.7°N 117.8°W	Stevens County, Washington
November 2, 1906	01:49	V	48.5°N 117.9°W	Reported felt information
February 18, 1907	12:20 LT	V	47.8°N 120.0°W	Chelan, Washington
January 21, 1909	05 LT	IV	47.8°N 120.0°W	Chelan, Washington
May 24, 1909	22 LT	V	47.7°N 120.4°W	Chelan-Leavenworth, Washington
June 12, 1908	Unknown	V	45.0°N 117.25°W	Cornucopia, Oregon
July 5, 1911	08:00	V	47.0°N 120.5°W	Ellensburg, Washington
October 14, 1913	23:00	V	45.7°N 117.1°W	Seven Devils, Idaho
March 5, 1915	05:10	IV	47.8°N 120.0°W	Lakeside, Washington
March 5, 1915	05:30	IV	47.8°N 120.0°W	Lakeside, Washington
July 18, 1915	20:54	IV	47.8°N 120.0°W	Lakeside, Washington
August 18, 1915	14:05	V	48.5°N 121.4°W	Felt over 78,000 km^2 (30,000 mi^2)
December 10, 1915	20:45	IV	47.7°N 117.4°W	Spokane, Washington
February 21, 1918	LT	IV	46.9°N 121.3°W	Bumping Lake, Washington
February 28, 1918	23:15	V	46.5°N 120.5°W	Near Yakima, Washington
March 12, 1918	03:26	V	47.6°N 117.0°W	Spokane, Washington
April 18, 1918	21:13	IV	47.6°N 117.4°W	White Bluffs Prairie, Washington
November 1, 1918	17:20	VI	46.7°N 119.5°W	Corfu, Washington
October 7, 1920	02 LT	V	47.6°N 120.1°W	Waterville, Washington
November 28, 1920	11:30	IV–V	45.7°N 121.5°W	Hood River, Oregon
September 14, 1921	11:00	VI	46.1°N 118.2°W	Dixie-Walla Walla, Washington
June 1, 1922	23:30	IV	47.7°N 117.4°W	Spokane, Washington
January 6, 1924	13:09	IV	46.1°N 118.3°W	Walla Walla, Washington
January 6, 1924	23:10	V	45.8°N 118.3°W	Milton and Weston, Oregon
May 27, 1924	00:19:00	IV	46.1°N 118.3°W	Walla Walla, Washington
November 28, 1925	01:25:00	4.30 ML	47.5°N 116.0°W	—
April 23, 1926	13:56:00	IV	46.1°N 118.3°W	Walla Walla, Washington
October 17, 1926	02:45:00	V	45.7°N 121.5°W	White Salmon, Washington
November 27, 1926	18:25 LT	V	47.5°N 116.0°W	Near Rathdrum, Idaho
December 30, 1926	17:57:00	VI	47.7°N 120.2°W	Chelan-East Central Washington
January 3, 1927	04:58:00	VI	47.6°N 120.6°W	Leavenworth, Washington
April 8, 1927	05:00	V	44.8°N 117.2°W	Richland, Washington
September 3, 1930	13:00:00	V	47.3°N 117.8°W	Near Lamont, Washington
December 8, 1931	14:25:00	IV	47.8°N 120.0°W	Lakeside-Chelan Falls, Washington

Table 7.4. (contd)

Date	Universal Time	Intensity[(d)]/ Magnitude	Coordinates	Remarks
Earthquakes with Magnitude ≥3 or Intensity ≥IV, 1866 to 1966				
May 31, 1933	20:20:00	IV	47.8°N 120.0°W	Chelan, Washington
May 31, 1933	20:30:00	IV	47.8°N 120.0°W	Chelan, Washington
March 9, 1934	16:00:00	IV	47.8°N 120.0°W	Lakeside, Washington
September 18, 1934	24 LT	V	47.0°N 120.5°W	Ellensburg, Washington
September 22, 1934	11:30 LT	IV	47.0°N 120.5°W	Ellensburg, Washington
September 22, 1934	17:37 LT	IV	47.0°N 120.5°W	Ellensburg, Washington
September 26, 1934	16:15 LT	V	47.0°N 120.5°W	Ellensburg, Washington
September 26, 1934	16:45 LT	V	47.0°N 120.5°W	Ellensburg, Washington
September 26, 1934	21:15 LT	V	47.0°N 120.5°W	Ellensburg, Washington
October 4, 1934	02:26 LT	IV	47.0°N 120.5°W	Ellensburg, Washington
October 11, 1934	21:19 LT	IV	47.0°N 120.5°W	Ellensburg, Washington
October 19, 1934	23:31 LT	V	47.0°N 120.5°W	Ellensburg, Washington
October 29, 1934	18:36 LT	IV	47.0°N 120.5°W	Ellensburg, Washington
November 1, 1934	07:28 LT	V	47.0°N 120.5°W	Ellensburg, Washington
November 2, 1934	15:17 LT	V	47.0°N 120.5°W	Ellensburg, Washington
July 9, 1935	22:45:00	V	47.7°N 120.0°W	Near Chelan Falls, Washington
October 12, 1935	01:03	V	47.7°N 120.2°W	Entiat, Washington
November 1, 1935	03:35	IV	47.5°N 115.9°W	Wallace, Idaho
July 16, 1936	07:07:49.0	VII 6.10 MS 5.75 ML	46.2°N 118.2°W	Milton-Freewater, Oregon
July 18, 1936	16:30	V	45.9°N 118.4°W	Milton-Freewater, Oregon
July 30, 1936	11:20	IV	45.9°N 118.4°W	Freewater, Oregon
July 30, 1936	12:00	IV	45.9°N 118.4°W	Freewater, Oregon
July 30, 1936	12:20	IV	46.1°N 118.3°W	Walla Walla, Washington
August 4, 1936	09:19	V	45.8°N 118.6°W	Helix, Oregon
August 28, 1936	04:39	V	45.9°N 118.8°W	Milton-Freewater, Oregon
February 9, 1937	22:20	IV	46.1°N 118.3°W	Walla Walla, Washington
June 4, 1937	14:43	IV	46.1°N 118.3°W	Walla Walla, Washington
August 11, 1938	18:52	IV	45.9°N 118.4°W	Milton, Oregon
October 27, 1938	23:10	IV	45.9°N 118.4°W	Milton, Oregon
January 26, 1939	07:59	IV	45.7°N 118.7°W	Mission, Oregon
November 29, 1939	04:39	V	47.7°N 120.0°W	Chelan Falls, Washington
March 24, 1940	03:04	IV	46.0°N 121.2°W	Mt. Rainier, Washington
April 7, 1941	09:25	VI 4.50 ML	48.3°N 119.6°W	Felt over 14,000 km^2 (5,500 mi^2) Mazanna, Washington
April 12, 1941	17:40	IV	47.6°N 120.1°W	Waterville, Washington
February 23, 1942	14:03	V	47.6°N 120.2°W	Wenatchee-Chelan, Washington
June 12, 1942	09:30	V	44.9°N 117.1°W	Halfway and Pine, Oregon
October 14, 1942	11:30	V	48.3°N 120.6°W	Stehekin, Washington
November 1, 1942	18:50:06.0	VI 5.50 ML	48.0°N 116.7°W	Sandpoint, Idaho
April 24, 1943	00:10:46.0	VI	47.3°N 120.6°W	Felt over 24,000 km^2 (10,000 mi^2) Leavenworth, Washington
September 22, 1943	21:50 LT	IV	48.0°N 119.0°W	Grand Coulee, Washington
September 2, 1944	01:25:14.0	IV	46.1°N 118.3°W	Walla Walla, Washington

Table 7.4. (contd)

Date	Universal Time	Intensity[(d)]/ Magnitude	Coordinates	Remarks
Earthquakes with Magnitude ≥3 or Intensity ≥IV, 1866 to 1966				
September 20, 1944	03:00	IV	44.9°N 116.9°W	Rockville, Oregon
October 31, 1944	11:34:28.7	V	47.8°N 120.6°W	Fish Lake, Washington
December 25, 1944	13:12:08.8	IV	47.7°N 120.2°W	Entiat, Washington
January 4, 1945	02:34:48.7	V	47.7°N 120.2°W	Entiat, Washington
February 27, 1945	11:00	IV	48.5°N 121.2°W	Winthrop, Washington
March 2, 1945	07:54:59.3	IV	47.7°N 120.2°W	Entiat, Washington
September 23, 1945	02:40	IV	46.1°N 118.3°W	Walla Walla, Washington
February 5, 1946	16:12:42.0	IV	47.8°N 120.2°W	Chelan-Ardenvoir, Washington
February 6, 1946	03:20	IV	48.5°N 121.4°W	Marblemount, Washington
December 22, 1947	10:30	IV	47.7°N 120.2°W	Entiat, Washington
January 13, 1948	06:55	V	47.9°N 120.3°W	Lucerne-Waterville, Washington
August 28, 1948	22:25	IV	48.0°N 117.5°W	Deer Park, Washington
October 25, 1948	19:50	IV	47.8°N 120.0°W	Chelan, Washington
December 20, 1948	16:18	IV	45.0°N 120.2°W	Fossil, Oregon
March 15, 1949	20:53:11.0	4.80 ML	45.5°N 117.0°W	Joseph, Oregon
October 20, 1949	16:00	IV	48.5°N 120.5°W	Lost River, Washington
March 8, 1950	06:25	IV	47.6°N 120.2°W	Entiat, Washington
June 25, 1950	23:45	IV	47.5°N 117.6°W	Cheney, Washington
January 4, 1951	13:45	V	47.7°N 120.0°W	Chelan-Waterville, Washington
January 7, 1951	22:45	V	45.9°N 119.2°W	McNary, Oregon
March 4, 1951	13:45:00.0	V	47.7°N 120.0°W	Chelan-Waterville, Washington
March 4, 1952	19:42	V	47.7°N 117.4°W	Spokane, Washington
September 9, 1952	09:30	IV	48.7°N 116.3°W	Felt Bonners Ferry, Idaho
September 9, 1952	09:45	IV	48.7°N 116.3°W	Felt Bonners Ferry, Idaho
September 9, 1953	09:30	IV	48.7°N 116.3°W	Felt Bonners Ferry, Idaho
May 23, 1954	13:41:42.0	V	48.342°N 120.137°W	Twisp, Washington
June 8, 1954	00:16:13.0	V	47.5°N 116.0°W	Mortaern-Coeur d'Alene, Idaho
February 6, 1955	LT	IV	47.967°N 119.000°W	Grand Coulee, Washington
May 31, 1955	23:35	IV	47.7°N 116.8°W	Felt Coeur d'Alene, Idaho
February 24, 1956	22:00	V	47.9°N 119.1°W	Electric City, Washington
November 1, 1957	10:12:02.0	4.2 ML	46.7°N 121.5°W	Mt. Rainier, Washington
December 18, 1957	25:25	5.0 ML	47.5°N 116.0°W	—
April 12, 1958	00:00	IV	47.9°N 119.1°W	Electric City, Washington
April 12, 1958	22:37:11.0	4.1 ML	48.0°N 120.0°W	Chelan, Washington
January 20, 1959	About 23:15	V	26.2°N 118.2°W	Milton-Freewater, Oregon
January 21, 1959	07:15	IV	46.1°N 118.3°W	Walla Walla, Washington
July 11, 1959	15 LT	IV	47.6°N 119.3°W	Deep Lake, Washington
August 6, 1959	03:44:32.0	4.4 ML	47.8°N 119.9°W	Chelan, Washington
November 9, 1959	21:10	IV	45.4°N 119.6°W	Heppner, Oregon
May 22, 1961	01:57:51.4	IV	47.6°N 120.2°W	—
June 28, 1961	10:22:52.9	IV	47.537°N 120.293°W	Rocky Reach Dam, Washington

Table 7.4. (contd)

Date	Universal Time	Intensity[(d)]/ Magnitude	Coordinates	Remarks
Earthquakes with Magnitude ≥3 or Intensity ≥IV, 1866 to 1966				
October 31, 1961	02:35	4.3 ML	48.4°N 120.0°W	—
October 31, 1961	03:34:29.8	V	48.4°N 120.0°W	Felt over 3,000 km^2 (1,200 mi^2)
January 15, 1962	05:29	4.3 ML	47.8°N 120.2°W	Chelan, Washington
December 22, 1963	02:54:04.9	V 4.4MB	48.59°N 119.76°W	Reported felt information
April 28, 1965	19:00	4.3 ML	48.6°N 116.9°W	—
November 7, 1965	16:41:47.4	4.3 MB	44.9°N 117.0°W	—
July 23, 1966	01:57:08.8	4.3 MB	47.2°N 119.5°W	Ephrata, Washington
December 30, 1966	03:51:40.3	4.2 MB	44.9°N 117.0°W	—

(a) Davis (1981).
(b) DOE (1988).
(c) Latitude and longitude are used to define the location of historical earthquakes. Some times and coordinates have been modified from the original source times and coordinates to better reflect the possible error of these early earthquakes.
(d) Modified Mercalli Intensity.
LT = Local time.
MB = Body-wave magnitude.
ML = Local magnitude.
MS = Surface-wave magnitude.

Volcanoes in the Cascade Range are currently considered to be active, but activity associated with flood basalt volcanism has ceased. The flood basalt volcanism that produced the CRBG occurred between 17 million and 6 million years BP. Most of the lava was extruded during the first 2 to 2.5 million years of the 11-million-year volcanic episode. Volcanic activity has not recurred during the last 6 million years, suggesting that the tectonic processes that created the episode have ceased. The recurrence of Columbia River basalt volcanism is not considered to be a credible volcanic hazard (DOE 1988).

Volcanism in the Cascade Range has been active throughout the Pleistocene Epoch (approximately 2 million years BP to 10,000 years BP) and through the Holocene Epoch (10,000 years BP to present). The eruption history of the Holocene best characterizes the most likely types of activity in the next 100 years. Many of the volcanoes have been active in the last 10,000 years, including Mount Mazama (Crater Lake) and Mount Hood in Oregon, and Mount St. Helens, Mount Adams, and Mount Rainier in Washington. The Hanford Site is approximately 150 km from Mount Adams, 175 km from Mount Rainier, and 200 km from Mount St. Helens, the three closest active volcanoes. At these distances, tephra (ash) is the only hazard. Mount St. Helens has been considerably more active throughout the Holocene than Mount Rainier or than Mount Adams, which is the least active of the three. Probabilistic volcanic hazard studies of the Cascade Range have been completed by the U.S. Geological Survey (DOE 1988; Scott et al. 1995).

7.4.2 Seismic Hazard Assessment

A seismic hazard analysis was completed for the Hanford Site (Geomatrix 1996). Previous seismic hazard analyses were done for Washington Public Power Supply System WNP 1/4 and WNP/2, which also are located on the Hanford Site.

The following discussion is based on the current seismic hazard analysis (Geomatrix 1996) that incorporates seismo-tectonic data and interpretations that postdate the earlier assessment of the Washington Public Power Supply System. For details of the source models and attenuation relationships used in the hazard assessment, see Geomatrix (1996).

The following potential seismic sources were determined to be the major contributors to the seismic hazard in and around the Hanford Site:

- crustal sources
  - fault sources related to the Yakima Folds
  - shallow basalt sources that account for the observed seismicity within the CRBG and not associated with the Yakima Folds
  - crystalline basement source region.

- Cascadia Subduction Zone earthquakes.

The Geomatrix (1996) analysis is currently being revised based on data collected since that report. That analysis will not be complete until 2007.

8.0 References

Alexander DJ, SD Evelo, VG Johnson, and MD Sweeney. 1995. *Groundwater Impact Assessment Report for the 216-T-4-2 Ditch*. WHC-EP-0815, Westinghouse Hanford Company, Richland, Washington.

Baker VR and RC Bunker. 1985. "Cataclysmic Late Pleistocene Flooding from Glacial Lake Missoula: A Review." *Quaternary Science Reviews*, Vol. 4, pp. 1–41.

Baker VR, BN Bjornstad, AJ Busacca, KR Fecht, EP Kiver, UL Moddy, JG Rigby, DF Stradling, and AM Tallman. 1991. "Quaternary Geology of the Columbia Plateau." In *The Geology of North America, Quaternary Nonglacial Geology: Conterminous U.S.*, Vol. K-2, Chapter 8, pp. 215-250, Geological Society of America, Boulder, Colorado.

Barnett DB, KR Fecht, SP Reidel, BN Bjornstad, DC Lanigan, and CF Rust. 2007. *Geology of the Waste Treatment Plant Seismic Boreholes*. PNNL-16407, Rev. 1, Pacific Northwest National Laboratory, Richland, Washington.

Bentley RD. 1977. "Stratigraphy of the Yakima Basalts and Structural Evolution of the Yakima Ridges in the Western Columbia Plateau." In *Geological Excursions in the Pacific Northwest*, 1977 Annual Meeting, Geological Society of America, Seattle, Washington, pp. 339-389, Geological Society of America, Boulder, Colorado.

Bergeron MP and SK Wurstner. 2000. *Groundwater Flow and Transport Calculations Supporting the Immobilized Low-Activity Waste Disposal Facility Performance Assessment*. PNNL-13400, Pacific Northwest National Laboratory, Richland, Washington.

Bjornstad BN. 1990. *Geohydrology of the 218-W-5 Burial Ground, 200 West Area, Hanford Site*. PNL-7336, Pacific Northwest Laboratory, Richland, Washington.

Bjornstad BN. 2004. *Geologic Contacts Database for the 200 Areas of the Hanford Site*. WMP-22817, Rev. 0, Fluor Hanford, Inc., Richland, Washington.

Bjornstad BN, KR Fecht, and CJ Pluhar. 2001. "Long History of Pre-Wisconsin, Ice Age Cataclysmic Floods: Evidence from Southeastern Washington State." *Journal of Geology*, Vol. 109, pp. 695-713. DOI: 10.1086.323190.

Bretz JH, HTU Smith, and GE Neff. 1956. "Channeled Scabland of Washington: New Data and Interpretations." *Geological Society of America Bulletin*, Vol. 67, No. 8, pp. 957-1049.

Brown CF, RJ Serne, BN Bjornstad, DG Horton, DC Lanigan, RE Clayton, MM Valenta, TS Vickerman, IV Kutnyakov, KN Geiszler, SR Baum, KE Parker, and MJ Lindberg. 2006. *Characterization of Vadose Zone Sediments Below the C Tank Farm: Borehole C4297 and RCRA Borehole 299-E27-22*. PNNL-15503, Pacific Northwest National Laboratory, Richland, Washington.

Brown DJ. 1959. *Subsurface Geology of the Hanford Separation Areas*. HW-61780, Hanford Atomic Products Operation, General Electric Company, Richland, Washington.

Brown DJ. 1960. *An Eolian Deposit Beneath 200-West Area*. HW-67549, General Electric Company, Richland, Washington.

Caggiano JA. 1993. *Hydrologic Testing of the Single-Shell Tanks, 1989*. WHC-SD-EN-TI-147, Rev. 0, Westinghouse Hanford Company, Richland, Washington.

Caggiano JA and SM Goodwin. 1995. *Interim Status Groundwater Monitoring Plan for the Single-Shell Tanks*. WHC-SD-EN-AP-012, Rev. 1, Westinghouse Hanford Company, Richland, Washington.

Camp VE, ME Ross, and WE Hanson. 2003. "Genesis of Flood Basalts and Basin and Range Volcanic Rocks from Steens Mountain to the Malheur River Gorge, Oregon." *Geological Society of America Bulletin*, Vol. 115, No. 1, pp. 105-128.

Campbell NP. 1989. "Structural and Stratigraphic Interpretation of Rocks under the Yakima Fold Belt, Columbia Basin, Based on Recent Surface Mapping and Well Data." In *Volcanism and Tectonism on the Columbia River Flood-Basalt Province*, Special Paper 239, Geological Society of America, Boulder, Colorado.

Connelly MP, JV Borghese, CD Delaney, BH Ford, JW Lindberg, and SJ Trent. 1992. *Hydrogeologic Model for the 200 East Groundwater Aggregate Area*. WHC-SD-EN-TI-019, Rev. 0, Westinghouse Hanford Company, Richland, Washington.

Connelly MP, BH Ford, and JV Borghese. 1992. *Hydrogeologic Model for the 200 West Groundwater Aggregate Area*. WHC-SD-EN-TI-014, Rev. 0, Westinghouse Hanford Company, Richland, Washington.

Davis GA. 1981. "Late Cenozoic Tectonics of the Pacific Northwest with Special Reference to the Columbia Plateau," *Final Safety Analysis Report: Washington Public Power Supply System Nuclear Projects Number 2*, Amendment No. 18, Appendix 2.5N, Washington Public Power Supply System, Richland, Washington.

DOE. 1988. *Consultation Draft: Site Characterization Plan, Reference Repository Location, Hanford Site, Washington*. DOE/RW-0164, U.S. Department of Energy, Washington, D.C.

DOE. 1996. *Natural Phenomena Hazards Characterization Criteria*. DOE-STD-1022-94, Change Notice #1, U.S. Department of Energy, Washington, D.C.

DOE-GJO. 1996. *Vadose Zone Characterization Project at the Hanford Tank Farms: SX Tank Farm Report*. DOE/ID/12584-268, GJPO-HAN-4, U.S. Department of Energy, Grand Junction Office, Grand Junction, Colorado.

DOE-GJO. 1997. *Hanford Tank Farms Vadose Zone: TX Tank Farm Report*. GJO-97-13-TAR, GJO-HAN-11, U.S. Department of Energy, Grand Junction Office, Grand Junction, Colorado.

DOE-ORP. 2006. *Initial Single-Shell Tank System Performance Assessment for the Hanford Site.* DOE/ORP-2005-01, Rev. 0, U.S. Department of Energy, Office of River Protection, Richland, Washington.

DOE-RL. 1992. *Hanford Site Groundwater Background*. DOE/RL-92-23, U.S. Department of Energy, Richland Operations Office, Richland, Washington.

DOE-RL. 1993. *Phase I Remedial Investigation Report for 200-BP-1 Operable Unit*. DOE/RL-92-70, Rev. 0, U.S. Department of Energy, Richland Operations Office, Richland, Washington.

DOE-RL. 1997. *Hanford Site Background: Part 3, Groundwater Background*. DOE/RL-96-61, Rev. 0, U.S. Department of Energy, Richland Operations Office, Richland, Washington.

DOE-RL. 2002. *Standardized Stratigraphic Nomenclature for Post-Ringold-Formation Sediments Within the Central Pasco Basin*. DOE/RL-2002-39, Rev. 0, U.S. Department of Energy, Richland Operations Office, Richland, Washington.

Fecht KR, SP Reidel, and AM Tallman. 1987. "Paleodrainage of the Columbia River System on the Columbia Plateau of Washington State - A Summary." In *Selected Papers on the Geology of Washington*, Bulletin 77, pp. 219-248, Division of Geology and Earth Resources, Washington State Department of Natural Resources, Olympia.

Fecht KR, KA Lindsey, BN Bjornstad, DG Horton, GV Last, and SP Reidel. 1999. *Clastic Injection Dikes of the Pasco Basin and Vicinity – Geologic Atlas Series*. BHI-01103, Rev. 0, Bechtel Hanford, Inc., Richland, Washington.

Geomatrix. 1996. *Probabilistic Seismic Hazard Analysis DOE Hanford Site, Washington*. WHC-SD-W236A-TI-002, Rev. 1, Westinghouse Hanford Company, Richland, Washington.

Goff FE. 1981. *Preliminary Geology of Eastern Umtanum Ridge, South-Central Washington*. RHO-BWI-C-21, Rockwell Hanford Operations, Richland, Washington.

Grolier MJ and JW Bingham. 1971. *Geologic Map and Sections of Parts of Grant, Adams, and Franklin Counties, Washington*. Miscellaneous Geologic Investigations Map I-589, U.S. Geological Survey, Reston, Virginia.

Hagood MC. 1986. *Structure and Evolution of the Horse Heaven Hills in South-Central Washington*. RHO-BW-SA-344 P, Rockwell Hanford Operations, Richland, Washington.

Hajek BF. 1966. *Soil Survey: Hanford Project in Benton County Washington*. BNWL-243, Pacific Northwest Laboratory, Richland, Washington.

Hartman MJ, LF Morasch, and WD Webber (editors). 2001. *Hanford Site Groundwater Monitoring for Fiscal Year 2000*. PNNL-13404, Pacific Northwest National Laboratory, Richland, Washington.

Hartman MJ, LF Morasch, and WD Webber (editors). 2003. *Hanford Site Groundwater Monitoring for Fiscal Year 2002*. PNNL-14187, Pacific Northwest National Laboratory, Richland, Washington.

Hartman MJ, LF Morasch, and WD Webber (editors). 2004. *Hanford Site Groundwater Monitoring for Fiscal Year 2003*. PNNL-14548, Pacific Northwest National Laboratory, Richland, Washington.

Hodges FN and CJ Chou. 2000. *Groundwater Quality Assessment for Waste Management Area U: First Determination*. PNNL-13282, Pacific Northwest National Laboratory, Richland, Washington.

Horton DG. 2007. *Data Package for Past and Current Groundwater Flow and Contamination Beneath Single-Shell Tank Waste Management Areas.* PNNL-15837, Pacific Northwest National Laboratory, Richland, Washington.

Horton DG. 2002. *Borehole Data Package for Calendar Year 2001 RCRA Wells at Single-Shell Tank Waste Management Area B-BX-BY*. PNNL-13827, Pacific Northwest National Laboratory, Richland, Washington.

Horton DG. 2002. *Borehole Data Package for Calendar Year 2001 RCRA Wells at Single-Shell Tank Waste Management Area U*. PNNL-13828, Pacific Northwest National Laboratory, Richland, Washington.

Horton DG and VG Johnson. 2000. *Borehole Data Package for Wells 299-W22-48, 299-W22-49, and 299-W22-50 at Single-Shell Tank Waste Management Area S-SX*. PNNL-13200, Pacific Northwest National Laboratory, Richland, Washington.

Horton DG and SM Narbutovskih. 2001. *RCRA Groundwater Monitoring Plan for Single-Shell Tank Waste Management Area C at the Hanford Site*. PNNL-13024, Pacific Northwest National Laboratory, Richland, Washington.

Jarchow CM. 1991. *Investigations of Magmatic Underplating Beneath the Northwestern Basin and Range Province, Nevada, Seismic Data Acquisition and Tectonic Problems of the Columbia Plateau, Washington, and the Nature of the Mohorovićić Discontinuity Worldwide.* Order Number 9206793, Stanford University, Stanford, California.

Johnson VG and CJ Chou. 1998. *Results of Phase I Groundwater Quality Assessment for Single-Shell Tank Waste Management Areas S-SX at the Hanford Site*. PNNL-11810, Pacific Northwest National Laboratory, Richland, Washington.

Johnson VG and CJ Chou. 2002. *Groundwater Quality Assessment Report for Waste Management Area S-SX (April 2000 through December 2001)*. PNNL-13801, Pacific Northwest National Laboratory, Richland, Washington.

Johnson VG, TE Jones, SP Reidel, and MI Wood. 1999. *Subsurface Physical Conditions Description of the S-SX Waste Management Area*. HNF-4936, Rev. 0, Lockheed Martin Hanford Corporation, Richland, Washington.

Jones TE, R Khaleel, DA Myers, JW Shade, and MI Wood. 1998. *A Summary and Evaluation of Hanford Site Tank Farm Subsurface Contamination*. HNF-2603, Rev. 0, Lockheed Martin Hanford Corporation, Richland, Washington.

Kipp KL and RD Mudd. 1974. *Selected Water Table Contour Maps and Well Hydrographs for the Hanford Reservation, 1944-1973*. BNWL-B-360, Pacific Northwest Laboratories, Richland, Washington.

Knepp AJ. 2002. *Field Investigation Report for Waste Management Area B-BX-BY*. RPP-10098, Rev. 0, CH2M HILL Hanford Group, Inc., Richland, Washington.

Last GV, DW Duncan, MJ Graham, MD Hall, VW Hall, DS Laudeen, JG Leitz, and RM Mitchell. 1994. *216-U-10 Pond and 216-Z-19 Ditch Characterization Studies*. WHC-EP-0707 (formerly RHO-ST-45), Westinghouse Hanford Company, Richland, Washington.

Last GV, BN Bjornstad, MP Bergeron, DW Wallace, DR Newcomer, JA Schramke, MA Chamness, CS Cline, SP Airhart, and JS Wilbur. 1989. *Hydrogeology of the 200 Areas Low-Level Burial Grounds – An Interim Report*. PNL-6820, Vol. 1, Pacific Northwest Laboratory, Richland, Washington.

Lindenmeier CW, RJ Serne, BN Bjornstad, GW Gee, HT Schaef, DC Lanigan, MJ Lindberg, RE Clayton, VL LeGore, IV Kutnyakov, SR Baum, KN Geiszler, CF Brown, MM Valenta, TS Vickerman, and LJ Royack. 2003. *Characterization of Vadose Zone Sediment: RCRA Borehole 299-E33-338 Located Near the B-BX-BY Waste Management Area*. PNNL-14121, Pacific Northwest National Laboratory, Richland, Washington.

Lindenmeier CW, RJ Serne, BN Bjornstad, GV Last, DC Lanigan, MJ Lindberg, RE Clayton, VL Legore, IV Kutnyakov, SR Baum, KN Geiszler, MM Valenta, and TS Vickerman. 2002. *Characterization of Vadose Zone Sediment: Borehole C3103 Located in the 216-B-7A Crib Near the B Tank Farm* . PNNL-14128, Pacific Northwest National Laboratory, Richland, Washington.

Lindsey KA. 1991. *Revised Stratigraphy for the Ringold Formation, Hanford Site, South-Central Washington*. WHC-SD-EN-EE-004, Rev. 0, Westinghouse Hanford Company, Richland, Washington.

Lindsey KA. 1995. *Miocene- to Pliocene-Aged Suprabasalt Sediments of the Hanford Site, South-Central Washington*. BHI-00184, Rev. 00, Bechtel Hanford, Inc., Richland, Washington.

Lindsey KA. 1996. *The Miocene to Pliocene Ringold Formation and Associated Deposits of the Ancestral Columbia River System, South-Central Washington and North-Central Oregon*. Open File Report 96-8, Division of Geology and Earth Resources. Washington State Department of Natural Resources, Olympia.

Lindsey KA, BN Bjornstad, JW Lindberg, and KM Hoffman. 1992. *Geologic Setting of the 200 East Area: An Update*. WHC-SD-EN-TI-012, Rev. 0, Westinghouse Hanford Company, Richland, Washington.

Lindsey KA, SP Reidel, KR Fecht, JL Slate, AG Law, and AM Tallman. 1994. "Geohydrologic Setting of the Hanford Site, South-Central Washington" In *Geologic Field Trips in the Pacific Northwest*, 1994 Geological Society of America Annual Meeting, Vol. 1, Chap. 1C, pp. 1-16, Geological Society of America, Boulder, Colorado.

Lindsey KA, SE Kos, and KD Reynolds. 2000. *Vadose Zone Geology of Boreholes 299-W22-50 and 299-W23-19 S-SX Waste Management Area, Hanford Site, South-Central Washington*. RPP-6149, Rev. 0, CH2M HILL Hanford Group, Inc., Richland, Washington.

Lindsey KA, KD Reynolds, and SE Kos. 2001. *Vadose Zone Geology of Boreholes 299-E33-45 and 299-E33-46 B-BX-BY Waste Management Area Hanford Site, South-Central Washington*. RPP-8681, Rev. 0, CH2M HILL Hanford Group, Inc., Richland, Washington.

Lindsey KA, SE Kos, and KD Reynolds. 2001. *Vadose Zone Geology of Boreholes 299-W10-27 and 299-W11-39 T-TX-TY Waste Management Area Hanford Site, South-Central Washington*. RPP-8531, Rev. 0, CH2M HILL Hanford Group, Inc., Richland, Washington.

Malde HE. 1968. *The Catastrophic Late Pleistocene Bonneville Flood in the Snake River Plain, Idaho.* Professional Paper 596, U.S. Geological Survey, Reston, Virginia.

Mann FM and MP Connelly. 2003. *Preliminary Performance Assessment for Waste Management Area C at the Hanford Site, Washington.* DOE/ORP-2003-11, Rev. 0, U.S. Department of Energy, Office of River Protection, Richland, Washington.

Mann FM, KC Burgard, WR Root, PJ Puigh, SH Finfrock, R Khaleel, DH Bacon, EJ Freeman, BP McGrail, SK Wurstner, and PE LaMont. 2001. *Hanford Immobilized Low-Activity Tank Waste Performance Assessment: 2001 Version.* DOE/ORP-2000-24, Rev. 0, U.S. Department of Energy, Office of River Protection, Richland, Washington.

Myers CW and SM Price, Principal authors, and JA Caggiano, MP Cochran, WJ Czimer, NJ Davidson, RC Edwards, KR Fecht, GE Holmes, MG Jones, JR Kunk, RD Landon, RK Ledgerwood, JT Lillie, PE Long, TH Mitchell, EH Price, SP Reidel, and AM Tallman. 1979. *Geologic Studies of the Columbia Plateau – A Status Report: October 1979*. RHO-BWI-ST-4, Rockwell Hanford Operations, Richland, Washington.

Narbutovskih SM and DG Horton. 2001. *RCRA Groundwater Monitoring Plan for Single-Shell Tank Waste Management Area A-AX at the Hanford Site*. PNNL-13023, Pacific Northwest National Laboratory, Richland, Washington.

Neitzel DA, BN Bjornstad, CJ Fosmire, and RA Fowler (editors). 1996. *Hanford Site National Environmental Policy Act (NEPA) Characterization*. PNL-6415, Rev. 8, Pacific Northwest National Laboratory, Richland, Washington.

Newcomb RC. 1958. "Ringold Formation of Pleistocene Age in Type Locality, the White Bluffs, Washington." *American Journal of Science*, Vol. 256, pp. 328-340.

Newcomb RC, JR Strand, and FJ Frank. 1972. *Geology and Ground-Water Characteristics of the Hanford Reservation of the U.S. Atomic Energy Commission, Washington*. Professional Paper 717, U.S. Geological Survey, Reston, Virginia.

O'Connor JE. 1993. "Hydrology, Hydraulics, and Geomorphology of the Bonneville Flood." Special Paper 274, p. 83, Geological Society of America, Boulder, Colorado.

O'Connor JE and VR Baker. 1992. "Magnitudes and Implications of Peak Discharges from Glacial Lake Missoula." *Geological Society of America Bulletin*, Vol. 104, No. 3, pp. 267-279.

Pluhar CJ. 2003. *Paleomagnetic and Geochemical Applications to Tectonics and Quaternary Geology: Studies at Coso Volcanic Field, CA and the Channeled Scabland, WA.* University of California, Santa Cruz, California.

Pluhar CJ, BN Bjornstad, SP Reidel, RS Coe, and PB Nelson. 2006. "Magnetostratiphic Evidence from the Cold Creek Bar for Onset of Ice-Age Cataclysmic Floods in Eastern Washington During the Early Pleistocene." *Quaternary Research*, Vol. 65, pp. 123-135.

Price WH and KR Fecht. 1976a. *Geology of the 241-A Tank Farm*. ARH-LD-127, Atlantic Richfield Hanford Company, Richland, Washington.

Price WH and KR Fecht. 1976b. *Geology of the 241-AX Tank Farm*. ARH-LD-128, Atlantic Richfield Hanford Company, Richland, Washington.

Price WH and KR Fecht. 1976c. *Geology of the 241-B Tank Farm*. ARH-LD-129, Atlantic Richfield Hanford Company, Richland, Washington.

Price WH and KR Fecht. 1976d. *Geology of the 241-BX Tank Farm*. ARH-LD-130, Atlantic Richfield Hanford Company, Richland, Washington.

Price WH and KR Fecht. 1976e. *Geology of the 241-BY Tank Farm*. ARH-LD-131, Atlantic Richfield Hanford Company, Richland, Washington.

Price WH and KR Fecht. 1976f. *Geology of the 241-C Tank Farm*. ARH-LD-132, Atlantic Richfield Hanford Company, Richland, Washington.

Price WH and KR Fecht. 1976g. *Geology of the 241-S Tank Farm*. ARH-LD-133, Atlantic Richfield Hanford Company, Richland, Washington.

Price WH and KR Fecht. 1976h. *Geology of the 241-SX Tank Farm*. ARH-LD-134, Atlantic Richfield Hanford Company, Richland, Washington.

Price WH and KR Fecht. 1976i. *Geology of the 241-T Tank Farm*. ARH-LD-135, Atlantic Richfield Hanford Company, Richland, Washington.

Price WH and KR Fecht. 1976j. *Geology of the 241-TX Tank Farm*. ARH-LD-136, Atlantic Richfield Hanford Company, Richland, Washington.

Price WH and KR Fecht. 1976k. *Geology of the 241-TY Tank Farm*. ARH-LD-137, Atlantic Richfield Hanford Company, Richland, Washington.

Price WH and KR Fecht. 1976l. *Geology of the 241-U Tank Farm*. ARH-LD-138, Atlantic Richfield Hanford Company, Richland, Washington.

Price EH and AJ Watkinson. 1989. "Structural Geometry and Strain Distribution Within Eastern Umtanum Fold Ridge, South-Central Washington." In *Volcanism and Tectonism in the Columbia River Flood-Basalt Province*, Special Paper 239, pp. 265-282, Geological Society of America, Boulder, Colorado.

PSPL. 1981. *Skagit/Hanford Nuclear Project, Preliminary Safety Analysis Report*. Puget Sound Power and Light Company, Vol. 1, Tacoma, Washington.

Raisz E. 1945. "The Olympic-Wallowa-Lineament." *American Journal of Science*, Vol. 243-a, No. 5, pp. 479-485.

Reidel SP. 1984. "The Saddle Mountains: The Evolution of an Anticline in the Yakima Fold Belt." *American Journal of Science*, Vol. 284, No. 8, pp. 942-978.

Reidel SP. 2005. *Geologic Data Package for 2005 Integrated Disposal Facility Performance Assessment*. PNNL-14586 Rev. 1, Pacific Northwest National Laboratory, Richland, Washington.

Reidel SP and NP Campbell. 1989. "Structure of the Yakima Fold Belt, Central Washington," *Geologic Guidebook for Washington and Adjacent Areas*. Information Circular 86, pp. 275-303, Division of Geology and Earth Resources, Washington State Department of Natural Resources, Olympia.

Reidel SP and KR Fecht. 1994. *Geologic Map of the Priest Rapids 1:100,000 Quadrangle, Washington*. Open File Report 94-13, p. 22, Division of Geology and Earth Resources, Washington State Department of Natural Resources, Olympia.

Reidel SP and KR Fecht. 1994. *Geologic Map of the Richland 1:100,000 Quadrangle, Washington*. Open File Report 94-8, p. 21, Division of Geology and Earth Resources, Washington State Department of Natural Resources, Olympia.

Reidel SP and PR Hooper (eds). 1989. *Volcanism and Tectonism in the Columbia River Flood-Basalt Province*. Special Paper 239, p. 386, plate 1, Geological Society of America, Boulder, Colorado.

Reidel SP, KR Fecht, MC Hagood, and TL Tolan. 1989a. "The Geologic Evolution of the Central Columbia Plateau." In *Volcanism and Tectonism in the Columbia River Flood-Basalt Province*, Special Paper 239, pp. 247-264, Geological Society of America, Boulder, Colorado.

Reidel SP, TL Tolan, PR Hooper, MH Beeson, KR Fecht, RD Bentley, and JL Anderson. 1989b. "The Grande Ronde Basalt, Columbia River Basalt Group; Stratigraphic Descriptions and Correlations in Washington, Oregon, and Idaho." In *Volcanism and Tectonism in the Columbia River Flood-Basalt Province*, Special Paper 239, pp. 21-53, Geological Society of America, Boulder, Colorado.

Reidel SP, KA Lindsey, and KR Fecht. 1992. *Field Trip Guide to the Hanford Site*. WHC-MR-0391, Westinghouse Hanford Company, Richland, Washington.

Reidel SP, NP Campbell, KR Fecht, and KA Lindsey. 1994. "Late Cenozoic Structure and Stratigraphy of South-Central Washington." In *Regional Geology of Washington State*, Bulletin 80, pp. 159-180, Division of Geology and Earth Resources, Washington State Department of Natural Resources, Olympia.

Reidel SP, DG Horton, Y Chien, DB Barnett, and KM Singleton. 2006. *Geology, Hydrogeology, Geochemistry, and Mineralogy Data Package for the Single-Shell Tank Waste Management Areas at the Hanford Site*. RPP-23748, CH2M HILL Hanford Group, Inc., Richland, Washington.

Resource Conservation and Recovery Act of 1976, Public Law 94-580, 90 Stat. 2795, 42 USC 6901 et seq.

Saltus RW. 1993. "Upper-Crustal Structure Beneath the Columbia River Basalt Group, Washington: Gravity Interpretation Controlled by Borehole and Seismic Studies." *Geological Society of America Bulletin*, Vol. 105, pp. 1247-1259.

Scott WE, RM Iverson, JW Vallance, and W Hildreth. 1995. *Volcano Hazards in the Mount Adams Region, Washington.* Open-File Report 95-492, U.S. Geological Survey, Reston, Virginia.

Serne RJ, BN Bjornstad, GW Gee, HT Schaef, DC Lanigan, RG Mccain, CW Lindenmeier, RD Orr, VL Legore, RE Clayton, MJ Lindberg, IV Kutnyakov, SR Baum, KN Geiszler, MM Valenta, TS Vickerman, and LJ Royack. 2002c. *Characterization of Vadose Zone Sediment: Borehole 299-E33-46 Near Tank B-110 in the B-BX-BY Waste Management Area*. PNNL-14119, Pacific Northwest National Laboratory, Richland, Washington.

Serne RJ, BN Bjornstad, HT Schaef, BA Williams, DC Lanigan, DG Horton, RE Clayton, AV Mitroshkov, VL LeGore, MJ O'Hara, CF Brown, KE Parker, IV Kutnyakov, JN Serne, GV Last, SC Smith, CW Lindenmeier, JM Zachara, and DS Burke. 2002a. *Characterization of Vadose Zone Sediment: Uncontaminated RCRA Borehole Core Samples and Composite Samples*. PNNL-13757-1, Pacific Northwest National Laboratory, Richland, Washington.

Serne RJ, HT Schaef, BN Bjornstad, DC Lanigan, GW Gee, CW Lindenmeier, RE Clayton, VL Legore, RD Orr, MJ O'Hara, CF Brown, GV Last, IV Kutnyakov, D Burke, TC Wilson, and BA Williams. 2002b. *Characterization of Vadose Zone Sediment: Borehole 299-W23-19 [SX -115] in the S-SX Waste Management Area*. PNNL-13757-2, Pacific Northwest National Laboratory, Richland, Washington.

Serne RJ, BN Bjornstad, DG Horton, DC Lanigan, CW Lindenmeier, MJ Lindberg, RE Clayton, VL LeGore, KN Geiszler, SR Baum, MM Valenta, IV Kutnyakov, TS Vickerman, RD Orr, and CF Brown. 2004a. *Characterization of Vadose Zone Sediments Below the T Tank Farm: Boreholes C4104, C4105, 299-W10-196 and RCRA Borehole 299-W11-39.* PNNL-14849, Pacific Northwest National Laboratory, Richland, Washington

Serne RJ, BN Bjornstad, DG Horton, DC Lanigan, CW Lindenmeier, MJ Lindberg, RE Clayton, VL LeGore, RD Orr, IV Kutnyakov, SR Baum, KN Geiszler, MM Valenta, and TS Vickerman. 2004b. *Characterization of Vadose Zone Sediments Below the TX Tank Farm: Boreholes C3830, C3831, C3832 and RCRA Borehole 299-W10-27*. PNNL-14594, Pacific Northwest National Laboratory, Richland, Washington.

Serne RJ, GV Last, GW Gee, HT Schaef, DC Lanigan, CW Lindenmeier, MJ Lindberg, RE Clayton, VL Legore, RD Orr, IV Kutnyakov, SR Baum, KN Geiszler, CF Brown, MM Valenta, and TS Vickerman. 2002. *Characterization of Vadose Zone Sediment: Borehole 299-E33-45 Near BX-102 in the B-BX-BY Waste Management Area*. PNNL-14083, Pacific Northwest National Laboratory, Richland, Washington.

Shaw J, M Munro-Stasiuk, B Sawyer, C Beaney, J-E Lesemann, A Musacchio, B Rains, and RR Young. 1999. "The Channeled Scabland: Back to Bretz?," *Geology*, Vol. 27, No. 7, pp. 605-608.

Singleton KM and KA Lindsey. 1994. *Groundwater Impact Assessment Report for the 216-U-14 Ditch*. WHC-EP-0698, Westinghouse Hanford Company, Richland, Washington.

Slate JL. 1996. "Buried Carbonate Paleosols Developed in Pliocene-Pleistocene Deposits of the Pasco Basin, South-Central Washington, U.S.A." *Quaternary International*, Vol. 34-36, pp. 191-196.

Slate JL. 2000. *Nature and Variability of the Plio-Pleistocene Unit in the 200 West Area of the Hanford Site*. BHI-01203, Rev. 0, Bechtel Hanford, Inc., Richland, Washington.

Smith RM, FN Hodges, and BA Williams. 2001. *Groundwater Quality Assessment Plan for Single-Shell Tank Waste Management Area U*. PNNL-13612, Pacific Northwest National Laboratory, Richland, Washington.

Sobczyk SM. 2000. *Subsurface Interpretation of the SX Tank Farm Hanford Site, Washington Based on Gamma-Ray Logging*. Nez Perce Tribe Environmental Restoration Waste Management Program, Lapwai, Idaho.

Spane FA Jr., PD Thorne, and DR Newcomer. 2001a. *Results of Detailed Hydrologic Characterization Tests – Fiscal Year 1999*. PNNL-13378, Pacific Northwest National Laboratory, Richland, Washington.

Spane FA Jr., PD Thorne, and DR Newcomer. 2001. *Results of Detailed Hydrologic Characterization Tests – Fiscal Year 2000*. PNNL-13514, Pacific Northwest National Laboratory, Richland, Washington.

Spane FA, Jr., PD Thorne, and DR Newcomer. 2002. *Results of Detailed Hydrologic Characterization Tests – Fiscal Year 2001*. PNNL-14113, Pacific Northwest National Laboratory, Richland, Washington.

Spane FA Jr., PD Thorne, and DR Newcomer. 2003. *Results of Detailed Hydrologic Characterization Tests – Fiscal Year 2002*. PNNL-14186, Pacific Northwest National Laboratory, Richland, Washington.

Swanson DA, JL Anderson, RD Bentley, VE Camp, JN Gardner, and TL Wright. 1979a. *Reconnaissance Geologic Map of the Columbia River Basalt Group in Eastern Washington and Northern Idaho*. Open File Report 79-1363, U.S. Geological Survey, Reston, Virginia.

Swanson DA, TL Wright, PR Hooper, and RD Bentley. 1979b. *Revisions in Stratigraphic Nomenclature of the Columbia River Basalt Group*. Bulletin 1457-G, U.S. Geological Survey, Reston, Virginia.

Tabor RW, VA Frizzell Jr., JA Vance, and CW Naeser. 1984. "Ages and Stratigraphy of Lower and Middle Tertiary Sedimentary and Volcanic Rocks of the Central Cascades, Washington: Application to the Tectonic History of the Straight Creek Fault." *Geological Society of America Bulletin*, Vol. 95, pp. 26-44.

Tallman AM, KR Fecht, MC Marratt, and GV Last. 1979. *Geology of the Separations Areas, Hanford Site, South-Central Washington*. RHO-ST-23, Rockwell Hanford Operations, Richland, Washington.

Tallman AM, JT Lillie, and KR Fecht. 1981. "Suprabasalt Sediment of the Cold Creek Syncline Area." Chapter 2 in *Subsurface Geology of the Cold Creek Syncline*. RHO-BWI-ST-14, Rockwell Hanford Operations, Richland, Washington.

Thorne PD, MA Chamness, FA Spane Jr., VR Vermeul, and WD Webber. 1993. *Three-Dimensional Conceptual Model for the Hanford Site Unconfined Aquifer System, FY93 Status Report*. PNL-8971, Pacific Northwest Laboratory, Richland, Washington.

Waitt RB Jr. 1980. "About Forty Last-Glacial Lake Missoula Jökulhlaups through Southern Washington." *Journal of Geology*, Vol. 88, pp. 653-679.

Waldrop WR and HS Pearson. 2000. *Results of Field Tests with the Electromagnetic Borehole Flowmeter at the Pacific Northwest National Laboratory Richland, WA*. QEC-T-132, Quantum Engineering Corporation, Loudon, Tennessee.

Waters AC. 1961. "Stratigraphic and Lithologic Variations in the Columbia River Basalt." *American Journal of Science*, Vol. 259, pp. 583-611.

WHC. 1991. *Geology and Hydrology of the Hanford Site: A Standardized Text for Use in Westinghouse Hanford Company Documents and Reports*. WHC-SD-ER-TI-003, Rev. 0, Westinghouse Hanford Company, Richland, Washington.

Williams BA and SM Narbutovskih. 2003. *Borehole Data Package for RCRA Wells 299-E25-93 and 299-E24-22 at Single-Shell Tank Waste Management Area A-AX, Hanford Site, Washington*. PNNL-14538, Pacific Northwest National Laboratory, Richland, Washington.

Williams BA and SM Narbutovskih. 2004. *Borehole Data Package for Four CY 2003 RCRA Wells 299-E27-4, 299-E27-21, 299-E27-22, and 299-E27-23 at Single-Shell Tank, Waste Management Area C, Hanford Site, Washington*. PNNL-14656, Pacific Northwest National Laboratory, Richland, Washington.

Williams BA, BN Bjornstad, R Schalla, and WD Webber. 2000. *Revised Hydrogeology for the Suprabasalt Aquifer System, 200-East Area and Vicinity, Hanford Site, Washington*. PNNL-12261, Pacific Northwest National Laboratory, Richland, Washington.

Williams BA, BN Bjornstad, R Schalla, and WD Webber. 2002. *Revised Hydrogeology for the Suprabasalt Aquifer System, 200-West Area and Vicinity, Hanford, Washington*. PNNL-13858, Pacific Northwest National Laboratory, Richland, Washington.

Wood MI and TE Jones. 2003. *Subsurface Conditions Description of the U Waste Management Area*. RPP-15808, Rev. 0, CH2M HILL Hanford Group, Inc., Richland, Washington.

Wood MI, TE Jones, R Schalla, BN Bjornstad, and SM Narbutovskih. 2000. *Subsurface Conditions Description of the B-BX-BY Waste Management Area*. HNF-5507, Rev. 0A, CH2M HILL Hanford Group, Inc, Richland, Washington.

Wood MI, TE Jones, R Schalla, BN Bjornstad, and FN Hodges. 2001. *Subsurface Conditions Description of the T and TX-TY Waste Management Areas*. HNF-7123, Rev. 0, CH2M HILL Hanford Group, Inc, Richland, Washington.

Wood MI, TE Jones, BN Bjornstad, DG Horton, SM Narbutovskih, and R Schalla. 2003. *Subsurface Conditions Description of the C and A-AX Waste Management Area*. RPP-14430, Rev. 0, CH2M HILL Hanford Group, Inc., Richland, Washington.

Distribution

DOE Office of River Protection

R. W. Lober	H6-60

CH2M HILL Hanford Group, Inc.

F. M. Mann	H6-03

Pacific Northwest National Laboratory

R. W. Bryce	K6-75
K. M. Krupka	K6-81
Hanford Technical Library	P8-55